CORA Cork Open Research Archive
Cartlann Taighde Oscailte Chorcaí

Title	Vaccinia virus assembly and motility
Authors	Cudmore, Sally
Publication date	1996
Original Citation	Cudmore, S. 1996. Vaccinia virus assembly and motility. PhD Thesis, University College Cork.
Type of publication	Doctoral thesis
Link to publisher's version	http://library.ucc.ie/record=b1255996~S0
Rights	© 1996, Sally Cudmore. - http://creativecommons.org/licenses/by-nc-nd/3.0/
Download date	2026-10-30 14:13:51
Item downloaded from	https://hdl.handle.net/10468/1627

UCC
University College Cork, Ireland
Coláiste na hOllscoile Corcaigh

Tionól agus Gluaiseacht an Víorais Vaccinia

Sally Cudmore

Téis a thugadh d'Ollscoil na h-Éireann chun na riachtanais i gcóir céim Dochtúra Fealsúnachta a chomhlíonadh go páirteach.

Márta1996

Stiúrthoirí :
Dr. Gareth Griffiths, Cell Biology Programme, European Molecular Biology Laboratory, Heidelberg, An Ghearmáin.
Dr. David Sheehan, An Roinn Bithcheimic, Coláiste na h-Ollscoile, Corcaigh, Éire.
Prof. Thomas Cotter, An Roinn Bithcheimic, Coláiste na h-Ollscoile, Corcaigh, Éire.

UNIVERSITY

Vaccinia Virus Assembly and Motility

Sally Cudmore

A thesis submitted to the National University of Ireland in partial fulfilment of the requirements for the degree of Doctor of Philosophy

March 1996

Supervisors:
Dr. Gareth Griffiths, Cell Biology Programme, European Molecular Biology Laboratory, Heidelberg, Germany.
Dr. David Sheehan, Biochemistry Department, University College Cork, Ireland.
Prof. Thomas Cotter, Biochemistry Department, University College Cork, Ireland.

To my family

Table of Contents

Declaration i
Acknowledgements ii
Abbreviations iv
Abstract v

Chapter 1 : 1
Introduction

1.1 Poxviridae 2
1.2 Vaccinia Virus 3
1.3 Vaccinia life cycle 4
1.3.1 Vaccinia entry 4
1.3.2 Gene expression and DNA replication 6
1.3.3 Virion assembly and release 7
1.4 Vaccinia structural proteins 8
1.4.1 Core proteins 8
1.4.2 Membrane proteins of the IMV 9
1.4.3 Membrane proteins of the EEV 10
1.5 Drugs which inhibit the vaccinia life cycle 11
1.6 Vaccinia assembly mutants 13
1.7 Interactions of intracellular pathogens with the actin cytoskeleton 13
1.8 Viruses and the actin cytoskeleton 18
1.9 Vaccinia-actin interactions 19
1.10 Thesis aims 20

Chapter 2 : 22
A vaccinia virus core protein, p39, is membrane associated
Submitted to Journal of Virology

Chapter 3 : 62
Actin-based vaccinia virus motility
Nature **378;** 636-638 (1995)

Chapter 4 : 67

Vaccinia virus: a model system for actin-membrane interactions

Submitted to Journal of Cell Science

Chapter 5 : 95

Discussion

5.1 What has been learnt from this work? 96

5.1.1 Review of vaccinia virus lifecycle 96

5.2 Future Questions 102

5.2.1 Structure of the IMV 102

5.2.2 Vaccinia-actin motility: future questions 103

Bibliography to chapters 1 and 5 106

Appendix: Additional papers 119

1. Assembly of vaccinia virus: incorporation of p14 and p32 into the membrane of the intracellular mature virus. (1995) Sodeik, B., Cudmore, S., Ericsson, M., Esteban, M., Niles, E.,G., and Griffiths, G. J Virol. 69, 3560-3574.
2. Characterization of *ts*16, a temperature-sensitive mutant of vaccinia virus. (1995) Ericsson, M., Cudmore,S., Shuman,S., Condit, R.,C., Griffiths, G. and Krijnse Locker, J. J. Virol. 69, 7072-7086
3. A novel immunogold cryoelectron microscopic approach to investigate the structure of intracellular and extracellular forms of vaccinia virus. (1996) Roos, N., Cyrklaff, M., Cudmore, S., Blasco, R., Krijnse Locker, J. and Griffiths, G. EMBO J. in press

DECLARATION

This thesis has not been submitted before, in whole or in part, to this or any other University for any degree, and is, except where otherwise stated, the original work of the author.

Signed: Sally Cudmore, March 1996

Sally Cudmore

ACKNOWLEDGEMENTS

First and foremost I would like to thank Gareth Griffiths for offering me a position in his lab. From him I have learnt that science comes in different flavours and textures, such as mountain hiking in the French Alps to skiing in various parts of Europe. He always found time to help with problems and to offer valuable advice and I hope that we will always remain friends and collaborators. Thanks to Gareth, I have spent a wonderful time at EMBL, a unique environment full of multicultural experiences and surprises of all sorts. The first line of the abstract is dedicated especially to Gareth !

My gratitude also to the members of my thesis comittee, Kai Simons and Steve Fuller for advice throughout this research, and to my supervisors in UCC, Thomas Cotter and David Sheehan, for their recommendations during the writing of this thesis.

To Beate Sodeik and Jacomine Krijnse Locker I am gratefully indebted for almost everything I have learnt about viruses, tissue culture, immunofluorescence microscopy and radioactivity. Thank you for all this support and help, especially at the beginning stages of my thesis when I so badly needed it.

For my electron microscopy experience, there are many people to whom I would like to express my gratitude. Maria Ericsson and Heinz Horstmann both spent enormous amounts of time demonstrating many various techniques from knife making to cryosectioning. Brent Gowen taught me how to embed samples in Lowacryl, while many different members of the Leonard lab, Chas Ferguson, David Goulding and Vincent Guenebaut, came to my aid frequently on beam searching missions !!!

I would like to thank all the members of the Griffiths lab, both past and present, for proving such a convivial, and occasionally fiery, working atmosphere. From vla to sekt, snow balls to Mossbach petrol station, I will always have a lot of fond memories of great times. Thank you to Beate, Heinz, Maria, Michel, Jan, Jacomine, Andrea, Ariel, Masha, Sibylle, Anja, Hanry, Eric, Yvonne, Marlies, Torunn, Norbert and Victoria.

I spent a great two weeks in Madrid with Rafa Blasco. During this time I learnt both how to clone and to come to terms with a society whose time schedule operates about three hours

behind my normal routine and stomach growlings !!! Not only did I learn most of my molecular biology from Rafa, but I also used many of his virus mutants throughout the course of this work.

I would also like to thank all the people who proof read various parts of this thesis: Gareth Griffiths, Jacomine Krijnse Locker, Michael Way, Janis Burkhardt, Rafa Blasco and Vincent Guénebaut. Petra Riedinger provided a lot of help with figure 8.

Michael Way, with whom I collaborated on the subject of actin-based vaccinia motility, played a tremendous role in this thesis. He spent many hours sitting in front of the confocal microscope, and even more hours again at his computer generating many of the images in chapters 3 and 4. And even more hours, on top of all that, drinking beers !!! This thesis was written on a computer which he generously lent to me. I would also like to thank the other members of his lab, Inge Reckmann and Sidney Higley.

My family have always been a constant source of support, letters, faxes and telephone calls. They unerringly visited every year, even parting occasionally with broken bones and great impressions of Swiss nurses! Mum was always at the other end of the phone when I needed someone to talk to while Dad always kept a crewing position available, even amongst fierce competition from my sisters, Wendy and Ruth. Ronan, my "little" brother who unfortunately is no longer as little as when I left Ireland, always provided entertainment when he came to visit, and was especially amused at all the Ein- und Aus-"fahrts" on the German autobahns.

And finally Vincent, it is he that I followed to the top of the Matterhorn and to the bottom of the Red Sea. With him I climbed frozen ice falls, jumped gaping crevasses and almost floated away in our tent. He taught me to appreciate French cheeses that smelt worse than β-mercaptoethanol, whilst failing to persuade me to even taste Corsican worm cheese. He has spent unfaltering hours baking the very best Apfel Strudel ever spacially for me, and even more dedicated minutes helping me to devour it. His constant love, understanding, support and enthusiasm have been instrumental in shaping this thesis.

ABBREVIATIONS

β Me	β mercaptoethanol
CEV	cell-associated enveloped virus
DTT	dithiotreitol
D	DNA crystalloid
DNA	deoxyribonucleic acid
EEV	extracellular enveloped virus
FCS	foetal calf serum
h	hour
HU	hydroxyurea
IC	intermediate compartment
IEV	intracellular enveloped virus
IMCBH	N_1-isonicotinoyl-N_2-3-methyl-4-chlorobenzoyl hydrazine
IMV	intracellular mature virus
IV	immature virus
kD	kilo Dalton
µg	microgram
µm	micrometer
min	minute
MOI	multiplicity of infection
mRNA	messenger RNA
N	nucleus
nm	nanometer
Na_2CO_3	sodium carbonate
NP 40	nonidet P 40
PAGE	polyacrylamide gel electrophoresis
PBS	phosphate buffered saline
p.i.	post infection
RB	rifampicin body
Rif	rifampicin
RNA	ribonucleic acid
SDS	sodium dodecyl sulphate
TGN	*trans* Golgi network
Tris	tris(hydroxymethyl)amino-methane
TX-114	triton X-114

ABSTRACT

Vaccinia virus, the prototype member of the orthopoxviruses, is the largest and the most complex virus known. After replication of its genome and expression of the viral proteins, vaccinia undergoes a complicated assembly process which produces two distinct infectious forms. The first of these, the intracellular mature virus (IMV), develops from the immature virion (IV) after packaging of the genome and cleavage of the core proteins. During the transition of the IV to the IMV, a new core structure develops in the centre of the virion, concomitantly with the appearance of spike-like structures which extend between this core and the surrounding membranes of the IMV. I describe the characterization of p39 (gene A4L) which is hypothesized to be one component of these spikes. p39 is a core protein, but has strong associations with the membranes surrounding the IMV, possibly due to an interaction with p21 (A17L). Due to its location between the core and the membranes of the IMV, p39 is ideally situated to act as a matrix-like linker protein and may play a role in the formation of the core during the transition of the IV to the IMV.

The IMV is subsequently wrapped by a membrane cisterna derived from the *trans* Golgi network, to form the intracellular enveloped virus (IEV). I show that the IEV can co-opt the actin cytoskeleton of the host cell in order to induce the formation of actin tails which extend from one side of the virion. These actin tails propel the virus particle, both intra- and intercellularly, at speeds of up to 2.8μm/min. On reaching the plasma membrane, the virus particles project out from the cell surface at the tip of virally induced microvilli. The outer membrane of the IEV is thought to fuse with the plasma membrane at the tip of these projections, thus exposing the second infectious form of vaccinia. This is thought to be the means by which the cell-associated enveloped virus is presented to neighbouring cells, thereby facilitating the direct cell-to-cell spread of virus particles.

CHAPTER I

Introduction

The work presented in this thesis encompasses two different stages of the life cycle of vaccinia virus; (i) the early stages of vaccinia assembly and (ii) the actin-based motility of vaccinia virus. In this introduction I will present a brief synopsis of the life cycle of vaccinia and, as a basis for comparison with vaccinia motility, I will review the field of actin-based bacterial motility as there are many parallels, as well as differences, between the two systems.

1.1 Poxviridae

The *poxviridae* form a diverse family of DNA viruses which infect both vertebrate and invertebrate hosts. They are the largest known viruses, reaching sizes of approximately 200nm in width x 400nm in length. Pox virions consist of a double stranded DNA genome of between 130 and 280kbp, which is surrounded by a number of membranes of different sub-cellular origin. The poxviruses encode most of the proteins required for their own replication and transcription, which occurs independently of the host cell nucleus, unlike other DNA viruses (Moss, 1990). Most members of the *poxviridae* which have been investigated thus far have two distinct infectious forms, the intracellular mature virus (IMV) and the extracellular enveloped virus (EEV), which appear at different stages during the life-cycle.

A scheme depicting the members of the poxvirus family is shown in figure 1. The *poxviridae* consist of two subfamilies, *Chordopoxvirinae* (vertebrate poxviruses) and *Entomopoxvirinae* (insect poxviruses). The *Chordopoxvirinae* are further divided into eight genera; *orthopoxvirus*, *parapoxvirus*, *avipoxvirus*, *capripoxvirus*, *leporipoxvirus*, *suipoxvirus*, *yatapoxvirus* and *molluscipoxvirus* (Murphy and Kingsbury, 1990). The most well known of these genera is *orthopoxvirus*, which is comprised of variola virus, the causative agent of human smallpox, as well as vaccinia virus, cowpox virus and monkeypox virus. The members of the orthopox genus are famous for a number of different reasons. Smallpox has been known as a severe disease for over 2000 years. Originating in India or western Asia, smallpox spread to eastern Asia, Europe and north Africa by 700AD. From Europe it was spread to most of the rest of the world by colonisers, arriving in North America in 1617 and Australia in 1789 (Fenner, 1990). Smallpox was one of the first diseases against which preventative measures were taken. In ancient China dried material was taken from skin lesions of people recovering from a mild infection and this was administered to other individuals by inhalation, a process known as variolation, *varus* being the Latin for pimple. Vaccination, as we know it today, was pioneered by Edward Jenner (*1749-1823†). He used material from the pocks of milk maids infected with cowpox which he then injected into uninfected people to confer immunity against smallpox (Jenner, 1799). Hence the name vaccination which is derived from *vacca* , the Latin word for cow. Due to a

global eradication programme co-ordinated in 1958 by the World Health Organization (WHO), the world was declared free of endemic smallpox in 1979 (WHO, 1980).

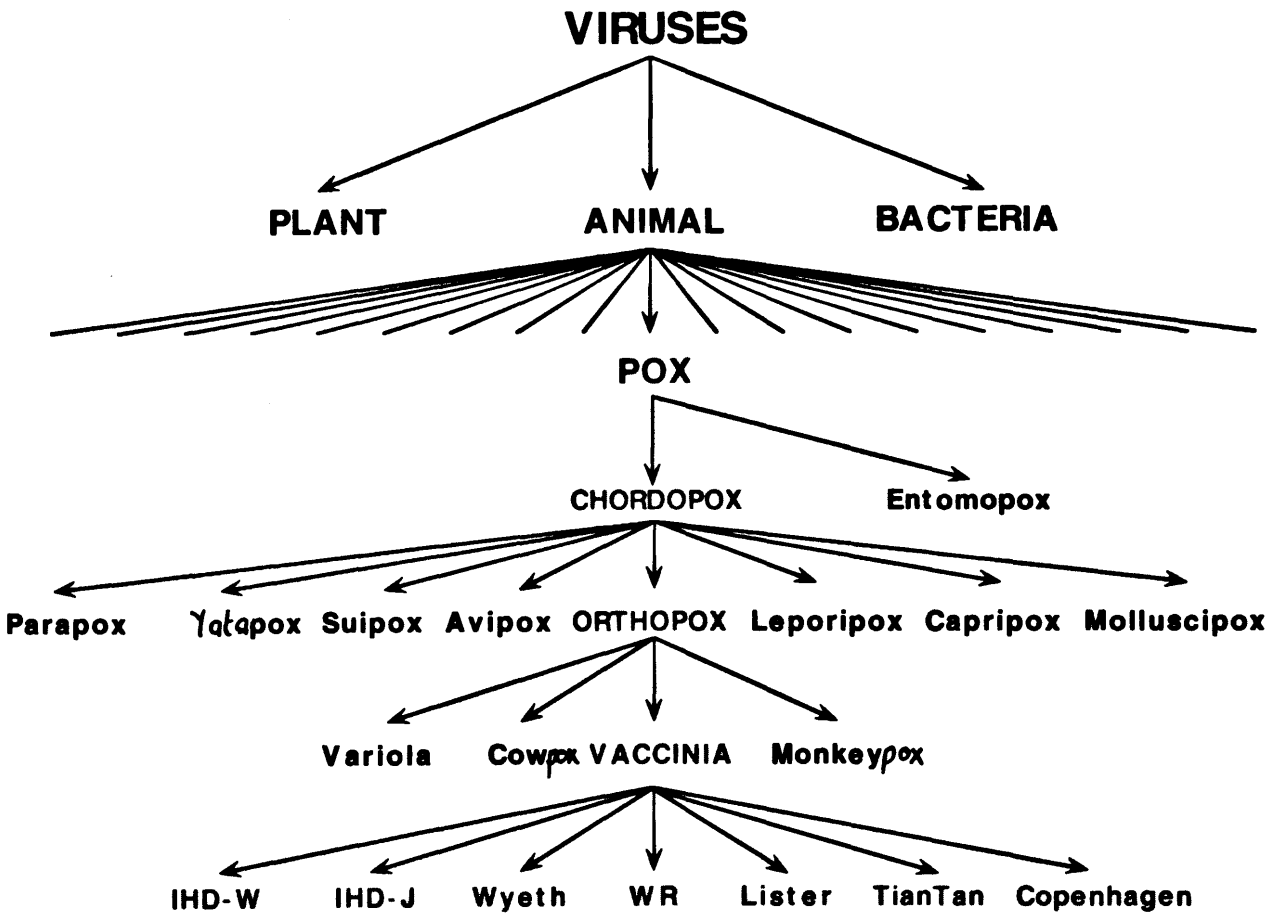


FIGURE 1: A tree diagram depicting the members of the poxvirus family

1.2 Vaccinia Virus

Vaccinia virus is the prototype member of the orthopoxviruses. It was the first virus to be seen microscopically (in 1887 by Buist), to be associated with an infectious disease (Ledingham and Aberd, 1931), accurately titrated, physically purified and chemically analysed (Craigie, 1932; Ledingham and Aberd, 1931). The main constituents of vaccinia virus are protein, lipid and DNA which account for 90%, 5-6% and 3.2% respectively of the dry weight of the particle (Zwartouw, 1964). Vaccinia is a valuable tool which is used as an expression system, and recombinant vaccinia is being considered for use as a live vaccine against many diseases, including herpes and AIDS (Moss, 1991). There are a number of different vaccinia strains which include WR (Western Reserve), Copenhagen, Lister, Wyeth, IHD-J, IHD-W (International Health Department) and Tian Tan (figure 1).

The ends of the genome consist of terminal hairpin loops which covalently connect the two DNA strands into one continuous polynucleotide chain (Baroudy et al., 1982). The genome of vaccinia strain Copenhagen is composed of 191kbp of a linear duplex DNA molecule. This genome has been completely sequenced and shown to code for a potential 263 open reading frames, which encode proteins of over 65 amino acids (Goebel et al., 1990; Johnson et al., 1993). However many of the proteins encoded by these genes still await identification and functional characterization.

1.3 Vaccinia life cycle

For ease of description, the life cycle of vaccinia virus will be reviewed under the following headings; virus entry, regulated gene expression and replication of the dsDNA genome, virion assembly and virus dissemination. Figure 2 shows a general scheme depicting the life cycle.

1.3.1 Vaccinia entry

There are a number of different stages in vaccinia entry: adsorption, penetration and uncoating. First vaccinia adsorbs to the cell surface. This may occur due to an interaction with a receptor on the plasma membrane, however a receptor for vaccinia virus has

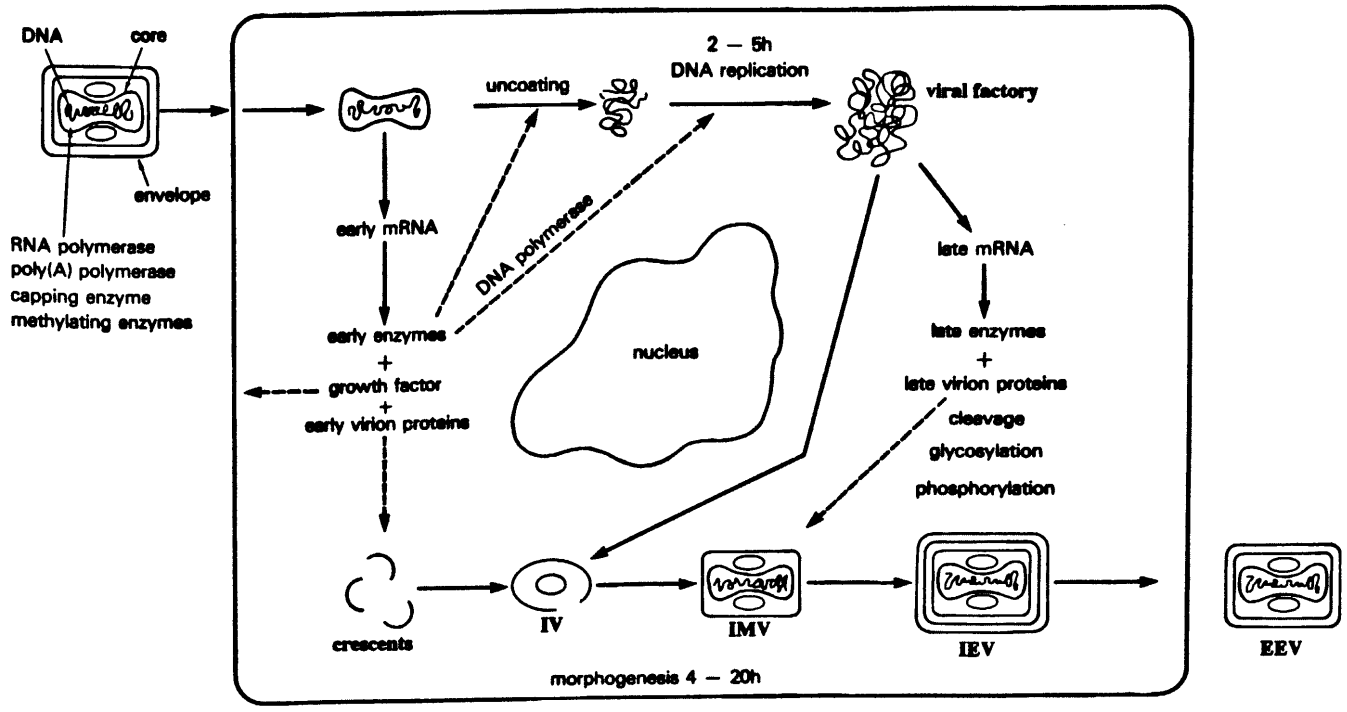


FIGURE 2: Outline of the life-cycle of vaccinia virus (modified from Moss, 1990)

not yet been identified [1]. Adsorption to the cell surface can occur at 4°C whereas penetration, the second stage of entry, requires physiological temperatures. Enveloped viruses normally penetrate cells either by fusion of their outer membrane with the plasma membrane or alternatively they can be endocytosed, whereupon low pH triggers a conformational change in a viral fusion protein leading to fusion of the viral membrane with the endosomal membrane, releasing the nucleocapsid (for a review see Marsh and Helenius, 1989). Fusion with the plasma membrane is currently accepted as the method of vaccinia penetration (Doms et al., 1990). Due to the fact that vaccinia has two infectious forms (see section 1.4), the intracellular mature virus (IMV) and the extracellular enveloped virus (EEV), the process of vaccinia entry is complicated. Early work on vaccinia virus used preparations of IMV as the importance of the EEV for infection had not been recognized. Electron micrographs show IMVs fused to the plasma membrane (Chang and Metz, 1976) or within vacuoles formed by membrane invagination (Dales and Kajioka, 1964). Fluorescence assays have also demonstrated that vaccinia membranes fuse with the plasma membrane (Doms et al., 1990). In addition, other reports have suggested that vaccinia virus is activated by interaction with the plasma membrane (Ichihashi and Oie, 1983) and viral proteins are found associated with the plasma membrane after subcellular fractionation of infected cells (Janeczko et al., 1987; Mallon (Ruszala) and Holowczac, 1985). In agreement, plaque formation is not inhibited by lysomotrophic agents indicating that endocytosis is not essential for vaccinia entry (Doms et al., 1990; Janeczko et al., 1987).

There is very little information concerning the entry of the EEV, which has an additional membrane in comparison to the IMV. Current understanding is that enveloped virus is essential for cell-to-cell and long range spread of the virus (Appleyard et al., 1971; Blasco and Moss, 1991; Blasco and Moss, 1992; Boulter and Appleyard, 1973; Payne, 1980). EEV fuses twice as rapidly and efficiently with cell surfaces than the IMV (Doms et al., 1990; Payne and Norrby, 1978). According to this model, an IMV would be released into the cytoplasm and therefore it is likely that a different mechanism of virion disassembly exists in order to release the viral cores after EEV entry.

The third step in vaccinia entry involves uncoating of the virus core to release the DNA. Unlike the earlier two steps of vaccinia entry, it requires both viral RNA and protein synthesis (Joklik, 1964). It is thought that an early viral protein, a putative 23kD uncoating protein with trypsin-like activity, may be involved in this uncoating process (Pedley and

---

[1] It has been proposed, based on infectivity-blocking studies with epidermal growth factor (EGF), synthetic peptides and antibodies to the EGF receptor (EGF-R), that the EGF-R acts as a portal of entry for vaccinia virus (Eppstein et al., 19985; Marsh and Eppstein, 1987). However, it has been shown more recently that EGF-R is not a receptor for vaccinia (Hugin and Hauser, 1994; Stroobant et al., 1985).

Cooper, 1987). Isolated cores can be purified and have been shown to be capable of *in vitro* transcription (Kates and McAuslan, 1967; Kates and Beeson, 1970; Munyon et al., 1967). The cores contain all the proteins necessary for this process e.g., VETF (vaccinia early transcription factor) (Li and Broyles, 1995), RNA polymerase (Kates and McAuslan, 1967), deoxyribonuclease (Pogo and Dales, 1969), nucleoside triphosphate phosphohydrolase (Gold and Dales, 1968) and DNA topoisomerase (Bauer et al., 1977). The core of vaccinia can be visualized by electron microscopy as a distinct physical entity in the cytoplasm of the infected cell and it appears that the nucleoprotein complex passes out through a breach in the wall of this core, leaving behind empty shells (Dales, 1965; Dales, 1963; Dales and Kajioka, 1964).

1.3.2 Gene expression and DNA replication

Vaccinia gene expression is divided into three groups on a temporal basis ; the early genes are transcribed prior to DNA replication [2], while the transcription of both the intermediate and late genes occurs during or after DNA replication (Moss, 1990; Moss, 1990; Moss, 1990). Transcription of the early genes by enzymes which are present in the core produces functional mRNA (Kates and McAuslan, 1967). These early genes encode proteins such as the putative uncoating protein (Pedley and Cooper, 1987), growth factors (Stroobant et al., 1985) and DNA polymerase (Challberg and Englund, 1979). Once the virion has been uncoated, the DNA released and early gene expression has taken place, genome replication can commence.

As previously mentioned, the transcription and replication of the vaccinia genome takes place in the cytoplasm of the host cell. This occurs in structures called "viral factories" which are found in the perinuclear region of infected cells approximately 1 to 2 hours after infection (Cairns, 1960; Dales, 1963; Harford et al., 1966; Minnigan and Moyer, 1985). DNA replication commences at about 1.5 h after infection (Cairns, 1960) and by 4.5h, 90% of the replication has occurred (Joklik and Becker, 1964). Cells infected with vaccinia contain up to six times more DNA polymerase activity than uninfected cells, despite the fact that the replication of the host cell nuclear DNA is greatly diminished (Green and Pina, 1962; Joklik and Becker, 1964; Magee, 1962). Up to 10,000 copies of the viral genome are generated per infected cell (Joklik and Becker, 1964; Salzman, 1960).

Coincident with the onset of DNA replication, a dramatic change in gene expression occurs as the intermediate and late genes are switched on. The intermediate proteins are

---

[2] These early genes account for approximately half of the genome. The transcription of the early genes continues, to a lesser extent, even after the late genes have been switched on (Boone and Moss, 1978; Oda and Joklik, 1967; Paoletti and Grady, 1977).

synthesised immediately after DNA replication, whereas the synthesis of the late proteins is somewhat delayed (Moss, 1990). The late genes encode most of the structural proteins which are needed for virion assembly, as well as many different enzymes including a DNA topoisomerase (Bauer et al., 1977) and deoxyribonucleases (McAuslan and Kates, 1967; Pogo and Dales, 1969).

1.3.3 Virion assembly and release

Once genome replication and protein synthesis have occurred, virion assembly can commence. The first sign of viral membrane formation is the appearance of rigid, curved membrane structures called "crescents" (see figure 2), which appear to bud from the viral factories, already described as the sites of DNA replication. These "crescents" consist of a membrane with a border of spicules on the convex surface and electron dense granular material on the concave surface (Dales, 1963). It is believed by some that these crescents are synthesised *de novo* in the cell, without a pre-existing membrane template, as they do not appear to have any definite continuation with membranes from cellular organelles (Stern and Dales, 1974; Stern and Dales, 1976; Mohondas and Dales, 1995). However, it was shown by Sodeik (1993) that these membranes are derived from a cisterna of the intermediate compartment (IC) and that they are therefore composed of two tightly apposed membrane bilayers. These membranes have a very rigid structure and it is thought that p65, the gene product of D13L, may contribute to this rigidity as it localizes to the concave surface of the "crescents". In the presence of the drug rifampicin, p65 fails to localize to the membranes surrounding the viral factories and the crescents do not form (see sections 1.4.1 and 1.5) (Essani et al., 1982; Sodeik et al., 1994).

The crescents develop into completely spherical immature virions (IV) which undergo further maturational changes, such as the packaging of DNA and cleavage of core proteins (Moss and Rosenblum, 1973; VanSlyke et al., 1991; VanSlyke et al., 1991), to produce the first of two infectious forms of vaccinia, the intracellular mature virus (IMV), which are first seen about 3 to 4 hours after infection. Almost nothing is known about the transition from the IV to the IMV. Whereas the IV is completely spherical and has not yet packaged its complement of DNA, the IMV is a parallelepiped with a definite internal core structure. Release of IMV can occur when the cell lyses due to the cytotoxic effects of infection.

A fraction of IMV, varying between 5 and 40% according to virus strain and cell type (Payne, 1979), can undergo a second wrapping step by another membrane cisterna (Dales, 1971; Hiller and Weber, 1985; Ichihashi et al., 1971; Morgan, 1976), this time from the *trans* Golgi network (TGN) (Schmelz et al., 1994), producing the intracellular enveloped virus

(IEV) (figure 2). The IEV is released from the cell when its outermost membrane fuses with the plasma membrane, thus producing the extracellular enveloped virus (EEV) (Dales, 1971; Ichihashi et al., 1971; Morgan, 1976; Payne, 1980; Payne and Kristensson, 1985). It has also been demonstrated that thick actin-containing microvilli, which have virus particles at their tips, are induced at late times during infection, possibly facilitating the release of virus particles (Hiller et al., 1981; Hiller et al., 1979; Krempien et al., 1981; Stokes, 1976). The majority of enveloped virus can remain bound to the outer cell surface and this is referred to as cell-associated enveloped virus (CEV) (Blasco et al., 1991; Blasco and Moss, 1992). EEV is important for long range virus transmission and the ability of a given vaccinia strain to cause long range spread of infection is directly related to the amount of EEV it produces (Appleyard et al., 1971; Boulter and Appleyard, 1973; Payne, 1979; Payne, 1980). It has been suggested that the CEV is involved in direct cell-to-cell spread of infection (Blasco and Moss, 1991; Blasco and Moss, 1992).

1.4 Vaccinia virus structural proteins

Of the 263 potential reading frames in the vaccinia genome (Goebel et al., 1990; Johnson et al., 1993), approximately 100 proteins are packaged into the mature virion (Carrasco and Bravo, 1986; Essani and Dales, 1979). Many of these are post-translationally modified by proteolytic cleavage, glycosylation, phosphorylation and fatty acid acylation (for a review see (VanSlyke and Hruby, 1990). Vaccinia structural proteins, which are the products of late genes, can be separated into two groups according to their location within the virion: (i) core proteins and (ii) envelope proteins. This classification is based on the traditional method used to separate vaccinia membranes from the cores, which employs a combination of a detergent, usually Nonidet P 40 (NP 40), and a reducing agent, usually either dithiothreitol or β-mercaptoethanol (Easterbrook, 1966; Essani and Dales, 1979; Holowczak and Joklik, 1967; Oie and Ichihashi, 1981; Sarov and Joklik, 1972).

1.4.1 Core proteins

In combination with the structural proteins, the core also contains soluble enzymes which are necessary for the transcription of the early genes (see section 1.3.2). The potential structural proteins described to date are: (i) p11 (gene F18R), a basic, phosphorylated, 11kD DNA-binding protein which accounts for 11% of the total weight of the particle (Kao et al., 1981; Pogo et al., 1975; Wittek et al., 1984). p11 is implicated in the condensation of the DNA and its incorporation into the virion (Kao and Bauer, 1987). Inactivation of the gene demonstrated that p11 is essential for viral assembly (Zhang and Moss, 1991; Zhang and Moss, 1991). It has also been reported that an 11kD phosphorylated protein interacts with the actin cytoskeleton, but it remains to be established if this is the same protein (Hiller and

Weber, 1982). (ii) p25 (gene L4R) is a 25kD protein which is derived from a larger precursor of 28kD (p28) by post-translational cleavage (Sarov and Joklik, 1972; VanSlyke et al., 1991; Vanslyke and Hruby, 1994; Weir and Moss, 1984; Weir and Moss, 1985; Yang et al., 1988). p25 comprises 6.5% of the virion weight and it has been suggested that it may have a histone like-function as it can bind to DNA (Yang et al., 1988). (iii) p4a (gene A10L) and (iv) p4b (gene A3L) are also proteolytically processed (Katz and Moss, 1970; Rosel and Moss, 1985; Sarov and Joklik, 1972; vanMeir and Wittek, 1988; VanSlyke et al., 1991; Vanslyke and Hruby, 1994; VanSlyke and Hruby, 1990; Wittek et al., 1984). p4a (105kD) is cleaved to yield a 68kD protein, 4a, while p4b (74kD) is cleaved to the resultant 4b (62kD). These two proteins are additionally modified by ADP-ribosylation (Child et al., 1988). The post-translational cleavage of p28, p4a and p4b is prevented by addition of the drug, rifampicin (see section 1.5) (Katz and Moss, 1970). (v) The product of the gene I7L is another structural protein of the core. A virus, ts16, which has a temperature sensitive mutation in this protein does not assemble IVs (Condit et al., 1983; Ericsson et al., 1995; Kane, 1993). (vi) p65 (D13L), the target of the drug rifampicin (discussed in section 1.5) (Baldick and Moss, 1987; Moss et al., 1971; Nagayama et al., 1970; Tartaglia and Paoletti, 1985; Tartaglia et al., 1986), has been localized to the concave surface of the IVs and is thought to play a role in the development and rigidity of these intermediate compartment derived membranes (Sodeik et al., 1994). (vii) p39 (gene A4L) is a highly immunogenic core protein which is synthesized at late times during infection (Demkowicz et al., 1992; Maa and Esteban, 1987; Paez et al., 1987). This protein is the focus of chapter 2 of this thesis.

1.4.2 Membrane proteins of the IMV

To date, six proteins have been described as components of the IMV membranes. (i) p14 (gene A27L) was identified when monoclonal antibodies against a 14kD protein were shown to neutralise IMV infectivity, indicating that p14 may play a role in virus penetration (Rodriguez and Esteban, 1987; Rodriguez et al., 1985). It was later confirmed that p14 is involved in fusion of the viral envelope with the cell plasma membrane (Doms et al., 1990; Rodriguez et al., 1987) and is also involved in cell-cell fusion late in infection (Gong et al., 1990; Rodriguez et al., 1985; Rodriguez et al., 1987). p14 can form trimers which are covalently linked by disulphide bonds (Rodriguez et al., 1987). p14 does not seem to be essential for the infectivity of the IMV, but rather for wrapping of the IMV by the TGN due to interactions with another vaccinia membrane protein, p37 (F13L) (see sections 1.4.3 and 1.5), which is targetted to the TGN membranes (Rodriguez and Smith, 1990). Immunoprecipitation with antibodies to p14 identified another membrane protein of the IMV, (ii) p21 (A17L) (Rodriguez et al., 1993; Rodriguez and Esteban, 1987). p21 is a quadruple spanning membrane protein which is present in the inner of the two membranes

surrounding the IMV (Krijnse Locker et al., submitted) and which may act to anchor p14 in the membrane as p14 does not have a membrane spanning domain. (iii) M25 (L1R) is a 25kD protein which is covalently modified by the addition of the C_{14} fatty acid, myristate (Franke et al., 1989; Franke et al., 1990). The signal which localizes this protein to the IMV membranes appears to reside in both the fatty acid moiety and the first 12 N-terminal amino acids (Franke et al., 1989; Ravanello and Hruby, 1994; Ravanello et al., 1992). (iv) p32 (D8R) has a C-terminal membrane spanning domain and was shown to be non-essential for virus propagation in tissue culture (Niles and Seto, 1988; Rodriguez et al., 1992). It is thought that p32 facilitates the binding of IMV to the plasma membrane during infection (Lai et al., 1991; Maa et al., 1990). (v) There has been some discrepancy over the identity of a 35kD component of the IMV membranes. It was originally identified as the gene product of H6R, an early gene (Gordon et al., 1988; Gordon et al., 1991; Wilton et al., 1986), but was later attributed to the late gene H3L (Zinov'ev et al., 1992). (vi) The surface of the IMV has been shown to be covered with protrusions called surface tubular elements (STE). These STEs are composed of a 58kD protein that elicits an antibody which can suppress vaccinia infectivity and cell-cell fusion (Stern and Dales, 1976). More recently, the core protein 4b (gene A3L, see section 1.4.1) was also identified as a component of these STEs (Wilton et al., 1995).

1.4.3 Membrane proteins of the EEV

In its additional TGN-derived outer membrane, the EEV has a number of extra virally-encoded membrane proteins, of which five have been identified (Hiller and Weber, 1985; Payne, 1979; Payne, 1978). (i) HA or haemagglutinin has been sequenced in four different strains of vaccinia; gene salG1R in vaccinia strain WR (Smith et al., 1991); gene A56R in Copenhagen (Goebel et al., 1990); IHD-J (Shida, 1986) and Tian Tan (Jin et al., 1989). It has an apparent molecular weight of 89kD and is found on both the plasma membrane of infected cells and in the outer membrane of the EEV. HA is a type I integral membrane protein which shows sequence homology to the immunoglobulin (Ig) superfamily (Jin et al., 1989; Shida, 1986). HA is thought to play a role in EEV adsorption to the cell surface, and prevents polykariocytosis of infected cells (Ichihashi and Dales, 1971; Payne and Norrby, 1976). It is a non-essential protein as vaccinia strains which are HA$^-$(IHD-W) are infectious. It is glycosylated with both N- and O-linked carbohydrates (Shida and Dales, 1981). (ii) The major, and until recently the only recognised nonglycosylated protein of the EEV membrane, p37 (gene F13L), has already been mentioned due to its role during wrapping of the IMV by a cisterna from the TGN (section 1.4.2) (Hiller and Weber, 1985; Payne, 1992). p37 contains bound palmitate and oleate which are thought to facilitate its binding to the viral membrane (Hiller and Weber, 1985; Payne, 1992; Schmutz et al., 1991). p37 is the only protein thus identified which is cytoplasmically exposed on the outside of the

IEV (Schmutz et al., 1995). As will be discusssed in more detail, deletion of p37 prevents wrapping of the IMV (section 1.6) (Blasco and Moss, 1991; Blasco and Moss, 1992) and a mutation in the gene encoding p37 confers resistance to the drug, IMCBH (see also section 1.6) (Schmutz et al., 1991). (iii) gp42 (gene B5R in vaccinia strain WR (Smith et al., 1991), Copenhagen (Goebel et al., 1990), Lister (Takahashi-Nishimaki et al., 1991) is another acylated EEV glycoprotein. It is a type I integral membrane protein with homology to complement control factors . gp42 is very conserved among the vaccinia strains within which it has been identified to date; cowpox virus, rabbitpox virus, and seven different vaccinia strains (WR, Lister, Copenhagen, TianTan, Wyeth, Tashkent and IHD-W) (Engelstad et al., 1992) and is also thought to participate in the envelopment of IMV by TGN membranes (Engelstad and Smith, 1993; Wolffe et al., 1993). (iv) gp21 (salL4R in WR and A34R in Copenhagen) is a phosphorylated, sulphated, palmitoylated glycoprotein (Payne, 1992). This protein displays homology to C-type animal lectins (Duncan and Smith, 1992) and the lectin domain of this glycoprotein is thought to be involved in the retention of CEV at the plasma membrane in the WR strain (Blasco et al., 1993). (v) A36R encodes a 43-50kD type II integral membrane protein of the EEV. It is a 221 amino acid protein with a N-terminal hydrophobic sequence and seven potential sites for attachment of N-linked carbohydrate, but despite this does not appear to be N-glycosylated. p43-50 does not play a role in binding of the EEV to the cell surface during virus entry, but is required for the formation of normal levels of EEV (Parkinson and Smith, 1994).

1.5 Drugs which inhibit the vaccinia life cycle

There are a number of different drugs which block the life cycle of vaccinia virus at various stages. For many of these drugs, inhibitor resistant mutants have been isolated which have given valuable insights into vaccinia assembly and especially functional information on the mutant protein in question. Those inhibitors which have been used during the course of this research will be described here, while the stage at which they prevent viral assembly is shown in figure 3. Hydroxyurea (HU) can be used to reversibly block vaccinia DNA replication and therefore prevents intermediate and late gene expression. For this reason it has been traditionally used to synchronize DNA replication and viral assembly (Morgan, 1976; Pogo and Dales, 1971; Rosenkranz et al., 1966). It also provides a means to identify the temporal class of gene encoding a particular protein, as intermediate and late genes are not expressed in the presence of this drug. Rifampicin (Rif), a macrolide antibiotic, specifically blocks vaccinia assembly from proceeding past the viral factory stage (Moss et al., 1969). Rif resistant mutants allowed the identification of the gene responsible for the sensitivity to this drug, D13L, which encodes a 65 kD protein (Baldick

and Moss, 1987; Nagayama et al., 1970; Tartaglia and Paoletti, 1985; Tartaglia et al., 1986). Rif prevents p65 from being targeted to the membranes surrounding the viral factories, and hence the "crescents" fail to develop and viral assembly is blocked. The effects of this drug are also reversible, with normal viral assembly continuing after washout. Rif does not block viral protein synthesis (but does prevent cleavage of the core proteins p4a, p4b and p28, see section 1.4.1) and thus acts as an ideal way to prevent virus formation at a stage subsequent to viral structural protein synthesis. Rifampicin was used in chapter 2 of this study to prevent virus assembly, as viral proteins are more accessible to biochemical analysis in the absence of virion formation. IMCBH, or N_1-isonicotinoyl-N_2-3-methyl-4-chlorobenzoyl-hydrazine, prevents wrapping of the IMV by membranes from the TGN thus blocking assembly of the IEV (Hiller et al., 1981; Kato et al., 1969; Payne and Kristensson, 1979). The target of this drug was identified as being the 37kD protein (gene F13L) of the IEV (section 1.4.2) (Hiller et al., 1981; Schmutz et al., 1991). During normal virion assembly this protein is targeted to the membranes of the TGN where it is thought to interact with the 14kD peripheral protein which is exposed on the outer surface of the IMV, thus initiating IMV wrapping by TGN cisternae (sections 1.4.2 and 1.4.3). IMCBH was used in chapter 3 to prevent IEV formation.

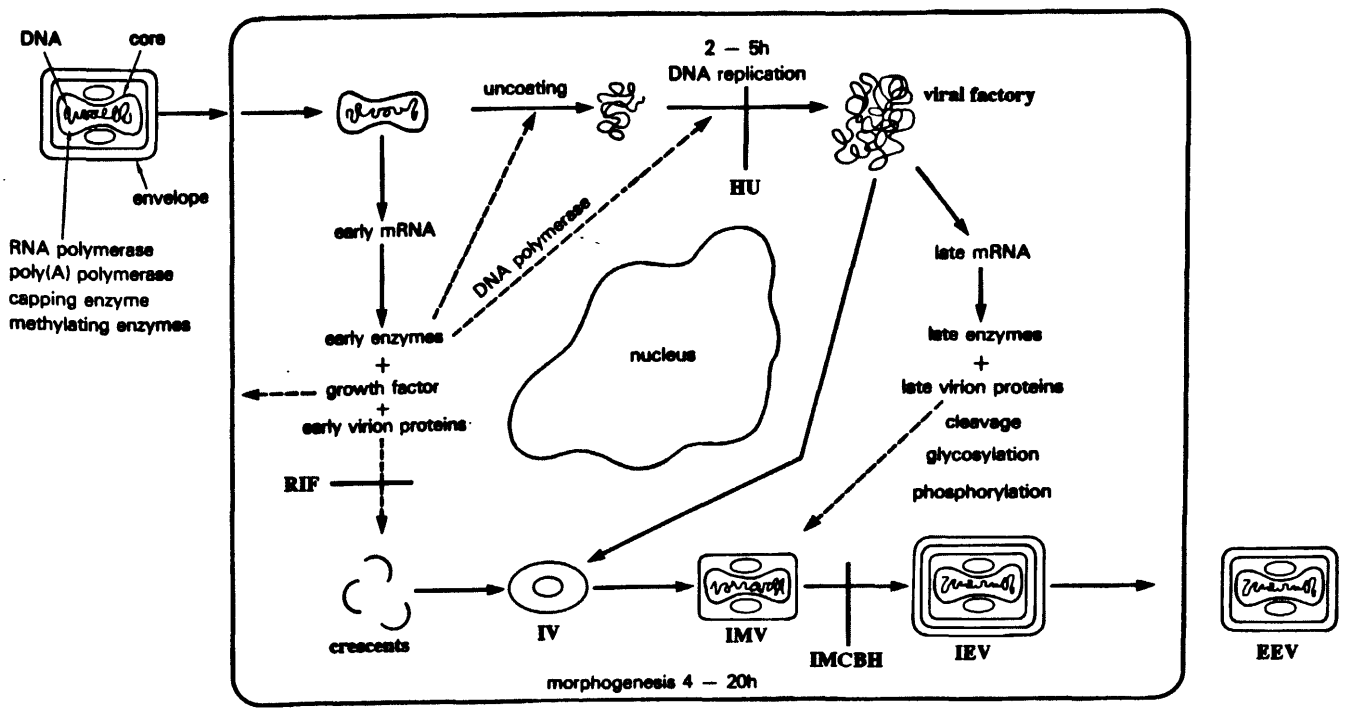


FIGURE 3: A scheme of the vaccinia life cycle showing the stages at which the various drugs block the assembly process.

1.6 Vaccinia assembly mutants

There are many different mutants of vaccinia assembly which have greatly facilitated the understanding of the vaccinia lifecycle. Three different mutants have been used in the present study. vRB12 and vRB10 are both deletion mutants in which the gene encoding the 37kD protein of the IEV, (gene F13L), has been deleted in WR and IHD-J respectively (Blasco and Moss, 1991; Blasco and Moss, 1992). Therefore these mutant viruses are unable to wrap with membranes from the TGN and consequently do not form IEV.

Vaccinia virus encodes a protein which is 31% identical to cellular profilin (Blasco et al., 1991). In chapter 3, I used a deletion mutant in which the A42R gene, which encodes vaccinia profilin, was deleted. All of these mutants were generous gifts of Dr. Rafael Blasco, Madrid, Spain.

1.7 Interactions of intracellular pathogens with the actin cytoskeleton

A number of different pathogenic bacteria have been shown to utilize the host cell actin cytoskeleton in order move within the cell and from one cell to another. This system can provide insight into the mechanism by which local actin polymerization is controlled in cells, in the absence of complex plasma membrane mediated cellular signalling processes. The first bacterium discovered to move in this manner was *Shigella flexneri*, a gram negative, enteroinvasive bacterium which causes bacillary dissentry (Adam et al., 1995; Bernardini et al., 1989; Goldberg and Sansonetti, 1993; Ogawa et al., 1968; Vasselon et al., 1991). Other obligate intracellular bacteria capable of actin-based intra- and intercellular motility include *Listeria ivanovii*, which is pathogenic exclusively for animals, causing abortions, neonatal sepsis and enteritis (Karunasagar et al., 1993) and *Rickettsia conorii*, along with *Rickettsia rickettsii*, which cause serious diseases in humans such as Mediterranean spotted fever and Rocky Mountain spotted fever respectively (Heinzen et al., 1993; Teysseire et al., 1992). Another bacterium which moves in this manner is *Listeria monocytogenes*, and, as it has been the most thoroughly studied in respect to its actin-based motility, it will be described below in more detail.

Listeria monocytogenes is a ubiquitous, rapidly growing, gram positive bacterium which is responsible for severe food borne infections which can cause meningitis, encephalitis and septicemia causing a high mortality rate in newborns, elderly and immunocompromised persons (Gellin and Broome, 1989). Electron microscopy studies have shown the life cycle of *L. monocytogenes*, in respect to its associations with actin at different stages of infection (Tilney et al., 1990; Tilney et al., 1992; Tilney et al., 1992, Tilney and Portnoy, 1989). A cartoon depicting the life cycle of *Listeria* is shown in figure

4A. After phagocytosis by the host cell, the bacterium, whose virulence genes encode proteins such as listeriolysin O (Geoffroy et al., 1987; Mengaud et al., 1988), breaks down the membranes of the phagosome and escapes into the cytoplasm of the host cell where it starts to multiply with a doubling time of about 1 hour. The dividing bacterium becomes surrounded by a cloud of actin which is subsequently organized at one pole. Thus, the bacterium begins to move through the cytoplasm of the host cell within 2 hours after infection, leaving behind an actin tail, also called an "actin comet", which can reach lengths of up to 40μm. An immunofluorescence micrograph of a cell infected with *Listeria* , where the actin tails are visible (green), is shown in figure 4B. Using these actin tails, the bacterium moves towards the cell surface and when it reaches the plasma membrane it projects outwards at the tip of large protrusion which can contact a neighbouring cell and be phagocytosed. This gives rise to a bacterium within a two-membraned phagosome in the new host cell, one membrane derived from the old cell and the other arising from the newly infected cell (figure 4A). As mentioned above, *Listeria* lyses these phagosome membranes to escape into the cytoplasm of the new cell and the cycle is repeated. Thus, once it has infected a host cell, *Listeria* can continue to spread from cell-to-cell avoiding the humoral immune response of the host as it is never exposed extracellularly.

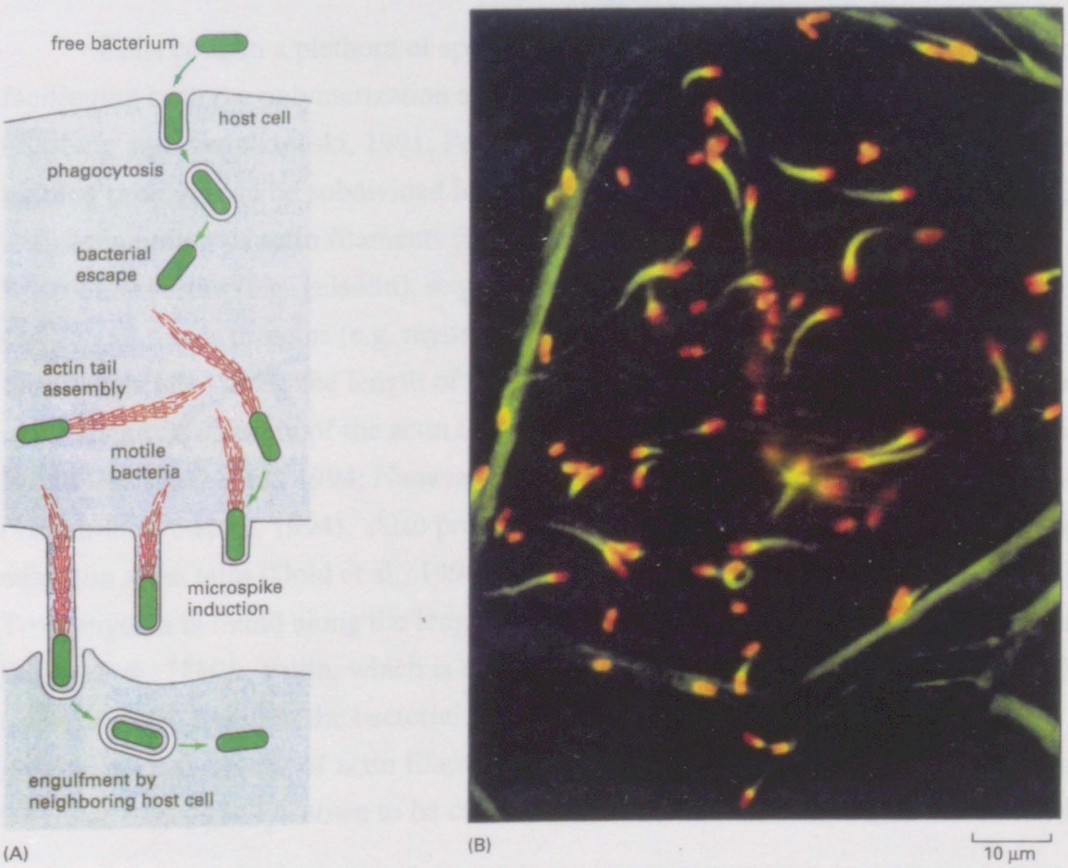


FIGURE 4: (A) depicts the life cycle of Listeria monocytogenes. (B) Fluorescence image of Listeria monocytogenes moving in a cell which has been stained to reveal the bacteria (red) and the actin (red). The actin comets are clearly visible extending from behind the bacteria. From (Alberts et al., 1994).

These actin tails are the means by which the bacterium moves within the host cell. They are composed of apparently short, 0.2μm actin filaments which are oriented unidirectionally with their barbed, or fast growing, ends towards the bacterium (Tilney et al., 1992) [3]. Fluorescence polarization ratio images show that the filament organization in outer shell of the actin tail appears to be parallel while the filaments in the core of the tail are more disordered (Zhukarev et al., 1995). Video microscopy of infected cells which were microinjected with fluorescently labelled G-actin indicated that actin nucleation and filament elongation occur close to the bacterial surface (Sanger et al., 1992). The elongation of the comets is caused by the addition of actin monomers to the barbed end of the filaments, which are present at the bacterial surface. This actin tail formation induces bacterial movement which can be very rapid, up to 1.46μm/sec, but the range of *Listeria* motility rates varies from one cell type to another (Dabiri et al., 1990; Nanavati et al., 1994). There is a positive correlation between the rate of actin polymerization and bacterial movement, with the faster moving bacteria having longer tails (Theriot et al., 1992). Comet length is dependant on the rate of actin polymerization at the bacterial end of the tail, which occurs at varying rates. In contrast, depolymerization occurs at a constant rate and throughout the length of the tail (Nanavati et al., 1994).

Cells contain a plethora of special actin binding proteins (ABP) which play a role in facilitating both the polymerization and depolymerization of filaments (for reviews see (Hartwig and Kwiatkowski, 1991; Pollard and Cooper, 1986; Stossel et al., 1985). Actin binding proteins can be subdivided into different classes based on their functions (figure 5), such as bundling of actin filaments (e.g. alpha actinin and fimbrin), cross-linking (e.g. filamin), severing (e.g. gelsolin), sequestering (e.g. β thymosin and profilin), capping (e.g. cap Z) and motor proteins (e.g. myosins). Many of these actin-binding proteins have been found associated along the length of the bacterial comets and are presumed to play a role in the dynamic stability of the actin tails. These include alpha actinin which is crucial for tail formation (Dold et al., 1994; Nanavati et al., 1994), filamin (Dabiri et al., 1990) and fimbrin (Temm-Grove et al., 1994). Also present are vinculin, which is normally found at focal adhesion sites, talin (Dold et al., 1994), and ezrin-radixin (Temm-Grove et al., 1994). Tropomyosin is found along the length of the tails and may act to protect the filaments (Dabiri et al., 1990). Villin, which is normally limited to microvilli in vertebrate epithelial cells, was also found in the bacterial tails (Temm-Grove et al., 1994). Profilin is concentrated at the site of actin filament formation, rather than being incorporated into the tails, and was initially shown to be essential for bacterial movement (Theriot et al., 1994).

---

[3] Due to the harsh extraction techniques used in this study, this filament length is most likely an underestimation of the true filament length. There is evidence that the filaments are longer than this, reaching lengths of over 0.5μm (Dr.s Peg Sievert and Tim Mitchison, personal communication).

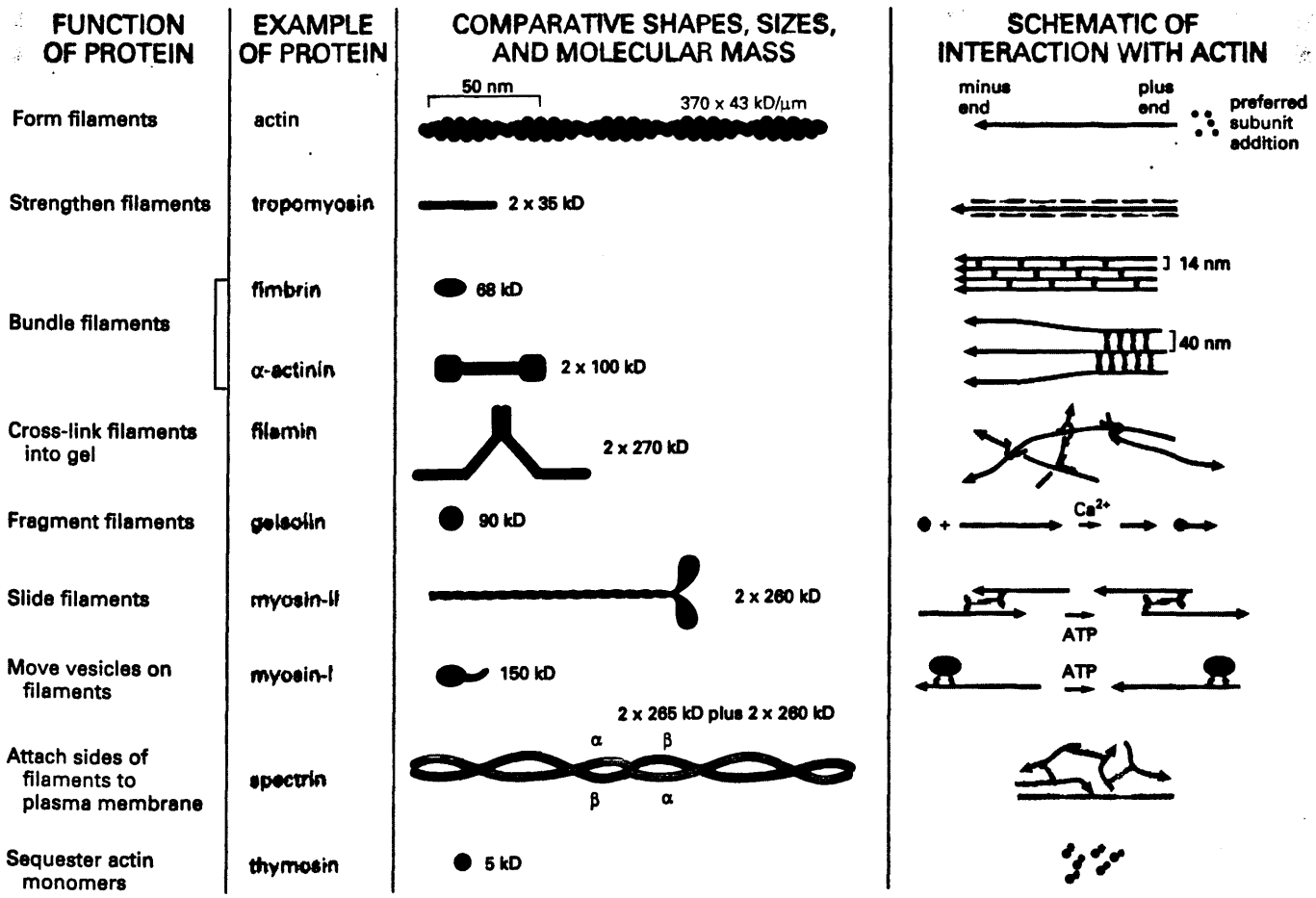
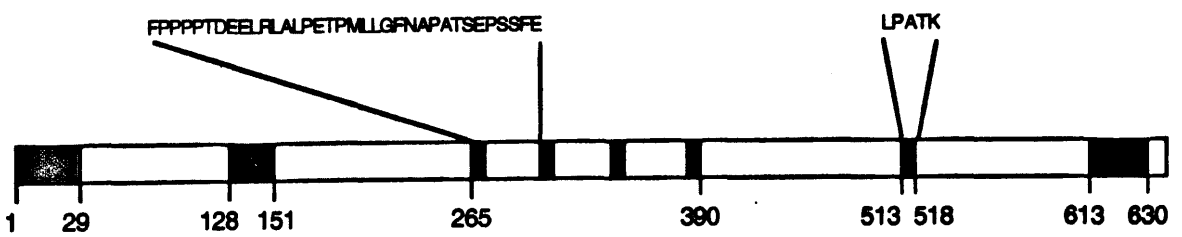


FIGURE 5: Some of the major classes of actin binding proteins found in most vertebrate cells. Actin is shown in red, while the actin binding proteins are in green. From (Alberts et al., 1994)

More recently, however, profilin has been shown not to be strictly necessary for *Listeria* movement, but when present participates in actin assembly and may even stimulate this process (Marchand et al., 1995). There is no indication that any myosin is present in the tails, further supporting the hypothesis that actin polymerization itself produces the force to generate motility.

These motile bacteria also encode virulence genes which are required for the actin-based motility. This became apparent when it was discovered that mutants defective in the *act A* gene could not form actin tails and hence bacterial spread was abolished (Domann et al., 1992; Kocks et al., 1992). The 90kD Act A protein (figure 6) is located on the outer surface of the bacterium, anchored to the bacterial membrane by a hydrophobic C-terminal sequence (Domann et al., 1992; Kocks et al., 1992; Vasquez-Boland et al., 1992). The distribution of Act A is polarised and this is thought to arise when the bacteria divide as the membrane which forms at the site of septation is devoid of Act A, with the protein being concentrated at the opposite "older" pole of the cell (Kocks et al., 1993). This is thought to

be the determining factor which causes *Listeria* movement in one direction, that is, in the direction of the non-Act A expressing pole. Act A has four polyproline repeats in the middle of the sequence which are not essential for actin motility (Pistor et al., 1995). Initially postulated as a possible profilin binding site due to the high affinity of profilin for polyproline (Perelroizen et al., 1994), these polyproline repeats were later shown not to bind profilin (Marchand et al., 1995) but are responsible for binding to VASP (vasodilator-stimulated phosphoprotein, discussed later). The N-terminal part of Act A (amino acids 128-151) is required for actin assembly (Pistor 1995, Friedrich 1995). When the protein was transiently expressed in uninfected cells, it was targetted to the host cell mitochondria, but the mitochondria remained immobile (Pistor et al., 1994). A 130kD protein, Ics A, which has a similar function, but no homology, to Act A was previously identified in *Shigella flexneri* (Bernardini et al., 1989; Lett et al., 1989). Unlike Act A, it is present throughout the comets of moving Shigella, as well as on the outer bacterial membrane (Goldberg and Sansonetti, 1993). The virulence gene necessary for actin-assembly in *L. ivanovii, iact A*, has also been identified and this protein shows low homology to Act A (Gouin et al., 1994).



- N-terminal bacterial singal sequence
- F actin recruitment site
- Polyproline repeats - bind VASP
- LPATK motif typical of cell wall proteins of Gram-positive bacteria
- C-terminal anchor region

FIGURE 6: Schematic representation of the Act A protein

Although required for actin assembly and profilin concentration at the pole of the bacterium, Act A does not bind directly to either protein. This together with the finding that *Listeria* grown in broth will not induce the assembly of actin comets (Tilney et al., 1992). indicates that the presence of host proteins is probably necessary for motility. The development of a cell-free system of concentrated *Xenopus* egg extracts, in which *Listeria* movements can be reproduced has made biochemical analysis of these cellular factors possible (Theriot et al., 1994).

One candidate cellular component is vasodilator-stimulated phosphoprotein (VASP), a highly abundant substrate of both cAMP- and cGMP-dependant protein kinases which co-localises with actin filaments in focal contacts, stress fibres and membrane ruffles (Haffner et al., 1995; Reinhard et al., 1992). VASP, a 40kD protein, has three distinct phosphorylation sites and is also rich in proline residues which are concentrated in the central region of the protein (Haffner et al., 1995). It was shown that profilin can bind to the polyproline regions of VASP, thereby identifying VASP as the first endogenous proline-rich ligand of profilin (Reinhard et al., 1992). Subsequently it was shown that VASP accumulates on the surface of *Listeria* in a polarised fashion, prior to the detection of the actin clouds but it is not incorporated into the actin tails (Chakraborty et al., 1995). VASP can bind directly to Act A polyproline repeats, and therefore provides the first physical connection between a bacterial protein and the cytoskeleton (Pistor et al., 1995). VASP also associates with the actin tails of *Shigella*, being incorporated evenly along the complete length of the actin tail, as is Ics A. However an overlay blot with radiolabelled VASP indicated that it does not interact directly with Ics A (Chakraborty et al., 1995).

Now that three major proteins involved in the process of *Listeria* actin-based motility have been identified, Act A, profilin and VASP, it is possible to hypothesize as to how these bacteria co-opt the actin cytoskeleton of the host cell. Three possible models for actin recruitment and tail elongation at the pole of *Listeria* are shown in figure 7. Profilin is thought to play a role in delivering the actin monomers to the growing ends of the filaments, but more direct evidence will be needed to establish the complete mechanism.

1.8 Viruses and the actin-cytoskeleton

Many reports have indicated that viruses can associate with the actin cytoskeleton. In the mid 1970s a 42 kD protein identified as cellular actin, was found to be present in the virions of many enveloped viruses, such as Sendai virus (Lamb et al., 1976), a number of different mammalian RNA tumour viruses (Wang et al., 1976), murine mammary tumour virus (Damsky et al., 1977), measles virus (Wechsler and Fields, 1978) and rabies virus (Naito and Matsumoto, 1978). The M protein of paramyxoviruses was also shown to interact with cellular actin (Giuffre et al., 1982). Later studies with cytochalasin B, a drug which inhibits actin polymerisation, prevented the release of infectious measles virus in a manner that was not related to a defect in glycosylation (as cytochalasin B also affects protein glycosylation) (Stallcup et al., 1983). It was later suggested that actin filaments are involved in the formation of viral buds at the plasma membrane, as actin filaments were observed to protrude into measles particles, which were in the process of budding from the plasma membrane, with the barbed ends of the filaments in close association with the

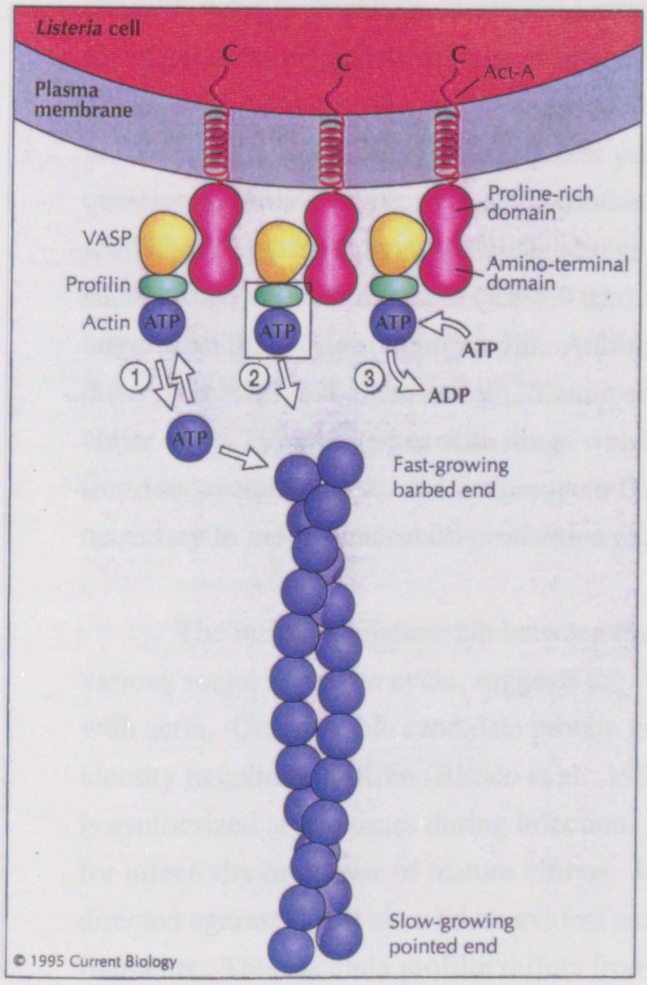


FIGURE 7: A model of actin assembly at the pole of Listeria. VASP forms a link between Act A bound to the bacterial cell surface and profilin which concentrates profilin at the assembly site. Profilin may promote actin polymerization in three ways (i), by rapidly binding and dissociating actin, raising the local concentration of free actin subunits available for assembly, (ii), by providing actin-profilin complexes (boxed) to add directly to the barbed end of the actin filaments, followed by the dissociation of profilin, or (iii), by promoting nucleotide exchange on the actin subunits. (From Pollard, 1995)

nucleocapsids (Bohn et al., 1986). Therefore, it was hypothesized that the vectorial growth of actin filaments facilitated the budding of measles virions. Other viral systems where actin has been implicated in budding include paramyxoviruses (Giuffre et al., 1982) and frog virus 3 (Murti et al., 1985).

Several viruses have also been shown to interact with the actin cytoskeleton during the replication and transcription of their genomes in the nuclei of host cells (Charlton and Volkman, 1991; Ciampor, 1988; De et al., 1993; Luftig, 1982) and the actin cytoskeleton is also implicated in the transport of viral structural proteins (Bohn et al., 1986; Kasamatsu et al., 1983). Therefore actin plays a role in many different stages of virus assembly and maturation.

1.9 Vaccinia-actin interactions

To date, vaccinia is the best studied virus which has been shown to have close associations with the actin cytoskeleton. This was first observed by Stokes (1976) who

showed, using high voltage electron microscopy, that the migration of vaccinia virions from factories to the plasma membrane of infected cells involved an association with the host cell cytoplasmic network. He also demonstrated the presence of specialized microvilli with virus particles at the tip (Stokes, 1976). A few years later it was demonstrated that the filaments in question in Stokes' report were actin-containing microfilaments (Hiller et al., 1979). The specialised microvilli, conspicuously absent from uninfected cells, were characterized and shown to be variable in length (1.8-3.0 μm), with a constant diameter (0.30-0.35 μm), much larger than that of normal microvilli. Antibodies to myosin and tropomyosin failed to label these microvilli, but alpha-actinin, filamin and fimbrin were identified (Hiller et al., 1981; Hiller et al., 1979). Studies with drugs which arrest vaccinia assembly, such as sodium fluoride, cycloheximide, and actinomycin D, showed that virus particle formation is necessary to induce microvilli production (Krempien et al., 1981).

The intimate relationship between the actin cytoskeleton and vaccinia virus at the various stages of its life cycle, suggests the vaccinia may contain proteins which interact with actin. One possible candidate protein is the gene product of A42R that displays 31% identity to cellular profilin (Blasco et al., 1991). This viral profilin is a 15kD protein which is synthesized at late times during infection. Deletion of A42R showed that it is not required for infectivity or release of mature virions. Immunofluoresence studies with an antibody directed against A42R showed no evident association of vaccinia profilin with actin filaments. This vaccinia profilin differs from its cellular counterparts in that it has a higher affinity for phosphoinositides than for actin or polyproline, suggesting that it may rather play a role in cellular signalling (Machesky et al., 1994).

1.10 Thesis Aims

During the initial stages of my thesis, I set out to characterize the proteins in the virus which may play a role during the transition of the IV to the IMV. As one of the changes which occurs during this maturation step is a major shape rearrangement from a spherical IV to a parallelepiped or "brick" -shaped IMV, I began with the identification of the membrane proteins in the IMV, assuming that they play a structural role in this shape transition. Vaccinia membranes were separated from the viral cores using a combination of 1% NP 40 and 20mM DTT, a classical method used for this purpose (Easterbrook, 1966; Essani and Dales, 1979; Holowczak and Joklik, 1967; Oie and Ichihashi, 1981; Sarov and Joklik, 1972). The resultant sample was centrifuged through a 36% sucrose cushion, whereby the cores pelleted, while the viral membranes remained on top of the cushion. The membrane proteins were subsequently identified by peptide sequencing. After this NP 40 / DTT treatment, there

was one protein which behaved in an unusual manner in that it was present in both the membrane and core fractions, in variable proportions. Therefore I investigated this protein further, as due to its presence in both the membrane and core fractions, it was plausible that it could act as a possible link between the core and the surrounding membranes of the IMV. This protein is p39, gene A4L, and is the subject of chapter 2.

Nothing was known about how vaccinia moves in the cell or even if the associations between the virus and actin which have been reported (Hiller et al., 1981; Hiller et al., 1979; Krempien et al., 1981; Stokes, 1976) are sufficient to actually support viral movement. Therefore, during the later part of my thesis research, I examined the subject of both inter- and intracellular motility of vaccinia virus more thoroughly. I demonstrated that vaccinia-virus can co-opt the actin cytoskeleton of the host cell, in a manner not unlike *Listeria*, in order to move both within the cell and from one cell to another, in order to cause direct cell-to-cell spread of the disease. This work is presented in chapters 3 and 4.

CHAPTER 2

A Vaccinia Virus Core Protein, p39, is Membrane Associated

Submitted to the Journal of Virology

A Vaccinia Virus Core Protein, p39, is Membrane Associated.

Sally Cudmore[1], Rafael Blasco[2], Renaud Vincentelli[3], Beate Sodeik[1,4], Gareth Griffiths[1]*and Jacomine Krijnse Locker[1].

1 Cell Biology Programme, [3] Structures and Biocomputing Programme, European Molecular Biology Laboratory, Meyerhofstr. 1, D-69117 Heidelberg, Germany.

2 Centro de Investigacion en Sanidad Animal, INIA-MAPA, Valdeolmos, E28130 Madrid, Spain.

4 Present address : Department of Cell Biology, Yale University School of Medicine, New Haven, CT 06520-8002, USA

* To whom correspondence should be addressed:
Tel: (49) (6221) 387267
Fax: (49) (6221) 387306

ABBREVIATIONS

IV	Immature virus
IMV	Intracellular mature virus
p.i.	post-infection
NP 40	Nonidet P 40
DTT	Dithiothreitol
TX-114	Triton X-114
Rif	Rifampicin
PBS	Phosphate buffered saline
PNS	Post nuclear supernatant
MEM	Minimal essential medium
Na_2CO_3	Sodium carbonate

ABSTRACT

We describe the characterization of the product of the A4L gene of vaccinia virus, p39. Using immunolabelling of thawed cryosections from infected HeLa cells, we show that this protein is initially located in the central region, or "viroplasm", of the viral factories, as well as the immature virions (IV), with very low amounts of labelling observed on the surrounding membranes. The localization of p39 changes dramatically during the transition of the IV to the intracellular mature virus (IMV), coincident with the appearance of the core structure in the centre of the IMV, and it is now located between this core and the surrounding membranes. Complementary biochemical data, such as partitioning into Triton X-114 detergent phase and stripping of the viral membranes with Nonidet P 40 and dithiothreitol, suggest that p39 is strongly associated with the inner of the two membranes surrounding the core. Sodium carbonate treatment also indicates that p39 is associated with membranes, even at the early stages of viral assembly. However, following *in vitro* translation of p39 in the presence of microsomal membranes we failed to detect any membrane association of the independently expressed protein. We also failed to detect any post-translational acylation of p39 with myristate or palmitate, suggesting that p39 does not achieve its membrane association through lipid anchors. Therefore, p39 is most likely membrane-associated through an interaction with integral membrane protein(s) present in the inner of the two membranes surrounding the IMV. Together with our recent data showing that p39 co-localizes with the spike-like protrusions on the IMV core (47)(Roos et al., (1996) EMBO J., in press), we suggest that p39 may form part of this spike and possibly functions as matrix-like linker protein between the core and the inner of the two membranes surrounding the IMV.

INTRODUCTION

Vaccinia virus, the prototype member of the Poxviridae, has a 190kb dsDNA genome which has been completely sequenced (17, 24). This genome codes for 263 potential open reading frames, of which approximately 100 proteins are associated with the virus particle (12). The transcription and translation of these genes can be divided into three temporal classes ; early, intermediate and late (36, 41). The early genes are those which are transcribed prior to DNA replication, while the intermediate and late genes are only transcribed after the viral genome has been replicated. The vaccinia structural proteins are normally encoded by the late proteins (36).

Vaccinia virus assembly has been extensively studied by electron microscopy but little is known about the molecular events which take place during the assembly process. The first morphological evidence of the infection process is the appearance of large structures enriched in DNA (2, 20, 25) at about 1-2 hours post infection. These structures, which are also visible by light microscopy, referred to as "viral factories", are thought to be the site of viral DNA replication and transcription (2, 36, 37). The first sign of viral membrane assembly is the appearance of rigid, curved membrane structures referred to as "crescents", which appear to bud in the region of the viral factories. Once thought to be the only example of *de novo* membrane synthesis (5, 6, 59), it now appears that the first membranes of vaccinia are derived from a cisterna of the intermediate compartment between the rough endoplasmic reticulum and the Golgi complex (28, 53). These crescents, which are the progenitors of the immature virion (IV), normally appear as one membrane profile in electron micrographs but have been shown to consist of two tightly apposed membrane bilayers (53). The spherical shaped IV, after the packaging of the viral genome and cleavage of some of the core proteins (26, 27, 39, 49, 56, 57), develops a core structure surrounding the DNA and matures into the brick-shaped intracellular mature virus (IMV), the first of two distinct infectious forms.

There is a marked difference between the structure of the IV and the IMV. The IMV has two "membrane-like" profiles when viewed by both conventional thin sectioning and cryo electron microscopy, the innermost of these representing the newly formed core structure, while the outer profile is qualitatively the same as the two membranes surrounding the IV, i.e. it represents the two tightly apposed membranes derived from the intermediate compartment (47, 53). While the central region of the IV clearly consists of electron-dense material that can be labelled with antibodies to vaccinia core proteins (11, 54, 58) , it has not yet packaged the DNA and does not contain the

final internal core-structure (see e.g. (11). Nothing is known about either the origin or the composition of the inner "membrane-like" structure surrounding the DNA or how it is formed during the transition from IV to IMV. A possible explanation for the sudden appearance of the core during the assembly process may be that the insertion of the DNA into the IV (see (35), which coincides with the proteolytic cleavage of some of the major core proteins (26, 27, 39, 56, 57, 60), may lead to a rearrangement of these core proteins to form the core structure. Following this process, the IMV membranes appear brick-shaped, rather than spherical as they were in the IV. This change in shape is possibly caused by an interaction of one or several inner membrane protein(s) with components on the surface of the newly formed core.

In pioneering electron microscopic studies of IMV particles, Dales (1963) clearly showed the presence of spike-like protrusions extending between the core and the surrounding membranes, using a combination of thin sectioning and negative staining. In a more recent study, Dubochet et al. (1994) performed cryoelectron microscopy, a method that does not involve chemical fixation, dehydration or embedding techniques, on intact IMV as well as isolated vaccinia cores. Isolated cores are operationally defined as the particle which remains intact after treatment of IMV with Nonidet P-40 and a reducing agent such as dithiotreitol or β-mercaptoethanol (10, 43, 55). In these later studies, the spikes were clearly visualized on the outer surface of the isolated cores, as well as in untreated IMV. These data were extended by combining cryoelectron microscopy with immunogold labelling of antigens on the surface of the core (47), which suggested that these spike-like protrusions may be composed of p39, the focus of this paper.

p39 was first identified by Maa and Esteban (1987) as a highly antigenic protein that produced a strong immune response in mice and rabbits. They demonstrated that p39, a product of the late class of genes, is an acidic polypeptide which is present in the core. The protein was later identified as the product of the A4L gene and it was established that the C-terminal 103 amino acids were the most immunogenic region of the protein, eliciting an antibody response in vaccinated humans which persists for years (7). Due to both its location on the outside of the core and its abundance in virions, we suspected that p39 might play an important role during the transition of the IV to the IMV. We therefore attempted to establish a function for p39 during virion assembly and maturation. We propose that p39 plays a matrix-like role in the virion, acting as a link between the core and the surrounding membranes in the IMV.

MATERIALS AND METHODS

Cells, virus and antibodies: HeLa cells were grown and infected with vaccinia virus strain WR as previously described (53). Two different antibodies were used in the present study. First, we used the rabbit antiserum raised against p39 previously described by Demkowicz et al. (1992), a kind gift from M. Esteban. In addition, we made a new rabbit polyclonal. A peptide representing the C-terminal residues 267-281 of the protein product of gene A4L was synthesised (pI of 10.78), and was solubilized in PBS prior to covalent coupling to keyhole limpet hemocyanin. Rabbits were immunized in the popliteal lymph node on day 1 with 200μg of peptide in Freund's complete adjuvant (Sigma). They received subscapular boosts of 50μg peptide in Freund's incomplete adjuvant (Sigma) on days 21 and 42 and 50ml bleeds were taken 10 days after each boost. On day 63 the rabbits received an intramuscular boost of 25μg of peptide in phosphate-buffered saline (PBS) followed on 2 consecutive days by intravenous boosts of 25μg. Ten days later the animals were sacrificed and serum prepared. Western blot analysis showed that this peptide antibody recognised p39.

Metabolic labelling of virus and infected cells: Four 175 cm^2 flasks of subconfluent HeLa cells were infected at a MOI of 10. Two mCi of ^{35}S Express Methionine Cysteine (Du Pont, NEN, Boston, MA) in 20 mls of labelling medium (10% MEM containing 5% FCS; 90% methionine and cysteine free DMEM; Sigma) was added to the infected cells at 6 hours post-infection. After 24 hours of infection, the radioactive label was chased for 2 hours by replacing the labelling medium with MEM containing 5% FCS. The virus was purified using a 36% sucrose cushion, followed by a 15-40% sucrose gradient in a SW40 rotor (8). ^{35}S-labelled post-nuclear supernatant from infected cells was prepared as follows. HeLa cells were infected as above and incubated in MEM/FCS containing 100μg/ml of rifampicin (Sigma). The cells were labelled with 40μCi/ml of ^{35}SExpress from 6 to 8 hours post-infection in labelling medium and chased for one hour, still in the presence of rifampicin. Cells were then scraped from the dish in PBS-Ca^-, gently pelleted and resuspended in 10mM Tris-Cl, pH 9. The cells were broken by 10 to 12 strokes of a dounce homogenizer and the nuclei removed by centrifugation at 3000rpm for 10 mins. For the pulse-chase analysis, infected cells were pulse-labelled at 7 hours post-infection (p.i.) for 5 minutes with 100μCi/ml ^{35}SExpress and subsequently chased for the indicated times. The labelled cells were lysed as described (29), the lysates concentrated by acetone precipitation at -20°C and the precipitate dissolved in first dimension lysis buffer

(9.8M urea, 2% ampholines (Pharmacia, Uppsala, Sweden), pH 7-9, 4% NP-40 and 100mM DTT).

For preparation of PNS labelled with either ^{3}H-myristate or ^{3}H-palmitate (250μCi/ml of each) (13), the labelled lipids were added to infected cells, in D-MEM with 2% delipidated FCS, at 4h after infection.. PNS was prepared at 24h p.i., as described above. For ^{32}P-labelled PNS, infected cells were starved of phosphate for 30 minutes (in D-MEM without Na_2PO_4 containing 2% dialysed FCS) prior to adding 400μCi of ^{32}P at 6h p.i.. The labelled cells were harvested at 24h p.i. and a PNS prepared as described above. ^{3}H-glucosamine labelling was carried out in RPMI medium (glucose free) containing 2% dialysed FCS, 2mM glutamine and 10μg/ml glucose. 75mCi/ml of ^{3}H-glucosamine was added to a 3cm dish of cells at 4h p.i. and PNS was prepared at 24h p.i.. Immunoprecipitation with antibodies to p39 (7) or p21 (A17L) (28) was carried out as previously described (29) followed by analysis on 15% SDS-PAGE.

Protein microsequencing : Purified IMV was resolved on a 15% SDS-PAGE. After electrophoresis the gel was stained with Coomassie Brillant Blue (R250) and a band, which comigrated with p39 on western blots was excised. The gel piece was subjected to tryptic digestion, the peptides separated by HPLC and two resulting peptides were sequenced using Edman automated degradation (30). The two 7 amino acid sequences were used to search for homologies in the Swissprot data bank using Blitz, Brookhaven data bank, PIR and Swissprot using Blast, and Genbank and the EMBL Data Library using TFasta. These peptides are identical to amino acids 42-50 and 59-66 of the vaccinia WR strain A4L gene (AC P29191).

Immunofluorescence microscopy: Cells grown on coverslips were infected as described above and, following 3 washes in PBS, were fixed at 8h p.i. with 3% paraformaldehyde in CB (10mM MES, 150mM NaCl, 5mM EGTA, 5mM $MgCl_2$, 5mM glucose, pH 6.1) for 10 minutes at room temperature. Following 3 washes in CB, cells were permeabilised with 0.1% TX-100 for 60 seconds and then blocked with 1% FCS and 1% BSA for 10 minutes. The infected cells were labelled with the antiserum against the C-terminus of p39 (diluted 1: 300) for 30 minutes and subsequently incubated with FITC-conjugated goat anti-rabbit antibody (Dianova-immunotech GmBH, Germany) together with 5μg/ml Hoechst (No. 33258, Sigma) for 30 minutes. The coverslips were washed 3 times in CB, rinsed in distilled water and mounted on slides in moviol. The samples were examined with a Zeiss axiophot microscope.

Electron microscopy: For negatively stained samples, IMV was adsorbed to a glow-discharged, formvar- and carbon coated EM grid for 2 minutes. The sample on the grid was subsequently treated with either 1% NP-40 or 20mM DTT or both, for 30 minutes at 37°C. The IMV absorbed to the grid was also treated with either 50µg/ml proteinase K for 30 minutes on ice or 50µg/ml trypsin for 30 minutes at 37°C. Following 3 washes in 10mM Tris pH 9, the grids were incubated with 10% fetal calf serum in PBS and subsequently with primary antibody (p39 antiserum or a monoclonal antibody against p14 (mAbC3, 46) both from M. Esteban) diluted in 5% FCS-PBS for 15 minutes. In the case of p14 the labelling was followed by incubation with a rabbit anti-mouse antibody (Cappel, USA). Subsequently the grids were incubated for 15 minutes with 10nm protein-A gold and then briefly washed in triple distilled water before staining with 1.5% uranyl acetate for 60 seconds (52).

Cells which were infected for 8 h, and cells which were infected in the presence of rifampicin for 16 h, were fixed and prepared for cryo sectioning as previously described (18, 54). Purified IMV were prepared by pelleting at 14,000rpm in an eppendorf centrifuge and were then fixed with 4% paraformaldehyde and 0.1% glutareldehyde for 30 minutes. The pellet was subsequently infiltrated with 2.1M sucrose for 15 mins and rapidly frozen in liquid nitrogen. Immunolabelling of frozen hydrated cryosections was performed as previously described (48, 52, 53).

Protease treatment : Purified IMV was incubated on ice for 30 minutes with proteinase K (Merck, Darmstadt, Germany) at 5, 10, 20, 30, 50, 100, 200 and 300 µg/ml in 10mM Tris pH9.0 (made from a 1mg/ml stock solution in isopropanol, stored at -80°C). Reactions were stopped by the addition of PMSF (polymethylsulphonylfluoride; stock 10mM in isopropanol, stored at -20°C,Sigma) to a final concentration of 1mM. Purified virus was also treated with 50µg/ml of α-chymotrypsin (TLCK treated; Sigma; stock solution 1mg/ml, stored at -20°C), 100µg/ml of thermolysin (Boehringer, Mannheim; stock solution 10mg/ml in 20mM $CaCl_2$, stored at -20°C,) and 250µg/ml V8 (endoproteinase Glu-C, Boehringer; stock solution 10mg/ml, stored at -20°C). All incubations were carried out for 30 minutes at 37°C. The reactions were terminated by the addition of 3,4-dichloroisocoumarin to a final concentration of 0.1mM (stock solution 40mM, stored at -20°C; Boehringer) to the chymotrypsin and V8 treated samples and 5mM EDTA (ethylenedinitrolo tetraacetic acid, Merck) to the thermolysin sample. After digestion, the samples were immediately frozen in liquid nitrogen and stored at -20°C to prevent further digestion. All samples were heated for 3 minutes at 95°C in Laemmli sample buffer just prior to electrophoresis.

Detergent extraction and sodium carbonate treatment of IMV and PNS: Viral membranes were separated from the cores as described by Oie (1981) with the following modifications: virus was (i) disaggregated before treatment by a 30 sec sonication in a water bath sonicator, (ii) incubated with 1% NP-40 (Sigma) and 20mM DTT (Sigma) in 10mM Tris, pH9 rather than 100mM Tris pH 7.5. The incubation was carried out for 30 mins at 37°C with gentle shaking. The sample was then loaded on top of a 36% sucrose cushion and spun in an airfuge at 26psi for 30 mins to separate the membranes, which remained on top of the sucrose cushion, from the cores which pelleted. The cores were subsequently incubated with 0.5% deoxycholate (DOC, Sigma) and 0.5% sodium dodecyl sulphate (SDS, Serva) at 56°C for 10 min to ensure solubilization prior to adding Laemmli sample buffer.
For the TX-114 extraction (1), following a brief sonication, intact virus was solubilized in an equal volume of 2% TX-114 in 300mM NaCl, 1mM DTT and 10mM Tris pH 10. An additional 400 µl of 1% TX-114 and 150mM NaCl in 10mM Tris, pH 9was added and the mixture was incubated at 37°C for 15 minutes followed by 20 minutes at 4°C and centrifuged for 2 minutes at 14,000rpm to separate the phases. Both phases were subjected to a second round of TX-114 extraction. TX-114 extraction of radiolabelled post-nuclear supernatants from cells infected in the presence of rifampicin (see above) was performed in the same way, with the exception that the DTT was omitted. For the Na_2CO_3 extraction of post-nuclear supernatants from cells infected in the presence of rifampicin, the pH of the sample was adjusted to pH 11 by the addition of an equal volume of 200mM Na_2CO_3. The sample was incubated for 30 minutes on ice and then spun at 150,000xg (Beckman TLA100 rotor) to pellet the membranes. All samples were concentrated by acetone precipitation at -20°C and the pellet dissolved in Laemmli sample buffer or first dimension lysis buffer prior to electrophoresis.

Cloning, transfection and *in vitro* translation of A4L : Gene A4L from vaccinia strain WR was PCR amplified using the following primers ;
TCGGAATTCAATTTTAAAGC (EcoRI site underlined) and
TTTACTCGAAAAGCTTGATT (HindIII site underlined). It was then digested with EcoRI and HindIII and inserted into plasmid pGEM7. P39 was transcribed and translated *in vitro* using pGEMA4L and a coupled T7-driven transcription/translation system (Promega) according to the instructions of the manufacturer. When dog pancreas microsomes (a kind gift from K. Schroeder and B. Dobberstein) were used, they were added at 100 OD_{280} units per translation. To remove endogenous mRNAs, the microsomes were treated with micrococcal nuclease (Sigma) before translation (Krijnse Locker et al., submitted). Soluble p39 was separated from (putative)

membrane bound protein by pelleting the membranes in a Beckman airfuge through a cushion of 0.5M sucrose in RM-buffer (50mM Hepes-KOH, pH 7.5, 50mM KOAC, 2mM MgAc, 1mM DTT) for 10 minutes at 24 psi. All fractions were diluted in 500µl of detergent solution, and SDS was added to a final concentration of 0.2% along with 2µl of the anti-p39 antibody. The subsequent immunoprecipitation steps (as described in (29) were followed by analysis on 15% SDS-PAGE.
For the transient expression in HeLa cells, A4L was cloned into the pCMUII plasmid (a kind gift from Tommy Nilsson; (45) using XbaI and BAMHI. As the A4L sequence contained both these restriction sites a two step cloning was performed. First the 5' region of A4L was inserted into pCMUII using XbaI digested pGEMA4L. Similarly the 3' end of A4L was digested from pGEMA4L and insertion of A4L into pCMUII was completed to generate the vector pCMUIIA4L. Transient transfection was then performed according to Pääbo et al. (1986) using pCMUIIA4L and cells were fixed at 48 hours post-transfection and immunolabelled as described above.

Gel electrophoresis and western blotting: Proteins were separated using standard SDS-polyacrylamide gel electrophoresis (SDS PAGE) (32) with a 15% resolution gel and a 4% stacking gel. Samples were incubated in Laemmli sample buffer containing 1% SDS and 0.5% ß-mercaptoethanol for 5 mins at 95°C. In some experiments, samples dissolved in first dimension lysis buffer were subjected to 2D gel analysis using a Biorad (Richmond, CA) mini 2D gel system. Samples were separated by isoelectric focusing (IEF) from pH 4.0 to pH 7.0 in the first dimension and 15% SDS PAGE in the second dimension. The gels were either fluorographed using Entensify (Du Pont de Nemours, Brussels, Belgium) or electrophoretically transferred to nitrocellulose membranes for immuno-blotting, using the BioRad semi-dry transfer system. The nitrocellulose was blocked in PBS with 0.2% Tween 20 and 5% non-fat skim milk (PBS-T milk) overnight at 4°C prior to incubation with anti-p39 serum diluted 1:10,000 in PBS-T milk. The nitrocellulose was then incubated with horseradish peroxidase tagged goat anti-rabbit antibody (Biorad). Antibody was detected by ECL (Amersham Life Sciences, England).

Gel filtration: *In vitro* translated p39 was resolved by high performance size-exclusion chromatography (HPSEC, Gilson ,France). The 5 µm TSKG2000 SWXL column (Toyosoda Inc., Japan) was precalibrated with a mixture of gel filtration molecular weight standards (ferritin, 440kD; catalase, 232kD; bovine serum albumin, 66kD; carbonic anhydrase, 29kD and cytochrome c, 12.4kD). The column was then pre-equilibrated with 50mM Na_2PO_4 and 100mMKCl, pH7.4, and 1µl of sample was injected into the column.

RESULTS:

Identification of p39 (A4L) and synthesis of antibodies : As a first step towards the characterization of p39, we decided to ensure its identity by peptide sequencing. A 43kD band, reactive by immunoblot with the antiserum raised against the complete p39 (7), was excised from an SDS polyacrylamide gel and sequenced using Edman degradation. Two peptides were found that showed a 100% homology to the gene product of the vaccinia WR A4L open reading frame. This protein has a predicted molecular weight of 30.9kD but, since it has been previously referred to as p39 due to its mobility on gels (7, 33), we adhere to this terminology throughout this paper. To facilitate further characterization studies, we raised a COOH-terminal peptide antibody against residues 267 to 281 of p39 which also recognised p39 on western blots (data not shown).

p39 labels viral factories by immunofluorescence microscopy: We first investigated the localization of p39 in infected cells at the light microscopy level. Infected HeLa cells were fixed at 8 hours post infection and labelled with the COOH-terminal specific peptide antiserum. As can be seen from figure 1, clear labelling of structures in the peri-nuclear region of the cell could be detected. This labelling co-localized with the viral DNA factories which were identified by Hoechst-staining (arrowheads in fig. 1b). In addition, p39 antiserum decorated punctate structures throughout the cell, which probably represent individual virus particles (arrows in fig. 1a).

Electron microscopy localisation of p39: A more precise localization of p39 throughout the different stages of viral assembly was subsequently carried out using immunolabelling of thawed cryosections from aldehyde fixed infected cells. The earliest viral structures to appear in infected cells are termed viral factories (2, 20, 25) (F in fig. 2a). These electron dense structures, which are predominantly found in the peri-nuclear region, labelled strongly with antibodies against p39 in their central region. From these viral factories crescent shaped membranes develop (fig. 2a). p39 was preferentially associated with the viroplasm underlying these membranes, with a very low amount of label occasionally visible on the membranes themselves (arrows in 2a). These "crescents" eventually form IVs (fig. 2b) which labelled throughout the electron-dense viroplasm with anti-p39 antibodies. The labelling with anti-p39 at these different early stages of assembly resembles the pattern that is seen with antibodies against vaccinia-core proteins, such as p4a or p65 (11, 54, 58).

As the virus particles mature to form IMV (IMV in figs. 2b and g), the p39 labelling was found predominantly in the space between the newly developed core structure and the outer IMV membranes, i.e. in the space between the two visible IMV membrane profiles (see introduction). Panels c to h of figure 2 depict what we believe to be the different stages of viral assembly with p39 labelling. Figures 2c and 2d show developing IVs. The "viroplasm", which is being present in these structures, labels strongly with anti-p39. These IVs have not yet packaged the DNA which is visible above the virion in figure 2d and is clearly devoid of any labelling (arrowhead in 2d). Figure 2e shows an IV which has packaged its DNA, which is visible to one side of the particle (arrowhead). A transitional intermediate between the IV and the IMV is shown in figure 2f, where the core structure is beginning to form. At this stage of development, p39 appears to be excluded from the centre of the developing core and is found in the space between this and the surrounding IMV membranes. The IMV (fig. 2g) and IEV (fig. 2h) show a similar labelling pattern, with labelling of the space between the core and the surrounding membranes.

We also investigated the localization of p39 in cells which were infected in the presence of rifampicin, which blocks viral assembly prior to the IV-stage (19, 38, 42),. When cells were infected in the presence of rifampicin, typical electron dense structures called rifampicin bodies (RB in fig. 3a) were observed in the cytoplasm close to the nucleus (N in 3a) (19, 42, 54). As for the viral factories, the rifampicin bodies were strongly and uniformly labelled throughout by antibodies against p39. These rifampicin bodies were surrounded by membrane structures which, after release of the rifampicin block, formed the characteristic crescent shaped membranes (stars in fig. 3b). There was only a very low amount of p39 labelling on these membranes (within the ≈20nm resolution of this labelling method, (18), whereas the core material labelled very strongly. As maturation continued the IVs developed (fig. 3b), the viroplasm of which labelled strongly with p39. In addition to the rifampicin bodies, another especially distinct structure can be observed in cells infected in the presence of rifampicin. These are crystalline-like arrangements of DNA (D in figs. 3a and b), which are prevented from packaging into virions due to the rifampicin block. Consequently they accumulate into crystalline arrays which are much larger than those seen in normally infected cells. These rifampicin-induced periodic DNA structures were also devoid of any p39 labelling.

The localization of p39 in the IMVs was subjected to a closer inspection by processing purified IMV for cryosectioning and subsequent immunolabelling with anti-p39 (fig. 3c). In these sectioned particles, spike-like

protrusions, which have been previously described (4, 9, 47) can be seen to extend outwards from the internal core structure (arrowheads in 3c). The structure, composition and function of these spikes is unknown. Recent evidence makes it conceivable that the spikes may in part be composed of p39 (47) and the co-localization of the p39 labelling with the spikes in figure 3c further support this possibility. In some views of the purified IMV particles, the whole virion labels with p39, but this is probably due to the plane of the section through the virus particle, as any particle which is sectioned between the core and the membranes may label all over this accessible surface.

Immunolabelling of intact and treated IMV particles : In order to confirm the localization of p39, electron microscopic experiments were performed, in which purified IMV preparations were subjected to different treatments on the EM grids, followed by immunolabelling and negative staining. Intact IMV particles did not label significantly with antibodies against p39 (fig. 4a). This is in stark contrast to the labelling obtained for another vaccinia protein, p14 (A27L; fig. 4b), previously described as being exposed on the outside of the virion (52). As can be seen from table 1, intact IMV labelled with anti-p39 only occasionally, with less than 1 gold particle per virion. A small proportion of particles which were disrupted by the preparation also labelled strongly (data not shown). On treatment of the particles with NP-40 and DTT, a classical method used to remove IMV membranes (10, 43), the labelling with p39 increased dramatically (inset in fig. 4a), while p14 labelling was lost (inset in fig. 4b).

The data in table 1 show the corresponding numerical values for the p39 labelling. When viral particles were treated with NP 40 alone, there was very little increase in labelling. However, treatment with DTT alone caused a significant increase in the number of gold particles per virion. This is in agreement with other data using a novel cryo electron microscopy immunolabelling procedure which showed that DTT alone is sufficient to cause a dramatic loosening of the membranes surrounding the IMV (47). In this process the core became exposed and labelled strongly on its outside with antibodies to p39. In our experiments, a combination of both NP 40 and DTT caused an almost 500-fold increase in labelling relative to the untreated control, indicating that p39 is associated with the external surface of the core structure.

p39 is protected from protease digestion in intact IMV particles : We confirmed the internal location of p39 by carrying out experiments in which intact purified IMV were treated with different proteases. Virions were incubated with increasing

concentrations of proteinase K from 5 to 300µg/ml for 30 minutes on ice. Under these conditions, even the highest concentrations of proteinase K did not cause any digestion of p39, while two membrane proteins which are exposed on the outside of the IMV, p32 (D8L) and p14 (A27L) (52), were completely digested (fig. 5a). Other core proteins such as 4a/4b (A10L and A3L) and p11 (F18R) were also protected. Additional proteases, chymotrypsin and thermolysin, failed to digest p39, while they removed p32 and p14 from the outside of the virion (fig. 5b). V8 had no effect, even on these latter membrane proteins. When longer incubation times of 2 hours were used, the core proteins were eventually digested (results not shown), in agreement with our previous studies (47). When NP40 and DTT isolated cores were treated with protease for 30 minutes, the particles were completely digested (ascertained by electron microscopy), and there were no polypeptide bands, other than small digestion products, remaining on the gel (data not shown).

p39 associates with viral membranes: Kyte and Doolittle hydrophobicity plots of the p39 sequence show that it does not have any hydrophobic sequence typical of membrane spanning proteins, i.e. a stretch of 17 to 22 hydrophobic amino acids that may adopt an alpha helical structure but, data in the literature showed that a small amount of p39 was found in the membrane fraction after NP 40 and DTT treatment (33). Therefore we decided to undertake a detailed biochemical characterization of p39. We used a number of different criteria which are widely used to categorize the physical properties of proteins. First, the membrane proteins of purified IMV were extracted using a classical method for vaccinia virus which involves removal of the viral membranes using a combination of 1% NP 40 and 20mM DTT, along with some modifications which improved the extraction of membrane proteins, such as p32 (see Materials and Methods). Following this treatment, about 60% of p39 remained with the core fraction while the remaining 40% was in the membrane fraction (fig. 6a). As expected, the core proteins 4a, 4b, p25 and p11 were present exclusively in the core fraction. The extraction of p39 was highly variable and in some experiments the majority of p39 was found in the membrane fraction. When separated on 2D gels (fig. 6b), the p39 pattern appeared complex as the protein was resolved into a number of different spots, the identity of which were confirmed by western blotting (data not shown). This pattern is very similar to that seen in 2D gels by Oie and Ichihashi (1981), where this protein is referred to as p37.

In another series of experiments, purified IMV were subjected to treatment with TX-114. Following phase separation, TX-114 separates proteins predominantly according to their hydrophobicity, with hydrophobic proteins tending to partition into the detergent phase and hydrophilic proteins into the aqueous phase (1).

Since membrane proteins contain hydrophobic sequences that anchor them in the membrane, this phase separation can be operationally used to separate membrane proteins from soluble proteins. Using this extraction technique, p39 was found completely in the detergent phase indicating that it behaves more like a membrane protein (fig. 6c, lane 7). In order to study its behaviour in the absence of IMV formation, cells were infected in the presence of rifampicin to block virus assembly. Post-nuclear supernatants from these cells were treated with TX-114. Again, p39 was found exclusively in the detergent phase, as was p32 (D8L) which has been previously described as a membrane protein (52) (fig. 6c lane 3). These results were unexpected due to the predicted hydrophilic nature of p39 by the Kyte and Doolittle algorithm.

In order to further characterize the membrane association of p39, post-nuclear supernatants from rifampicin-blocked, infected cells were treated with Na_2CO_3. This treatment is typically used to establish whether proteins are associated with membranes in a peripheral or integral manner (15). The sample was adjusted to pH 11 by adding an equal volume of 0.2M Na_2CO_3, which removes the peripherally associated and luminal proteins, after which the membranes, along with their integral proteins, were separated from the soluble proteins by centrifugation. In such experiments, approximately 60% of p39 was found associated with the pelleted membrane fraction (fig. 6c lane 5), while the remainder was present in the supernatant (fig. 6c lane 4).

When isolated IMV were subjected to a single round of solubilization with 7M urea for 60 minutes at 37°C, approximately 30% of p39 was extracted, despite the fact that most of the membrane proteins, with the exception of p14 (A27L), a soluble, peripheral membrane protein, and a protein with a molecular weight of approximately 60kD, remained in the virion (not shown).

***In vitro* and *in vivo* translation studies show that p39 is not an integral membrane protein:** The biochemical results encouraged us to further investigate the membrane association of p39. In order to ascertain by an independent approach whether p39 is an integral membrane protein or merely peripherally associated with membranes, for instance via protein-protein interactions, the gene for p39, A4L, was cloned and inserted into the pGEM vector under the control of the T7 promoter in order to carry out *in vitro* translation and membrane translocation experiments. Upon *in vitro* translation and immunoprecipitation with antibodies to p39, three bands could be detected, the most prominent of which (upper bands in fig. 7) co-migrated with p39 immunoprecipitated from IMV (fig. 7 lane 7). The faster migrating species are possibly due to incomplete translation products . When in vitro translated p39 was treated with TX-114, most of the protein was found in the detergent phase (fig. 7, lane

2) showing, again, that p39 behaves as a "hydrophobic" protein, even in the absence of other viral proteins. When microsomes were added to the translation system at the beginning of the reaction, p39 failed to insert into these membranes suggesting that it is not a typical endoplasmic reticulum-synthesised integral membrane protein (fig. 7,lane 5).

p39 was also expressed transiently in HeLa cells using pCMUII to transfect the A4L gene. In transfected cells, p39 gave a predominantly cytosolic staining pattern. However, as this labelling was very strong, it could not be ruled out that some underlying membrane-like labelling was also present (fig. 8a). Further studies at the ultrastructural level will be needed to establish this point.

We also investigated whether the membrane association of p39 could be accounted for by fatty acid acylation. However, metabolic labelling with ^{3}H-palmitate or ^{3}H-myristate, followed by immunoprecipitation with anti-p39, indicated that p39 was not modified by the addition of fatty acids (results not shown). However, immunoprecipitation experiments with p39 showed that a number of other proteins were co-immunoprecipitated, with three of these especially abundant (fig 9a, lane 6). One of these proteins was identified as p21 (gene A17L) by immunoprecipitation with antibodies against the C-terminal region of this protein (fig 9a, lane 7) (28). This is an integral membrane protein which is present in the inner membrane surrounding the IMV (28). The identity of the other bands remains to be established.

Is p39 glycosylated ? As early as 1940 it was suggested by Smadel et al. (1940) that a vaccinia virus, heat stable, basic protein contained small amounts of glucosamine (50). Moreover, a number of different groups have reported the presence of a glycoprotein with an electrophoretic mobility of 37-40kD (16, 22, 23, 40, 44). This protein, which can be completely extracted from virions by two rounds of urea extraction (23, 43), has not yet been identified and therefore we investigated whether p39, which has a similar mobility, could be this glycoprotein. When infected cells were labelled with ^{3}H-glucosamine, the radiolabelled sugar which was reported in the previous studies, a faint band of very similar molecular weight was found (fig 9a, lane 1), but unfortunately was no longer detectable when combined with immunoprecipitation with anti-p39 antibodies (fig 9a, lane 3). Also when IMV was subjected to blotting with a monoclonal antibody specific for the O-linked N-acetyl glucosamine modification (51), a modification that is commonly seen in an ever increasing list of cytoplasmic proteins (21), a protein which corresponded in molecular weight to p39 was detected (data not shown). However, these results were not reproducible and so we cannot unequivocally conclude whether or not p39 is

modified by the addition of O-linked N-acetyl glucosamine residues. Thus our results still leave open the possibility that p39 represents the glycoprotein first described by Smadel et al (1940) and further characterized by Holowczak (1970), Garon and Moss (1971) , Moss et al. (1973), Ichihashi and Oie (1980) and Oie and Ichihashi (1987).

As most of the proteins which posess this cytoplasmic O-linked sugar are also phosphorylated (21), we also investigated whether p39 was phosphorylated. While a number of viral proteins were labelled by ^{32}Phosphate, immunoprecipitation of p39 from the ^{32}P labelled virus preparation failed to yield any band suggesting that p39 is not phosphorylated (results not shown). We also tested for N-linked glycosylation by infecting the cells in the presence of tunicamycin, a N-glycosylation inhibitor, followed by immunoprecipitation with anti-p39. There was no apparent shift in molecular weight of p39 synthesised in the presence of the drug (fig 9a, lane 5) suggesting that it is not post-translationally modified by N-glycosylation.

Pulse chase experiments : p39 showed a pattern of multiple polypeptides on a 2D gel, similar to the pattern observed by Oie and Ichihashi (1981, referred to as p37). We next investigated if these different forms were synthesized in a temporal fashion during viral infection by performing pulse-chase labelling experiments followed by separation on 2D gels. In these experiments the different forms of p39 indeed appeared at different stages during the viral maturation. These different migrating forms have been numbered 1 to 6 in fig 9d. The larger central form (no. 1) appeared first and was seen after a 5 minute pulse with a very faint trace of 5 and 6 (fig. 10a). After a 30 minute chase a fourth form (no. 2) appeared (fig. 10b). Two further species (nos. 3 and 4) were apparent after 60 minute chase (fig. 10c) with little change in the pattern after 120 minutes chase (fig. 10d).

p39 does not form oligomers *in vitro* : The spike-like structure, observed between the membranes and the core in the IMV by all electron microscopic techniques, is approximately 20nm in length. Therefore, if p39, does form part of this spike, it would most likely need to oligomerize, either forming homo-oligomers or hetero-oligomers with other core proteins. In order to find out if p39 forms homo-oligomers and to obtain a more accurate measure of the apparent molecular weight, *in vitro* translated p39 was subjected to high performance size-exclusion chromatography. As can be seen in figure 11, p39 behaved as a monomer, eluting from the column with a molecular weight corresponding to 41.5 (+/- 5%). The peak at 16.3 minutes, which is less than 1% of the total protein, corresponds to a molecular weight of 122kD (+/- 5%). However, it was confirmed that this peak did not correspond to p39, as the

A_{280nm}/A_{220nm} ratio was different. Two other smaller peaks of less than 10kD were also eluted. This data indicates that p39 does not form homo-oligomers *in vitro*. These experiments were very difficult to perform on *in vivo* synthesised protein as p39 cannot be isolated from virions or infected cells without the use of detergent and a reducing agent, both of which could disrupt any potential oligomerization. Therefore it remains possible that p39 may form homo-oligomers, or even hetero-oligomers, in the virus.

DISCUSSION :

The gene product of A4L, a late vaccinia gene, has been previously described as a core protein (33). The amino acid sequence of this protein indicates a predicted molecular weight of 30.9kD, but it migrates anomalously on SDS gels at a position of 39kD and was therefore referred to as p39 in previous studies (7, 33, 46). It has an unusually high proline content of 30 residues, concentrated mainly in the central region of the protein, which account for 10.6% of the entire protein. From sequence analysis there are also a number of internal repeats in p39 which could indicate gene duplication. It has a predominantly hydrophilic nature as determined by the Kyte and Doolittle algorithm (31) and does not posses a long stretch of hydrophobic amino acids, which protein prediction (PhD prediction of secondary structure, EMBL) indicates could form a putative membrane-spanning alpha helix. Sequence comparison (Blast programme, NIH) suggests that p39 has some homology with proteins which have a coiled-coil structure, such as eutrophin and myosins.

We investigated the localization of p39 throughout the early assembly stages of vaccinia using immunogold labelling of cryosections. p39 labels the viral factories very strongly and also the central region of the IVs, in a manner which resembles the more typical core proteins, such as p4a (11, 58), with only a very low amount of membrane association apparent. However, the Na_2CO_3 experiments indicate that a significant amount of p39 is associated with membranes in cells which were infected in the presence of rifampicin, showing that even before virion assembly has commenced p39 attains a certain degree of membrane association. Upon transition of the IV to the IMV, the pattern of p39 labelling changes dramatically. In the IMV, p39 is located between the two membrane profiles, which are apparent in electron micrographs (fig 2b,g and 3c). According to our current interpretation of the IMV structure (see introduction), this would mean that p39 is present in the space between the core and the inner of the two tightly apposed membranes. In this model p32 (D8L) is located in the outer of the two membranes (52) while p21 (A17L) is an

integral protein of the inner membrane (28). This interpretation of the IMV structure is supported by the fact that when isolated IMV are treated with DTT alone, the cisternal membranes surrounding the IMV are loosened and begin to come off the virus as one continuous membrane sheath, thereby exposing the underlying core (47). This fact could also explain why p39, a core-associated protein, produces a strong humoral immune response in humans (7, 34), as when the virus particles are disrupted in any way, the highly abundant p39 is readily exposed on the outside of the cores. Upon DTT treatment of the IMV, spike-like structures which are present between the outer surface of the core and the surrounding membranes of the IMV (4, 9) become exposed and recent work suggested that p39 might be a component of these spikes (47). All our electron microscopy results further support this possibility as both chemically prepared cores, as well as "natural" cores which arise during vaccinia entry into cells (Snijder et al, manuscript in preparation), are labelled by anti-p39 on their external surface where the spikes are exposed.

On our gels, p39 had a molecular weight of 43k which is even higher than the 39kD previously reported (7, 33, 46), and when ascertained by gel filtration, the molecular weight of the native protein was 41kD. It is difficult to reconcile such a large discrepancy between the predicted molecular weight of 30.9kD and the apparent molecular weight, even by co- or post-translational modifications. Radiolabelling experiments with ^{32}P, ^{3}H-myristate and ^{3}H-palmitate indicated that p39 is neither modified by fatty acid acylation nor by phosphorylation. We also showed that this protein is not modified by the addition of N-linked oligosaccharides. However, there was an indication that p39 may be glycosylated by the addition of N-acetyl glucosamine, suggesting that it may be the glycoprotein reported by (16, 22, 23, 40, 43), but due to the very low levels of ^{3}H-glucosamine which were incorporated, this point will need further investigation. Therefore, the aberrant migration of p39 on denaturing gels cannot be reconciled by co- or post-translational modifications, but may in part be due to the high number of proline residues.

Although our detailed sequence analysis failed to reveal a typical membrane spanning region, our biochemical data show that p39 has many physical characteristics typical of a membrane protein. Therefore, we investigated the possibility that p39 may be membrane-associated through the addition of a lipid moiety. It has indeed been shown that a number of vaccinia proteins can be acylated by the addition of palmitate or myristate (3, 13, 14). Albeit, the membrane association of p39 cannot be accounted for by a myristate of palmitate anchor, as the protein does not label with either ^{3}H-myristate or ^{3}H-palmitate. Moreover, *in vitro* translation and translocation

experiments indicate the protein does not associate with rough endoplasmic reticulum membranes. Therefore, we postulate that p39 attains its membrane association through interaction with other viral membrane protein(s) in the inner of the two membranes surrounding the IMV. Co-immunoprecipitation experiments suggest that p21 (A17L) could possibly interact with p39. We have recently identified p21 as an integral protein in the inner membrane of the IMV which spans this membrane four times, with both the N- and C-termini exposed on membrane surface which faces the core (28). Thus, the N- or C-terminal regions of p21, as well as the loop region between residues 98 and118, are ideally located to interact with p39.

Collectively, our data suggest the following model for p39 in the context of vaccinia assembly. We propose that p39 is synthesised on free ribosomes in the cytosol and is then transported to the viral factories, as it labels the "viroplasm" of these factories. It is packaged into the IV, apparently as part of this material, possibly facilitated by its association with viral membranes even at this early stage (as suggested by the Na_2CO_3 extraction of membranes from cells infected in the presence of rifampicin) and, subsequently, is predominantly located in their central region. However during transition to the IMV, a new internal core structure develops and p39 is now located in the space between this newly formed core and the surrounding cisternal envelope, an ideal position to act as a matrix protein and to make the link between the core structure and the surrounding membranes. The identity of the spike-like structures, long seen on the surface of the core, must be further investigated in order to establish if p39, possibly along with other proteins, is a structural component of this spike.

ACKNOWLEDGEMENTS:

We would like to thank R. Jacob for peptide synthesis, R. Kellner for peptide sequencing, M. Esteban for the generous gift of the polyclonal anti-p39 antibody and the mAbC3 against p14, L. Gerace for the antibody against the O-linked sugar motif, T. Nilsson for the gift of the pCMUII plasmid and B. Dobberstein and K. Schroeder for providing the microsomes as well as technical advice. We would also like to thank A. Sawyer for advice concerning antibody production and G. Vriend for discussions about the sequence of p39.

REFERENCES:

1. **Bordier, C.** 1981. Phase separation of integral membrane proteins in Triton X 114 solution. J.B.C. **256**:1604-1607.

2. **Cairns, J.** 1960. The initiation of vaccinia infection. Virology. **11**:603-623.

3. **Child, S. J., and D. E. Hruby.** 1992. Evidence for multiple species of vaccinia virus-encoded palmitylated proteins. Virology. **191**:262-271.

4. **Dales, S.** 1963. The uptake and development of vaccinia virus in strain L cells followed with labeled viral deoxyribonucleic acid. J. Cell Biol. **18**:51-72.

5. **Dales, S., and E. H. Mossbach.** 1968. Vaccinia as a model for membrane biogenesis. Virology. **35**:564-583.

6. **Dales, S., and B. G. T. Pogo.** 1981. Biology of poxviruses. Springer-Verlag, Wien/New York.

7. **Demkowicz, W. E., J. S. Maa, and M. Esteban.** 1992. Identification and characterization of vaccinia virus genes encoding proteins that are highly antigenic in animals and are immunodominant in vaccinated humans. J. Virol. **66**:386-398.

8. **Doms, R. W., R. Blumenthal, and B. Moss.** 1990. Fusion of intracellular- and extracellular forms of vaccinia virus with the cell membrane. J. Virol. **64**:4884-4892.

9. **Dubochet, J., M. Adrian, K. Richter, J. Garces, and R. Wittek.** 1994. Structure of intracellular mature vaccinia virus observed by cryoelectron microscopy. J. Virol. **68**:1935-1941.

10. **Easterbrook, K. B.** 1966. Controlled degradation of vaccinia virions *in vitro*: an electron microscopic study. J. Ultrastruct. Res. **14**:484-496.

11. **Ericsson, M., S. Cudmore, S. Shuman, R. Condit, C., G. Griffiths, and J. Krijnse Locker.** 1995. Characterization of ts16, a temperature-sensitive mutant of vaccinia virus. J. Virol. **69**:7072-7086.

12. **Essani, K., and S. Dales.** 1979. Biogenesis of vaccinia: evidence for more than 100 polypeptides in the virion. Virology. **95**:385-94.

13. **Franke, C. A., P. L. Reynolds, and D. E. Hruby.** 1989. Fatty acid acylation of vaccinia virus proteins. J. Virol. **63**:4285-4291.

14. **Franke, C. A., E. M. Wilson, and D. E. Hruby.** 1990. Use of a cell-free system to identify the vaccinia virus L1R gene product as the major late myristylated virion protein M25. J. Virol. **64**:5988-5996.

15. **Fujiki, Y., A. Hubbard, L., S. Fowler, and P. Lazarov, B.** 1982. Isolation of intracellular membranes by means of sodium carbonate treatment. Application to endoplasmic reticulum. J.C.B. **93**:97-102.

16. **Garon, C. F., and B. Moss.** 1971. Glycoprotein synthesis in cells infected with vaccinia virus. II. A glycoprotein component of the virion. Virology. **46**:223-246.

17. **Goebel, S. J., G. P. Johnson, M. E. Perkus, S. W. Davis, J. P. Winslow, and E. Paoletti.** 1990. The complete DNA sequence of vaccinia virus. Virology. **179**:247-266.

18. **Griffiths, G.** 1993. Fine Structure Immunocytochemistry. Springer Verlag. Heidelberg.

19. **Grimley, P. M., E. N. Rosenblum, S. J. Mims, and B. Moss.** 1970. Interruption by rifampin of an early stage in vaccinia virus morphogenesis: Accumulation of membranes which are precursors of virus envelopes. J. Virol. **6**:519-533.

20. **Harford, C. G., A. Hamlin, and E. Riders.** 1966. Electron microscopic autoradiography of DNA synthesis in cells infected with vaccinia virus. Exp. Cell Res. **42**:50-57.

21. **Hart, G., W.** 1992. Glycosylation. Curr. Op. Cell Biol. **4**:1017-1023.

22. **Holowczak, J. A.** 1970. Glycopeptides of vaccinia virus. I. Preliminary characterization and hexosamine content. Virology. **42**:87-99.

23. **Ichihashi, Y., and M. Oie.** 1980. Adsorption and penetration of the trypsinized vaccinia virion. Virology. **101**:50-60.

24. **Johnson, G., P., S. Goebel, J., and E. Paoletti.** 1993. An update on the vaccinia virus sequence. Virol. **196**:381-401.

25. **Joklik, W. K., and Y. Becker.** 1964. The replication and coating of vaccinia DNA. J. Mol. Biol. **10**:452-474.

26. **Katz, E., and B. Moss.** 1970. Formation of a vaccinia virus structural polypeptide from a high molecular weight precursor: Inhibition by rifampicin. Proc. Natl. Acad. Sci. USA. **66**:677-684.

27. **Katz, E., and B. Moss.** 1970. Vaccinia virus structural polypeptide derived from a high-molecular-weight precursor: Formation and integration into virus particles. J. Virol. **6**:717-726.

28. **Krijnse Locker, J., S. Schleich, D. Rodriguez, B. Goud, G. Vriend, E. Snijder, and G. Griffiths.** The role of a 21kDa viral membrane protein in the assembly of vaccinia virus from the intermediate compartment. Submitted for publication.

29. **Krijnse-Locker, J., J. K. Rose, M. C. Hornizek, and P. J. M. Rottier.** 1992. Membrane Assembly of the triple-spanning Coronavirus M Protein - Individual transmembrane domains show preferred orientation. J. Biol. Chem. **in press**.

30. **Kurzchalia, T., V., J. Gorvel, P., P. Dupree, R. Parton, R. Kellner, T. Houthaeve, J. Gruenberg, and K. Simons.** 1992. Interaction of rab 5 with cytosolic proteins. J. Biol. Chem. **267:**18419-18423.

31. **Kyte, J., and R. Doolittle, F.** 1982. A simple method for displaying the hydropathic character of a protein. J. Mol. Biol. **157:**105-132.

32. **Lämmli, U. K.** 1970. Cleavage of structural proteins during the assembly of the head of the bacteriophage T4. Nature. **227:**680-685.

33. **Maa, J. S., and M. Esteban.** 1987. Structural and functional studies of a 39,000 Mr immunodominant protein of vaccinia virus. J. Virol. **61:**3910-3919.

34. **Maa, J. S., J. F. Rodriguez, and M. Esteban.** 1990. Structural and functional characterization of a cell surface binding protein of vaccinia virus. J. Biol. Chem. **265:**1569-1577.

35. **Morgan, C.** 1976. The insertion of DNA into vaccinia virus. Science. **193:**591-592.

36. **Moss, B.** 1990. Poxviridae and their replication, p. 2079-2111. *In* B. N. Fields and D. M. Knipe (ed.), Virology, 2nd ed. Raven Press, Ltd., New York.

37. **Moss, B.** 1990. Regulation of vaccinia virus transcription. Annu. Rev. Biochem. **59:**661-688.

38. **Moss, B., E. Katz, and E. N. Rosenblum.** 1969. Vaccinia virus directed RNA and protein synthesis in the presence of rifampicin. Biochem. Biophys. Res. Comm. **36:**858-865.

39. **Moss, B., and E. N. Rosenblum.** 1973. Protein cleavage and poxvirus morphogenesis: Tryptic peptide analysis of core precursors accumulated by blocking assembly with rifampicin. J. Mol. Biol. **81:**267-269.

40. **Moss, B., E. N. Rosenblum, and C. F. Garon.** 1973. Glycoprotein synthesis in cells infected with vaccinia virus. III. Purification and biosynthesis of the virion glycoprotein. Virology. **55:**143-156.

41. **Moss, B., and N. P. Salzman.** 1968. Sequential protein synthesis following vaccinia virus infection. J. Virol. **2:**1016-1027.

42. **Nagayama, A., B. G. T. Pogo, and S. Dales.** 1970. Biogenesis of vaccinia: separation of early stages from maturation by means of rifampicin. Virology. **4:**1039-1051.

43. **Oie, M., and Y. Ichihashi.** 1981. Characterization of vaccinia polypeptides. Virology. **113:**263-276.

44. **Oie, M., and Y. Ichihashi.** 1987. Modification of vaccinia virus penetration proteins analyzed by monoclonal antibodies. Virology. **157:**449-459.

45. **Pääbo, S., F. Weber, T. Nilsson, W. Schaffner, and P. Peterson, A.** 1986. Structural and functional dissection of an MHC class I antigen-binding adenovirus glycoprotein. EMBO J. **5**:19921-1927.

46. **Paez, E., S. Dallo, and M. Esteban.** 1987. Virus attenuation and identification of structural proteins of vaccinia virus that are selectively modified during virus persistence. J. Virol. **61**:2642-2647.

47. **Roos, N., M. Cyrklaff, S. Cudmore, R. Blasco, J. Krijnse-Locker, and G. Griffiths.** 1996. The use of a novel immunogold cryoelectron microscopic method to investigate the structure of the intracellular and extracellular forms of vaccinia virus. EMBO J. **In press.**

48. **Schmelz, M., B. Sodeik, M. Ericsson, E. J. Wolffe, H. Shida, G. Hiller, and G. Griffiths.** 1994. Assembly of vaccinia virus: The second wrapping cisterna is derived from the trans Golgi network. J. Virol. **68**. 130-147

49. **Silver, M., and S. Dales.** 1982. Biogenesis of vaccinia: Interrelationship between posttranslational cleavage, virus assembly, and maturation. Virology. **117**:341-356.

50. **Smadel, J., E., G. Lavin, I., and R. Dubos, J.** 1940. Some constituents of elementary bodies of vaccinia virus. J. Exp. Med. **71**:373-389.

51. **Snow, C., M., A. Senior, and L. Gerace.** 1987. Monoclonal antibodies identify a group of nuclear pore complex glycoproteins. J. Cell. Biol. **104**:1143-1156.

52. **Sodeik, B., S. Cudmore, M. Ericsson, M. Esteban, E. Niles, G., and G. Griffiths.** 1995. Assembly of vaccinia virus: Incorporation of p14 and p32 into the membrane of the intracellular mature virus. J. Virol. **69**:3560-3574.

53. **Sodeik, B., R. W. Doms, M. Ericsson, G. Hiller, C. E. Machamer, W. v. t. Hof, G. v. Meer, B. Moss, and G. Griffiths.** 1993. Assembly of vaccinia virus: Role of the intermediate compartment between the endoplasmic reticulum and the Golgi stacks. J. Cell Biol. **121**. 521-541

54. **Sodeik, B., G. Griffiths, M. Ericsson, and R. Doms, W.** 1994. Assembly of vaccinia virus:effects of rifampicin on the intracellular distribution of viral protein p65. J. Virol. **68**:1103-1114.

55. **Stern, W., and S. Dales.** 1976. Biogenesis of vaccinia: Isolation and characterization of a surface component that elicits antibody suppressing infectivity and cell-cell fusion. Virology. **75**:232-241.

56. **VanSlyke, J., S. S. Whitehead, E. M. Wilson, and D. E. Hruby.** 1991. The multistep proteolytic maturation pathway utilized by vaccinia virus P4a protein: A degenerate conserved cleavage motif within core proteins. Virology. **183**:467-478.

57. **VanSlyke, J. K., C. A. Franke, and D. E. Hruby.** 1991. Proteolytic maturation of vaccinia virus core proteins: identification of a conserved motif at the N termini of the 4b and 25K virion proteins. J. Gen. Virol. **72:**411-416.

58. **Vanslyke, J. K., and D. E. Hruby.** 1994. Immunolocalization of Vaccinia Virus Structural Proteins during Virion Formation. Virology. **198:**624-635.

59. **Wilton, S., A. Mohandas, R., and S. Dales.** 1995. Organisation of the vaccinia envelope and relationship to the structure of the intracellular mature virions. Virol. **214:**503-511.

60. **Yang, W. P., S. Y. Kao, and W. R. Bauer.** 1988. Biosynthesis and post-translational cleavage of vaccinia virus structural protein VP8. Virology. **167:**585-590.

Table 1. Labeling of intact IMV with α p39 on EM grids

Treatment	Gold particles/ virion (mean +/- SEM) [a]	ratio [b]
Control	0.1 +/- 0.01	1.0
NP-40	2.5 +/- 0.45	25
DTT	7.5 +/- 1.45	75
NP-40/DTT	47.4 +/- 2.08	474
Trypsin	3.1 +/- 0.47	31
Proteinase K	0.6 +/- 0.02	6

Table 1 : Purified IMV were adsorbed to formvar- and carbon-coated 100 mesh electron microscopy grids and treated as described in Materials and Methods. The grids were subsequently blocked and labelled with anti-p39 antibodies followed by 10nm protein A-gold.

[a] Mean values +/- standard error of the mean (SEM) (n=20).

[b] For the ratios, the data from the treated samples were compared to the untreated control sample which was normalised to 1.

FIGURE LEGENDS:

Figure 1 : Immunofluorescence localization of p39 in vaccinia infected HeLa cells 8h after infection. Panel a) shows an infected cell labelled with antibodies against p39. There is strong labelling of the peri-nuclear region of the cell most likely corresponding to the viral factories, which can also be seen by Hoechst staining of DNA (arrowheads in panel b). The punctate structures seen throughout the cell (arrows in a) probably represents individual virions. Scale bar 20μm.

Figure 2 : Immunolabelling of thawed cryosections of fixed HeLa cells, infected with vaccinia for 8h, with antibodies against p39. Panel a) shows a viral factory (F) which labels strongly with anti-p39. Crescent shaped membranes (star) are visible protruding from the factories, which display a very low amount of p39 labelling (arrows). In panel b) immature virions (IV) clearly label in their central region with antibodies against p39. In the intracellular mature virus (IMV) p39 labelling is observed in the space between the core and the envelope. The IMVs always appear to label less than the IVs, most likely due to a problem of access of the antibody to p39 in the IMV. Panels c) through to h) show virus particles at various stages during maturation labelled with anti-p39. In c) a developing IV is packaging "viroplasm" while in d) the IV has not yet packaged DNA, which is visible above the particle in a crystalline-like array (arrowhead). In panel e) the DNA (arrowhead), which does not label with p39, has been packaged and is seen as an electron dense structure on the left side of the virion. An intermediate stage between the IV and IMV is seen in f) where the label starts to associate with what is interpreted as the surface of the developing core. The IMV in (g) and EEV in (h) label between the core and the IMV membranes. Scale bar 200nm.

Figure 3 : Cryosections of cells infected for 16h in the presence of rifampicin and immunolabelled with anti-p39. In panel a) rifampicin bodies (RB) are clearly visible which label strongly with antibodies against p39. Also visible are crystalline arrays of DNA (D) which are devoid of labelling. Panel b) shows viral crescents (stars) protruding from the rifampicin bodies, as well as immature virions (IV), seen here 15 minutes after rifampicin release. In panel c) purified IMV were used to make pellets which were cryosectioned and labelled with anti-p39. The label is most frequently found in the region between the core and surrounding IMV membranes. This labelling appears to colocalise with the spikes which extend between the core and IMV membranes (arrowheads). Scale bar in (a) 400nm, in (b) 250nm and in (c) 50nm.

Figure 4 : Immunolabelled and negatively stained IMV viewed by electron microscopy. Purified IMV were adsorbed to an EM grid and labelled with antibodies against a) p39 and b) p14, followed by protein A gold. The inserts show IMV particles which were treated with 1% NP 40 and 20mM DTT to remove the viral membranes prior to labelling. In contrast to anti-p14, antiserum against p39 does not significantly label intact IMV. However, after NP 40 and DTT treatment, the cores are devoid of p14 labelling, while the p39 labelling has dramatically increased. In panel A, virus particles are visible which are open to the negative stain (arrowheads) but do not label with anti-p39, suggesting that the epitope is still masked by the surrounding envelope. Scale bars in (a) 200nm, in the inset 100nm; in (b) 200nm.

Figure 5 : p39 is not digested during protease treatment of IMV. a) ^{35}S labelled and purified IMV was treated with proteinase K for 30 mins on ice. Lane 1; mock treated control ; lanes 2-9; samples treated with 5, 10, 20, 30, 50, 100, 200 and 300 µg/ml proteinase K respectively ; lane 10, untreated IMV sample. The positions of 4a, 4b, p11 and p39 which are not digested, as well as the position of p32 which is sensitive to proteinase K, are indicated on the left. b) IMV was also subjected to treatment with 50µg/ml α-chymotrypsin (lane 1), 100µg/ml thermolysin (lane 2), 250µg/ml V8 (lane 3) at 37°C for 30 minutes. In lane 4 samples were treated with 50µg/ml proteinase K for 30 minutes on ice. Lane 5, untreated control IMV. The positions of the major core proteins, 4a, 4b and p11, as well the membrane protein p14 are indicated on the left, with the positions of three molecular weight markers (45kD, 30kD and 14kD) indicated on the right. p39 is not digested by any of the proteases assayed, even at concentrations of 300µg/ml of proteinase K indicating it is protected from protease treatment due to its internal location.

Figure 6 : Membrane association of p39. a) ^{35}S-labelled purified IMV was incubated with 1% NP 40 and 20mM DTT for 30 minutes after which the sample was centrifuged through a 36% (w/v) sucrose cushion to pellet the cores. Lane 1 shows the membrane proteins, while lane 2 comprises the core proteins. Lane 3, untreated control IMV. Approximately 40% of p39 is found in the membrane fraction along with other membrane proteins like p32 (indicated on the left). The core proteins 4a and 4b (indicated on the left) are found exclusively in the pelleted core fraction. b) 2D gel electrophoresis of NP 40 and DTT treated samples. Isoelectric focusing was used in the first dimension and SDS polyacrylamide gel electrophoresis in the second dimension. The top panel shows the pelleted core proteins while the bottom panel shows the membrane protein fraction. When separated in this fashion, it is clear that p39 separates into both the membrane and core fractions and that it is composed of a

complex pattern of polypeptides. The protein pattern on the right side of the autoradiogram represents the same samples which are only subjected to SDS-PAGE. The position of p39 is indicated on the right. The pH range of the IEF is shown at the bottom of the gels. c) Post nuclear supernatants from infected cells were subjected to treatment with 1% TX-114 or Na_2CO_3. Lane 1 untreated control PNS. Lane 2 shows the aqueous phase and lane 3 the detergent phase of TX-114 treated PNS samples. Lane 6 shows the aqueous phase of TX-114 treated purified IMV and lane 7 the detergent phase. p39, as well as p32 (indicated), are found exclusively in the detergent fraction under both conditions, indicating their hydrophobic nature. Lane 4 comprises the supernatant and lane 5 the pellet fraction from Na_2CO_3 treated PNS. Approximately 60% of p39 is found associated with the pelleted membranes from infected cells, while p32 quantitatively pellets, indicating that p39 associates strongly with membranes. Numbers on the right of a) and c) indicate the positions of molecular weight marker proteins in kD.

Figure 7 : ***In vitro*** translation and translocation of p39. p39 was translated ***in vitro*** using a rabbit reticulocyte lysate system. The samples were then immunoprecipitated with antibodies against p39, which yielded three different bands (lane 8), the uppermost of which co-migrates with p39 immunoprecipitated from IMV (lane 7). The faster migrating bands are most likely due to premature termination or internal initiation of the translation. Upon extraction of the ***in vitro*** translation reaction with 1% TX-114,. p39 is found almost exclusively in the detergent phase (lane 2) with only a small amount of p39 apparent in the aqueous phase (lane 1). In lanes 3 through to 6, p39 was translated in vitro in the absence (lanes 3 and 4) or presence (lanes 5 and 6) of dog microsomes, after which the soluble protein (lanes 3 and 5) was seperated from the putative membrane-associated protein (lanes 4 and 6) by centrifugation. p39 does not associate with rough microsome membranes when they are added co-translationally, as indicated by the absence of p39 in the pelleted membrane fraction (lane6). The number on the right indicates the 45kD molecular weight standard.

Figure 8 : HeLa cells transiently transfected with p39. Panel a) shows transfected cells labelled with antiserum against p39 that indicate a predominantly cytosolic labelling, suggesting that p39 behaves as a soluble protein in the absence of other late viral proteins. Panel b) shows a phase contrast image of the same field showing that the morphology of the transfected cells, in comparison with the untransfected cells, remained normal. Scale bar represents 50μm.

Figure 9 : Immunoprecipitation of p39 from cells infected in the presence of ^{3}H-glucosamine, ^{35}S or ^{32}P. Panel (a): Lane 1, ^{3}H-glucosamine labelled PNS and lane 2, ^{35}S-labelled PNS without immunoprecipitation. A faint band apparently co-migrating with p39 is labelled with ^{3}H-glucosamine(lane 1). When this sample is immunoprecipitated with antibodies against p39, the labelled protein is no longer detectable, lane 3 The major glycosylated band, running at approximately 90kD, most likely represents the EEV HA protein. Lane 4 shows a control p39 immunoprecipitation from ^{35}S-labelled PNS, while lane 5 indicates that the molecular weight of p39 is not affected by the addition of tunicamycin which prevents N-glycosylation. The co-immunoprecipitation of p39 in lane 6 shows that p39 may interact with a number of other proteins. One of these was identified as p21 (gene A17L) by immunoprecipitation with antibodies against the C-terminus of this protein (lane7).
lane 3: immunoprecipitation of a ^{3}H glucosamine labelled PNS with α-p39.

Figure 10 : Pulse-chase analysis of p39. infected HeLa cells pulse-labelled for 5 minutes at 7 hours p.i. (a), and chased for (b) 30 minutes, (c) 60 minutes and (d) 120 minutes. The different forms of p39, that occured during the various chase times, have been numbered 1 to 6 in (d). Initially the p39 pattern is quite simple with a central major spot (no. 1) with some minor species visible (nos. 5 and 6). By 60 mins chase and even more noticeably by 120 mins chase, the p39 pattern is more complex with the central, most abundant form of p39 now surrounded by 6 other species of varying intensity.

Figure 11 : A graph showing the elution profile of *in vitro* translated p39 after high performance size-exclusion chromatography. The Y-axis represents the optical density at 280nm while the elution time, in minutes, is shown on the X-axis. p39 eluted at 19.42 minutes, which corresponds to 41.5 +/- 5% when compared to the calibration standards. Two smaller peaks of 8.9 and 7kD are also visible. The peak at 12.5 minutes is the void volume while the peak at 16.3 minutes corresponds to 122kD but analysis of the A_{280nm}/A_{220nm} ratio indicated that it is not a trimer of p39.

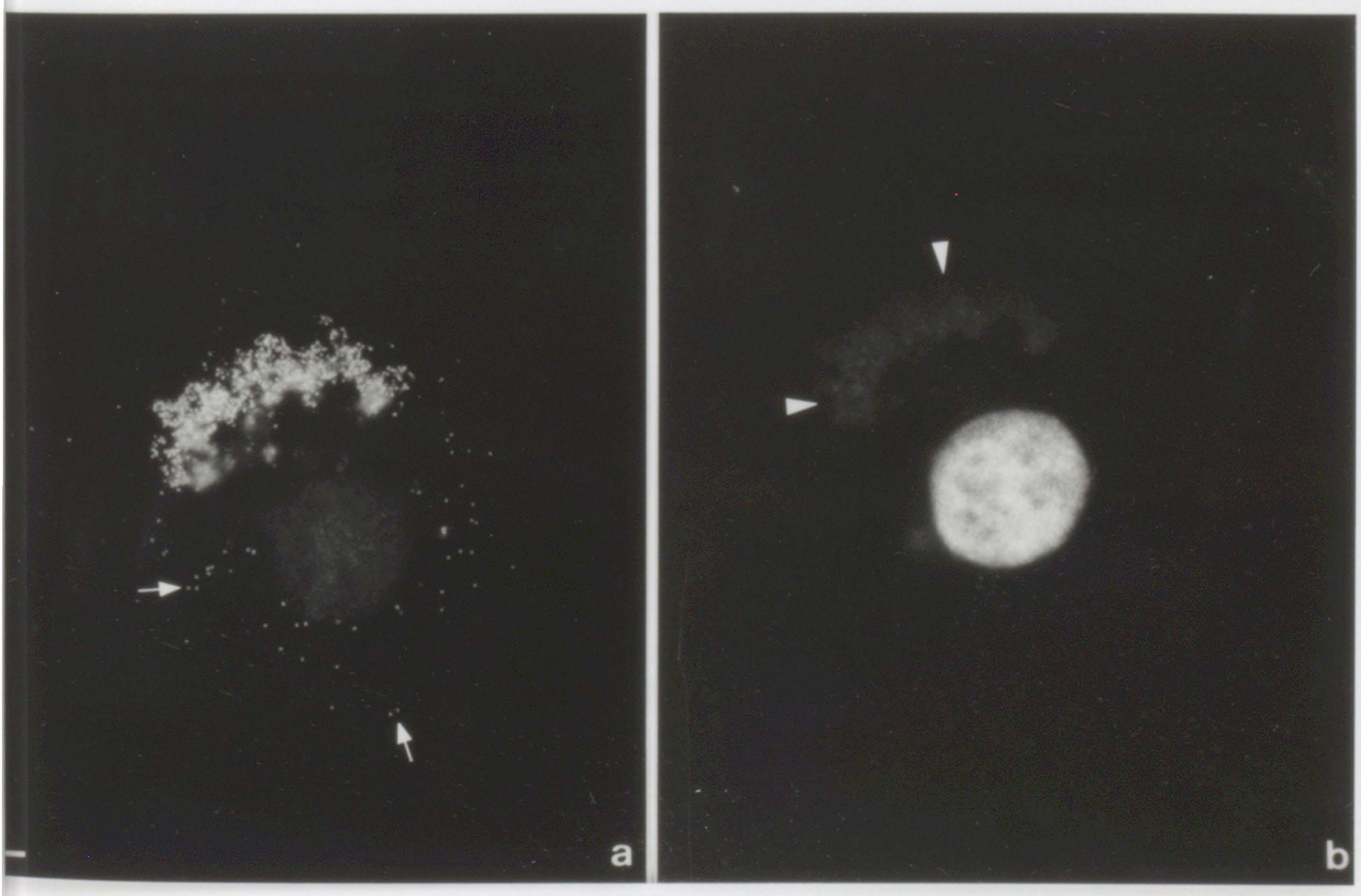


Fig 1 Cudmore et al. 1996

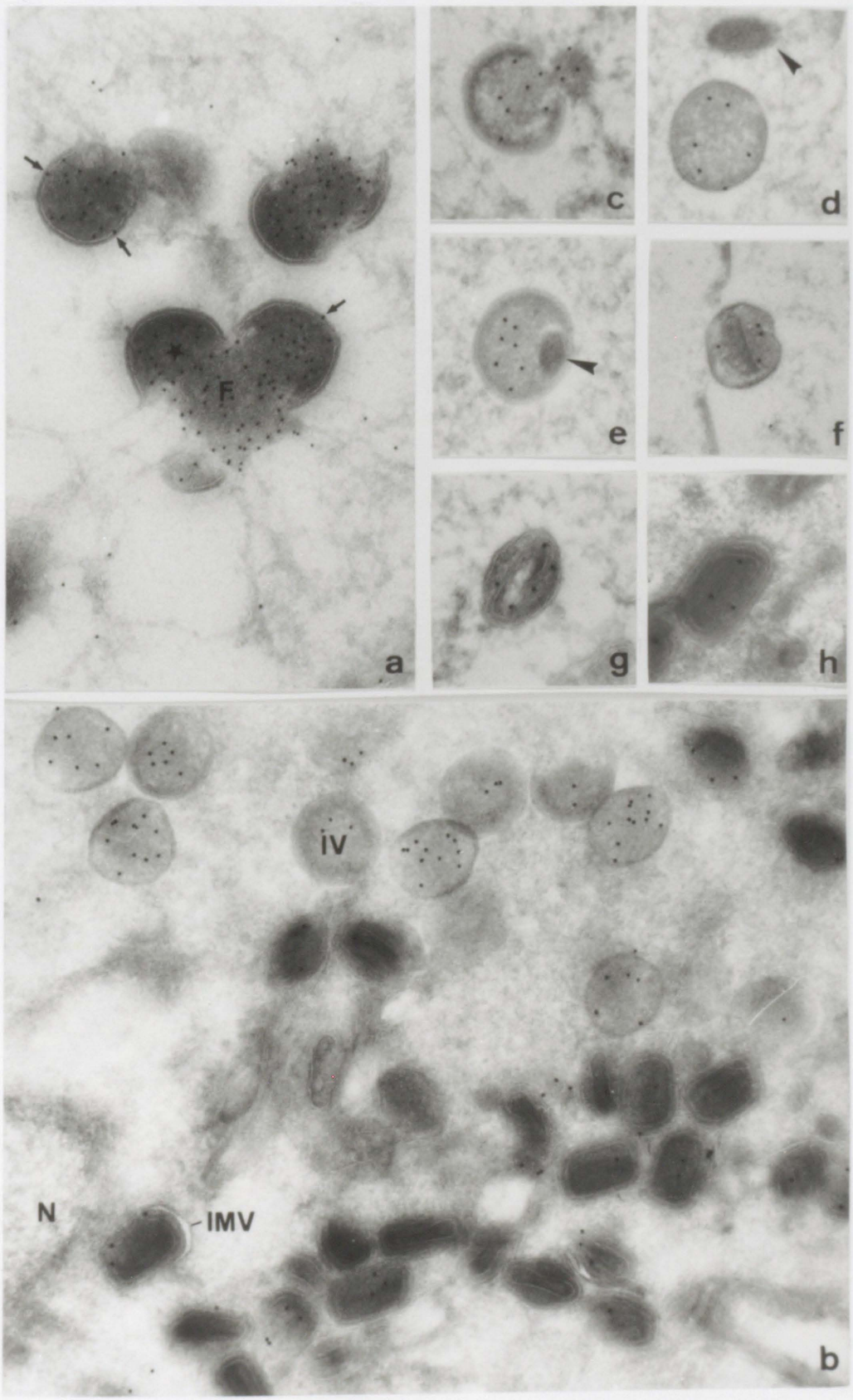


Fig 2 Cudmore et al. 1996

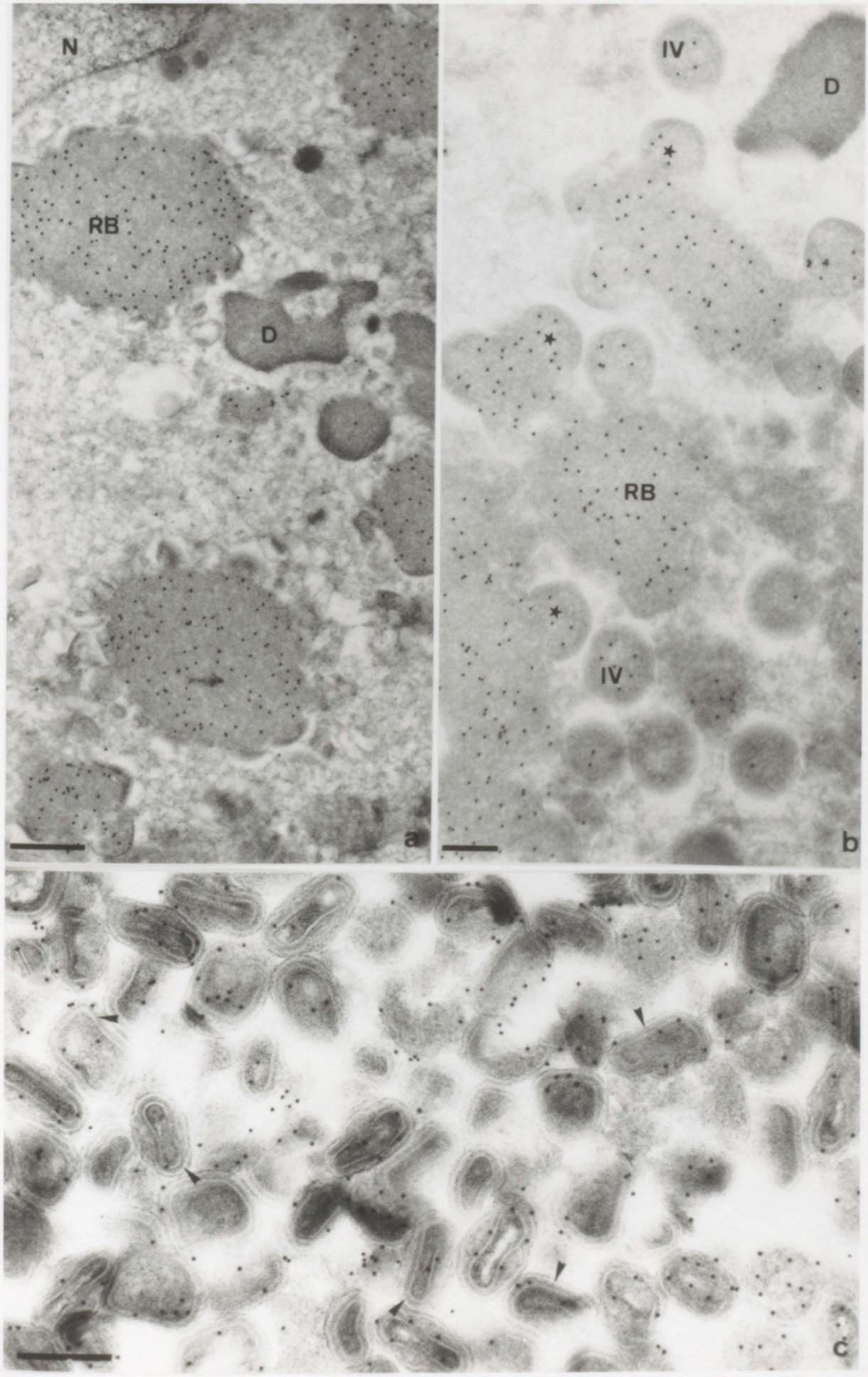


Fig 3 Cudmore et al. 1996

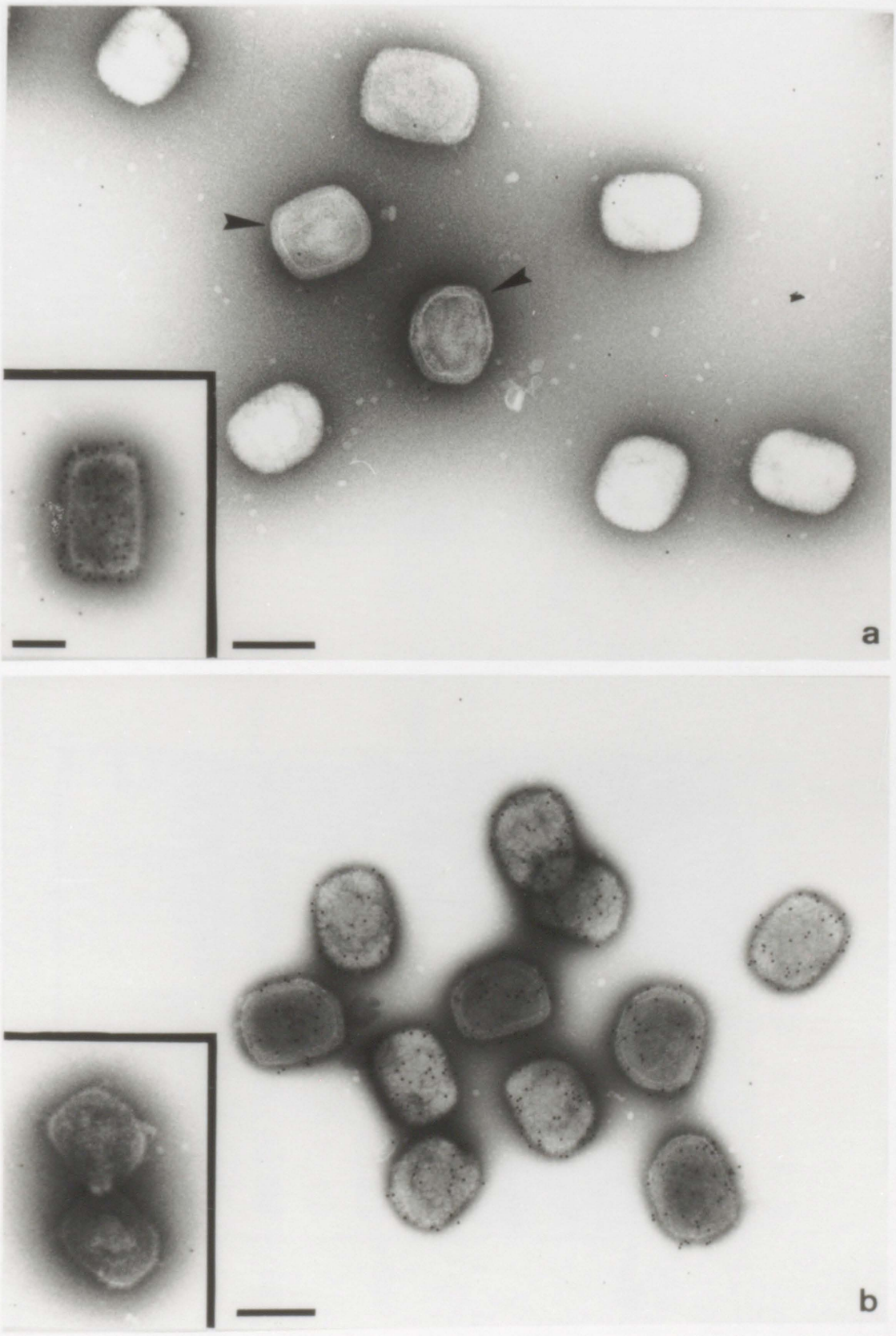


Fig 4 Cudmore et al. 1996

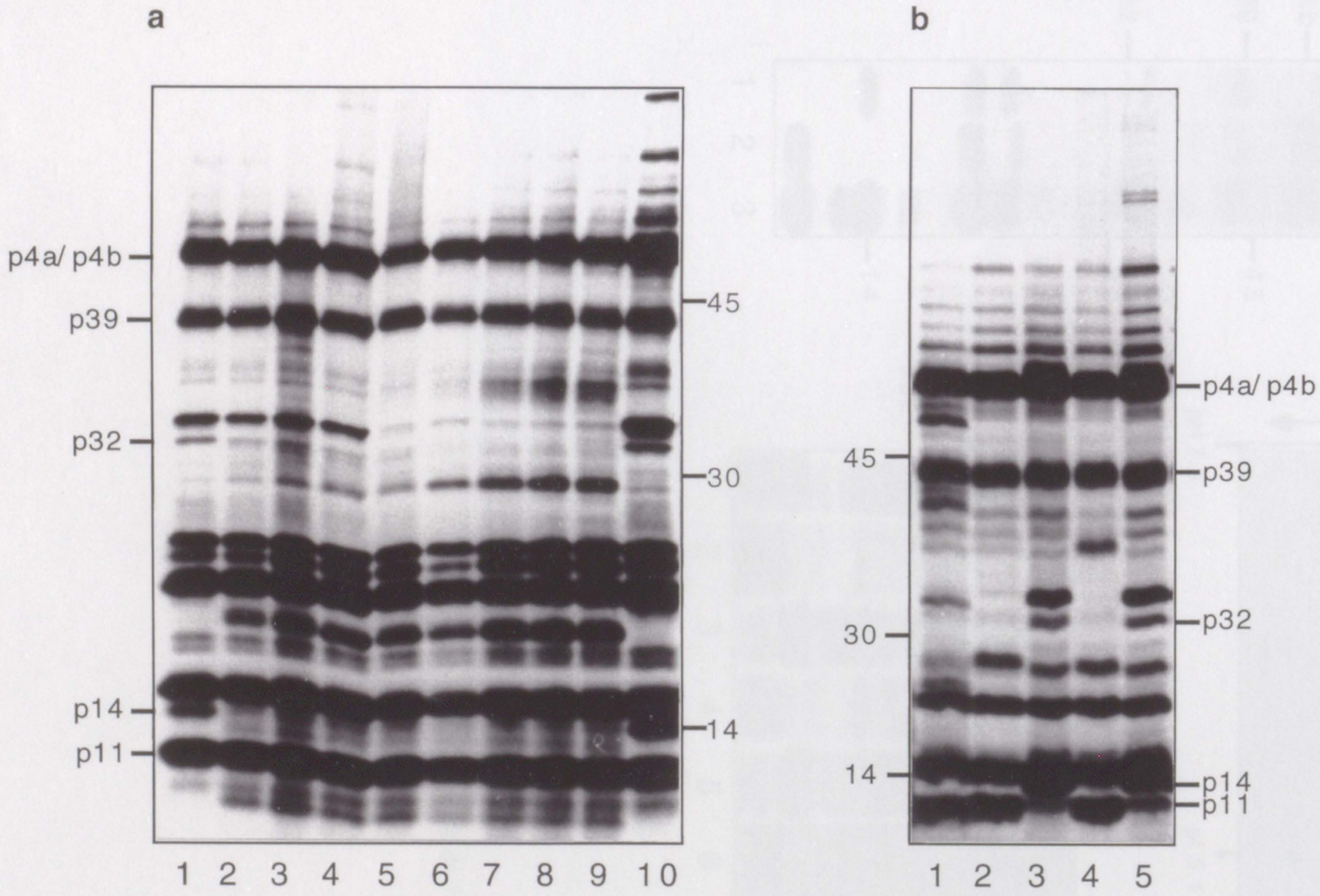


Fig 5 Cudmore et al 1996

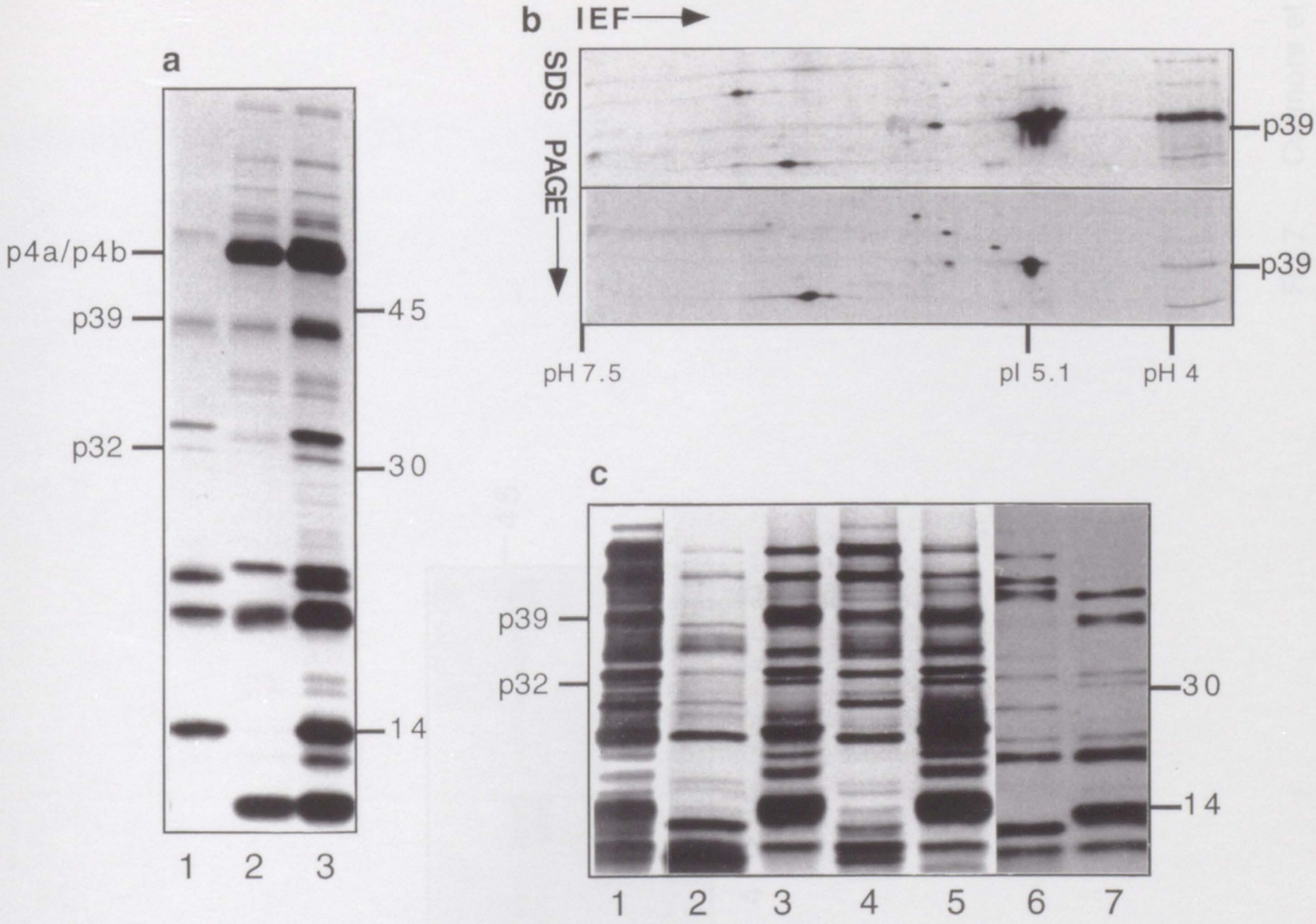


Fig 6 Cudmore et al 1996



Fig 7 Cudmore et al 1996

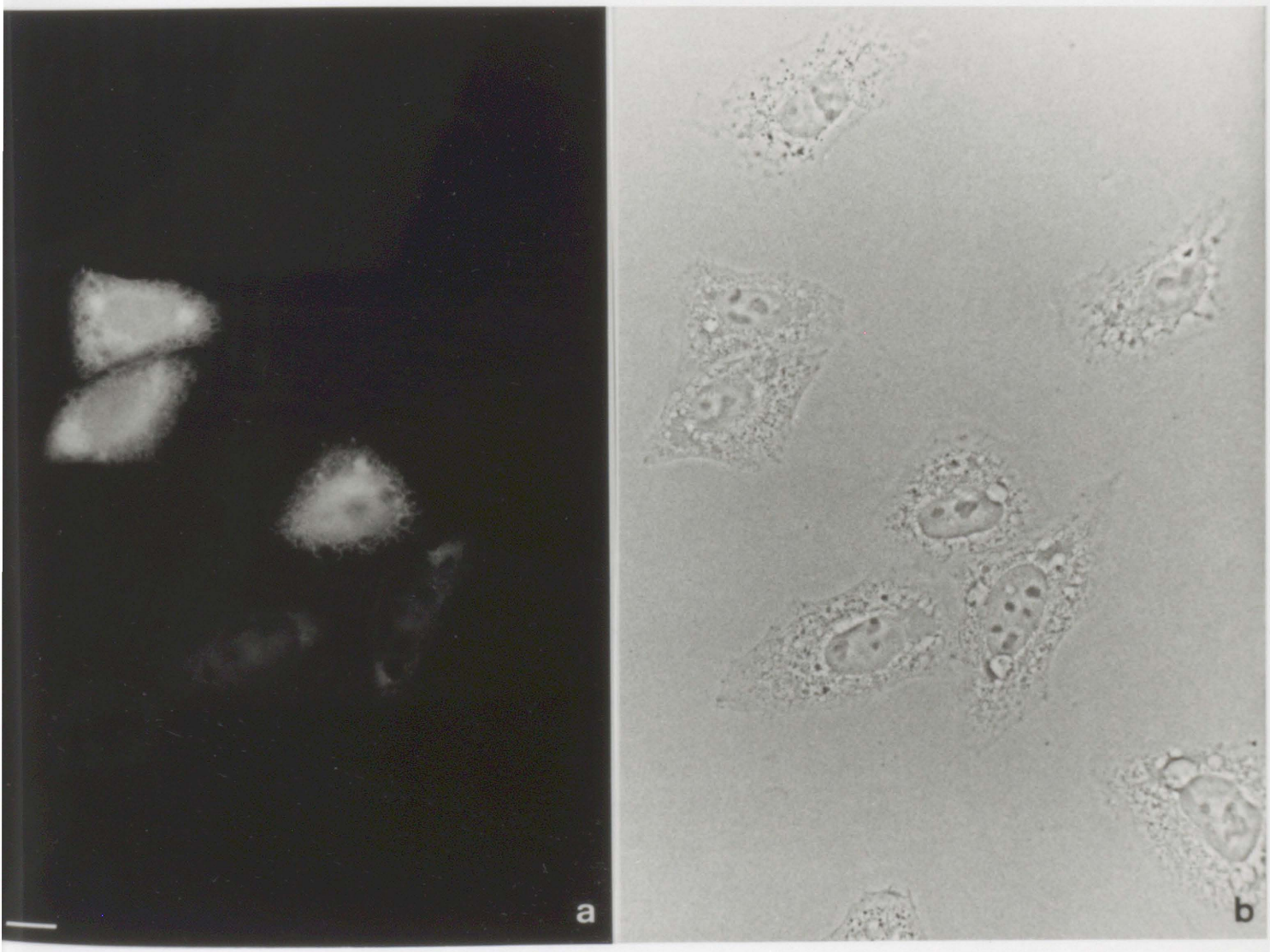


Fig 8 Cudmore et al. 1996

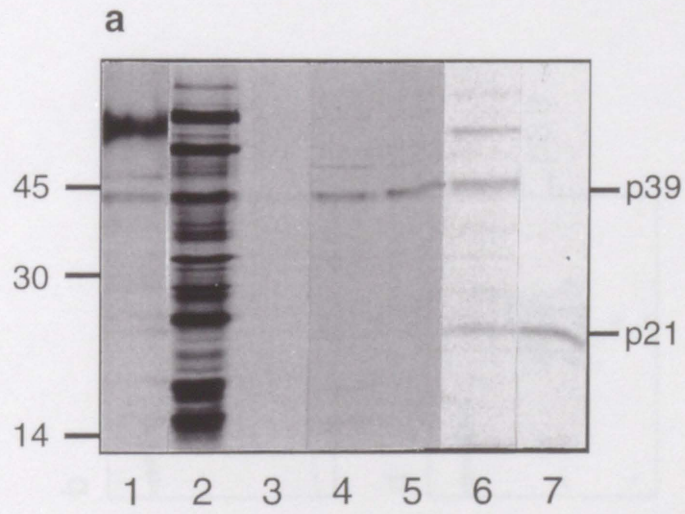


Figure 9 Cudmore et al 1996

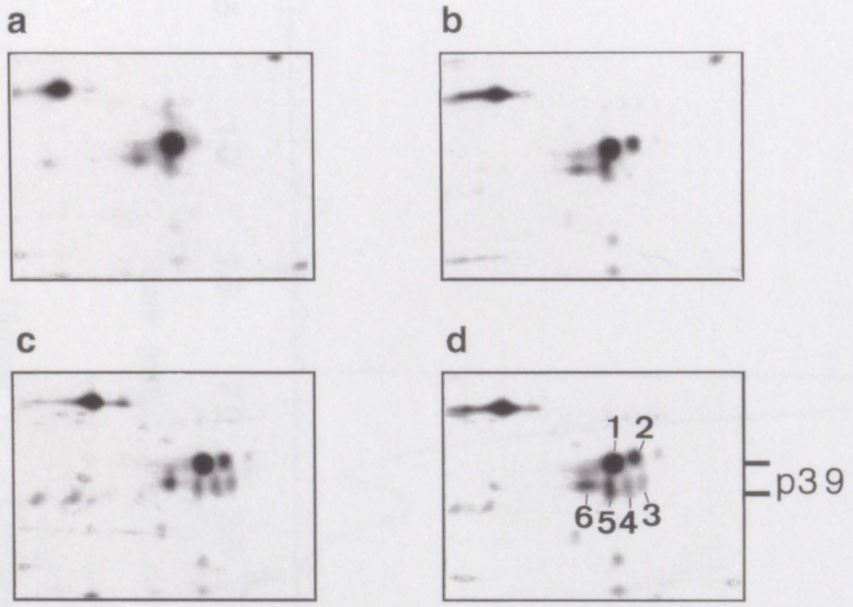


Fig 10 Cudmore et al 1996

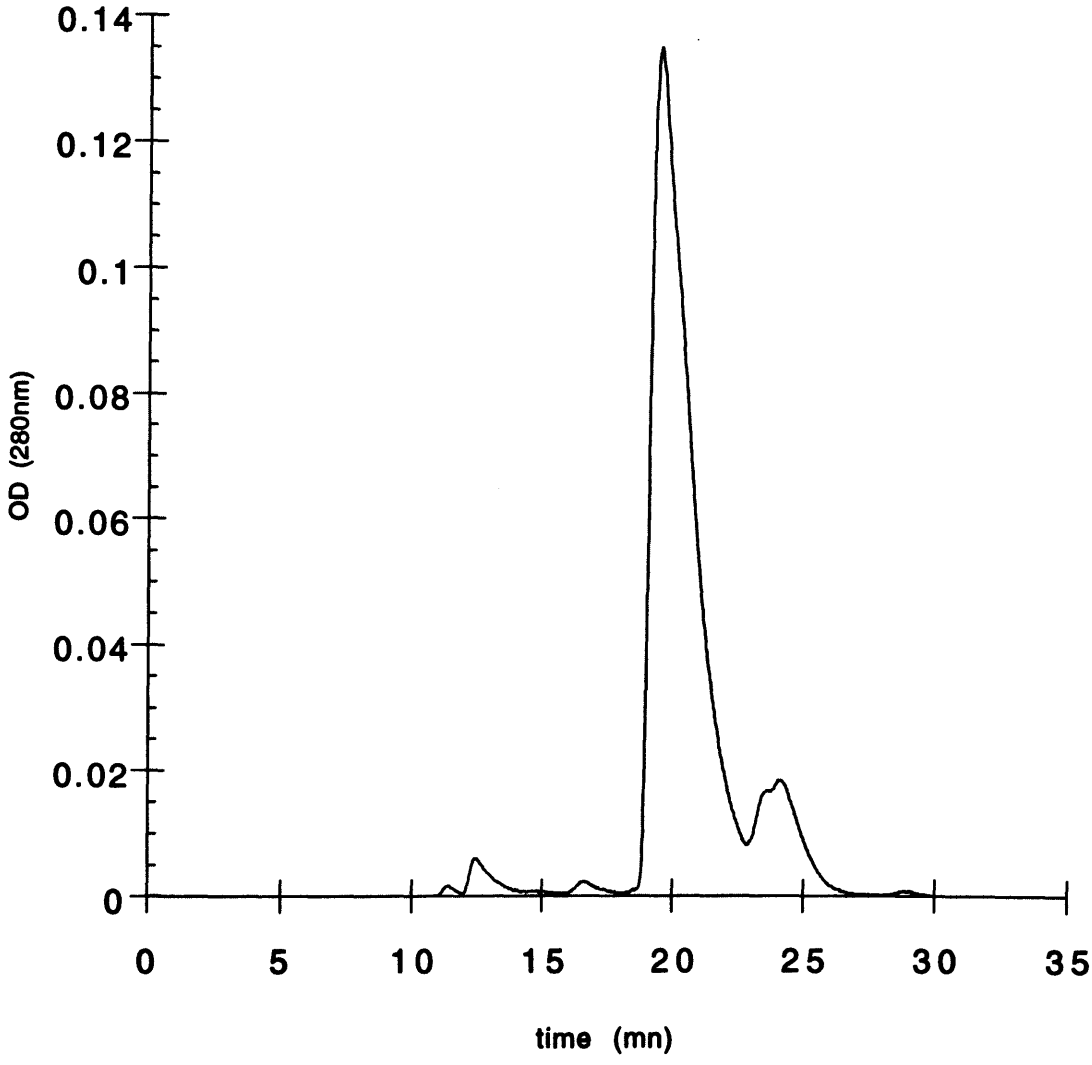


Figure 11 Cudmore et al. 1996

CHAPTER 3

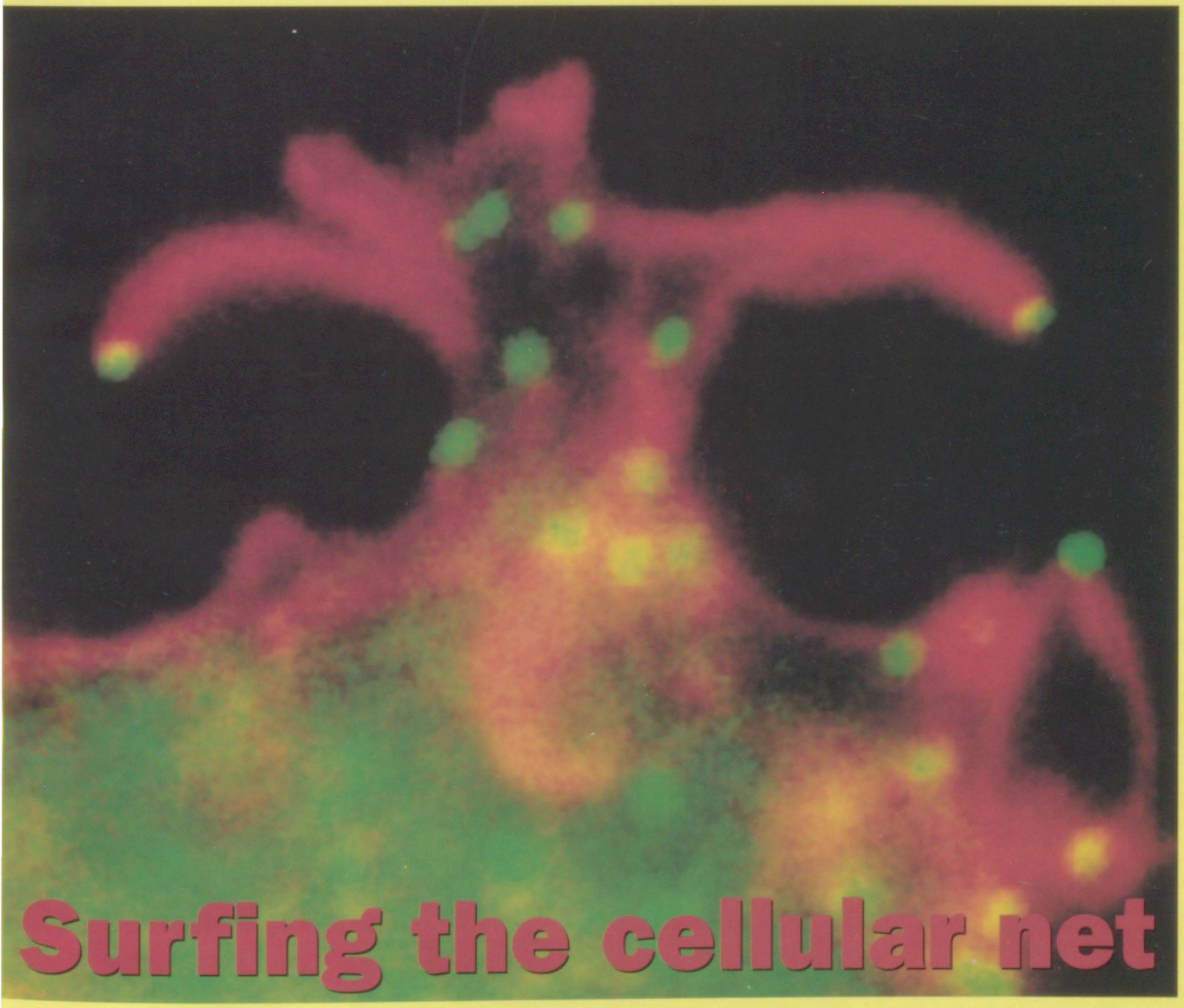
Actin Based Motility of Vaccinia Virus

Nature 378 ; 636-638 (1995)

nature

INTERNATIONAL WEEKLY JOURNAL OF SCIENCE

Volume 378 No. 6557 7 December 1995 $10.00



Surfing the cellular net

Cosmic dust: a climate connection?

Making continental crust

Science in China

Cell biology
PRODUCT REVIEW

region of the cell, and no actin tails are seen while the actin cytoskeleton appears normal (Fig. 2). Subsequent removal of IMCBH results in the appearance of actin tails with associated viral particles (Fig. 2*c*).

We observed individual viral particles *in vivo* by video microscopy (Fig. 3). Phase-dense structures, the actin tails, were only observed behind moving viral particles and were completely absent from vRB12-infected cells. The number of moving particles and tails is consistent with fluorescence images of fixed cells, although the tails generally appear shorter. Movement within cells appears to be random with an average speed of 2.8 μm min^{-1} (s.d. 0.5 μm min^{-1}, $n=44$), which is similar to that observed for *Listeria*[21,22]. On reaching the cell surface, virus particles project up to 20 μm at the same rate (Fig. 3). Projections are always much larger than the normal cell-surface microvilli, and presumably correspond to the virally induced projections previously described[6,7].

Cytochalasin D has previously been shown to prevent the release of IEV, which suggests that actin is involved in this process[23]. Our immunofluorescence images clearly show viral-tipped actin projections extending into uninfected cells (Fig. 4*a*). Electron microscopy also shows virus particles at the tip of a dense actin network projecting from one cell into another (Fig. 4*b*). Taken together, our results suggest that IEV are able to recruit and exploit actin to facilitate their spread from cell to cell. Given that the rates at which intracellular tails move and projections extend are identical, it is likely that these two events are driven by the same mechanism. However, the stability of actin in tails and projections is very different: the actin at the distal end of the intracellular tail is unstable and depolymerizes as the tail continues to extend, but it is stable in the elongating projection. This stability may be explained in part by membrane interactions in the projection that are absent in intracellular tails.

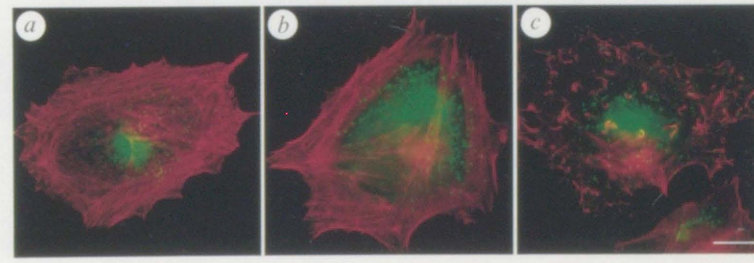


FIG. 2 IEV induces actin tail formation. *a*, HeLa cells infected with a mutant vaccinia strain, vRB 12. *b*, Cells infected with wild-type WR in the presence of IMCBH. The virus is concentrated in the perinuclear area of both cells and there are no actin tails. *c*, Viral particles are seen on actin tails 1 h after IMCBH removal. Scale bar, 50 μm.
METHODS. Cells were infected with WR or vRB12 as described above. IMCBH was added to a final concentration of 10 μg ml^{-1} 1 h post-infection. At 8 h post-infection cells were washed 5 times with PBS and fixed 1 h after washout.

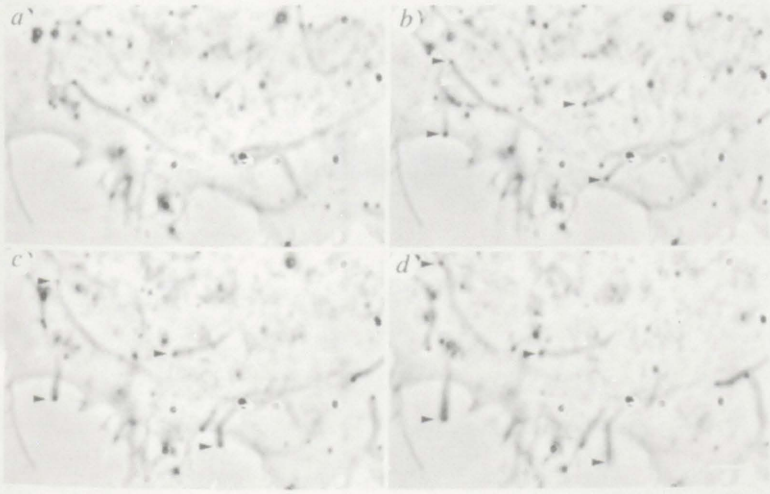


FIG. 3 Virus motility *in vivo*. Frame stills 40 s apart, from the video microscope, showing virus particles moving through the cell at the tip of actin tails and inducing the formation of protrusions from the cell surface. White arrowheads are fixed reference points, and black arrows indicate moving virus particles. Scale bar, 3.0 μm.
METHODS. Cells were infected with WR and viewed 10 h post-infection with a Zeiss axiovert microscope using a Sony CCD IRIS camera.

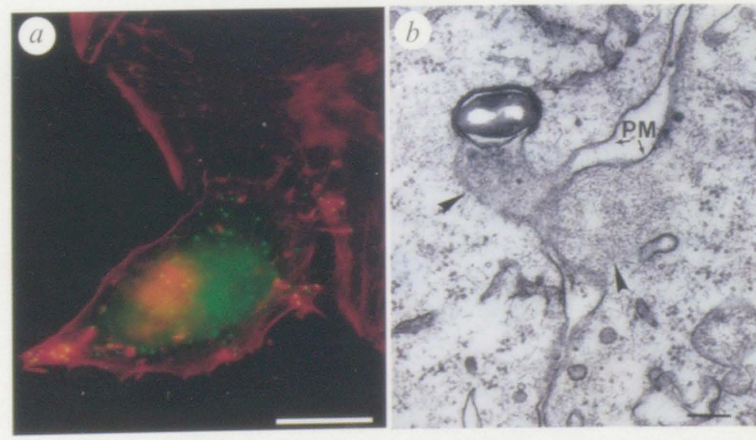


FIG. 4 Spread of vaccinia virus from cell to cell. *a*, Virus particles moving from an infected cell to an uninfected cell at the tip of actin-rich projections. Scale bar, 50 μm. *b*, Electron micrograph of a virus particle moving into a neighbouring cell. Black arrowheads show actin, and PM indicates the plasma membrane of the two cells. Scale bar, 400 nm.
METHODS. *a*, Cells were infected in the presence of IMCBH. Then, 5 h post-infection, the cells were washed once with warm PBS + IMCBH and uninfected cells were seeded on the same coverslips; 3 h later the IMCBH was washed out, and the cells were fixed after 1 h and stained as described above. *b*, Infected cells were fixed in 1% gluteraldehyde, 0.5 mg ml^{-1} saponin, 2% tannic acid, 50 mM KCl, 5 mM $MgCl_2$ for 30 min, post-fixed in 1% osmium on ice for 30 min, dehydrated in ethanol, and embedded in EPON.

The intimate relationship between the IEV and the actin cytoskeleton suggests that the virus contains protein(s) that can associate directly or indirectly with actin. In *Listeria* species and *Shigella*, the proteins ActA, IactA and IcsA are critical for the nucleation of actin filaments at the bacterium surface[15,24,26]. Sequence comparisons of the vaccinia virus genome with ActA, IactA or IcsA failed to identify any ORF that contains significant homologous sequences. One possible candidate for viral interactions with actin is the A42R ORF, which is 32.1% identical to human profilin[27]. However, deletion of A42R has previously shown that it is not required for infectivity or release of mature virions[27]. Moreover, we found that vaccinia virus lacking A42R is still able to form actin tails and projections (data not shown), which is consistent with the recent observation that profilin is not required for actin-based motility of *Listeria* in the cell-free *Xenopus* system[28]. Whether profilin is involved in vaccinia motility will require further characterization, as the virus may be able to utilize cellular profilin isoforms. Given the similarities between the motility of bacterial pathogens and vaccinia virus, we suggest that intracellular pathogens have developed a common mechanism to exploit the actin cytoskeleton for their own purposes. □

Received 25 August; accepted 6 October 1995.

1. Goebel, S. J. *et al. Virology* **179**, 247–266 (1990).
2. Moss, B. in *Virology* (eds Fields, B. N. *et al.*) 2079–2111 (Raven, New York, 1990).
3. Payne, L. G. *J. gen. Virol.* **50**, 89–100 (1980).
4. Schmelz, M. *et al. J. Virol.* **68**, 130–147 (1994).
5. Morgan, C. *Virology* **73**, 43–58 (1976).
6. Stokes, G. V. *J. Virol.* **18**, 636–643 (1976).
7. Hiller, G., Weber, K., Schneider, L., Parajsz, C. & Jungwirth, C. *Virology* **98**, 142–153 (1979).
8. Hiller, G. & Weber, K. *J. Virol.* **44**, 647–657 (1982).
9. Hiller, G., Jungwirth, C. & Weber, K. *Expl Cell Res.* **132**, 81–87 (1981).
10. Krempien, U. *et al. Virology* **113**, 556–564 (1981).
11. Pollard, T. D. *Curr. Biol.* **5**, 837–840 (1995).
12. Cossart, P. *Curr. Opin. Cell Biol.* **7**, 94–101 (1995).
13. Tilney, L. G. & Portnoy, D. A. *J. Cell Biol.* **109**, 1597–1608 (1989).
14. Heinzen, R. A., Hayes, S. F., Peacock, M. G. & Hackstead, T. *Infect. Immun.* **61**, 1926–1935 (1993).
15. Bernardini, M. L., Mounier, J., d'Hauteville, H., Coquis-Rondon, M. & Sansonetti, P. J. *Proc. natn. Acad. Sci. U.S.A.* **86**, 3867–3871 (1989).
16. Blasco, R. & Moss, B. *J. Virol.* **66**, 4170–4179 (1992).
17. Hiller, G., Eibl, H. & Weber, K. *J. Virol.* **39**, 903–913 (1981).
18. Kato, N., Eggers, H. J. & Rolly, H. *J. exp. Med.* **129**, 795–808 (1969).
19. Payne, L. G. & Kristenson, K. *J. Virol.* **32**, 614–622 (1979).
20. Schmutz, C., Payne, L. G., Gubser, J. & Wittek, R. *J. Virol.* **65**, 3435–3442 (1991).
21. Dabiri, G. A., Sanger, J. M., Portnoy, D. A. & Southwick, F. S. *Proc. natn. Acad. Sci. U.S.A.* **87**, 6068–6072 (1990).
22. Theriot, J. A., Mitchison, T. J., Tilney, L. G. & Portnoy, D. A. *Nature* **357**, 257–260 (1992).
23. Payne, L. G. & Kristensson, K. *Archs Virol.* **74**, 11–20 (1982).
24. Kocks, C. *et al. Cell* **68**, 521–531 (1992).
25. Gouin, E., Dehoux, P., Mengaud, J., Kocks, C. & Cossart, P. *Infect. Immun.* **63**, 2729–2737 (1995).
26. Domann, E. *et al. EMBO J.* **11**, 1981–1990 (1992).
27. Blasco, R., Cole, N. B. & Moss, B. *J. Virol.* **65**, 4598–4608 (1991).
28. Marchand, J.-B. *et al. J. Cell Biol.* **130**, 1–13 (1995).
29. Herzog, M., Draeger, A., Ehler, E. & Small, J. V. *Cell Biology: A Laboratory Handbook* (Academic, San Diego, 1994).
30. Rodriguez, J. F., Janeczko, R. & Esteban, M. *J. Virol.* **56**, 482–488 (1985).

ACKNOWLEDGEMENTS. We thank Y. Rivière, V. David and E. Gouin for help in preliminary experiments; R. Blasco for vRB 12 and profilin null virus; D. Klaus and M. Esteban for the S1 myosin and C3 antibody, respectively; C. Dotti for help and suggestions concerning video microscopy; I. Reckmann for vaccinia virus preparations; S. Schleich for help with electron microscopy; and A. Hyman, K. Simons, M. Zerial, R. Parton and E. Karsenti for suggestions and comments on the manuscript.

CHAPTER 4

Vaccinia virus: a model system for actin-membrane interactions

Submitted to Journal of Cell Science

Vaccinia virus: a model system for actin-membrane interactions.

Sally Cudmore, Inge Reckmann, Gareth Griffiths and Michael Way*.

Cell Biology Programme, E.M.B.L., Meyerhofstr. 1, Heidelberg 69117, Germany.

* to whom correspondance should be addressed
Tel : 49 6221 387-288
Fax : 49 6221 387-512
Email : Way@EMBL-Heidelberg.de

RUNNING TITLE : Vaccinia virus and membrane-actin interactions
KEYWORDS: Vaccinia virus, actin tails, membranes

ABSTRACT

Our understanding of the interactions between the actin cytoskeleton and cellular membranes at the molecular level is rudimentary. One system that offers an opportunity to examine these interactions in greater detail is provided by vaccinia virus, which induces the nucleation of actin tails from the membrane surrounding the virion. To further understand the mechanism of their formation and how they generate motility, we have examined the structure of the actin tails in detail. Actin filaments in vaccinia tails are organized so they splay out at up to 45° from the centre of the tail and are up to 0.75μm in length, which is considerably longer than those reported in the *Listeria* system. Actin filaments show unidirectional polarity with their barbed filament ends associated with the surface of the virus particle. The overall organization of actin filaments in the vaccinia tail is very reminiscent of actin at the leading edge of motile cells. Rhodamine-actin incorporation experiments show that the first stage of tail assembly involves a polarized recruitment of G-actin, and not pre-formed actin filaments, to the membrane surrounding the virion. Incorporation of actin into the tail occurs by nucleation only from the viral surface at a rate consistent with the *in vivo* speed of virus particles. As virus particles fuse with the plasma membrane during extention of projections, actin nucleation sites previously in the viral membrane become localized to the plasma membrane, where they continue to nucleate actin polymerization in a manner analogous to the leading edge of motile cells.

INTRODUCTION

A key mechanism in the virulence of any cellular pathogen is its ability to move from cell to cell to facilitate spread of the infection. A group of unrelated bacterial pathogens *Shigella, Listeria* and *Rickettsia*, that are the causative agents of an number of important diseases including meningitis, septicaemia, dysentery and shigellosis have independently developed a similar actin based mechanism that is essential for their intercellular spread (Cossart, 1995, Cossart and Kocks, 1994, Tilney and Tilney, 1993). Initially, the bacterium enters the host cell by phagocytosis but rapidly escapes into the cytoplasm where it grows and divides by lysis of the phagosome. In the cytoplasm, the bacterium recruits a cloud of host actin which becomes arranged into an actin comet at one pole of the bacterium. The bacterium is then able to move around the cell by continued nucleation and unidirectional elongation of the actin filaments at the bacterial surface while the tail remains stationary in the cytoplasm (Theriot and Mitchison, 1992). Ultimately, interactions with the plasma membrane and continued motility result in the formation of long bacterial-tipped extentions that project from the cell surface. These projections are phagocytosed by neighbouring cells and a new infection cycle begins without the bacterium being exposed outside the cell, hence escaping the humoral immune response of the host. The ability to nucleate the formation of an actin tail is essential for the intercellular spread of these bacteria, as mutants which are unable to recruit actin are non-virulent.

Bacterial pathogens are not the only infectious agents that have profound effects on the actin cytoskeleton of their host cells. Many different viruses have been shown to disrupt or stabilize the actin cytoskeleton (Bohn, et al., 1986, Giuffre, et al., 1982, Murti, et al., 1985, Tyrell and Norrby, 1978). The best studied example is that of vaccinia virus, the prototype member of the orthopox genus and a close relative of variola virus. Vaccinia, one of the largest and most complex viruses known, has a programmed series of interactions with the host cell that involve wrapping by two membrane cisternae of different subcellular origin during its assembly and maturation. An intriguing characteristic of this assembly process of vaccinia virus is that it results in two different infectious forms. The first infectious form, the intracellular mature virus (IMV), is surrounded by a membrane cisterna derived from the intermediate compartment (Sodeik, et al., 1993). Infectious IMV are released when the cell lyses due to the cytotoxic effects of infection. Alternatively, a small proportion of IMV, can undergo a second wrapping step by a cisternal domain derived from the *trans* Golgi network (Payne, 1980, Payne and Kristensson, 1985, Schmelz, et al., 1994). This form is called the intracellular enveloped virus (IEV) and escapes from the cell by fusion of its outer membrane with the plasma membrane of the host, thereby releasing the second infectious form called the extracellular enveloped virus (EEV) (Blasco and Moss, 1991, Dales, 1971, Morgan, 1976,

Payne, 1980). During the fusion of IEV with the plasma membrane, a small proportion of EEV particles are not released into the media but remain associated with the outside of the cell. These particles are refered to as cell-associated enveloped virus (CEV) (Blasco and Moss, 1992).

The first indication that vaccinia virus was able to interact with the cytoskeleton during its complex assembly process came from high voltage electron microscopy studies which showed virus particles at the tips of large microvilli projections in infected cells (Stokes, 1976). These projections were larger than the normal cellular microvilli which lacked virus particles. Subsequent studies confirmed that these vaccinia-tipped projections contained actin, as well as the actin cross-linking proteins alpha actinin, filamin and fimbrin but not tropomyosin or myosin (Hiller, et al., 1981, Hiller, et al., 1979). Furthermore, inhibition of virus assembly prevented the formation of the large microvilli suggesting that these structures were virally induced (Krempien, et al., 1981).

In light of the effects of bacterial pathogens on the actin cytoskeleton we have recently re-examined the effects of vaccinia virus on the actin cytoskeleton (Cudmore, et al., 1995). Infection by vaccinia virus not only results in the formation of virally-induced microvilli on the cell surface but also in the disruption of actin stress fibres and the formation of actin tails in the cytoplasm of the host cell that are very reminiscent of those seen in bacterial systems. Studies using a mutant virus which cannot form IEV, as well as infection with wild type virus in the prescence of a drug which prevents IEV formation, demonstrated that it is the IEV that is able to recruit actin to form tails. Vaccinia virus uses these actin tails to move around in the cytoplasm of the host cell at a speed of 2.8 μm/min and to project into and infect neighbouring cells (Cudmore, et al., 1995). The existence of actin-based motility in vaccinia virus suggests that diverse cellular pathogens have developed a common mechanism to exploit the host actin cytoskeleton as a means to facilitate their spread between cells.

In order to learn more about the process of actin tail mediated motility, we have analyzed the structure and dynamics of actin filaments in tails induced by vaccinia virus. Using rhodamine actin incorporation into permeabilized cells, we have shown that nucleation and growth of actin filaments occurs in a polarized fashion from the viral surface. Furthermore, the appearance of the actin filaments in the tails nucleated by the viral membrane is strikingly similar to the organization and polarity of actin filaments at leading edge of motile cells.

MATERIALS AND METHODS

Immunofluorescence microscopy : HeLa cells were grown, infected and fixed at 8h post infection (p.i.) as previously described (Cudmore, et al., 1995). Infected cells were labelled with anti-14kD viral antibodies (Rodriguez, et al., 1985) and either rhodamine or bodipy phalloidin (Molecular Probes). For maximium resolution, all immunofluoresence experiments were examined and recorded with 63X or 100X lenses in a Zeiss Axiophot microscope. Negatives were printed and scanned on a flat bedscanner to convert prints to digital images that were enlarged and annotated using the Adobe 3.0 software package.

Electron microscopy: HeLa cells were grown and infected with vaccinia virus strain WR at a multiplicity of infection of 1 PFU/cell as described (Doms, et al., 1990). For S1 myosin labelling, infected cells were washed at 16 hours p.i. with ice cold PBS and incubated with 5mg/ml S1 myosin in 0.1M phosphate buffer pH 6.8 (PB) and 0.2 mg/ml saponin for 30 mins on ice. The cells were washed twice with PB and subsequently fixed in 1% gluteraldehyde, 2% tannic acid and 50mM phosphate buffer pH 6.8 for 30 mins at room temperature. After another wash in PB, the cells were post fixed in 1% OsO_4 and 1.5% $KFe(Cn)_6$ for 30 mins on ice in the dark. Following three rinses in distilled water, the samples were dehydrated in 50% ethanol and stained overnight in 70% ethanol saturated with uranyl acetate. The following day the dehydration was continued and the cell monolayers were embedded in EPON. Parallel sections of the embedded cell monolayers were cut using a Reichert microtome. Sections were post-stained with 4% uranyl acetate for 5 mins followed by 1% lead citrate for 3 mins, and observed in a Philips 400 electron microscope.

Cell permeabilisation experiments : For these experiments the method of Symons and Mitchison (1991) was used with some minor modifications. Briefly, HeLa cells were grown on uncoated 11mm glass coverslips for 24 hours before infection with virus. At 8h p.i. the cells were transferred to observation medium (OM ; Bicarbonate free MEM buffered with 20mM Hepes, pH 7.4, 10% FCS, penicillin and streptomycin) at 37°C. Before the experiment the cells were cooled to room temperature and the subsequent experiments carried out at this temperature. The coverslip was incubated cell side down on two drops of rinsing buffer (RB ; 20mM Hepes pH 7.5, 138mM KCl, 4mM $MgCl_2$ and 3mM EGTA) and and then permeabilised for 30 seconds on a drop of incubation buffer (IB ; RB plus 0.2mg/ml saponin). A 10 mg/ml stock solution of rhodamine G-actin (Cytoskeleton, USA) stored at -80°C was pre-thawed, diluted 1:10 with G-actin buffer (2mM Tris pH8.0, 0.1mM ATP, 0.1mM DTT and 0.1mM $CaCl_2$) and clarified for 20 mins at 26psi in an airfuge at 4°C. It was then diluted to a final concentration of 1.0 or 0.3 µM in IB plus 1 mM ATP. The coverslips were incubated on 20 µl drops of rhodamine actin for various times from 5 secs to 10 mins. After incubation in rhodamine actin

the cells were fixed in 3% PFA in CB for 10 mins. The coverslips were then permeablized in 0.1% TX-100 for 1 min and further fluorescence labelling carried out as described above.
For myosin inhibition experiments 3,4-butanedione monoximide (BDM) was added to rhodamine actin to a final concentration of 10 mM from a freshly made 1 M stock in water prior to incubation with permeablized cells as described above.
All permeabilzation incubation experiments were examined and recorded using the EMBL confocal microscope facility. The resulting aligned digital images were merged and false colour added using the Adobe 3.0 software package.

RESULTS

The structure of vaccinia actin tails: Cells stained with bodipy phalloidin 6 hours or later after infection with vaccinia virus show numerous actin tails and projections that are not seen in uninfected cells (Fig. 1). The number of actin tails and projections in each cell is variable, between 1-200 in the same infection experiment but their number increases with longer infection times. When virus particles extend from the plasma membrane the projections initially have a broad and constant diameter along their their length (Fig. 1). However, as the projections continue to extend, the region closer to the cell appears withered and thin (Fig. 1).

Closer inspection of the appearance of vaccinia-induced actin tails shows that although similar to those of bacterial pathogens, there are a number of differences in their organization. Rather than being smooth like those in the published images of bacterial comets, the vaccinia actin tails have a somewhat splayed appearance with branch like appendages extending outward randomly along their length (Fig. 2). These branches project out at an angle of about 45° with respect to the central axis of the tail , towards the virus particle end. This splayed appearance along the complete length is seen mainly in intracellular tails. Microvillar projections at the cell surface tend to be smoother with only the tips splaying outwards. In cases where projection tips do not splay, the region of actin in contact with the virus particle shows a clear cup-like structure (Fig. 2). The same cup-like structure is seen in intracellular tails but is less pronounced (data not shown).

For higher resolution studies using electron microscopy, we found that embedding the infected cells as a monolayer after myosin S1 decoration of the actin filaments and cutting sections parallel to the plane of the cells yielded the clearest images (Fig. 3 and 4). Despite this, it was difficult to obtain perfect sections along the plane of the virus and tail. Consequently, the lengths of tails observed in electron micrographs are shorter than in images obtained by fluorescence microscopy, since thin sections cut through a complete actin tail from head to tip will occur very rarely. However, the general overall appearance of the actin tail in the electron micrcosope is in good agreement with those in immunofluorescence microscopy (Figs. 3 & 4). In electronmicrographs actin filaments in the tail splay outwards, as suggested by the branches seen in fluorescence microsopy. This is especially evident in curled intracellular tails (Fig. 3). Thus the tail appears to be arranged almost like an "upside down Christmas tree" with the filaments oriented so that they extend outwards from the centre of the tail.

Although a number of different fixation and cell permeablization techniques were tried, it was difficult to preserve the structural integrity of membranes, both those surrounding the virus and

the plasma membrane, as well as the actin filaments. Consequently, the number of actin filaments that are seen to directly interact with virus particles is lower than predicted in comparison to the density of the tail immediately adjacent to the virus observed in immunofluoresce images. However, actin filaments are clearly seen in contact with the membrane around the virus particle (Figs. 3 and 4). In addition, when virus particles are projecting from the cell surface, a number of actin filaments from the tail are seen in contact the plasma membrane both in longitudinal (Fig. 4) and transverse sections (Fig. 5). From the transverse sections it is clear that actin filaments interact with the plasma membrane both at their fast-growing ends and along their lengths (Fig. 5). Electron micrographs of long projections with withered bases clearly show that actin is still present along the whole length of the projection, although at a much reduced density near the cell where they appear to be arranged in a much more parallel fashion (Fig. 5).

Polarity and length of actin filaments in the tail: Superposition of filaments over each other in the same section within the bulk of the tail viewed by electron microscopy makes polarity determination by myosin S1 decoration difficult. However, it is possible to discern the characteristic myosin S1 arrowhead polarity on filaments towards or at the edge of the actin tails in very thin sections (40-50nm). In all cases the barbed or fast growing end of the actin filaments point towards the virus (Fig. 4). Given that all filaments where arrowheads are visible show the same polarity, we assume that the filaments within the bundle also share the same polarity. As with filament polarity determination, it is difficult to measure the true length of individual actin filaments within the tail. In our electronmicrographs we find filaments of up to 0.74 μm, although this is probably an underestimation of the true length (Fig. 5).

Actin recruitment to viral particles is polarized: The fact that the barbed ends of the filaments point towards the virus particle suggests that actin monomers incorporate into tails at or near the virus surface. To investigate if this was indeed the case, we adopted the technique of Symons and Mitchison (1991), in which sites of actin polymerization are observed by the incorporation of rhodamine labelled G-actin into cells which are permeabilized with saponin. Phalloidin staining of uninfected cells permeablized with saponin confirmed that under conditions of our assay, cells still maintained a highly organized actin cytoskeleton that incorporated rhodamine actin into the leading edge, focal adhesions and stress fibres, even after 10 minutes of permeablization (Fig 6).

A 10 second incubation of permeabilized infected cells with 1.0 μM rhodamine G-actin resulted in incorporation of actin only at virus particles which had associated actin tails, but not into the tails themselves which were visualised with phalloidin, i.e. total F-actin (Fig. 7). Only a

proportion of virus particles recruited rhodamine actin, which is consistent with the proportion of virus particles which induce tails (Cudmore, et al., 1995). There was no apparent difference in the ability of virus particles to recruit rhodamine actin, whether they were on intracellular actin tails or extending outwards from the plasma membrane on actin projections (Figs. 7 & 8). Antibody labelling of virus particles together with rhodamine actin incorporation was used to examine whether the pool of dynamic actin was polarized in its distribution on the virus surface (Fig. 8). Both early and late incubation time-points actin recruitment onto the viral surface occurs in a polarized fashion immediately adjacent to the tail.

Incorporation of actin into the tail occurs at a similar rate to motility: When the length of incubation time with rhodamine G-actin was increased, incorporation of actin into the tail only occurred from the virus particle which remained covered in a bright cloud of G-actin (Fig. 7 & 8). No rhodamine actin incorporation was observed along the tail that did not originate from the virus particle, irrespective of incubation time. This observation suggests that the branch-like structures which extend along the length of intracellular tails do not form by the addition of actin monomers at their ends as they do not incorporate rhodamine actin from their tips. Although there is some varation between cells, generally after 1 minute, rhodamine actin incorporation was observed along 30-40% of the length of intracellular tails (Fig. 7). By 3 minutes the complete length of intracellular tails were labelled with rhodamine actin (Fig. 7). Incorporation of rhodamine actin into viral projections at the cell surface occurred at the same rate as that seen in intracellular tails. Experiments performed with 0.3 μM rhodamine actin, a value below the critical concentration for assembly of actin at the pointed end, 0.7-0.9 μM *in vitro*, but above the value of 0.1 μM for barbed end assembly, gave identical results with no qualitative difference in the rate of incorporation. The rate of rhodamine actin incorporation into tails in the presence of butanedione monoxime (BDM) was also indistinguible from control experiments (data not shown). BDM is a broad-spectrum inhibitor of the actin activated ATPase activity of non muscle myosin II, myosin V and probably most myosin isoforms (Cramer and Mitchison, 1995).

The site of actin incorporation becomes fragmented at the tip of projections: As figure 8 shows, the rhodamine actin incorporating structure in the virally induced projections from the cell surface, i.e. the actin nucleating surface on the virus particle, tends to be cup-shaped. However, in many cases these nucleating structures have fragmented into several foci, which are still able to actively recruit rhodamine actin (Fig. 9). We also occasionally see projections that are actively incorporating actin into these foci although there is no viral particle at the tip (data not shown). The simplest explaination for our observations is that the actin nucleation sites are now

present in the plasma membrane as a result of viral membrane fusion and are free to diffuse within the plasma membrane.

DISCUSSION

The interactions between actin filaments and membranes is poorly understood. Previous observations demonstrated that vaccinia virus is capable of inducing the formation of actin-rich microvilli during its infection cycle (Hiller, et al., 1981, Hiller, et al., 1979, Krempien, et al., 1981, Stokes, 1976). We have recently extended these earlier observations to show that the IEV form of vaccinia induces the formation of actin tails that are similar to the actin tails seen in cells infected with bacterial pathogens such as *Shigella, Listeria,* and *Rickettsia*(Cossart, 1995, Cossart and Kocks, 1994, Tilney and Tilney, 1993). The IEV form of vaccinia virus is surrounded by a membrane cisterna derived from the *trans* Golgi network (Schmelz, et al., 1994) and consequently it offers a unique opportunity to examine membrane-actin interactions in detail. As a first step towards a detailed characterization of the system, we have examined the structure and dynamics of the actin tail induced by IEV.

The ultrastructure of the vaccinia actin tail: Electron micrographs of both intracellular tails and microvilli-like projections, show many features that are consistent with the immunofluorescence images, suggesting that our fixation and extraction process has not drastically altered the structure of the tail. A common feature between the tails of vaccinia and *Listeria* is actin filament polarity. Although we cannot determine actin filament polarity in the bulk of the viral tail, both systems show that actin filaments at the edge of the tail have unidirectional polarity, with their barbed or fast-growing ends in the direction of motion (Fig. 3). Although similar in their polarity, we find that vaccinia tails contain longer actin filaments than the 0.2μm length filaments reported in bacterial systems (Tilney and Portnoy, 1989). Given the severe limitations for measurement from sections of actin tails, we suspect that the filaments may be significantly longer. The most striking difference between the two systems is seen in the organization of actin filaments in the tail. Actin filaments in vaccinia tails are oriented so that they splay outwards at a 45° angle from the central axis of the tail. This is not the case in *Listeria* tails where fluorescence polarization microscopy shows that filaments in the core of the tail appear to be randomly oriented, while those at the surface or shell of the tail are preferentially aligned parallel to the direction of movement (Zhukarev, et al., 1995). This difference in structural organization of actin filaments probably reflects a difference between the two systems in both the nature of the actin nucleation site, as well as the actin cross-linking proteins in the tail.

Nucleation of actin tails occurs asymmetrically at the viral surface: Under the conditions of our permeabilization assay the actin cytoskeleton remains intact and readily incorporates

rhodamine actin at leading edges and focal contacts. More importantly, the fact that actin tails show progressive rhodamine actin incorporation suggests that viral particles are still moving in our assay. From our results it is clear that the first stage of tail formation is the recruitment of G-actin, and not pre-formed actin filaments, to the virus particle. Furthermore, continued tail growth requires a constant recruitment of G-actin as viral particles remain coated in rhodamine actin at all stages of incorporation experiments. We observe that actin nucleation occurs in an asymmetric fashion on the virus particle surface, as is also observed for the bacterial comets (Kocks, et al., 1993). We are currently unable to explain why actin recruitement is polarized on the virus particle surface, given that the virus particle is covered in a membrane that has no obvious asymmetry. However, the virus particle is asymmetric in shape and in our electron micrographs, they are nearly always oriented with their long axes perpendicular to the tail.

Incorporation of rhodamine actin into the tail only occurs from the virus surface and not from internal sites along the tail. Thus, actin branches on intracellular tails do not incorporate label from their tips. This is an important observation as it suggests that the only free ends available for polymerization of actin monomers are found at, or near the virus surface and that filaments within the tail or branches are blocked from further addition of actin. We find that the rate of incorporation is the same in intracellular tails and projections at the cell surface. Given that the virus particle at the tip nucleates actin tail assembly, a constant supply of actin monomers must be provided at the projection tip even when extentions are more than 20 μm long. Due to the actin density within the tail, it is highly likely that the pool of actin is supplied by filaments depolymerizing at the base of the tail. We also find that the rate of incorporation of rhodamine actin is the same regardless of whether it is used above or below the critical concentration for assembly of actin at the pointed end *in vitro*. Hence polymerization only occurs at the free barbed ends found at the virus particle surface, in agreement with filament polarity.

Movement of the viral particle is driven by actin polymerization.

Elegant photoactivation experiments have shown that the rate of *Listeria* motility is proportional to the length of the tail (Theriot, et al., 1992). Furthermore, this rate is equal to the rate of actin filament growth at the bacterial surface suggesting that motility is driven by continuous polymerization and release of actin filaments and that mysoin motors are not involved (Theriot, et al., 1992). To date myosin has not been identified in the tail of any bacterial pathogen by immunofluorescence microscopy. We have previously shown that vaccinia moves at a rate of 2.8 μm/min (Cudmore, et al., 1995). If vaccinia virus moves by a similar mechanism, based on this average speed we would expect that tails of length between 6.4-9.6 μm would show 100% rhodamine incorporation in about 2.5-3.0 minutes. This calculation is consistent with our observations. Thus, qualitatively the rate of actin polymerization at the virus surface is equal to

its rate of movement, suggesting that actin assembly alone can generate vaccinia motility. Our BDM inhibition experiments, although not conclusive as it is not known whether BDM inhibits all myosin isoforms, are extremely suggestive that no myosin motor is involved in the motility process. This is not unexpected as based on the organization of myosin and actin in muscle, the actin filament polarity in the tail is incompatible with a myosin driven motility.

Given that a similar mechanism of actin polymerization drives the motility of vaccinia and bacterial pathogens, why are their rates of motility so different? We have measured vaccinia motility as 2.8 μm/min whereas values for *Listeria* between 6-60 μm/min can be found in the literature (Cossart, 1995, Dabiri, et al., 1990, Theriot, et al., 1992) . It is known that the rate of motility in *Listeria* is proportional to the tail length and we assume that the same holds true for vaccinia. Therefore, using the data in Theriot et al., (al. 1992) with a tail length distribution of 6.4-9.6 μm for vaccinia we would expect viral particles to move at 12-16 μm/min. The fact they do not suggests that other factors are important. Clearly, density of actin filaments will be an important determinant in the rate of movement. From our observations it is clear that actin filaments in the vaccinia tail are extremely dense and at least as dense as those in *Listeria* tails (compare Figs. 3-5 with Figs. 16 and 17 (Tilney and Portnoy, 1989) and Fig 4B (Kocks, et al., 1992)). The shape of the particle being propelled by the actin tail may play an important determining factor. However, the rate of movement of *E.coli* expressing IcsA from *Shigella flexneri* in *Xenopus* egg extracts shows a similar range of speeds irrespective of whether their long axis is parallel or perpendicular to the direction of movement (Goldberg and Theriot, 1995). Given that the shape of the object does not seem to effect the rate of movement, why then if vaccinia particles are smaller than bacteria and presumably easier to move through the cytoplasm are the rates of movements not similar? We would like to suggest that a large determining factor is the difference in actin filament organization between the two systems. However, the molecular mechanisms responsible for these differences must be addressed by more detailed analysis.

Transfer of viral-actin nucleation sites to the plasma membrane: One feature that was noticeable in rhodamine actin incorporation experiments was that in long projections emerging from the plasma membrane actin incorporation sites were often fragmented into several foci (Fig. 8). In the most extreme cases, the incorporation of rhodamine actin occured at the tips of these foci. We would like to suggest that these foci originate when the outer membrane of the IEV fuses with the plasma membrane to release the EEV, the second infectious form of vaccinia virus (Fig. 10). Such a fusion event would transfer actin nucleation sites from the membrane around the IEV to the plasma membrane where nucleation appears to continue, despite the fact that the particle is now localized on the outerside of the plasma membrane (Fig. 10). In support

of this hypothesis we often see virus particles which appear to be on the outside of microvillar projections, suggesting that they have already fused with the plasma membrane (Fig 3A). That these particles are indeed EEV, can be confirmed by conventional thin section electron microscopy analysis under conditions that avoid cell permeabilization (data not shown). A similar conclusion can be drawn from images in the original high voltage microscopy study of vaccinia virus release by Stokes (Stokes, 1976). Consistent with this, it has previously been reported that the IEV is released from the cell by fusion of its outer membrane with the plasma membrane, releasing the EEV (Blasco and Moss, 1991, Blasco and Moss, 1992, Dales, 1971, Ichihashi, et al., 1971, Morgan, 1976). However, some of the EEV can remain attached to the outer surface of the cell, these being refered to as CEV (Blasco and Moss, 1991, Blasco and Moss, 1992). It has been proposed that while the EEV is responsible for long range spread of virions (Appleyard, et al., 1971, Boulter and Appleyard, 1973, Payne, 1980), that the role of the CEV is in direct cell to cell spread (Blasco and Moss, 1992). We believe that the virus particles on the outer suface of projection tips are CEV and thus actin polymerzation provides the mechanism by which these particles contact neighbouring cells in order to cause the direct cell to cell spread of infection.

Conclusions: Actin filaments at the leading edge of motile cells are not organized perpedicular to the plasma membrane but rather in an orthogonal network at an angle of 45° (Small, et al., 1995). It is striking that the organization of actin filaments nucleated from the membrane surrounding vaccinia virus is very reminiscent of the leading edge, both in organization and polarity. Given the parallels between the two systems we believe that a detailed understanding of the interaction between the nucleating complex in the outer membrane of vaccinia virus and actin filaments will provide further insights into actin-membrane interactions at the leading edge of motile cells.

ACKNOWLEDGEMENTS

We would like to thank Dr.s Ernst Steltzer and Sigrid Reinsch for advice concerning confocal microscopy, Dr. Michael Glotzer for advice on imaging, Dr. Daniella Klaus for a gift of S1 myosin and Dr. Rafael Blasco for interesting discussions on virus-membrane fusion. We would also like to thank Cytoskeleton, USA for rhodamine-actin and Drs. Antony Hyman, Rebecca Heald and Sigrid Reinsch for critical reading of the manuscript.

REFERENCES

1. **Appleyard, G., A. J. Hapel, and E. A. Boulter.** 1971. An antigenic difference between intracellular and extracellular rabbitpox virus. *J. Gen. Virol.* **13**:9-17.

2. **Blasco, R., and B. Moss.** 1991. Extracellular vaccinia virus formation and cell-to-cell virus transmission are prevented by deletion of the gene encoding the 37,000-dalton outer envelope protein. *J. Virol.* **65**:5910-5920.

3. **Blasco, R., and B. Moss.** 1992. Role of cell-associated enveloped vaccinia virus in cell-to-cell spread. *J. Virol.* **66**:4170-4179.

4. **Bohn, W., G. Rutter, H. Hohenberg, K. Mannweiler, and P. Nobis.** 1986. Involvement of actin filaments in budding of measles virus: studies on cytoskeletons of infected cells. *Virol.* **149**:91-106.

5. **Boulter, E. A., and G. Appleyard.** 1973. Differences between extracellular and intracellular forms of poxvirus and their implications. *Progr. Med. Virol.* **16**:86-108.

6. **Cossart, P.** 1995. Actin based bacterial motility. *Curr. Opinion Cell Biol.* **7**:94-101.

7. **Cossart, P., and C. Kocks.** 1994. The actin-based motility of the faculative intracellular pathogen *Listeria monocytogenes. Molec Microbiol.* **13**:395-402.

8. **Cramer, L., P., and T. Mitchison, J.** 1995. Myosin is involved in postmitotic cell spreading. *J.C.B.* **131**:179-189.

9. **Cudmore, S., P. Cossart, G. Griffiths, and M. Way.** 1995. Actin-based motility of vaccinia virus. *Nature.* **378**:636-638.

10. **Dabiri, G. A., J. M. Sanger, D. A. Portnoy, and F. S. Southwick.** 1990. Listeria monocytogenes moves rapidly through the host-cell cytoplasm by inducing directional actin assembly. *Proc.Natl.Acad.Sci.USA.* **87**:6068-6072.

11. **Dales, S.** 1971. Involvement of membranes in the infectious cycle of vaccinia, p. 136-144. *In* G. W. Richter and D. G. Scarpelli (ed.), Cell Membranes: Biological and pathological aspects. Williams & Wilkins, Baltimore.

12. **Doms, R. W., R. Blumenthal, and B. Moss.** 1990. Fusion of intracellular- and extracellular forms of vaccinia virus with the cell membrane. *J. Virol.* **64**:4884-4892.

13. **Giuffre, R., M., D. Tovell, R., C. Kay, M., and D. Tyrell, L.** 1982. Evidence for an interaction between the membrane protein of a paramyxovirus and actin. *J. Virol.* **42**:963-968.

14. **Goldberg, M., B., and J. Theriot, A.** 1995. Shigella flexneri surface protein IcsA is sufficient to direct actin-based motility. *Proc.Natl.Acad.Sci. USA.* **92**:6572-6576.

15. **Hiller, G., C. Jungwirth, and K. Weber.** 1981. Fluorescence microscopical analysis of the life cycle of vaccinia virus in the chick embryo fibroblasts. *Exp Cell Res.* **132**:81-87.

16. **Hiller, G., K. Weber, L. Schneider, C. Parajsz, and C. Jungwirth.** 1979. Interaction of assembled progeny pox viruses with the cellular cytoskeleton. *Virology.* **98**:142-153.

17. **Ichihashi, Y., S. Matsumoto, and S. Dales.** 1971. Biogenesis of poxviruses: Role of A-type inclusions and host cell membranes in virus dissemination. *Virology.* **46:**507-532.

18. **Kocks, C., E. Gouin, M. Tabouret, P. Berche, H. Ohayon, and P. Cossart.** 1992. L. monocytogenes-induced actin assembly requires the actA gene product, a surface protein. *Cell.* **68:**521-531.

19. **Kocks, C., R. Hellio, P. Gounon, H. Ohayon, and P. Cossart.** 1993. Polarized distribution of Listeria monocytogenes surface protein ActA at the site of directional actin assembly. *J. Cell. Sci.* **105:**699-710.

20. **Krempien, U., L. Schneider, G. Hiller, K. Weber, E. Katz, and C. Jungwirth.** 1981. Conditions for pox virus specific microvilli formation studied during synchronized virus assembly. *Virol.* **113:**556-564.

21. **Morgan, C.** 1976. Vaccinia virus reexamined: Development and release. *Virology.* **73:**43-58.

22. **Murti, K., G., M. Chen, and R. Goorha.** 1985. Interaction of frog virus 3 with the cytomatrix. III. Role of microfilaments in virus release. *Virol.* **142:**317-325.

23. **Payne, L. G.** 1980. Significance of extracellular enveloped virus in the *in vitro* and *in vivo* dissemination of vaccinia. *J. Gen. Virol.* **50:**89-100.

24. **Payne, L. G., and K. Kristensson.** 1985. Extracellular release of enveloped vaccinia virus from mouse nasal epithelial cells *in vivo*. *J. Gen. Virol.* **66:**643-646.

25. **Rodriguez, J. F., R. Janeczko, and M. Esteban.** 1985. Isolation and characterization of neutralizing monoclonal antibodies to vaccinia virus. *J. Virol.* **56:**482-488.

26. **Schmelz, M., B. Sodeik, M. Ericsson, E. J. Wolffe, H. Shida, G. Hiller, and G. Griffiths.** 1994. Assembly of vaccinia virus: The second wrapping cisterna is derived from the trans Golgi network. *J. Virol.* **68.** 130-147

27. **Small, J., V., M. Herzog, and K. Anderson.** 1995. Actin filament organization in the fish keratocyte lamellipodium. *JCB.* **129:**1275-1286.

28. **Sodeik, B., R. W. Doms, M. Ericsson, G. Hiller, C. E. Machamer, W. v. t. Hof, G. v. Meer, B. Moss, and G. Griffiths.** 1993. Assembly of vaccinia virus: Role of the intermediate compartment between the endoplasmic reticulum and the Golgi stacks. *J. Cell Biol.* **121.** 521-541

29. **Stokes, G. V.** 1976. High-voltage electron microscope study of the release of vaccinia virus from whole cells. *J. Virol.* **18:**636-643.

30. **Theriot, J., A., and T. Mitchison, J.** 1992. The nucleation-release model of actin filament dynamics in cell motility. *Trends Cell Biol.* **2:**219-222.

31. **Theriot, J., A., T. Mitchison, J., L. Tilney, G., and D. Portnoy, A.** 1992. The rate of actin-based motility of intracellular Listeria monocytogenes equals the rate of actin polymerization. *Nature.* **357:**257-260.

32. **Tilney, L., G., and M. Tilney, S.** 1993. The wily ways of a parasite: induction of actin assembly by Listeria. *Trends Microbiol.* **1**:25-31.

33. **Tilney, L. G., and D. A. Portnoy.** 1989. Actin filaments and the growth,movement and spread of the intracellular bacterial parasite, *Listeria monocytogenes. J. Cell. Biol.* **109**:1597-1608.

34. **Tyrell, D., L., and E. Norrby.** 1978. Structural polypeptides of measles virus. *J. Gen. Virol.* **39**:219-229.

35. **Zhukarev, V., F. Ashton, J. M. Sanger, J. W. Sanger, and H. Shuman.** 1995. Organization and structure of actin filament bundles in *Listeria* infected cells. *Cell Motil Cytoskel.* **30**:229-246.

FIGURE LEGENDS

Figure 1 : Overall appearance of vaccinia infected cells by immunofluorescence microscopy. Panels A and B show entire cells containing numerous actin tails which were fixed at 8h and 16h post infection respectively. The higher magnification images, C and D, show long projections from the cell surface with withered bases as well as shorter, newly formed projections. Such long projections are often observed to be over 20μm in length. Scale bar in B represents 25μm in panels A and B while that in D represents 20μm in C and D.

Figure 2 : High resolution images of intracellular tails and projections stained with phalloidin. A and B show branch like structures splaying outwards from intracellular tails. Panel C shows that the region of the actin tail in contact with the virus particle has a cup-like shape. Virus particles lie at the broader, more brightly stained end of the tails. Scale bar represents 3μm in all panels.

Figure 3 : Electron microscopy of S1 myosin decorated intracellular tails. Panel A shows a highly curled tail with filaments splaying outwards at a 45° angle to the central axis of the tail. Panel B shows two intracellular tails with actin filaments interacting directly with the virus particles. Note that the virus particles are oriented with their longer axes perp ndicular to the long axis of the tail. Stars indicate virus particles. Scale bars represent 400nm.

Figure 4 : Electron microscopy of virally-induced projections. In panel A the polarity of the S1 myosin decorated actin filaments can be discerned and is indicated by closed arrowheads. The barbed or fast-growing end of the filaments are oriented towards the virus particle. Interactions

between individual actin filaments and the plasma membrane are indicated by open arrowheads. The virus particle, labelled by the star, appears to be outside the plasma membrane. The length of a single filament, 440nm, is indicated. Panel B shows another projection where the virus particle still appears to be inside the plasma membrane. Scale bars represent 400nm.

Figure 5 : Electron microscopy of vaccinia induced projections, both longitudinal and transverse sections. A shows a long projection that lacks a virus particle at its tip. Membrane interactions with actin filaments are indicated by open arrowheads and a single long actin filament is also indicated. The density of actin filaments at the base of the tail is clearly reduced in comparison to the top. In addition, the filaments in the base tend to have a more parallel arrangement than at the top of the tail. B shows a transverse section through the top of a projection. The density distribution of actin filaments is consistent with longitudinal sections. Two orientations of actin filaments interacting with the plasma membrane are discernable: open arrows indicate examples where filaments ends are in contact while closed arrows show filaments interacting along their length. Scale bars represent 400nm.

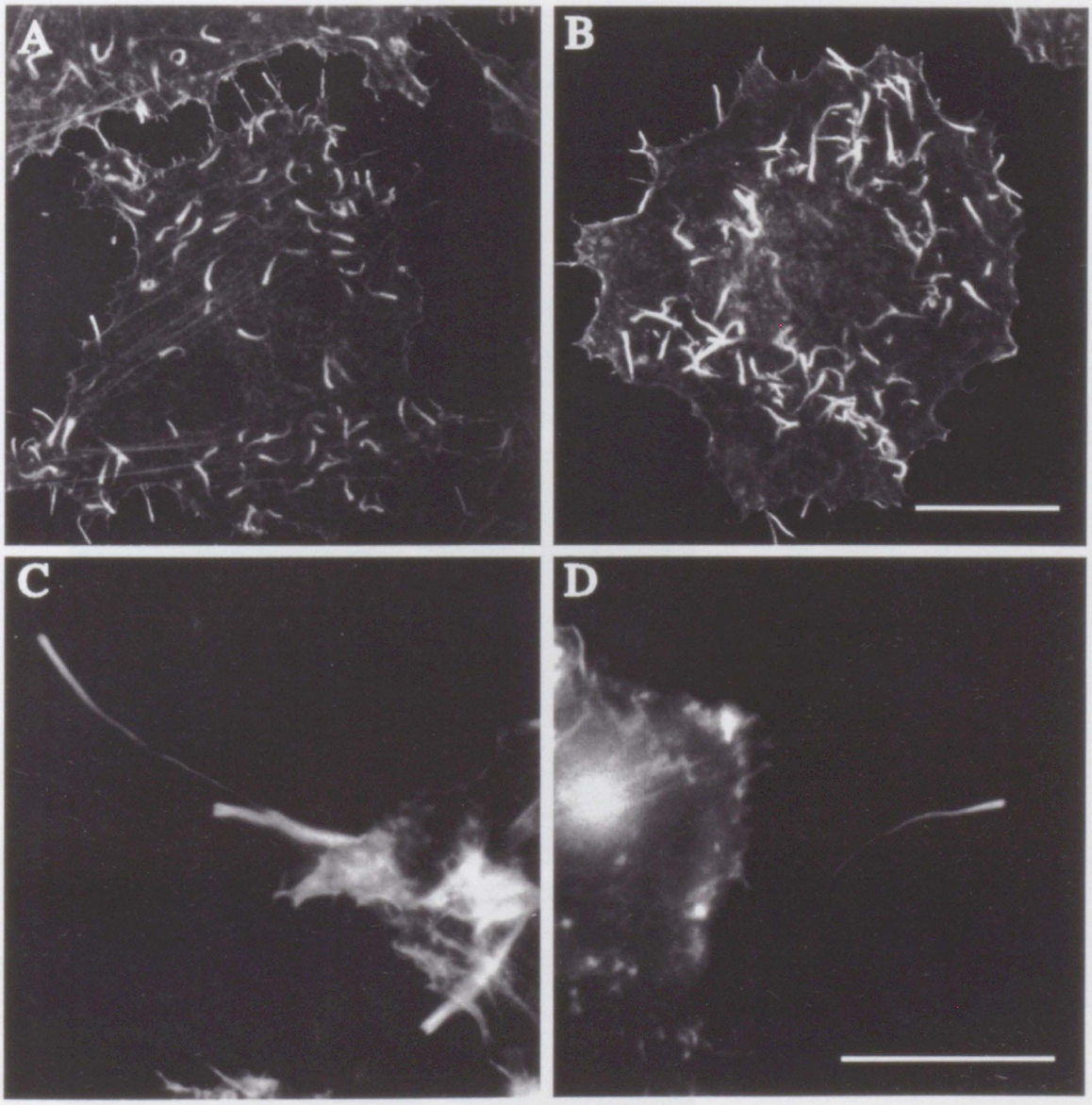
Figure 6 : Incorporation of rhodamine actin into permeabilized cells shows that actin cytoskeleton of an uninfected cell is both stable and dynamic after 10 minutes of permeabilization and incubation with exogenous rhodamine actin: A, the complete actin cytoskeleton visualised by biodipy phalloidin ; B, localization of rhodamine actin incorporation sites and C, merged false colour images of phalloidin (green) and rhodamine actin images (red) showing that although focal contacts have incorporated rhodamine actin, they also maintain a pool of unincorporated G-actin at their tips. Scale bar 20 μm.

Figure 7 : Incorporation of rhodamine actin into vaccinia actin tails occurs from the viral particle surface. Panels A, D, and G: total F-actin visualised by phalloidin; panels B, E and H: localization of rhodamine actin after 10 seconds, 1 minute and 3 minutes respectively. Panels C, F and I: merged false colour images of the phalloidin signal (green) and the rhodamine signal (red) for A & B; D & E and G & H respectively. From the images in the figure it is clear that viral particles recruit rhodamine G-actin to their surface which then becomes incorporated into the tail. After 10 seconds only virus particles are labelled with rhodamine G-actin but after 1 minute the rhodamine signal is seen about half way down the tail when compared to the phalloidin signal. After 3 minutes, rhodamine actin has incorporated down the complete length of the tails as judged by the rhodamine and phalloidin signals. In all merged panels it is noticeable that there is not 100% co-localization between the rhodamine signal on the virus particle and the phallodin signal of the tail suggesting the virus maintains a pool of G-actin on its surface. Scale bar 9 μm.

Figure 8 : Rhodamine actin incorporation combined with antibody labelling of virus particles. Panels A and D show virus particles while B and E show rhodamine actin incorporation after 10 seconds and 3 minutes respectively. C and F show merged false colour images of the virus particles (green) and the rhodamine signal (red). White arrows in the merged images highlight that there is not 100% co-localization of the virus particle and rhodamine signals indicating G-actin is recruited in a polarised fashion to the virus particle surface. Scale bar 8 μm.

Figure 9 : Actin nucleation sites at the projection tips fragment into foci. Panels A and D show rhodamine actin incorporation after 3 minutes. Panel B shows total F-actin visualised by biodipy phalloidin and panel E shows labelling of virus particles. C and F show merged false colour images of the rhodamine signal (red) and phalloidin or virus signal signal (green) for A & B and D & E respectively. White arrows in A to C indicate a branch near the tip of a projection incorporating rhodamine actin i.e. nucleating actin polymerization. White arrows in D to F highlight the fragmentation of the actin nucleating surface at the tip of a projection into discrete foci, many of which are not in contact with the virus particle. Scale bar 7 μm.

Figure. 10 : Model depicting the development of virally induced microvilli and fusion of the outer membrane of the IEV with the plasma membrane at the tip of this projection. The plasma membrane is shown in green and actin filaments in the projection are blue. The IEV is shown in black with its outer most membrane depicted in red. In panel A, the actin nucleation sites present in the viral membrane nucleate actin polymerization and consequently the projection extends outwards. B. The outer most membrane of the IEV form of vaccinia (red), along with its actin nucleation sites, fuses with the plasma membrane, releasing the CEV outsice the projection ready to infect neighbouring cells upon contact. C. The actin nucleation sites, which are now present in the plasma membrane, begin to diffuse but still continue to nucleate actin filaments as the projection extends.



Cudmore et al. Fig. 1

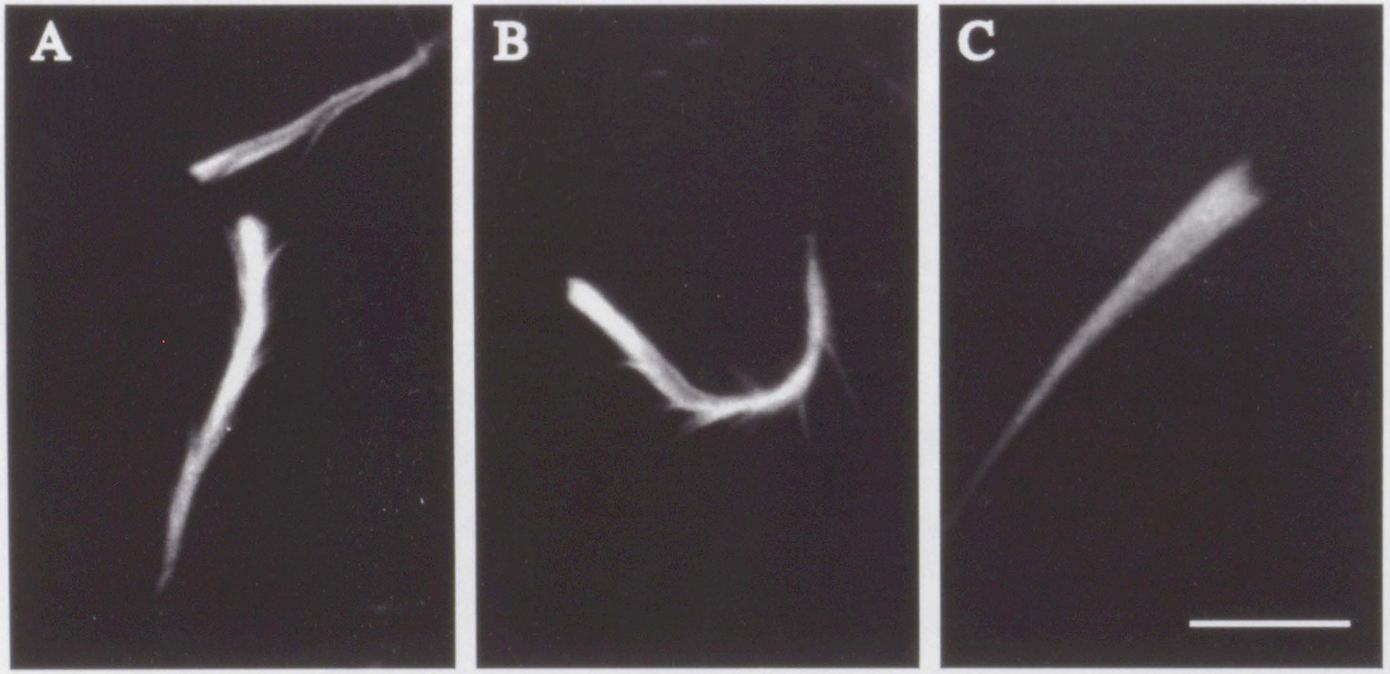


Figure 2 Cudmore et al

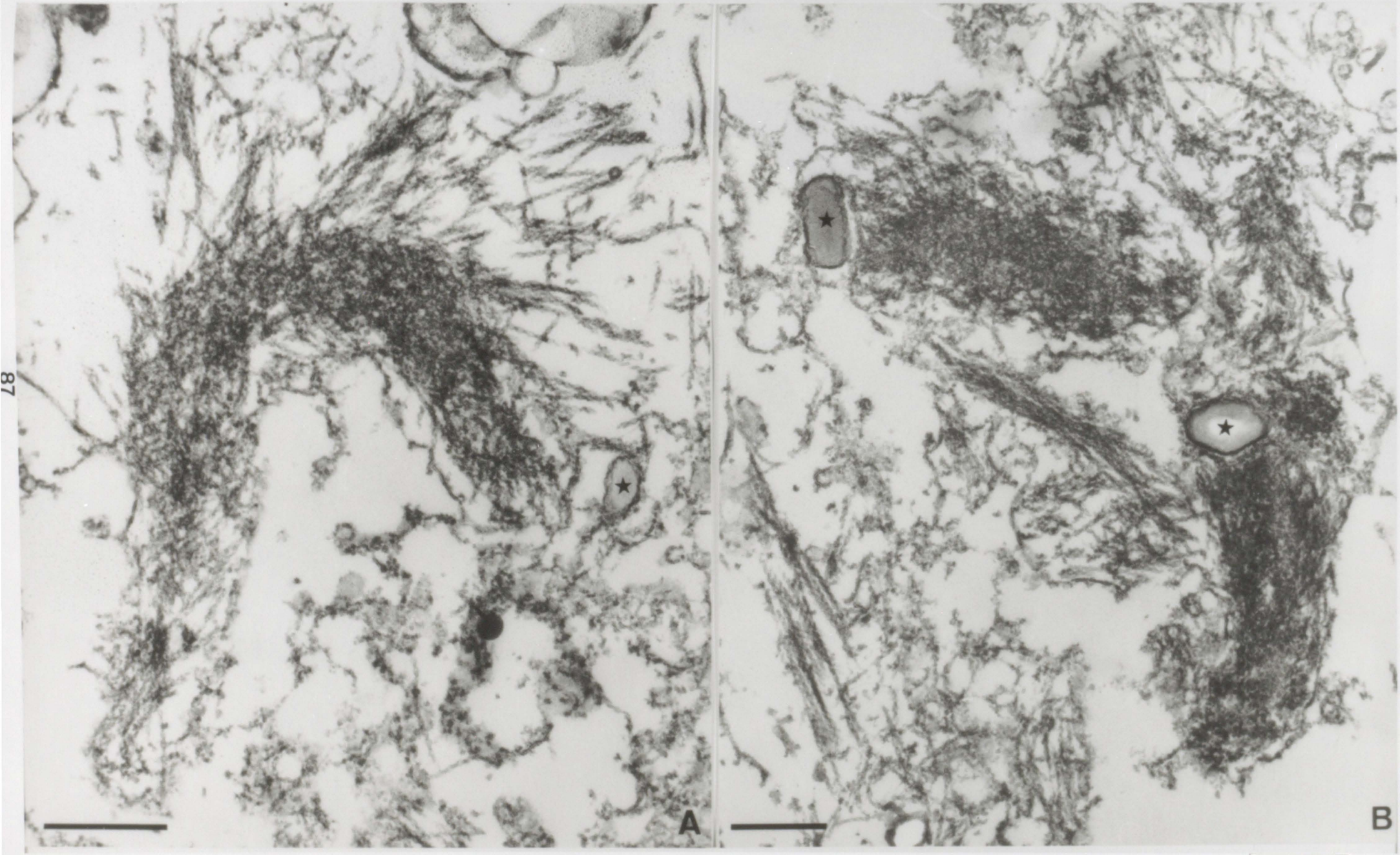


Figure 3

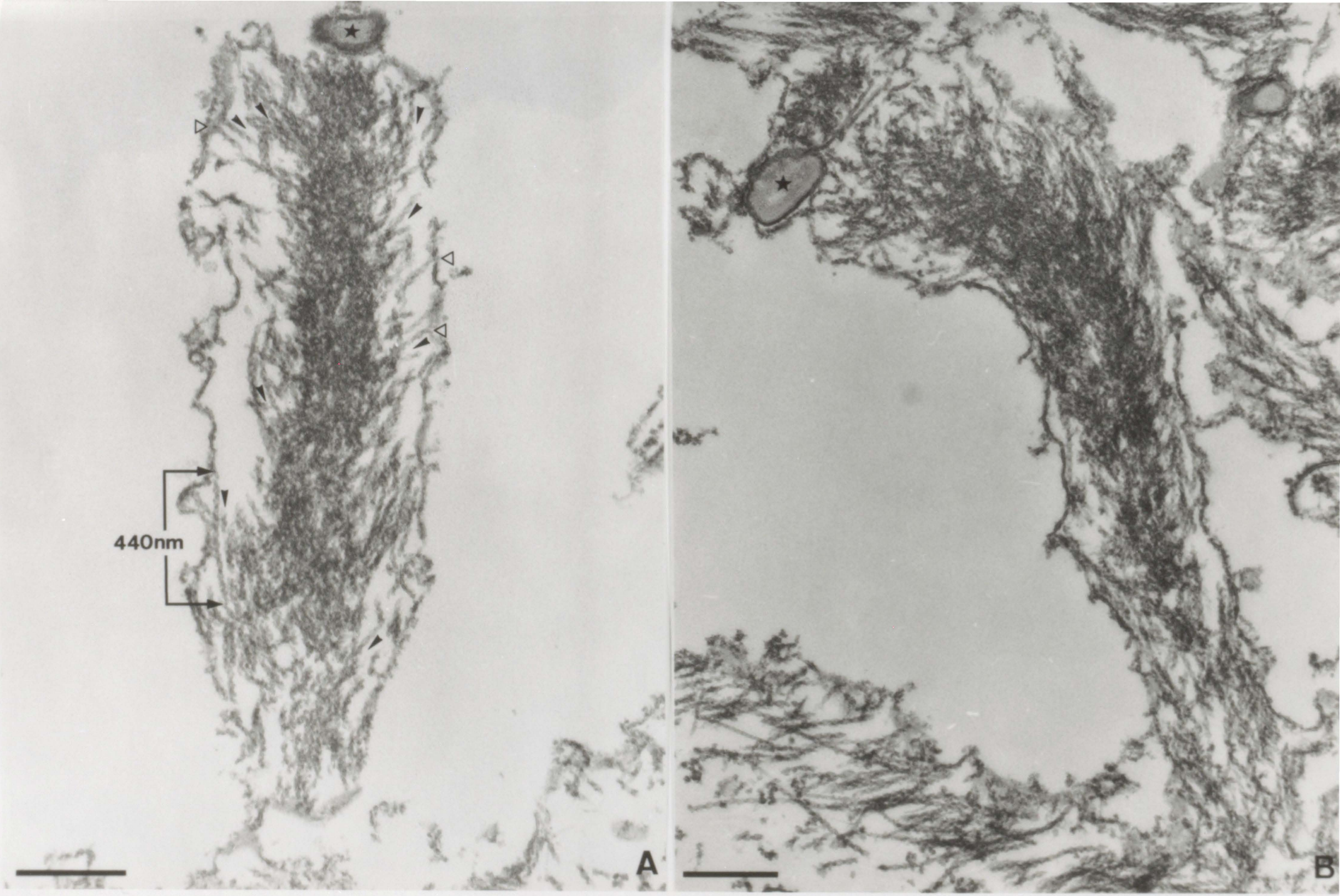


Fig 4

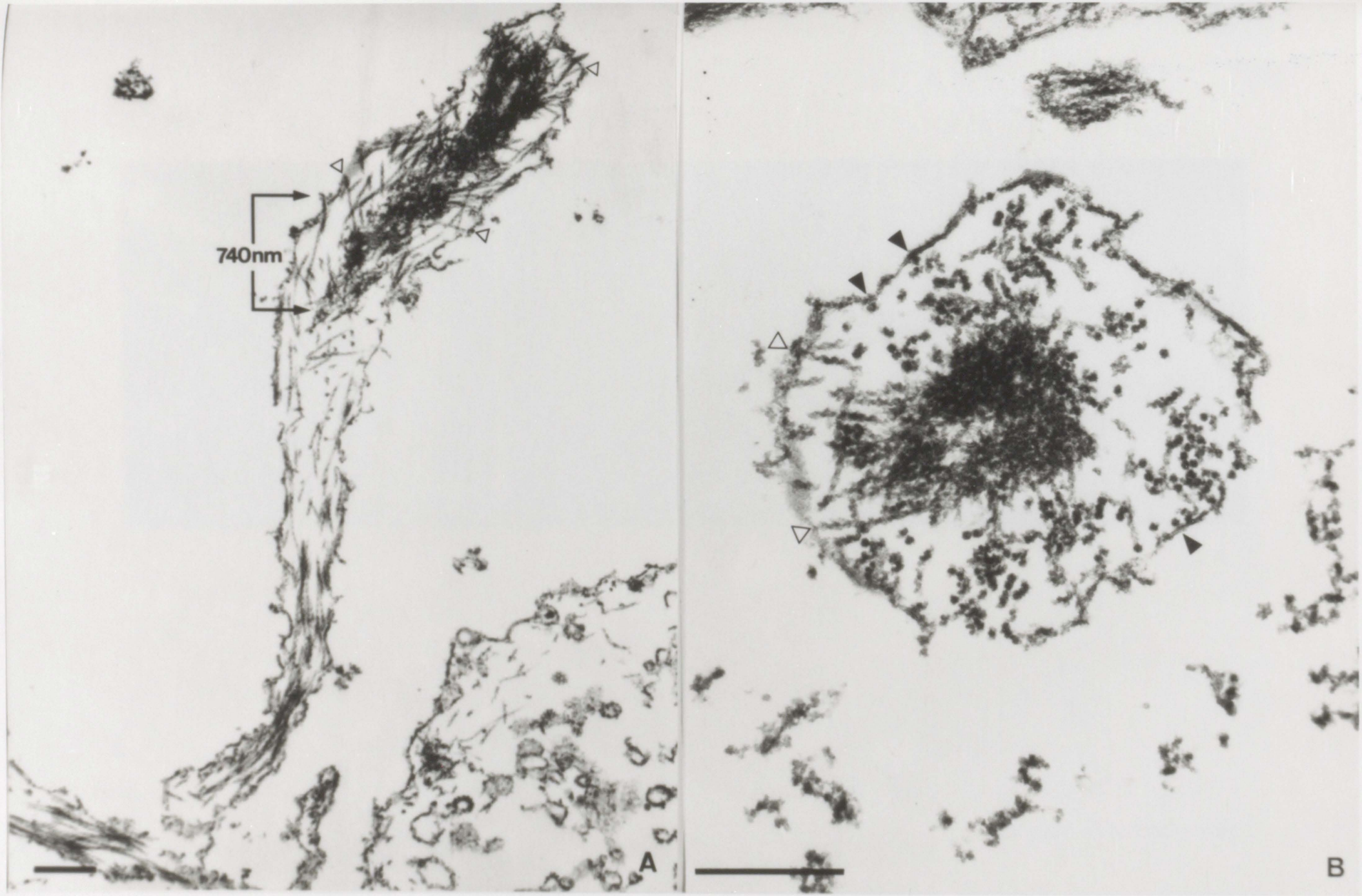


Fig 5

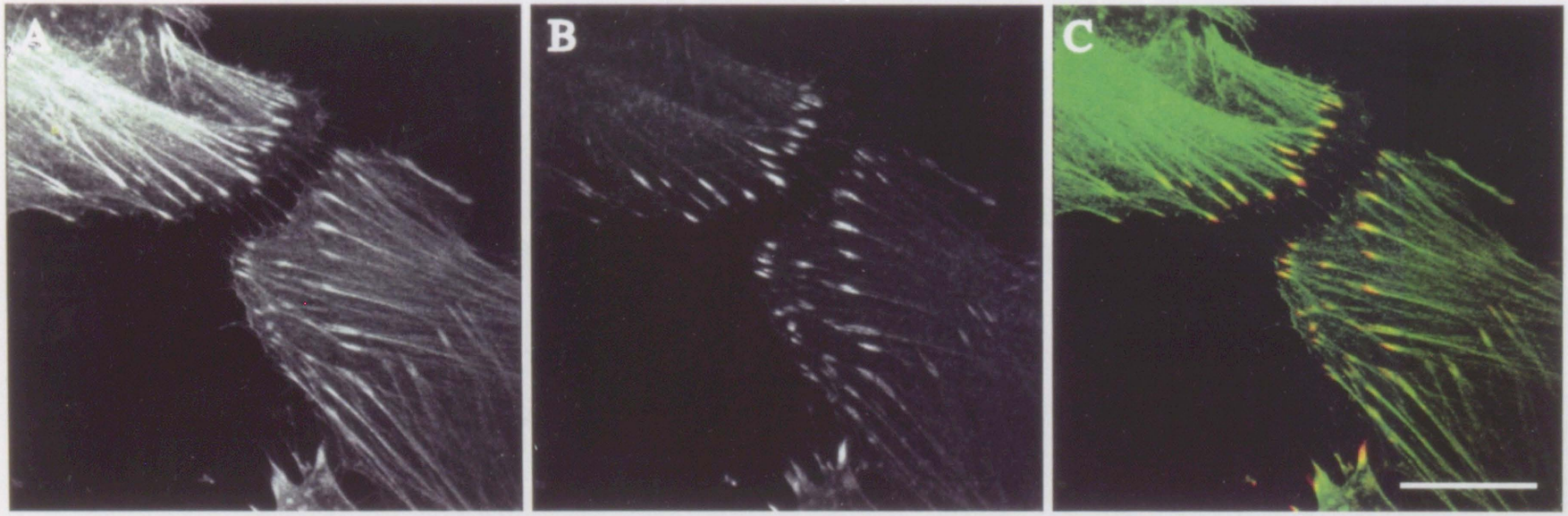


Figure 6 Cudmore et al.

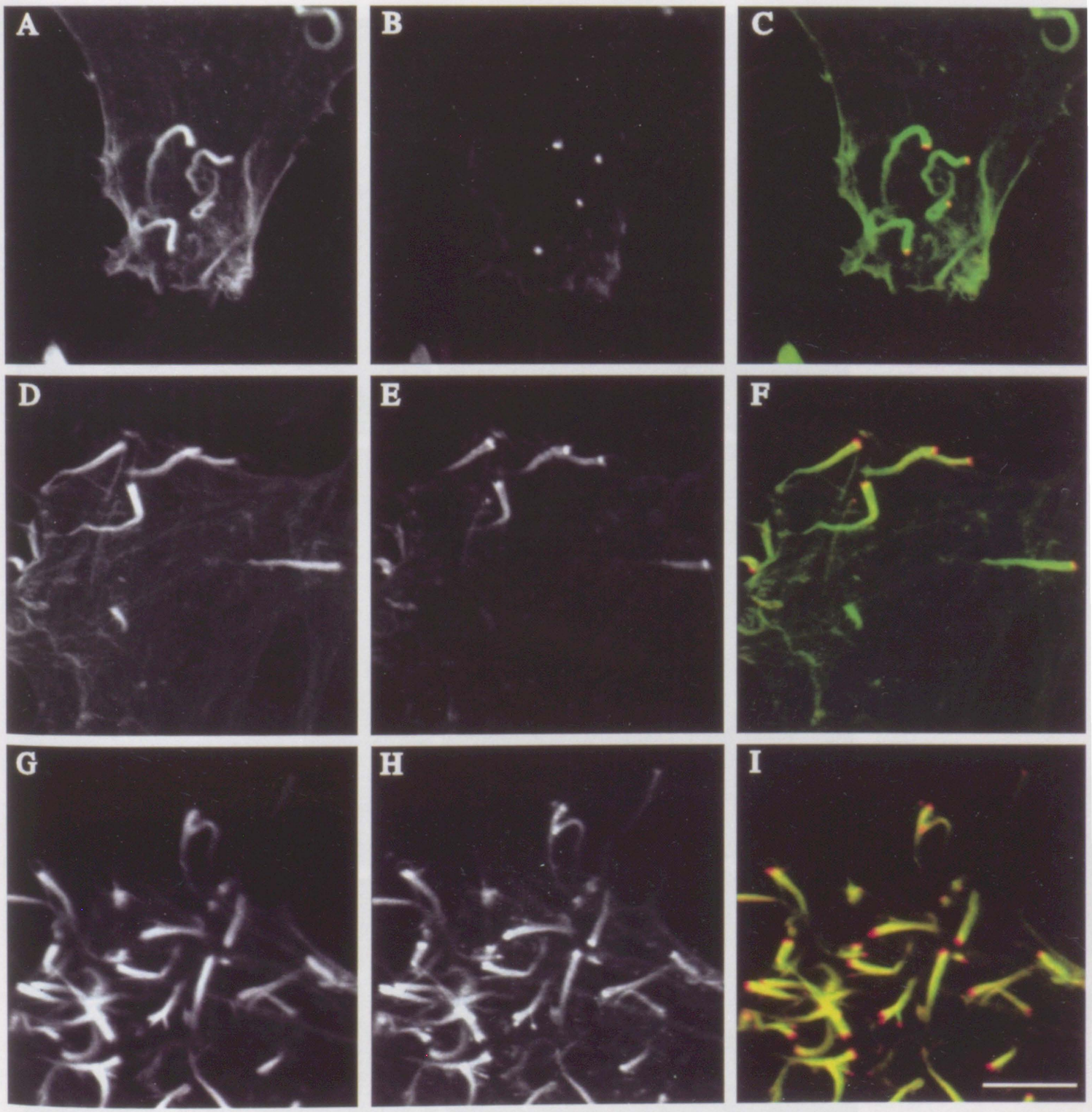


Figure7 Cudmore et al. 96

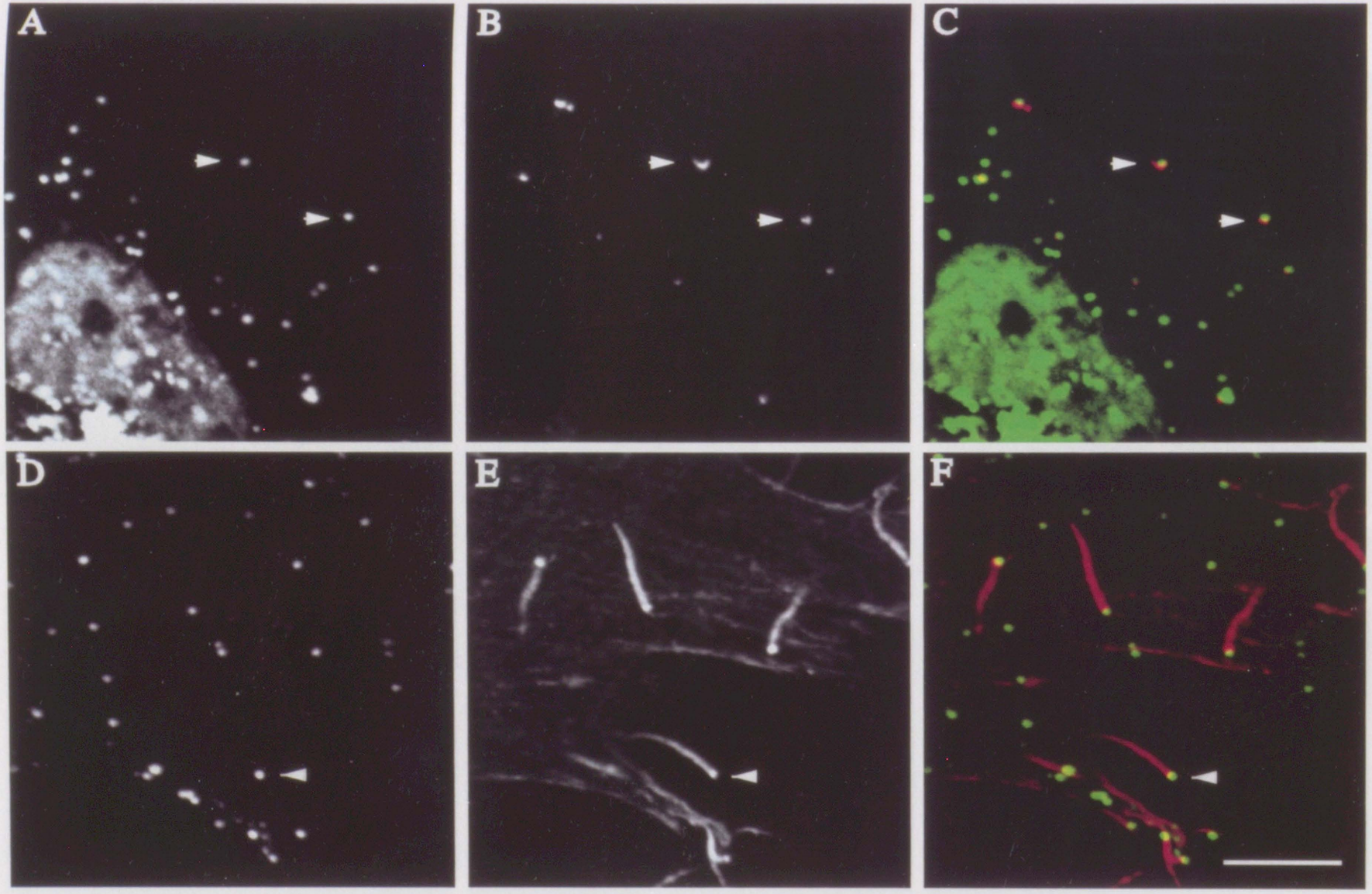


Figure 8 Cudmore et al.,

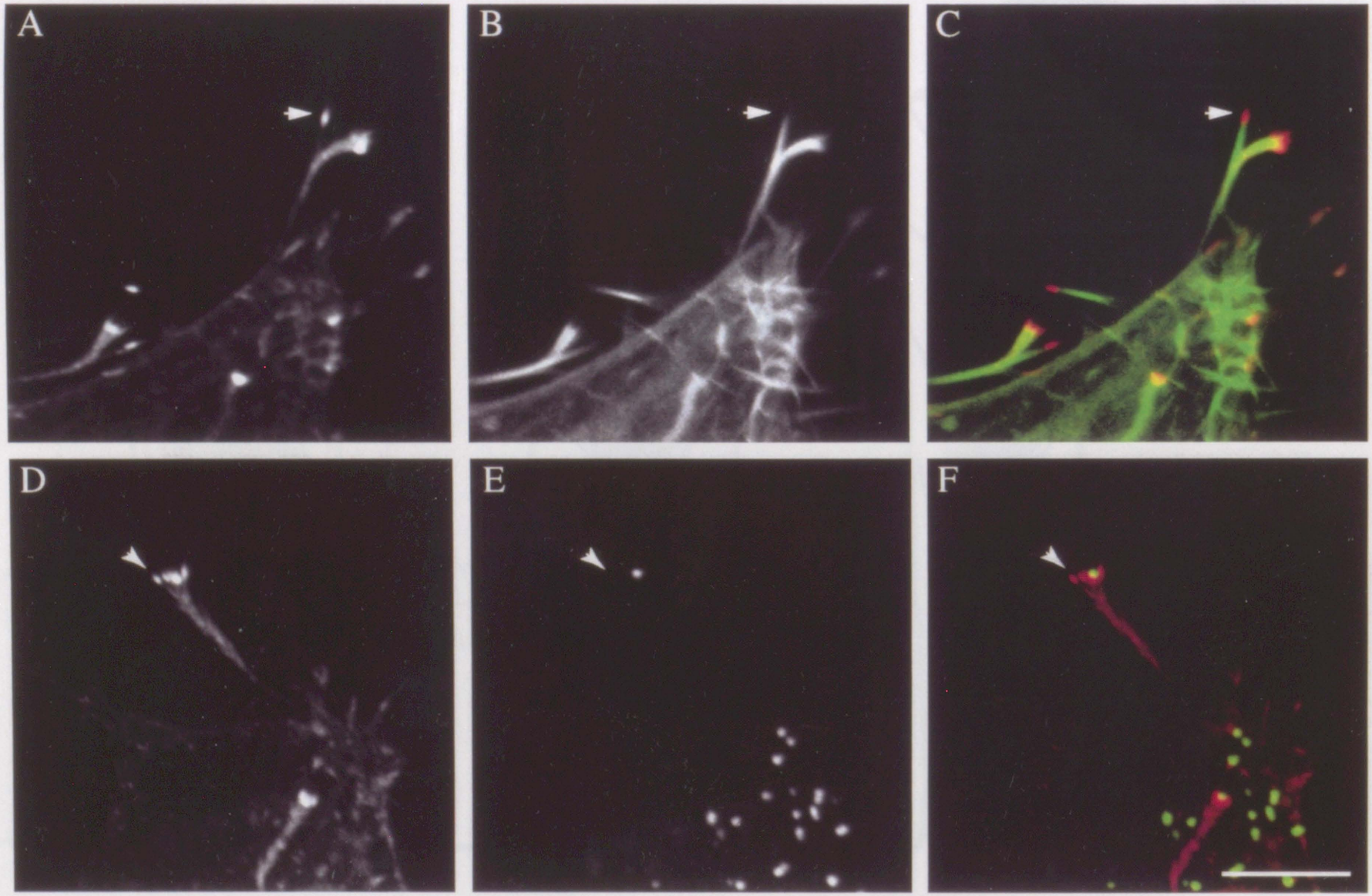


Figure9 Cudmore et al

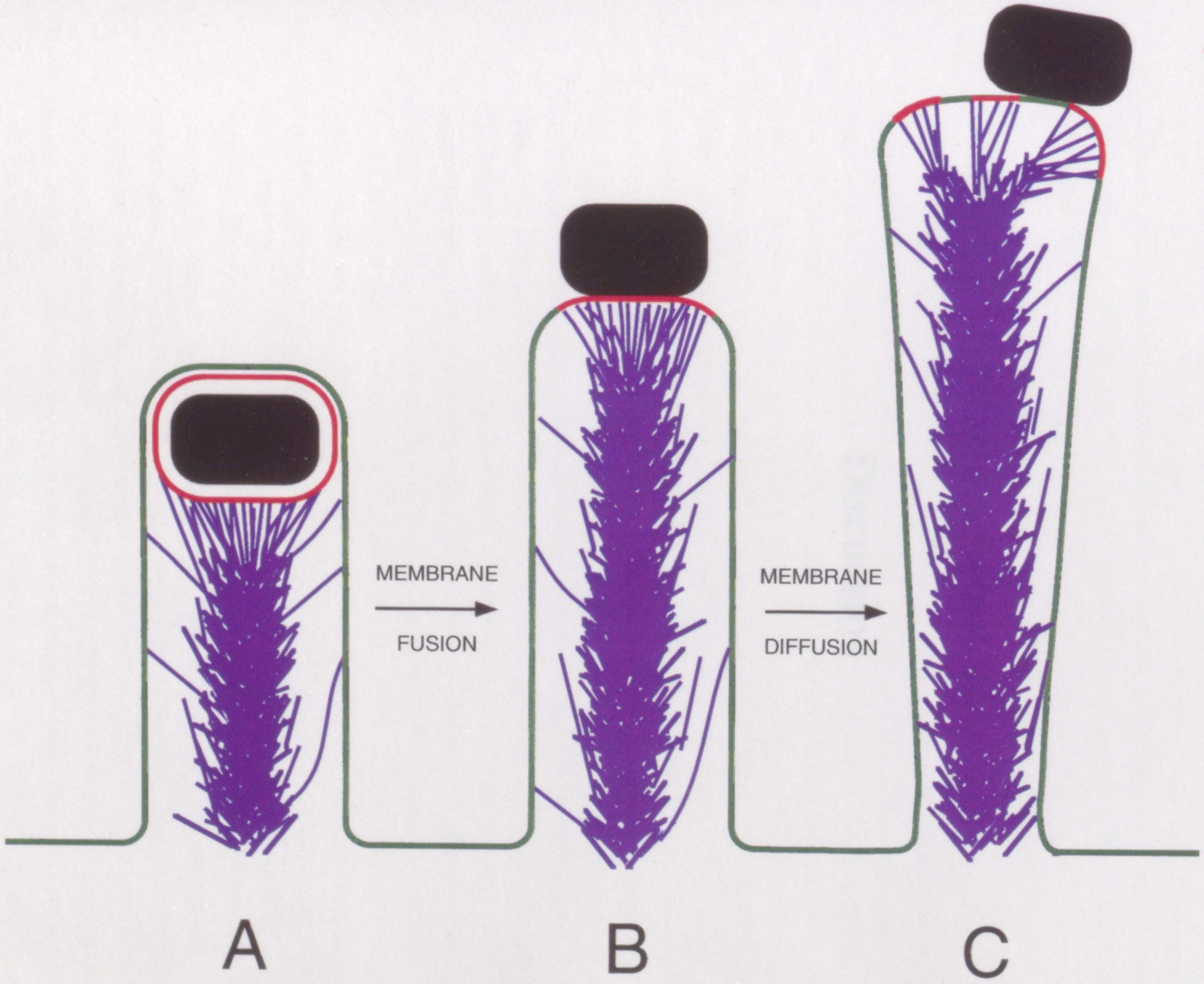


FIGURE 10

CHAPTER 5

Discussion

5.1 What has been learnt from this work ?

As most of the details of my work have been discussed at the end of the various chapters, I would like to present a review of the various assembly stages of vaccinia virus in relation to what has been learnt from both my research and the recent work of others. An updated version of the lifecycle is presented in figure 8, while a cartoon of the IMV structure is shown in figure 9.

5.1.1 Review of the vaccinia life-cycle

Vaccinia DNA is replicated in the cytoplasm of the infected host cell in specialised foci called "viral factories" (Cairns, 1960), which are observed close to the nucleus by immunofluorescence microscopy, when stained with DNA dyes such as DAPI or Hoechst. About 4 hours after infection late protein expression begins and infected cells can be labelled with antibodies to a variety of these viral proteins, including p35 (gene H3L) (Cudmore et al., manuscript in preparation), p32 (gene D8L) (see appendix for Sodeik et al., 1995), p39 (gene A4L) (chapter 2) and p21 (A17L) (Krijnse Locker et al., submitted). This labelling overlaps with that of the DNA but the signals do not co-localize completely (Sally Cudmore and Jacomine Krijnse Locker, unpublished observations) (Sodeik et al., 1994) suggesting that there are two distinct regions involved in the early steps of DNA replication and late protein expression. This was especially apparent when cells were labelled with antibodies against p39 (chapter 2), p35 (Cudmore et al, manuscript in preparation) or with antibodies against vaccinia core proteins (Krijnse Locker, unpublished results). The labelling of the protein factories occurs in distinct patches while the immunofluorescence staining of the DNA is more diffuse. These separate areas are also morphologically distinct by electron microscopy, with the protein factories apparent as electron dense areas close to the nucleus, while antibody labelling of the DNA indicates it is located in a more disperse pattern in the cytoplasm (Sodeik et al., 1993). There is no trace of DNA labelling in the protein factories, but it cannot be ruled out that this is not due to a problem of antibodies access in these factories. The distinction becomes even more obvious when cells are infected in the presence of rifampicin, which blocks viral assembly subsequent to DNA replication and protein expression (see section 1.5). Large electron-dense areas called "rifampicin bodies" accumulate in the peri-nuclear region of the cell which are composed of viral proteins (Payne and Kristensson, 1990) and are probably equivalent to the protein factories. Other structures, called inclusion bodies, have also been observed and shown to label with antibodies against p65, the target of rifampicin (see section 1.5) (Sodeik et al., 1994). The replicated DNA tends to accumulate in large striated structures, sometimes called "DNA crystalloids".

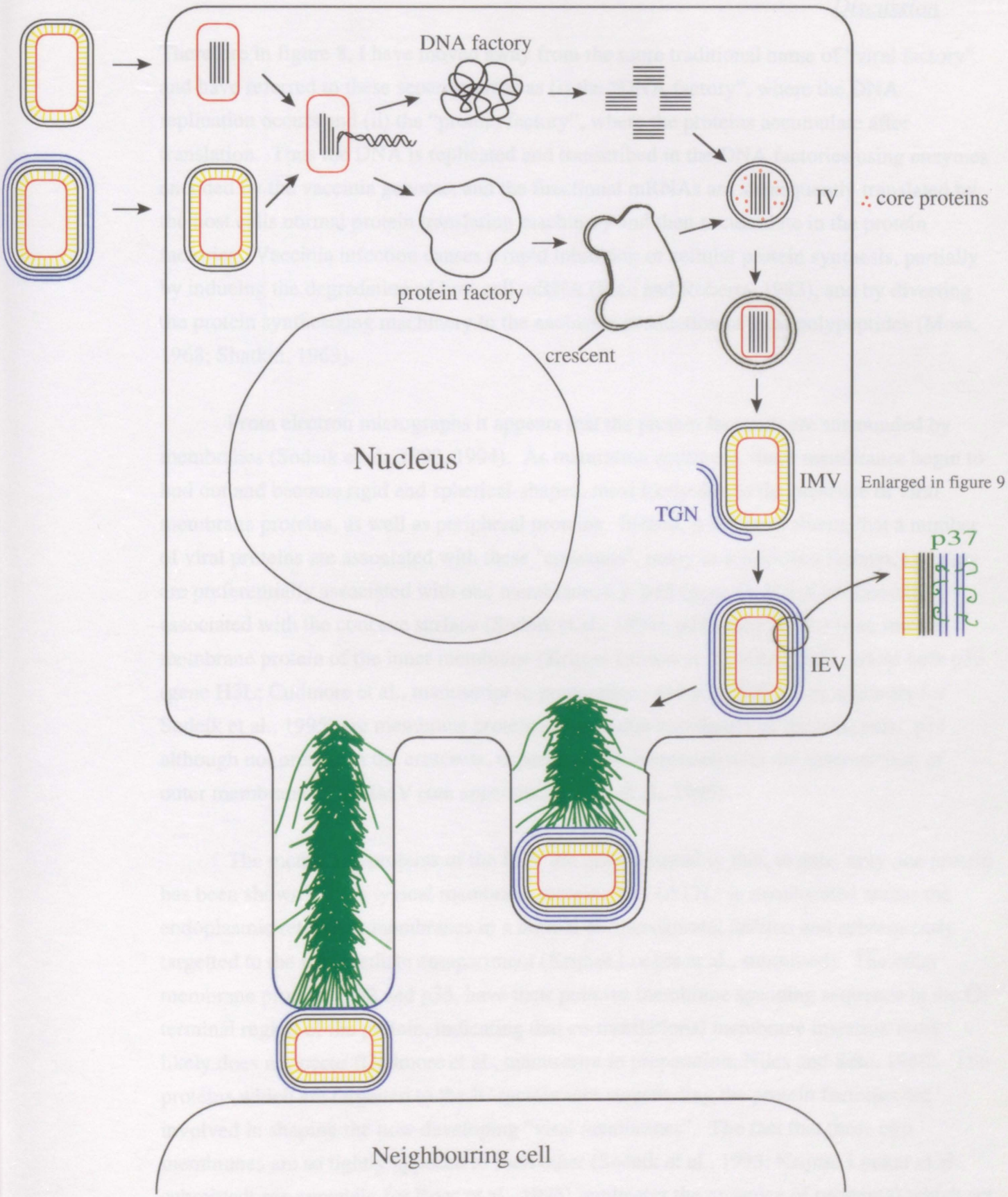


FIGURE 8: Vaccinia lifecycle

Therefore in figure 8, I have moved away from the more traditional name of "viral factory" and have referred to these separate areas as (i) the "DNA factory", where the DNA replication occurs and (ii) the "protein factory", where the proteins accumulate after translation. Thus the DNA is replicated and transcribed in the DNA factories using enzymes encoded by the vaccinia genome, and the functional mRNAs are subsequently translated by the host cells normal protein translation machinery and then accumulate in the protein factories. Vaccinia infection causes a rapid inhibition of cellular protein synthesis, partially by inducing the degradation of host cell mRNA (Rice and Roberts, 1983), and by diverting the protein synthesizing machinery to the exclusive production of viral polypeptides (Moss, 1968; Shatkin, 1963).

From electron micrographs it appears that the protein factories are surrounded by membranes (Sodeik et al., 1993, 1994). As maturation continues, these membranes begin to bud out and become rigid and spherical-shaped, most likely due to the presence of viral membrane proteins, as well as peripheral proteins. Indeed, it has been shown that a number of viral proteins are associated with these "crescents", many in a polarised fashion, i.e., they are preferentially associated with one membrane, e.g. p65 (gene D13L) is peripherally associated with the concave surface (Sodeik et al., 1994), p21 (gene A17L) is an integral membrane protein of the inner membrane (Krijnse Locker et al., submitted) , while both p35 (gene H3L; Cudmore et al., manuscript in preparation) and p32 (D8L) (see appendix for Sodeik et al., 1995) are membrane proteins of the outer membrane of the crescents. p14 , although not present in the crescents, is peripherally associated with the external face of outer membrane of the IMV (see appendix, Sodeik et al., 1995).

The membrane proteins of the IMV are quite unusual in that, to date, only one protein has been shown to be a typical membrane protein. p21 (A17L) is translocated across the endoplasmic reticulum membranes in a normal co-translational fashion and subsequently targetted to the intermediate compartment (Krijnse Locker et al., submitted). The other membrane proteins, p32 and p35, have their putative membrane spanning sequence in the C-terminal region of the protein, indicating that co-translational membrane insertion most likely does not occur (Cudmore et al., manuscript in preparation; Niles and Seto, 1988). The proteins which are targetted to the IC membranes surrounding the protein factories are involved in shaping the now developing "viral membranes". The fact that these two membranes are so tightly apposed to each other (Sodeik et al., 1993; Krijnse Locker et al., submitted; see appendix for Roos et al., 1996) implicates the presence of protein(s) which act to link them in some way (see section 5.2.1). Other viral proteins, those which are not integral membrane proteins, are most likely syntheized on free ribosomes and become

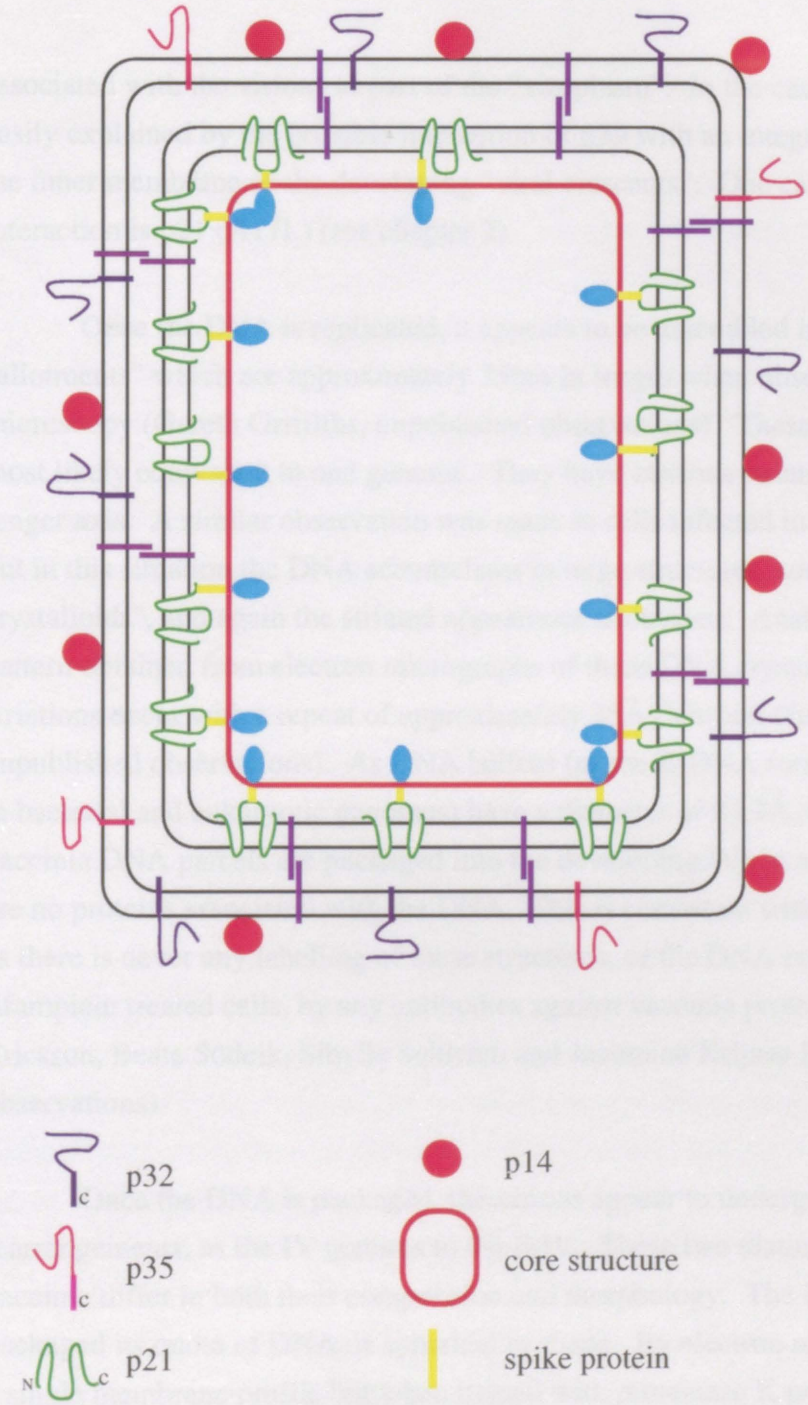


FIGURE 9: Schematic representation of an IMV particle

associated with the virions as part of the "viroplasm". In the case of p39 (A4L), this is most easily explained by the possible interaction of p39 with an integral membrane protein(s) in the inner membrane of the developing "viral crescents". One candidate for such an interaction is p21 (A17L) (see chapter 2)

Once the DNA is replicated, it appears to be assembled into specific sized "allotments" which are approximately 35nm in length when observed by electron microscopy (Gareth Griffiths, unpublished observations). These small DNA packages are most likely equivalent to one genome. They have obvious striations in one direction, the longer axis. A similar observation was made in cells infected in the presence of rifampicin, but in this situation the DNA accumulates in large structures, sometimes referred to as "DNA crystalloids", and again the striated appearance is obvious. Analysis of the diffraction pattern obtained from electron micrographs of these DNA crystalloids indicated that the striations occur with a repeat of approximately 25Å (Vincent Guénebaut and Sally Cudmore, unpublished observations). As DNA helices (of the B-DNA form which is normally found in bacterial and eukaryotic genomes) have a diameter of 23.7Å, this strongly suggests that vaccinia DNA parcels are packaged into the developing IVs in a naked fashion, that is, there are no proteins associated with the DNA. This is consistent with extensive labelling studies as there is never any labelling of these structures, or the DNA crystalloids which form in rifampicin treated cells, by any antibodies against vaccinia proteins (Sally Cudmore, Maria Ericsson, Beate Sodeik, Sibylle Schleich and Jacomine Krijnse Locker, unpublished observations)

Once the DNA is packaged, the virions appear to undergo a number of morphological rearrangements, as the IV matures to the IMV. These two distinct assembly stages of vaccinia differ in both their composition and morphology. The IV, which has not yet packaged its quota of DNA, is spherical in shape. By electron microscopy, it appears to have a single membrane profile but when treated with proteinase K prior to fixation, it is apparent that this single membrane profile is, in reality, two membrane bilayers (Sodeik et al., 1993). During maturation to the IMV, a new "core-like" structure forms, which appears to surround the recently packaged DNA. The IMV, in contrast to the IV, has two apparent membrane profiles when viewed by electron microscopy. One of these is the "core-like" structure which surrounds the DNA, while the other profile represents the membrane surrounding the IMV. It has been hypothesised that these two visible membrane profiles are qualitatively the same as those of the IV, with the inner membrane bilayer having collapsed to form the core structure which surrounds the DNA (Sodeik et al., 1993; see also appendix for figure 2b, Roos et al., 1996). This would mean that p39 would be located within the core. However,

this is not the case and due to the localization of p39 between the core and the surrounding membranes, it is more likely that outer membrane profile represents the two membranes of the IV and that the profile surrounding the DNA, the core structure, forms within the virion during maturation to the IMV (chapter 2) (see appendix for fig 2a, Roos et al., 1996) .

Other structures, whose appearance coincides with that of the core, are the spike-like protrusions which extend between the core and the surrounding membranes of the IMV. These are 20nm structures, first described by Dales (1963) and later observed by cryomicroscopy by Dubochet et al. (1994). These spikes probably function as a link between the core and the surrounding membranes. In chapter 2 of this thesis and in Roos et al. 1996, it is proposed that these spikes are composed, at least in part, by p39 (gene A4L).

The EEV has been described as the infectious form of vaccinia which is responsible for long range spread of virus *in vivo* (Appleyard et al., 1971; Boulter and Appleyard, 1973; Payne, 1980), while then CEV is thought to be responsible for the direct cell-to-spread (Blasco and Moss, 1991; Blasco and Moss, 1992). It is likely that these enveloped viral forms are the most important for the *in vivo* spread of the disease, as a clear and independent role for the IMV has not been established. It has been shown previously that actin is involved in the release of vaccinia virus (Hiller et al., 1981; Hiller et al., 1979; Krempien et al., 1981; Stokes, 1976). In chapter 3, I have elucidated the manner in which vaccinia moves through the cytoplasm of the host cell in an actin-based manner by inducing the formation of actin tails which are anchored in the cell, thereby pushing the virus particle forwards. I also demonstrated using a combination of drug and mutant studies that it is the IEV, the precursor of the second infectious form, which moves within the cell. Therefore, I have proposed that this mechanism of actin-based microvilli protrusion is the means by which CEV is presented to neighbouring cells. In chapter 4, it is hypothesised that the outer membrane of the IEV fuses with the plasma membrane during the extension of the microvilli, giving rise to a CEV at the tip of the projection. It is also noticeable that a greater number of virally induced projections are seen extending from the surface of the infected which is closest to a neighbouring cell (unpublished observations). This suggests that the infected cells are able to sense the presence of a neighbouring cell, in order to direct virus particles in this manner. Due to the fact that vaccinia is exposed at the tip of the projection, the virus can still enter a neighbouring cell by fusion of its outer membrane with the plasma membrane of the neighbouring cell, the currently accepted model of vaccinia entry (Doms et al., 1990) and does not necessarily invoke the need of either endocytosis or phagocytosis. This mechanism of entry is different to the bacterial pathogens which remain inside the tip of the extension, and are subsequently phagocytosed, still within the projection.

5.2 Future Questions

5.2.1 Structure of the IMV

As discussed in chapter 2, p39 (gene A4L) interacts with the viral membranes surrounding the IMV, without having any hallmarks of being a membrane spanning protein itself. Therefore, the association with membranes must be achieved through an interaction with an integral membrane protein(s) in the inner membrane of the IMV. What is the identity of this protein ? To date, only one protein has been preferentially localized to this inner membrane, p21 (gene A17L) (Krijnse Locker et al., submitted). This is an essential protein, which if deleted prevents crescent formation (Rodriguez et al., 1995). p21 is co-translationally inserted into the endoplasmic reticulum and is subsequently targetted to the intermediate compartment where it plays a role in the development of the crescent shaped membranes, which are the progenitors of the IVs (Krijnse Locker et al., submitted; Rodriguez et al., 1995). The co-immunoprecipitation experiment in chapter 2 suggests that p39 may interact with p21, thereby being responsible for the strong membrane association demonstrated by p39 in biochemical assays. As p21 is already present in the membranes surrounding rifampicin bodies and a significant proportion of p39 is also found associated with these membranes, it further strengthens the possibility that p21 could act as a membrane anchor for p39. p21 is predicted to span the inner membrane 4 times with both termini present in the space between the membranes and the viral core (Krijnse Locker et al., submitted). This topology results in three regions of the protein being candidates to interact with p39, the N-terminal 61 amino acids, the loop region between amino acids 98 and 118 and the C-terminal region (see figure 9).

Another question which awaits answering is the identity of the spike between the core and the membranes of the IMV. In chapter 2 and in Roos et al. (1996, see appendix), it is postulated that p39 may comprise part of this spike. If this is the case, it is likely that another protein(s) is also involved as p39 does not form homo-oligomers, at least *in vitro*, and alone is not large enough to form structures of 20nm in length. Other potential proteins could be the core proteins 4a, 4b, p11 and p25 (see section 1.4.1 and references therein).

The membranes of the IV and IMV are tightly apposed and therefore it is likely that a membrane protein(s) acts to keep them so tightly associated (figure 9). This protein(s) could be present in either or both membranes, but would probably need to have a significant proportion present in the lumenal space between the membrane bilayers in order to interact with either itself or other proteins.

5.2.2 Vaccinia-actin motility: future directions

Bacteria do it, and the results presented in chapters 3 and 4 demonstrate that viruses can do it too ! Therefore, two extremely diverse types of intracellular pathogens can commandeer the actin cytoskeleton of their host cells and rearrange it in a manner which enables them to move both within the cell, and to form projections which facilitate their direct spread from cell-to-cell. But is this phenomenon restricted to vaccinia virus or are there other, as yet undetected, viruses which move in a similar manner ? An even larger question: if extracellular pathogens induce motility such as this, is it not possible that intracellular organelles do the same? In other words, could actin nucleation and polymerization from membranes surrounding intracellular organelles provide a general mechanism of motility within cells. There is a small amount of evidence which suggests that this may not be as bizarre and outlandish as it seems.

Work by Heuser and Moriaski (1992, Mol. Cell. Biol. 3, 172a) demonstrated that actin polymerization is also involved in the propulsion of endosomes to and fro in the cell, in apparently random trajectories. This is observed after the application of lanadium followed by zinc, and this "phenomenon bears a striking similarity to the rocketing motility displayed by *Listeria...*" Thus the authors hypothesized that "organelle propulsion via actin polymerization or rocketting may play a normal role in delivering organelles to more directed microtubule-based trafficking pathways, and possibly, may be a mechanism to initiate segregation and processing of endosomal contents".

Though not often discussed, when using *Xenopus* egg extracts to reconstitute *in vitro* motility of bacteria (Theriot et al., 1992), the extracts alone also form actin tails which appear to elongate in a similar fashion to the bacterial tails. For the work with bacteria, this problem was generally overcome by the addition of TX-100 which disrupts the endogenous membrane vesicles which are responsible for tail formation[1]. The fact that TX-100 disrupted the endogenous vesicles which caused the actin tails, suggests that the factor inducing the formation of the actin assemblies in the absence of bacteria is membrane associated. It is thought that this factor may be a component of the egg cortex (Michael Glotzer, personal communication). In my attempts to establish an *in vitro* motility assay for vaccinia, it was not possible to use TX-100 as this also disrupted the membranes surrounding the virions and therefore work is continuing to attempt solving this problem.

[1] The only paper where this is actually mentioned, to the best of my knowledge, is Marchand et al., 1995.

What viral factors are involved in this actin assembly process ? A number of interacting components have been described for bacteria which are essential for their motility. These include the bacterial expressed membrane proteins, Act A in *Listeria monocytogenes* (Domann et al., 1992; Kocks et al., 1992), Ics A in *Shigella* (Bernardini et al., 1989) and Iact A in *Listeria ivanovii* (Gouin et al., 1994). Act A in turn has been shown to interact with a cellular component, VASP, which in turn can bind to an actin-sequestering protein, profilin (for a review see Pollard, 1995). Hence another interesting question will be to find the viral and cellular factors involved in vaccinia motility. As was shown in chapter 4, the recruitment of actin to the virus appears to occur in a polarised fashion as actin is often observed in a cup-shaped distribution surrounding the virus particle at the earlier stages of tail formation. What factor is responsible for this polarised assembly of actin ? Another interesting point is that the actin tails induced by vaccinia are almost exclusively seen to be at right angles to the long axis of the virus particle, in contrast to the bacterial tails which form prepindicularly to short axis. This means that the actin tail is pushing the longer viral surface through the cytoplasm and one would imagine that this would be more inefficient due to the greater friction. However, the larger surface area which is available to cause actin polymerization is sufficient to outweigh this problem of drag.

Vaccinia encodes a protein which is 31.8% identical to human profilin, but as yet a function has not been established for this protein, and it certainly is not essential for the actin-based motility as profilin deletion mutants still move (chapter 3). Whether cellular profilin plays a role is unknown, but a protein which would facilitate the recruitment of actin, is probably necessary. It is very likely that a membrane protein in the IEV is be involved in the process, either directly or indirectly recruiting actin to the membrane. One possible candidate, due to both its abundance and the fact that the protein is cytoplasmically exposed in the IEV, is p37 (gene F13L, see section 1.4.3). Another potential viral player is the protein product of the gene F8L. This is a 65 amino acid protein which has not yet been identified or functionally characterized, but its sequence shows a very low amount of homology to Act A in that it also has a number of proline residues. A knockout of F8L is currently being engineered to elucidate if this protein plays a role in the motility process (Sidney Higley and Michael Way, personal communication). It also remains to be established if host cell proteins such as VASP, or other cellular protein(s), also participate.

Our current understanding of the interactions between the actin cytoskeleton and membranes is rudimentary. Could vaccinia virus provide a means by which to study the complex interactions between membranes and actin ? The outer membranes surrounding the IEV are derived from cisternae of the *trans* Golgi network, and it is these membranes which

drive the nucleation and polymerization of actin, probably through the mediation of a virally-encoded, TGN targetted, membrane protein. Upon reaching the plasma membrane another set of complex membrane interactions take place and the actin-tail behind the virus particle drives the formation of a projection from the cell surface. As is clear from chapter 4, the actin in these projections interacts with the surrounding plasma membrane. Very little is known about the mechanisms of microspike protrusion in ordinary cells or about the interactions which occur between the actin and the membranes, especially at the tip of the microspikes where the addition of actin monomers is thought to play a key role in the extension of these structures.

Thus the in vitro permeabilized cell system used in chapter 4 [2] should provide a means to further investigate the key components involved in the actin-based motility of vaccinia virus.

2 This is the first time that such a permeabilised cell system has been used to observe particles or organelles moving within cells.

Bibliography to chapters 1 and 5

Adam, T., Arpin, M., Prevost, M.-C., Gounon, P., and Sansonetti, P. J. (1995). Cytoskeletal rearrangements and the functional role of T-plastin during entry of *Shigella flexneri* into HeLa cells. J. Cell. Biol. *129*, 367-381

Alberts, B., Bray, D., Lewis, J., Raff, M., Roberts, K., and Watson, J. D. (1994). Molecular Biology of the Cell, 3rd Edition (New York & London: Garland Publishing, Inc.).

Appleyard, G., Hapel, A. J., and Boulter, E. A. (1971). An antigenic difference between intracellular and extracellular rabbitpox virus. J. Gen. Virol. *13*, 9-17.

Baldick, C. J., and Moss, B. (1987). Resistance of vaccinia virus to rifampicin conferred by a single nucleotide substitution near the predicted NH_2 terminus of a gene encoding an Mr 62,000 polypeptide. Virology *156*, 138-145.

Baroudy, B., M., Venkatesan, S., and Moss, B. (1982). Incompletely base-paired flip-flop terminal loops link the two DNA strands of the vaccinia virus genome into one uninterrupted polynucleotide chain. Cell *28*, 315-324.

Bauer, W., R., Ressner, E., C., Kates, J., and Patzke, J. (1977). A DNA nicking-closing enzyme encapsidated in vaccinia virus. A partial purification and properties. Proc Natl Acad Sci USA *74*, 1841-1845.

Bernardini, M. L., Mounier, J., d'Hauteville, H., Coquis-Rondon, M., and sansonetti, P. J. (1989). Identification of *icsA*, a plasmid locus of *Shigella flexneri* that governs bacterial intra- and intercellular spread through interaction with F-actin. Proc.Natl.Acad.Sci.USA *86*, 3867-3871.

Blasco, R., Cole, N. B., and Moss, B. (1991). Sequence analysis, expression, and deletion of a vaccinia virus gene encoding a homolog of profilin, a eukaryotic actin-binding protein. J. Virol. *65*, 4598-4608.

Blasco, R., and Moss, B. (1991). Extracellular vaccinia virus formation and cell-to-cell virus transmission are prevented by deletion of the gene encoding the 37,000-dalton outer envelope protein. J. Virol. *65*, 5910-5920.

Blasco, R., and Moss, B. (1992). Role of cell-associated enveloped vaccinia virus in cell-to-cell spread. J. Virol. *66*, 4170-4179.

Blasco, R., Sisler, J., R., and Moss, B. (1993). Dissociation of progeny vaccinia virus from the cell membrane is regulated by a viral envelope glycoprotein : effect of a point mutation in the lectin homology domain of the A34R gene. J. Virol. *67*, 3319-3325.

Bohn, W., Rutter, G., Hohenberg, H., Mannweiler, K., and Nobis, P. (1986). Involvement of actin filaments in budding of measles virus : studies on cytoskeletons in uninfected cells. Virol. *149*, 91-106.

Boone, R. F., and Moss, B. (1978). Sequence complexity and relative abundance of vaccinia virus mRNA's synthesized *in vivo* and *in vitro*. J. Virol. *26*, 554-569.

Boulter, E. A., and Appleyard, G. (1973). Differences between extracellular and intracellular forms of poxvirus and their implications. Progr. Med. Virol. *16*, 86-108.

Cairns, J. (1960). The initiation of vaccinia infection. Virology *11*, 603-623.

Carrasco, L., and Bravo, R. (1986). Specific proteins synthesized during the viral lytic cycle in vaccinia virus-infected HeLa cells: Analysis by high-resolution, two-dimensional gel electrophoresis. J. Virol. *58*, 569-577.

Chakraborty, T., Ebel, F., Domann, E., Niebuhl, K., Gerstel, B., Pistor, S., Temm-Grove, C., J., Jockusch, B., M., Reinhard, M., Walter, U., and Wehland, J. (1995). A focal adhesion factor directly linking intracellularly motile *Listeria monocytogenes* and *Listeria ivanovii* to the actin-based cytoskeleton of mammalian cells. EMBO J. *14*, 1314-1321.

Challberg, M., D., and Englund, P., T. (1979). Purification and properties of the deoxyribonucleic acid polymerase induced by vaccinia virus. J. Biol. Chem. *254*, 7812-7819.

Chang, A., and Metz, D. H. (1976). Further investigations on the mode of entry of vaccinia virus into cells. J. Gen. Virol. *32*, 275-282.

Charlton, C., A., and Volkman, L., E. (1991). Sequential rearrangement and nuclear polymerization of actin in baculovirus-infected *Spodoptera frugiperda* cells. J. Virol. *65*, 1219-1227.

Child, S. J., Franke, C. A., and Hruby, D. E. (1988). Inhibition of vaccinia virus replication by nicotinamide: evidence for ADP-ribosylation of viral proteins. Vir. Res. *9*, 119-132.

Ciampor, F. (1988). The role of the cytoskeleton and nuclear matrix in virus replication. Acta Virol. *32*, 169-189.

Condit, R. C., Motyczka, A., and Spizz, G. (1983). Isolation and preliminary characterization, and physical mapping of temperature-sensitive mutants of vaccinia virus. Virology *128*, 429-443.

Craigie, J. (1932). The nature ofthe vaccinia flocculation reaction and observations on the elementary bodies of vaccinia. Brit. J. exp. Path. *13*, 368-380.

Dabiri, G. A., Sanger, J. M., Portnoy, D. A., and Southwick, F. S. (1990). Listeria monocytogenes moves rapidly through the host-cell cytoplasm by inducing directional actin assembly. Proc.Natl.Acad.Sci.USA *87*, 6068-6072.

Dales, S. (1971). Involvement of membranes in the infectious cycle of vaccinia. In Cell Membranes: Biological and pathological aspects, G. W. Richter and D. G. Scarpelli, eds. (Baltimore: Williams & Wilkins), pp. 136-144.

Dales, S. (1965). Relation between penetration of vaccinia, release of viral DNA, and initiation of genetic functions. In Perspectives in Virology, M. Pollard, ed. (New York: Harper & Row), pp. 47-71.

Dales, S. (1963). The uptake and development of vaccinia virus in strain L cells followed with labeled viral deoxyribonucleic acid. J. Cell Biol. *18*, 51-72.

Dales, S., and Kajioka, R. (1964). The cycle of multiplication of vaccinia virus in Earle's strain L cells. Virology *24*, 278-294.

Damsky, C., H., Sheffield, J., B., Tuszynski, G., P., and Warren, L. (1977). Is there a role for cellular actin in virus budding ? J. Cell Biol. *75*, 593-605.

De, B., P., Burdsall, A., L., and Banerjee, A., K. (1993). Role of cellular actin in human parainfluenza virus type 3 genome transcription. J.B.C. *268*, 5701-5710.

Demkowicz, W. E., Maa, J. S., and Esteban, M. (1992). Identification and characterization of vaccinia virus genes encoding proteins that are highly antigenic in animals and are immunodominant in vaccinated humans. J. Virol. *66*, 386-398.

Dold, F., G., Sanger, J., M., and Sanger, J., W. (1994). Intact alpha-actinin molecules are needed for both the assembly of actin into the tails and the locomotion of *Listeria monocytogenes* inside infected cells. Cell Mot.Cyto. *28*, 97-107.

Domann, E., Wehland, J., Rohde, M., Pistor, S., Hartl, M., Goebel, W., Leimeister-Wachter, M., Wuenscher, M., and Chakraborty, T. (1992). A novel bacterial virulence gene in Listeria monocytogenes required for host cell microfilament interaction with homology to the proline-rich region of vinculin. EMBO J. *11*, 1981-1990.

Doms, R. W., Blumenthal, R., and Moss, B. (1990). Fusion of intracellular- and extracellular forms of vaccinia virus with the cell membrane. J. Virol. *64*, 4884-4892.

Duncan, S. A., and Smith, G. L. (1992). Identification and characterization of an extracellular envelope glycoprotein affecting vaccinia virus egress. J. Virol. *66*, 1610-1621.

Easterbrook, K. B. (1966). Controlled degradation of vaccinia virions *in vitro*: an electron microscopic study. J. Ultrastruct. Res. *14*, 484-496.

Engelstad, M., Howard, S. T., and Smith, G. L. (1992). A constitutively expressed vaccinia gene encodes a 42-kDa glycoprotein related to complement control factors that forms part of the extracellular virus envelope. Virology *188*, 801-810.

Engelstad, M., and Smith, G., L. (1993). The vaccinia virus 42kD envelope protein is required for the envelopement and egress of extracellular virus and for virus virulence. Virol. *194*, 627-637.

Eppstein, D., A., Marsh, Y., V., Schreiber, A., B., Newman, S., R., Todaro, G., J., and Nestor, J., J.,Jnr. (19985). Epidermal growth factor receptor occupancy inhibits vaccinia virus infection. Nature *318*, 663-665.

Ericsson, M., Cudmore, S., Shuman, S., Condit, R., C., Griffiths, G., and Krijnse Locker, J. (1995). Characterization of ts16, a temperature-sensitive mutant of vaccinia virus. J. Virol. *69*, 7072-7086.

Essani, K., and Dales, S. (1979). Biogenesis of vaccinia: evidence for more than 100 polypeptides in the virion. Virology *95*, 385-94.

Essani, K., Dugre, R., and Dales, S. (1982). Biogenesis of vaccinia: Involvement of spicules of the envelope during virus assembly examined by means of conditional lethal mutants and serology. Virology *118*, 279-292.

Fenner, F. (1990). Poxviruses. In Virology, B. Fields, N. and D. Knipe, M., eds. (New York: Raven Press Ltd.), pp. 2113-2135.

Franke, C. A., Reynolds, P. L., and Hruby, D. E. (1989). Fatty acid acylation of vaccinia virus proteins. J. Virol. *63*, 4285-4291.

Franke, C. A., Wilson, E. M., and Hruby, D. E. (1990). Use of a cell-free system to identify the vaccinia virus L1R gene product as the major late myristylated virion protein M25. J. Virol. *64*, 5988-5996.

Gellin, B., R., and Broome, C., V. (1989). Listeriosis. J. Am. Med. Assoc. *261*, 1313-1320.

Geoffroy, C., Gaillard, J., L., Alout, J., E., and Berche, P. (1987). Purification,characterizatioon and toxicity of the sulfhydryl-activated hemolysin listeriolysin O from *Listeria monocytogenes*. Infect. Immun. *55*, 1641-1646.

Giuffre, R., M., Tovell, D., R, Kay, C., M., and Tyrrell, D., L.,J. (1982). Evidence for an interaction between the membrane protein of a paramyxovirus and actin. J. Virol. *42*, 963-968.

Goebel, S. J., Johnson, G. P., Perkus, M. E., Davis, S. W., Winslow, J. P., and Paoletti, E. (1990). The complete DNA sequence of vaccinia virus. Virology *179*, 247-266.

Gold, P., and Dales, S. (1968). Localization of nucleotide phosphohydrolase activity within vaccinia. Proc. Natl. Acad. Sci. USA *60*, 845-852.

Goldberg, M. B., and Sansonetti, P. J. (1993). *Shigella* subversion of the cellular cytoskeleton: a strategy for epithelial colonozation. Infection Immun *61*, 4941-4946.

Gong, S., Lai, C., and Esteban, M. (1990). Vaccinia virus induces cell fusion at acid pH and this activity is mediated by the N-terminus of the 14kDa virus envelope protein. Virology *178*, 81-91.

Gordon, J., Kovala, T., and Dales, S. (1988). Molecular characterization of a prominent antigen of the vaccinia virus envelope. Virology *167*, 361-369.

Gordon, J., Mohandas, A., Wilton, S., and Dales, S. (1991). A prominent antigenic surface polypeptide involved in the biogenesis and function of the vaccinia virus envelope. Virology *181*, 671-686.

Gouin, E., Mengaud, J., and Cossart, P. (1994). The virulence gene cluster of Listeria monocytogenes is also present in Listeria ivanovii, an animal pathogen and Listeria seeligeri, a nonpathogenic species. Infect. Immun. *62*, 3550-3553.

Green, M., and Pina, M. (1962). Stimulation of the DNA synthesizing enzyme of cultured human cells by vaccinia virus infection. Virol. *17*, 603-604.

Haffner, C., Jarchau, T., Reinhard, M., Hoppe, J., Lohmann, S., M., and Walter, U. (1995). Molecular cloning, structural analysis and functional expression of the proline-rich focal adhesion and microfilament-associated protein VASP. EMBO J. *14*, 19-27.

Harford, C. G., Hamlin, A., and Riders, E. (1966). Electron microscopic autoradiography of DNA synthesis in cells infected with vaccinia virus. Exp. Cell Res. *42*, 50-57.

Hartwig, J., H., and Kwiatkowski, D., J. (1991). Actin-binding proteins. Curr. Biol. *3*, 87-97.

Heinzen, R. A., Hayes, S. F., Peacock, M. G., and Hackstead, T. (1993). Directional actin polymerization associated with spotted fever group Rickettsia infection of Vero cells. Infection Immun *61*, 1926-1935.

Hiller, G., Eibl, H., and Weber, K. (1981). Characterization of intracellular and extracellular vaccinia virus variants: N_1-isonicotinoyl-N_2-3-methyl-4-chlorobenzoylhydrazine interferes with cytoplasmic virus dissemination and release. J. Virol. *39*, 903-913.

Hiller, G., Jungwirth, C., and Weber, K. (1981). Fluorescence microscopical analysis of the life cycle of vaccinia virus in the chick embryo fibroblasts. Exp Cell Res *132*, 81-87.

Hiller, G., and Weber, K. (1985). Golgi-derived membranes that contain an acylated viral polypeptide are used for vaccinia virus envelopment. J. Virol. *55*, 651-659.

Hiller, G., and Weber, K. (1982). A phosphorylated vaccinia virion polypeptide of molecular weight of 11,000 is exposed on the surface of mature particles and interacts with actin-containing cytoskeletal elements. J. Virol. *44*, 647-657.

Hiller, G., Weber, K., Schneider, L., Parajsz, C., and Jungwirth, C. (1979). Interaction of assembled progeny pox viruses with the cellular cytoskeleton. Virology *98*, 142-153.

Holowczak, J. A., and Joklik, W. K. (1967). Studies of the structural proteins of vaccinia virus. 1. Structural proteins of virions and cores. Virology *33*, 717-725.

Hugin, A., W., and Hauser, C. (1994). The epidermal growth factor receptor is not a receptor for vaccinia virus. J. Virol. *68*, 8409-8412.

Ichihashi, Y., and Dales, S. (1971). Biogenesis of poxviruses: Inter-relationship between hemagglutinin production and polykaryocytosis. Virology *46*, 533-543.

Ichihashi, Y., Matsumoto, S., and Dales, S. (1971). Biogenesis of poxviruses: Role of A-type inclusions and host cell membranes in virus dissemination. Virology *46*, 507-532.

Ichihashi, Y., and Oie, M. (1983). The activation of vaccinia virus infectivity by the transfer of phosphatidylserine from the plasma membrane. Virology *130*, 306-317.

Janeczko, R. A., Rodriguez, J. F., and Esteban, M. (1987). Studies on the mechanism of entry of vaccinia virus in animal cells. Arch. Virol. *92*, 135-150.

Jenner, E. (1799). An inquiry into the cause and effects of the variolae vaccinae, a disease discovered in some of the western counties of England, particularly Gloucestershire, and known by the name of cowpox. In Classics of Medicine and Surgery, r. i. C. N. B. Camac, ed. (New York, 1959: Dover), pp. 241.

Jin, D., Li, Z., Jin, Q., Yuwen, H., and Hou, Y. (1989). Vaccinia virus hemagglutinin - A novel member of the immunoglobulin superfamily. J. Exp. Med. *170*, 571-576.

Johnson, G., P., Goebel, S., J., and Paoletti, E. (1993). An update on the vaccinia virus sequence. Virol. *196*, 381-401.

Joklik, W. K. (1964). The intracellular uncoating of poxvirus DNA II. The molecular basis of the uncoating process. J. Mol. Biol. *8*, 277-288.

Joklik, W. K., and Becker, Y. (1964). The replication and coating of vaccinia DNA. J. Mol. Biol. *10*, 452-474.

Kane, E. M. and. Shuman, S. (1993). Vaccinia virus Morphogenesis is Blocked by a Temperature Sensitive Mutation in the I7 Gene that Encodes a Virion Component. J. of Virol. *67*, 2689-2698.

Kao, S. Y., and Bauer, W. R. (1987). Biosynthesis and phosphorylation of vaccinia virus structural protein VP11. Virology *159*, 399-407.

Kao, S. Y., Ressner, E., Kates, J., and Bauer, W. R. (1981). Purification and characterization of a superhelix binding protein from vaccinia virus. Virology *111*, 500-508.

Karunasagar, I., Krohne, G., and Goebel, W. (1993). *Listeria inanovii* is capable of cell-to-cell spread involving actin paolmerization. Infection Immun *61*, 162-169.

Kasamatsu, H., Lin, W., Edens, J., and Revel, J.-P. (1983). Visualization of antigens attached to cytoskeletal framework in animal cells: colocalization of simian virus 40 Vp1 polypeptide and actin in TC7 cells. Proc. Natl. Acad. Sci . USA *80*, 4339-4343.

Kates, J., R., and Beeson, J. (1970). Ribonucleic acid synthesis in vaccinia virus. I. The mechanism of synthesis and release of RNA in vaccinia cores. J. Mol. Biol. *50*, 1-18.

Kates, J., R., and McAuslan, B., R. (1967). Poxvirus DNA-dependent RNA polymerase. Proc. Natl. Acad. Sci. USA *58*, 134-141.

Kates, J. R., and Beeson, J. (1970). Ribonucleic acid synthesis in vaccinia virus. II. Synthesis of polyriboadenylic acid. J. Mol. Biol. *50*, 19-23.

Kates, J. R., and McAuslan, B. (1967). Messenger RNA synthesis by a "coated" viral genome. Proc. Natl. Acad. Sci. USA *57*, 314-320.

Kato, N., Eggers, H. J., and Rolly, H. (1969). Inhibition of release of vaccinia virus by N_1-isonicotinoyl-N-3-methyl-4-chlorobenzoylhydrazine. J. Exp. Med. *129*, 795-808.

Katz, E., and Moss, B. (1970). Formation of a vaccinia virus structural polypeptide from a high molecular weight precursor: Inhibition by rifampicin. Proc. Natl. Acad. Sci. USA *66*, 677-684.

Katz, E., and Moss, B. (1970). Vaccinia virus structural polypeptide derived from a high-molecular-weight precursor: Formation and integration into virus particles. J. Virol. *6*, 717-726.

Kocks, C., Gouin, E., Tabouret, M., Berche, P., Ohayon, H., and Cossart, P. (1992). L. monocytogenes-induced actin assembly requires the actA gene product, a surface protein. Cell *68*, 521-531.

Kocks, C., Hellio, R., Gounon, P., Ohayon, H., and Cossart, P. (1993). Polarized distribution of Listeria monocytogenes surface protein ActA at the site of directional actin assembly. J. Cell. Sci. *105*, 699-710.

Kotwal, G. J., Isaacs, S. N., and Moss, B. (1990). Inhibition of the complement cascade by the major secretory protein of vaccinia virus. Science *250*, 827-830.

Kotwal, G. J., and Moss, B. (1988). Vaccinia virus encodes a secretory polypeptide structurally related to complement control proteins. Nature *335*, 176-178.

Krempien, U., Schneider, L., Hiller, G., Weber, K., Katz, E., and Jungwirth, C. (1981). Conditions for pox virus specific microvilli formation studied during synchronized virus assembly. Virol *113*, 556-564.

Krijnse Locker, J., Schleich, S., Rodriguez, D., Goud, B., Vriend, G., Snijder, E., and Griffiths, G. The role of a 21kDa viral membrane protein in the assembly of vaccinia virus from the intermediate compartment. Submitted for publication.

Lai, C., Gong, S., and Esteban, M. (1991). The 32-kilodalton envelope protein of vaccinia virus synthesized in *Escherichia coli* binds with specificity to cell surfaces. J. Virol. *65*, 499-504.

Lamb, R., A., Mahy, B., W,.J., and Choppin, P., W. (1976). The synthesis of Sendai virus polypeptides in infected cells. Virol. *69*, 116-131.

Ledingham, J., C.,G., and Aberd, M., B. (1931). The aetiological importance of the elementary bodies in vaccinia and fowlpox. Lancet *221*, 525-526.

Lett, M., C., Sasakawa, C., Okada, N., Sakai, T., Makino, S., Yamada, M., Komatsu, K., and Yoshikawa, M. (1989). VirG, a plasmid-coded virulence gene of *Shigella flexneri*: identification of the virG protein and determination of the complete coding sequence. J. Bacteriol. *171*, 353-359.

Li, J., and Broyles, S., S. (1995). The DNA binding domain of the vaccinia virus early transcription factor small subunit is an extended helicase-like motif. Nuc. Acid Res. *23*, 1590-1596.

Luftig, R., B. (1982). Does the cytoskeleton play a significany role in animal virus replication? J. Theor. Biol. *99*, 173-191.

Maa, J. S., and Esteban, M. (1987). Structural and functional studies of a 39,000 Mr immunodominant protein of vaccinia virus. J. Virol. *61*, 3910-3919.

Maa, J. S., Rodriguez, J. F., and Esteban, M. (1990). Structural and functional characterization of a cell surface binding protein of vaccinia virus. J. Biol. Chem. *265*, 1569-1577.

Machesky, L., M., Cole, N., B., Moss, B., and Pollard, T., D. (1994). Vaccinia virus expresses a novel profilin with higher affinity for phosphoinositides than actin. Biochem. *33*, 10815-10824.

Magee, W., E. (1962). DNA poly and deoxyribonucleotide kinase activities in cells infected wth vaccinia virus. Virol. *17*, 604-607.

Mallon (Ruszala), V., and Holowczac, J. A. (1985). Vaccinia virus antigens on the plasma membrane of infected cells. Virology *141*, 201-220.

Marchand, J.-B., Moreau, P., Paoletti, A., Cossart, A., Carlier, M.-F., and Pantaloni, D. (1995). Actin based movement of Listeria Monocytogenes: actin assembly results from the local maintenance of uncapped filament barbed ends at the bacterium surface. J.C.B. *130*, 1-13.

Marsh, M., and Helenius, A. (1989). Virus entry into animal cells. Advan. Virus Res. *36*, 107-151.

Marsh, Y. V., and Eppstein, D. A. (1987). Vaccinia virus and the EGF receptor: A portal for infectivity. J. Cell. Biochem. *34*, 239-245.

McAuslan, B., R., and Kates, J., R. (1967). Poxvirus induced acid deoxyribonuclease: regulation of synthesis, control of activity in vivo, purification and properties of the enzyme. Virol *33*, 709-716.

Mengaud, J., Vicente, M.-F., Chenevert, J., Moniz Pereira, J., Geoffroy, C., Gicquel-Sanzey, B., Baquero, F., Perez-Diaz, J., C., and Cossart, P. (1988). Expression in *E. coli* and seqience analysis of the listeriolysin O determinant of *Listeria monocytogenes*. Infect. Immun. *56*, 766-772.

Minnigan, H., and Moyer, R. W. (1985). Intracellular location of rabbit poxvirus nucleic acid within infected cells as determined by in situ hybridization. J. Vir. *55*, 634-643.

Mohondas, A., and Dales, S. (1995). Function of spicules in the formation of vaccinia virus envelopes elucidated by a conditional lethal mutant. Virol. *214*, 494-502.

Morgan, C. (1976). The insertion of DNA into vaccinia virus. Science *193*, 591-592.

Morgan, C. (1976). Vaccinia virus reexamined: Development and release. Virology *73*, 43-58.

Moss, B. (1968). Inhibition of HeLa cell protein synthesis by the vaccinia virion. J. Virol. *2*, 1028-1037.

Moss, B. (1990). Poxviridae and their replication. In Virology, B. N. Fields and D. M. Knipe, eds. (New York: Raven Press, Ltd.), pp. 2079-2111.

Moss, B. (1990). Regulation of orthopoxvirus gene expression. Curr. Top. Microbiol. Immunol. *163*, 41-70.

Moss, B. (1990). Regulation of vaccinia virus transcription. Annu. Rev. Biochem. *59*, 661-688.

Moss, B. (1991). Vaccinia virus: A tool for research and vaccine development. Science *252*, 1662-1667.

Moss, B., and Rosenblum, E. N. (1973). Protein cleavage and poxvirus morphogenesis: Tryptic peptide analysis of core precursors accumulated by blocking assembly with rifampicin. J. Mol. Biol. *81*, 267-269.

Moss, B., Rosenblum, E. N., and Grimley, P. M. (1971). Assembly of vaccinia virus particles from polypeptides made in the presence of rifampicin. Virology *45*, 123-134.

Moss, B., Rosenblum, E. N., and Katz, E. (1969). Rifampicin: a specific inhibitor of vaccinia virus assembly. Nature *224*, 1280-1284.

Munyon, W., Paoletti, E., and Grace, J., Y. (1967). RNA polymerase activity in purified infectious vaccinia virus. Proc. Natl. Acad. Sci. USA *58*, 2280-2287.

Murphy, F. A., and Kingsbury, D. W. (1990). Virus taxonomy. In Virology, B. N. Fields and D. M. Knipe, eds. (New York: Raven Press), 9-37, vol 1.

Murti, K., G., Chen, M., and Goorha, R. (1985). Interaction of frog virus 3 with the cytomatrix. Virol. *142*, 31-325.

Nagayama, A., Pogo, B. G. T., and Dales, S. (1970). Biogenesis of vaccinia: separation of early stages from maturation by means of rifampicin. Virology *4*, 1039-1051.

Naito, S., and Matsumoto, S. (1978). Identification of cellular actin within the rabies virion. Virol *91*, 151-163.

Nanavati, D., Ashton, F., T., Sanger, J., M., and Sanger, J., W. (1994). Dynamics of actin and alpha-actinin in the tails of *Listeria monocytogenes* in infected PtK2 cells. Cell Mot. Cyto. *28*, 346-358.

Niles, E. G., and Seto, J. (1988). Vaccinia virus gene D8 encodes a virion transmembrane protein. J. Virol. *62*, 3772-3778.

Oda, K., and Joklik, W. K. (1967). Hybidization and sedimentation studies on "early" and "late" vaccinia messenger RNA. J. Mol. Biol. *27*, 395-419.

Ogawa, H., Nakamura, A., and Nakaya, R. (1968). Cinemicrographic study of tissue cell cultures infected with Shigella Flexneri. Japan J. Med. Sci. Biol. *21*, 259-273.

Oie, M., and Ichihashi, Y. (1981). Characterization of vaccinia polypeptides. Virology *113*, 263-276.

Paez, E., Dallo, S., and Esteban, M. (1987). Virus attenuation and identification of structural proteins of vaccinia virus that are selectively modified during virus persistence. J. Virol. *61*, 2642-2647.

Paoletti, E., and Grady, L. J. (1977). Transcriptional complexity of vaccinia virus *in vivo* and *in vitro*. J. Virol. *23*, 608-615.

Parkinson, J., E., and Smith, G., L. (1994). Vaccinia virus gene A36R encodes a Mr. 43-50 K protein on the surface of extracellular enveloped virus. Virol *204*, 376-390.

Payne, L. G. (1992). Characterization of vaccinia virus glycoproteins by monoclonal antibody precipitation. Virology *187*, 251-260.

Payne, L. G. (1979). Identification of the vaccinia hemagglutinin polypeptide from a cell system yielding large amounts of extracellular enveloped virus. J. Virol. *31*, 147-155.

Payne, L. G. (1978). Polypeptide composition of extracellular enveloped vaccinia virus. J. Virol. *27*, 28-37.

Payne, L. G. (1980). Significance of extracellular enveloped virus in the *in vitro* and *in vivo* dissemination of vaccinia. J. Gen. Virol. *50*, 89-100.

Payne, L. G., and Kristensson, K. (1979). Mechanism of vaccinia virus release and its specific inhibition by N_1-isonicotinoyl-N_2-3-methyl-4-chlorobenzoylhydrazine. J. Virol. *32*, 614-622.

Payne, L. G., and Kristensson, K. (1985). Extracellular release of enveloped vaccinia virus from mouse nasal epithelial cells *in vivo*. J. Gen. Virol. *66*, 643-646.

Payne, L. G., and Norrby, E. (1978). Adsorption and penetration of enveloped and naked vaccinia virus particles. J. Virol. *27*, 19-27.

Payne, L. G., and Norrby, E. (1976). Presence of hemagglutinin in the envelope of extracellular vaccinia virus particles. J. Gen. Virol. *32*, 63-72.

Payne, L. G., and Kristensson, K. (1990). The polypeptide composition of vaccinia-infected cell membranes and rifampicin bodies. Vir. Res. *17*, 15-30.

Pedley, C. B., and Cooper, R. J. (1987). The assay, purification and properties of vaccinia-virus-induced uncoating protein. J. Gen. Virol. *68*, 1021-1028.

Perelroizen, I., Marchand, J.-B., Blanchoin, L., Didry, D., and Carlier, M.-F. (1994). Interaction of profilin with G-actin and poly(L-proline). Biochem. *33*, 8472-8478.

Pistor, S., Chakraborty, T., Niebuhr, K., Domann, E., and Wehland, J. (1994). The ActA protein of *Listeria monocytogenes* acts as a nucleator inducing reorganization of the actin cytoskeleton. EMBO J. *13*, 758-763.

Pistor, S., Chakraborty, T., Walter, U., and Wehland, J. (1995). The bacterial actin nucleator protein Act A of *Listeria monocytogenes* contains multiple binding sites for host cell microfilaments. Curr. Biol. *5*, 517-525.

Pogo, B., G.,T., and Dales, S. (1969). Two deoxyribonuclease activities within purified vaccinia virus. Proc. Natl. Acad. Sci. USA *63*, 820-827.

Pogo, B. G. T., and Dales, S. (1971). Biogenesis of vaccinia: Separation of early stages from maturation by means of hydoxyurea. Virology *43*, 144-151.

Pogo, B. G. T., Katz, J. R., and Dales, S. (1975). Biogenesis of Poxviruses: Synthesis and phopshorylation of basic protein associated with the DNa. Virology *64*, 531-543.

Pollard, T., D., and Cooper, J., A. (1986). Actin and actin-binding proteins. A critical evaluation of mechanisms and functions. Ann. Rev. Biochem. *55*, 987-1035.

Pollard, T., D. (1995). Missing link for intracellular bacterial motility? Current Biology *5*, 837-840.

Ravanello, M., P., and Hruby, D., E. (1994). Conditional lethal expression of the vaccinia virus L1R myristylated protein reveals a role in virion assembly. J. Virol. *68*, 6401-6410.

Ravanello, M. P., Franke, C. A., and Hruby, D. E. (1995). An N-terminal peptide from the vaccinia virus L1R protein directs the myristylation and virion envelope localization of a heterologous fusion protein. J. Biol. Chem., *268*, 7585-7593

Reinhard, M., Giehl, K., Abel, K., Haffner, C., Jarchau, T., Hoppe, V., Jockusch, B., M., and Walter, U. (1992). The proline-rich focal adhesion and microfilament protein VASP is a ligand for profilins. EMBO J. *14*, 1583-1589.

Rice, A., P., and Roberts, B., E. (1983). Vaccinia virus induces cellular mRNA degradation. J. Virol. *47*, 529-539.

Rodriguez, D., Rodriguez, J.-R., and Esteban, M. (1993). The vaccinia virus fusion protein forms a stable complex with the processed protein encoded by the vaccinia virus A17L gene. J. Virol. *67*, 3435-3440.

Rodriguez, J. F., and Esteban, M. (1987). Mapping and nucleotide seqeunce of the vaccinia gene that encodes a 14-kilodalton fusion protein. J. Virol. *61*, 3550-3554.

Rodriguez, J. F., Janeczko, R., and Esteban, M. (1985). Isolation and characterization of neutralizing monoclonal antibodies to vaccinia virus. J. Virol. *56*, 482-488.

Rodriguez, J. F., Paez, E., and Esteban, M. (1987). A 14,000-M_r envelope protein of vaccinia virus is involved in cell fusion and forms covalently linked trimers. J. Virol. *61*, 393-404.

Rodriguez, J. F., and Smith, G. L. (1990). IPTG-dependent vaccinia virus: Identification of a virus protein enabling virion envelopment by Golgi membrane and egress. Nuc. Acid Res. *18*, 5347-5351.

Rodriguez, J. R., Rodriguez, D., and Esteban, M. (1992). Insertional inactivation of the vaccinia virus 32-kilodalton gene is associated with attenuation in mice and reduction of viral gene expression in polarized epithelial cells. J. Virol. *66*, 183-189.

Rodriguez, D., Esteban, M., and Rodriguez, J., R. (1995). Vaccinia virus A17L gene product is essential for an early step in virion morphogenesis. J. Virol. *69*, 4640-4648.

Roos, N., Cyrklaff, M., Cudmore, S., Blasco, R., Krijnse-Locker, J., and Griffiths, G. (1996). The use of a novel immunogold cryoelectron microscopic method to investigate the structure of the intracellular and extracellular forms of vaccinia virus. EMBO J. *In press.*

Rosel, J., and Moss, B. (1985). Transcriptional and translational mapping and nucleotide sequence analysis of a vaccinia virus gene encoding the precursor of the major core polypeptide 4b. J. Virol. *56*, 830-838.

Rosenkranz, H. S., Rose, H. M., Morgan, C., and Hsu, K. C. (1966). The effect of hydroxyurea on virus development: II. Vaccinia virus. Virology *28*, 510-519.

Salzman, N., P. (1960). The rate of formation of vaccinia deoxyribonucleic acid and vaccinia virus. Virol *10*, 150-152.

Sanger, J., M., Sanger, J., W., and Southwick, F., S. (1992). Host cell actin assembly is necessary and likely to provide propulsive force for intracellular movement of *Listeria monocytogenes*. Infect. Immun. *60*, 3609-3619.

Sarov, I., and Joklik, W. K. (1972). Studies on the nature and location of the capsid polypeptides of vaccinia virions. Virology *50*, 579-592.

Schmelz, M., Sodeik, B., Ericsson, M., Wolffe, E. J., Shida, H., Hiller, G., and Griffiths, G. (1994). Assembly of vaccinia virus: The second wrapping cisterna is derived from the trans Golgi network. J. Virol. *68*. 130-147

Schmutz, C., Payne, L. G., Gubser, J., and Wittek, R. (1991). A mutation in the gene encoding the vaccinia virus 37,000-M_r protein confers resistance to an inhibitor of virus envelopment and release. J. Virol. *65*, 3435-3442.

Schmutz, C., Rindisbacher, L., Galmiche, M., C., and Wittek, R. (1995). Biochemical analysis of the major vaccinia virus antigen. Virol. *213*, 19-27.

Shatkin, A., J. (1963). Actinomycin D and vaccinia virus infection of HeLa cells. Nature *199*, 357-358.

Shida, H. (1986). Nucleotide sequence of the vaccinia virus hemagglutinin gene. Virology *150*, 451-462.

Shida, H., and Dales, S. (1981). Biogenesis of vaccinia: Carbohydrate of the hemagglutinin molecule. Virology *111*, 56-72.

Smith, G. L., Chan, Y. S., and Howard, S. T. (1991). Nucleotide sequence of 42kbp of vaccinia virus strain WR from near the right inverted terminal repeat. J. Gen. Virol. *72*, 1349-1376.

Sodeik, B., Doms, R. W., Ericsson, M., Hiller, G., Machamer, C. E., Hof, W. v. t., Meer, G. v., Moss, B., and Griffiths, G. (1993). Assembly of vaccinia virus: Role of the intermediate compartment between the endoplasmic reticulum and the Golgi stacks. J. Cell Biol. *121*. 521-541

Sodeik, B., Griffiths, G., Ericsson, M., and Doms, R., W. (1994). Assembly of vaccinia virus:effects of rifampicin on the intracellular distribution of viral protein p65. J. Virol. *68*, 1103-1114.

Sodeik, B., Cudmore, S., Ericsson, M., Esteban, M., Niles, E., G., and Griffiths, G. (1995). Assembly of vaccinia virus: Incorporation of p14 and p32 into the membrane of the intracellular mature virus. J. Virol. *69*, 3560-3574.

Stallcup, K., C., Raine, C., S., and Fields, B., N. (1983). Cytochalasin B inhibits the maturation of measles virus. Virol *124*, 59-74.

Stern, W., and Dales, S. (1974). Biogenesis of vaccinia: Concerning the origin of the envelope phospholipids. Virology *62*, 293-306.

Stern, W., and Dales, S. (1976). Biogenesis of vaccinia: Isolation and characterization of a surface component that elicits antibody suppressing infectivity and cell-cell fusion. Virology *75*, 232-241.

Stern, W., and Dales, S. (1976). Biogenesis of vaccinia: Relationship of the envelope to virus assembly. Virology *75*, 232-241.

Stokes, G. V. (1976). High-voltage electron microscope study of the release of vaccinia virus from whole cells. J. Virol. *18*, 636-643.

Stossel, T., P., Chaponnier, C., Ezzell, R., M., Hartwig, J., H., Janmey, P., A., Kwiatkowski, D., J., Lind, S., E., Smith, D., B., Southwick, F., S., Yin, H., L., and Zaner, K., S. (1985). Nonmuscle actin binding proteins. Ann. Rev. Cell Biol. *1*, 353-402.

Stroobant, P., Rice, A. P., Gullick, W. J., Cheng, D. J., Kerr, I. M., and Waterfield, M. D. (1985). Purification and characterization of vaccinia virus growth factor. Cell *42*, 383-393.

Takahashi-Nishimaki, F., Funahashi, S. I., Miki, K., Hashizume, S., and Sugimoto, M. (1991). Regulation of plaque and host range by a vaccinia virus gene related to complement system proteins. Virology *181*, 158-164.

Tartaglia, J., and Paoletti, E. (1985). Physical mapping and DNA sequence analysis of the rifampicin resistance locus in vaccinia virus. Virology *147*, 394-404.

Tartaglia, J., Piccini, A., and Paoletti, E. (1986). Vaccinia virus rifampicin-resistance locus specifies a late 63,000 Da gene product. Virology *150*, 45-54.

Temm-Grove, C., J., Jockusch, B., M., Rohde, M., Niebuhr, K., Chakraborty, T., and Wehland, J. (1994). Exploitation of microfilament proteins by Listeria monocytogenes: microvillus-like composition of the comet tails and vectorial spreading in polarized epithelial sheets. J.C.S. *107*, 2951-2960.

Teysseire, N., Chiche-Portiche, C., and Raoult, D. (1992). Intracellular movements of Rickettsia conorii and R. typhi based on actin polymerization. Res. Microbiol. *143*, 821-829.

Theriot, J., A., Mitchison, T., J., Tilney, L., G., and Portnoy, D., A. (1992). The rate of actin-based motility of intracellular Listeria monocytogenes equals the rate of actin polymerization. Nature *357*, 257-260.

Theriot, J., A., Rosenblatt, J., Portnoy, D., A., Goldschmidt-Clermont, P., J., and Mitchison, T., J. (1994). Involvement of profilin in the actin-based motility of L. monocytogenes in cells and in cell-free extracts. Cell *76*, 505-517.

Tilney, L. G., Connelly, P. S., and Portnoy, D. A. (1990). Actin filament nucleation by the bacterial pathogen, *Listeria monocytogenes*. J. Cell. Biol. *111*, 2979-2988.

Tilney, L. G., DeRosier, D. J., and Tilney, M. S. (1992). How Listeria exploits host cell actin to form its own cytoskeleton.I. Formation of a tail and how that tail might be involved in movement. J. Cell. Biol., 71-81. *118*,

Tilney, L. G., DeRosier, D. J., Weber, A., and Tilney, M. S. (1992). How Listeria exploits host cell actin to form its own cytoskeleton. II Nucleation, actin filament polarity,filament assembly and evidence for a pointed end capper. J. Cell. Biol. *118*, 83-93.

Tilney, L. G., and Portnoy, D. A. (1989). Actin filaments and the growth,movement and spread of the intracellular bacterial parasite, *Listeria monocytogenes*. J. Cell. Biol. *109*, 1597-1608.

vanMeir, E., and Wittek, R. (1988). Fine structure of the vaccinia virus gene encoding the precursor of the major core protein 4a. Arch Virol. *102*, 19-27.

VanSlyke, J., Whitehead, S. S., Wilson, E. M., and Hruby, D. E. (1991). The multistep proteolytic maturation pathway utilized by vaccinia virus P4a protein: A degenerate conserved cleavage motif within core proteins. Virology *183*, 467-478.

VanSlyke, J. K., Franke, C. A., and Hruby, D. E. (1991). Proteolytic maturation of vaccinia virus core proteins: identification of a conserved motif at the N termini of the 4b and 25K virion proteins. J. Gen. Virol. *72*, 411-416.

Vanslyke, J. K., and Hruby, D. E. (1994). Immunolocalization of Vaccinia Virus Structural Proteins during Virion Formation. Virology *198*, 624-635.

VanSlyke, J. K., and Hruby, D. E. (1990). Posttranslational modifications of vaccinia virus proteins. Curr. Top. Microbiol. Immunol. *163*, 185-206.

Vasquez-Boland, J., A., Kocks, C., Dramsi, S., Ohayon, H., Geoffroy, C., Mengaud, J., and Cossart, P. (1992). Nucleotide sequence of the lecithinase operon of the *Listeria monocytogenes* and possible role in cell-to-cell spread. Infect. Immun. *60*, 219-230.

Vasselon, T., Mounier, J., Prevost, M., C., Hellio, R., and Sansonetti, P., J. (1991). Infection and Immunity *59*, 1723-1732.

Wang, E., Wolf, B., A., Lamb, R., A., Choppin, P., W., and Goldberg, A., R. (1976). The presence of actin in enveloped viruses. In Cell Motility, R. e. a. Goldman, ed.: Cold Spring Harbour), pp. 589-599.

Wechsler, S., L., and Fields, B. (1978). Intracellular synthesis of measles virus-specified polypeptides. J. Virol. *25*, 285-297.

Weir, J. P., and Moss, B. (1984). Regulation of expression and nucleotide sequence of a late vaccinia virus gene. J. Virol. *51*, 662-669.

Weir, J. P., and Moss, B. (1985). Use of a bacterial expression vector to identify the gene encoding a major core protein of vaccinia virus. J. Virol. *56*, 534-540.

WHO. (1980). The global eradication of small pox. Final report of the global commission for the certification of small pox eradication: World Health Organization). Geneva

Wilton, S., Gordon, J., and Dales, S. (1986). Identification of antigenic determinants by polyclonal and hybridoma antibodies induced during the course of infection by vaccinia virus. Virology *148*, 84-96.

Wilton, S., Mohandas, A., R., and Dales, S. (1995). Organisation of the vaccinia envelope and relationship to the structure of the intracellular mature virions. Virol *214*, 503-511.

Wittek, R., Hänggi, M., and Hiller, G. (1984). Mapping of a gene coding for a major late structural polypeptide on the vaccinia virus genome. J. Virol. *49*, 371-378.

Wittek, R., Richner, B., and Hiller, G. (1984). Mapping of the genes coding for the two major vaccinia virus core polypeptides. Nuc. Acid Res. *12*, 4835-4848.

Wolffe, E. J., Isaacs, S. N., and Moss, B. (1993). Deletion of the vaccinia virus B5R gene encoding a 42kD membrane glycoprotein inhibits extracellular virus envelope formation and dissemination. J. Virol *67*, 4732-4741.

Yang, W. P., Kao, S. Y., and Bauer, W. R. (1988). Biosynthesis and post-translational cleavage of vaccinia virus structural protein VP8. Virology *167*, 585-590.

Zhang, Y., and Moss, B. (1991). Inducer-dependent conditional-lethal mutant animal viruses. Proc. Natl. Acad. Sci. USA *88*, 1511-1515.

Zhang, Y., and Moss, B. (1991). Vaccinia virus morphogenesis is interrupted when expression of the gene encoding an 11-kilodalton phosphorylated protein is prevented by the *Escherichia coli* lac repressor. J. Virol. *65*, 6101-6110.

Zhukarev, V., Ashton, F., Sanger, J. M., Sanger, J. W., and Shuman, H. (1995). Organization and structure of actin filament bundles in *Listeria* infected cells. Cell Motil Cytoskel *30*, 229-246.

Zinov'ev, V., V., Ovechkina, L., G, Matskova, L., V., Balakhnin, S., M., Malygin, E., G, Yu Chertov, O., Telezhinskaya, I., N., Zaitseva, E., V., and Golubeva, T., B (1992). Identification of the immunodominant protein p35 gene of vaccinia virus. Mol. Biol. Moscow *26*, 142-149.

Zwartouw, H. T. (1964). The chemical composition of vaccinia virus. J. Gen. Microbiol. *34*, 115-123.

APPENDIX

Additional papers

1. Assembly of vaccinia virus: incorporation of p14 and p32 into the membrane of the intracellular mature virus. (1995) Sodeik, B., Cudmore, S., Ericsson, M., Esteban, M., Niles, E.,G., and Griffiths, G.
   J Virol. 69, 3560-3574.

2. Characterization of *ts*16, a temperature-sensitive mutant of vaccinia virus. (1995) Ericsson, M., Cudmore,S., Shuman,S., Condit, R.,C., Griffiths, G. and Krijnse Locker, J.
   J. Virol. 69, 7072-7086

3. A novel immunogold cryoelectron microscopic approach to investigate the structure of intracellular and extracellular forms of vaccinia virus. (1996) Roos, N., Cyrklaff, M., Cudmore, S., Blasco, R., Krijnse Locker, J. and Griffiths, G.
   EMBO J. in press

JOURNAL OF VIROLOGY, June 1995, p. 3560–3574
0022-538X/95/$04.00+0
Copyright © 1995, American Society for Microbiology
Vol. 69, No. 6

Assembly of Vaccinia Virus: Incorporation of p14 and p32 into the Membrane of the Intracellular Mature Virus

BEATE SODEIK,[1]† SALLY CUDMORE,[1] MARIA ERICSSON,[1] MARIANO ESTEBAN,[2] EDWARD G. NILES,[3] AND GARETH GRIFFITHS[1]*

Cell Biology Program, European Molecular Biology Laboratory, 69012 Heidelberg, Germany[1]; Centro Nacional de Biotecnologia, Consejo Superior de Investigaciones, Científicas, Campus Universidad Autonoma, 28049 Madrid, Spain[2]; and Department of Biochemistry, School of Medicine, State University of New York, Buffalo, New York 14214[3]

Received 9 June 1994/Accepted 14 March 1995

The cytoplasmic assembly of vaccinia virus begins with the transformation of a two-membraned cisterna derived from the intermediate compartment between the endoplasmic reticulum and the Golgi complex. This cisterna develops into a viral crescent which eventually forms a spherical immature virus (IV) that matures into the intracellular mature virus (IMV). Using immunoelectron microscopy, we determined the subcellular localization of p32 and p14, two membrane-associated proteins of vaccinia virus. p32 was associated with vaccinia virus membranes at all stages of virion assembly, starting with the viral crescents, as well as with the membranes which accumulated during the inhibition of assembly by rifampin. There was also low but significant labelling of membranes of some cellular compartments, especially those in the vicinity of the Golgi complex. In contrast, anti-p14 labelled neither the crescents nor the IV but gave strong labelling of an intermediate form between IV and IMV and was then associated with all later viral forms. This protein was also not significantly detected on identifiable cellular membranes. Both p32 and p14 were abundantly expressed on the surface of intact IMV. Our data are consistent with a model whereby p32 would become inserted into cellular membranes before being incorporated into the crescents whereas p14 would be posttranslationally associated with the viral outer membrane at a specific later stage of the viral life cycle.

Vaccinia virus is the best-studied member of the family *Poxviridae*, the largest and most complex of the animal viruses (for reviews, see references 5, 13, 18, and 28). Vaccinia virus replication and assembly occur in discrete cytoplasmic foci termed viral factories (1, 4, 24). The first morphological evidence for viral assembly is the formation of crescent-shaped membranes. On the basis of immunoelectron microscopy with antibodies specific to cellular membranes, in conjunction with a lipid analysis of purified virions, we have shown that these viral crescents are derived from a membrane cisterna of the intermediate compartment, which is located between the endoplasmic reticulum (ER) and the Golgi stacks (45). Our data also argue that the crescents are made up of two closely apposed membranes rather than one (45), as previous studies had suggested (5). The viral crescents eventually form spherical, immature virions which undergo additional maturational events such as proteolytic cleavages (5, 29), to give rise to the brick-shaped form of vaccinia virus, designated the intracellular naked virus (19, 31) or intracellular mature virus (IMV) (45). Data from both thawed cryosections of aldehyde-fixed vaccinia virus-infected cells (45) and cryoelectron microscopy (cryo-EM) of purified, frozen hydrated IMV (9) have also argued that the IMV contains at least two membranes. A fraction of the IMV becomes enwrapped by an additional cisterna, derived from the trans-Golgi network, thereby forming the intracellular enveloped virus (IEV), a form enveloped by four membranes (44). The outermost membrane of the IEV is thought to fuse with the plasma membrane, thereby releasing the extracellular enveloped virus (EEV), containing one fewer membrane than the IEV (44), into the medium (36).

By two-dimensional gel electrophoresis, purified IMVs have been shown to contain at least 111 different polypeptides (12). According to their solubility under reducing conditions in Nonidet P-40 (NP-40) or Triton X-100, the proteins of the IMV were classified into core proteins and envelope proteins (11, 21, 23, 34, 43). Envelope proteins of the IMV were also identified by surface labelling, by their accessibility to proteases on the surface of purified IMV, or by their capability to induce neutralizing antibodies against the IMV (3, 34, 35, 39, 47).

Probably the two best-characterized membrane proteins of the IMV are p32, encoded by the gene D8L (27, 32), and p14, encoded by the gene A27L (38). p32 was one of the first putative integral membrane proteins identified as being incorporated into the IMV. It has a molecular mass of 32 kDa, a C-terminal hydrophobic membrane anchor predicted from its sequence, and 36% homology to carbonic anhydrase. It is not glycosylated and is nonessential for the viral life cycle in cultured cells (32, 42). Further, p32 binds specifically to the plasma membrane. Inactivation of the gene results in reduced levels of gene expression and alternation of the virus, probably because of a function of p32 during virus entry (42). That deletion of p32 does not inhibit entry may be explained by redundancy: it seems likely that more than one protein can function as a ligand for the cellular receptors that facilitate entry.

p14 was first identified with a monoclonal antibody which neutralized IMV infectivity (6, 39). This 14-kDa protein has been postulated to exist as disulfide-linked trimers within the virus and to be involved in the fusion of the IMV with the plasma membrane upon virus entry, as well as in cell-cell fusion (16, 40). When p14 synthesis is repressed during the viral life cycle, normal infectious IMVs are formed, but they are not

* Corresponding author. Mailing address: EMBL, Meyerhofstr. 1, Postfach 10.2209, 69012 Heidelberg, Germany. Phone: 49-6221-387267. Fax: 49-6221-387306.

† Present address: Department of Cell Biology, Yale University School of Medicine, New Haven, CT 06520-8002.

wrapped by intracellular membranes and no IEVs or EEVs are formed (41). Thus, in contrast to p32, p14 is essential for the assembly of the IEV and consequently for the EEV.

While the protein composition of both IMV and EEV has been relatively well characterized, little is known about the proteins present in the immature viral structures because these particles have not been purified. Immunogold EM offers an alternative approach for asking whether or not a particular protein is enriched in the various morphological forms of the virus. With this rationale, we began a detailed analysis of the distribution of several vaccinia virus structural proteins (44–46). In this paper, we describe the subcellular localization of two vaccinia virus membrane proteins, p14 and p32. Our data show that p32 is associated with all morphologically detectable forms of the virus from the crescents onwards. In contrast, p14 is first detected on viral membranes at a later step during the transition from the intracellular immature virus (IV) to the IMV.

MATERIALS AND METHODS

Materials. Tissue culture reagents were obtained from Gibco BRL (Gaithersburg, Md.). HeLa cells (ATCC CCL 2) were grown in Eagle's minimal essential medium supplemented with 10% fetal calf serum (heat inactivated) and nonessential amino acids, and BHK-21 cells (ATCC CCL 10) were grown in Glasgow's modified Eagle's medium supplemented with 5% fetal calf serum and 10% tryptose phosphate broth. All media contained 2 mM glutamine, 100 U of penicillin per ml, and 10 mg of streptomycin per ml, and all cell lines were grown as adherent cultures in a 5% CO_2 incubator at 37°C. Virus propagation and titration with the vaccinia virus strain WR (ATCC VR 1354), kindly provided by B. Moss (National Institutes of Health, Bethesda, Md.), were performed as previously described (10). We used two rabbit antibodies (D8.1 and D8.2) raised against a region of p32 (gene D8L) consisting of amino acids 77 to 294 (32). We also used two antibodies against p14 (gene A27L), a mouse monoclonal antibody (C3) (39), and a rabbit antipeptide antibody (C4) raised against the first 20 amino acids of the N terminus of p14 (6). All secondary antibodies, rhodamine-coupled goat anti-rabbit or goat anti-mouse antibodies, and rabbit anti-mouse immunoglobulin G were obtained from Organon Teknika/Cappel (West Chester, Pa.).

Virus infections and drug treatments. Cells were grown for 2 days to approximately 90% confluency, washed once in phosphate-buffered saline (PBS), and then infected in serum-free Eagle's minimal essential medium at a multiplicity of infection of 10 to 20 PFU per cell (7). After 1 h at 37°C with intermittent agitation, the inoculum was aspirated off and the cells were placed in normal growth medium at 37°C with or without rifampin (final concentration, 100 μg/ml; Sigma, St. Louis, Mo.). Rifampin was stored as a 1,000-fold stock solution in dimethyl sulfoxide at −20°C. For chase experiments, the cells were washed three times with ice-cold PBS at the indicated times and then further incubated with prewarmed, normal rifampin-free medium at 37°C.

Microscopy. Vaccinia virus-infected HeLa and BHK cells were processed for microscopy as previously described (44–46). Briefly, for immunofluorescence experiments all incubations were carried out with PBS, pH 7.4, as a buffer. The cells were fixed with 3% paraformaldehyde for 20 min, quenched with 50 mM NH_4Cl for 10 min, and then permeabilized in 0.2% Triton X-100 for 4 min. They were labelled with the first antibody and subsequently with fluorescently labelled secondary antibodies, both in 0.2% gelatin for 20 min. Nuclear and viral DNAs were stained with 5 μg of *bis*-benzimide per ml (Hoechst no. 33258; Sigma) for 5 min. The coverslips were mounted in moviol on glass slides, examined with an Axiophot microscope (Carl Zeiss, Oberkochen, Germany), and photographed with TMAX Kodak film (ASA 400). For immunogold labelling on thawed cryosections, the cells were removed from the culture dish by proteinase K (25 μg/ml for HeLa cells and 50 μg/ml for BHK cells in 0.25 M HEPES [*N*-2-hydroxyethylpiperazine-*N'*-2-ethanesulfonic acid], pH 7.4) on ice for 2 to 3 min and fixed in 8% paraformaldehyde in 0.25 M HEPES, pH 7.4, overnight. Cell pellets were infiltrated with 2.1 M sucrose in PBS, frozen, and stored in liquid nitrogen. Ultrathin sections were cut at −90°C, transferred to Formvar-coated grids, and labelled (with protein A gold) and contrasted as described previously (17). The sequential procedure for double labelling is also described in reference 17. The treatment of cells with streptolysin O (SLO) (Wellcome Diagnostics, Dartford, United Kingdom) and their preparation for cryosectioning are described in reference 25.

For labelling whole virus, purified IMV was adsorbed onto glow-discharged grids that had been coated with Formvar and carbon. Grids with adsorbed virus were then treated with (i) NP-40 (1%) and dithiothreitol (DTT) (20 mM) for 30 min at 37°C, (ii) DTT alone (20 mM) at 37°C, (iii) trypsin (50 μg/ml) at 37°C, or (iv) proteinase K (50 μg/ml) at 4°C. Subsequently, the grids were rinsed with PBS, blocked for 10 min with 1% fetal calf serum, and labelled with either anti-p14 (followed by rabbit anti-mouse antibody) or anti-p32. The bound antibodies were visualized by protein A-gold (10 min). Following extensive rinses with PBS (20 min), the grids were rinsed with three changes (30 s total) of triple-distilled water and floated on 2% uranyl acetate for 30 s, and following removal of excess stain with filter paper, the grids were air dried.

RESULTS

Localization of p32. We began our analysis with p32, which is present in purified IMV and for which a transmembrane domain has been postulated on the basis of its predicted amino acid sequence (32). The two p32 antibodies that we used (32) gave identical results. By immunofluorescence microscopy at 8 h postinfection, anti-p32 strongly labelled the region of the viral factories (45, 46) (Fig. 1b) as defined by DNA staining (Fig. 1a, arrowheads). Additionally, there was strong labelling of punctate structures scattered throughout the whole cytoplasm and a weaker reticular labelling extending out to the periphery of the cells (Fig. 1b). We suggest that the punctate structures are IMV particles while the reticular labelling represents the ER. When the infection was carried out for 8 h in the presence of rifampin (30), anti-p32 labelled ring-shaped structures (Fig. 1e) which corresponded to the boundaries of the rifampin bodies, which we identified with phase-contrast microscopy (45, 46) (arrowheads in Fig. 1f). Additionally, we observed the same reticular labelling throughout the whole cytoplasm that was seen without rifampin. Both with and without rifampin, there was no labelling of the plasma membrane.

On ultrathin thawed cryosections of vaccinia virus-infected cells, anti-p32 labelled all identifiable forms of the virus (Fig. 2 to 5). Significant labelling for p32 was seen over the peripheral regions of many of the IVs (Fig. 4 and 5), the electron-dense intermediate form between the IV and the IMV (see references 45 and 46) (Fig. 2e and f), and the IMV particles (Fig. 2a to d, 3, and 4) which were strongly labelled on their membranes. The majority of label was associated with the outer of the two viral membranes of the IMV, but on many profiles of the IMV, the gold particles were also found over the inner membranes (Fig. 2b, c, and e). In the IEV, the second membrane and occasionally the inner membranes but in general not the two outermost membranes were labelled (Fig. 2g). There was also low but consistent labelling associated with the periphery of the Golgi stacks (Fig. 3). The central parts of the Golgi stacks (Fig. 3) and the plasma membrane (Fig. 2g) were essentially unlabelled. We also detected a low but significant labelling of the rough ER and the nuclear envelope (Fig. 4).

By evaluating a large number of preparations, it was clear that, on average, all viral forms were strongly labelled. However, for all forms individual examples that had low or no labelling were commonly seen (e.g., Fig. 3b). In our experience, such differences are often caused by variability in the access of antibodies to their antigens in the cryosections. Access is often improved on the surface of thawed cryosections from cells which were permeabilized with the bacterial, pore-forming toxin SLO prior to fixation (25). We therefore prepared HeLa cells infected with vaccinia virus (8 h) according to the same protocol. As shown in Fig. 5, after SLO extraction there was significantly more labelling of the IV (Fig. 5) and possibly of IMV (not shown). Not only the membranes of the IV but also those of the crescent were uniformly accessible for labelling with both peptide antibodies against p32. Moreover, labelled membranes that are apparently partially enclosed by the cup-shaped crescent structures were often seen (seen in section on the left of one crescent in Fig. 5b [arrowheads]). The significance of these internal membranes must await a more detailed study of the assembly process.

When cells were infected in the presence of rifampin, the viral precursor membranes surrounding the rifampin bodies

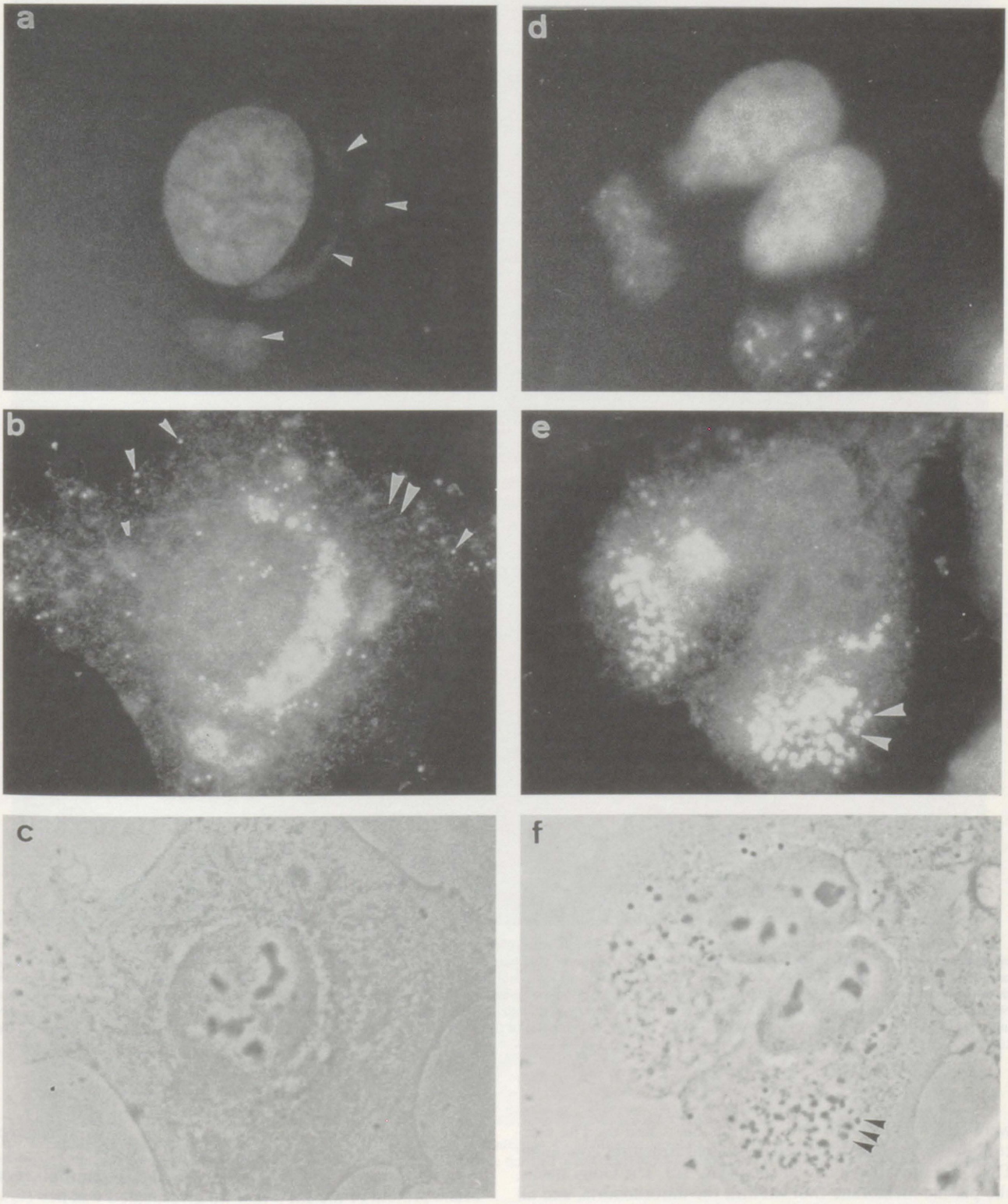


FIG. 1. Localization of p32 by immunofluorescence. Shown are vaccinia virus-infected HeLa cells 8 h postinfection in the absence (a to c) or presence (d to f) of rifampin. The cells were labelled with a fluorescent DNA dye (a and d) and with anti-p32 followed by rhodamine-conjugated goat anti-rabbit antibody (b and e). Panels c and f show the corresponding phase-contrast images. In the absence of rifampin, anti-p32 (b) shows a strong labelling in the region of the viral factories as defined by DNA staining (arrowheads in panel a). Additionally, there was strong labelling of punctate structures scattered throughout the cytoplasm (arrowheads in panel b) and a weaker reticular labelling extending out to the periphery of the cells. In the presence of rifampin, anti-p32 strongly labels the rifampin bodies (arrowheads in panel e) as defined in phase-contrast microscopy (arrowheads in panel f). Again, there is a weaker reticular labelling throughout the whole cytoplasm.

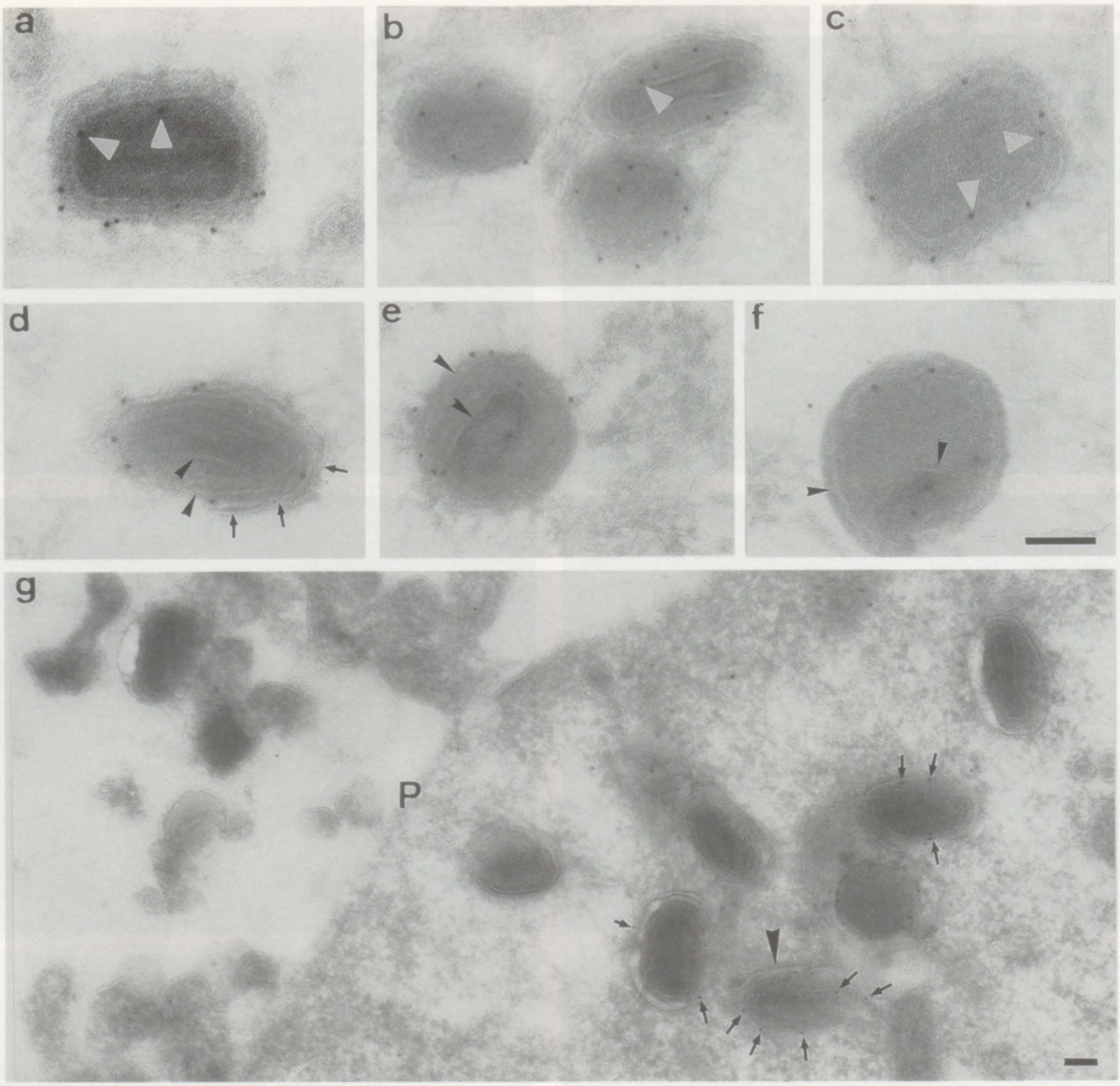


FIG. 2. EM immunogold localization of p32. Cryosections of vaccinia virus-infected HeLa cells at 8 h postinfection were labelled with anti-p32 antibody followed by protein A-gold. In panels a to c, labelling of IMV is shown. Most of the gold particles are associated with the outer membrane of the IMV; the arrowheads indicate label that appears to be associated with the inner membrane. In panel d, a p32-labelled IMV is partially enwrapped by a membrane cisterna (arrows); the arrowheads show the two membranes of the IMV. In panels e and f, intermediate-stage (between IV and IMV) particles are shown. The arrowheads indicate the two membranes. Note that some label is associated with the inner membrane. In panel g, a peripheral part of the cell is shown that contains a number of IEV profiles (the arrowhead indicates a cisterna that is tightly opposed to an IEV particle). Note that some of the IEVs are labelled significantly (small arrows), while others are unlabelled. Bars, 100 nm.

were clearly labelled by anti-p32 (Fig. 6a, c, and d). The electron-dense, irregularly shaped crystalloid structures containing DNA were invariably not labelled (Fig. 5d). The Golgi stacks, the plasma membrane (not shown), the mitochondria, and all other cell organelles had only occasional gold particles, which we assume to be background labelling (Fig. 6a). There was also a low labelling of the ER and nuclear envelope (not shown). When cells were incubated in drug-free medium for short time periods after the rifampin treatment, there was a synchronous assembly of viral crescents from the rifampin bodies (19, 46). As shown in Fig. 6b, when rifampin was chased for 15 min, there was significant labelling for p32 in the viral crescents which formed from the rifampin bodies.

Localization of p14. The second well-characterized membrane protein of the IMV that we investigated was p14 (6, 16, 37, 38, 40). In all our experiments, both anti-p14 antibodies that we have used gave identical results. By immunofluorescence microscopy at 4 h after vaccinia virus infection, anti-p14 gave a diffuse cytoplasmic labelling which did not show any reticular-like appearance (not shown). At 8 h postinfection, anti-p14 additionally labelled many distinct punctate structures, most probably single IMV particles, which accumulated

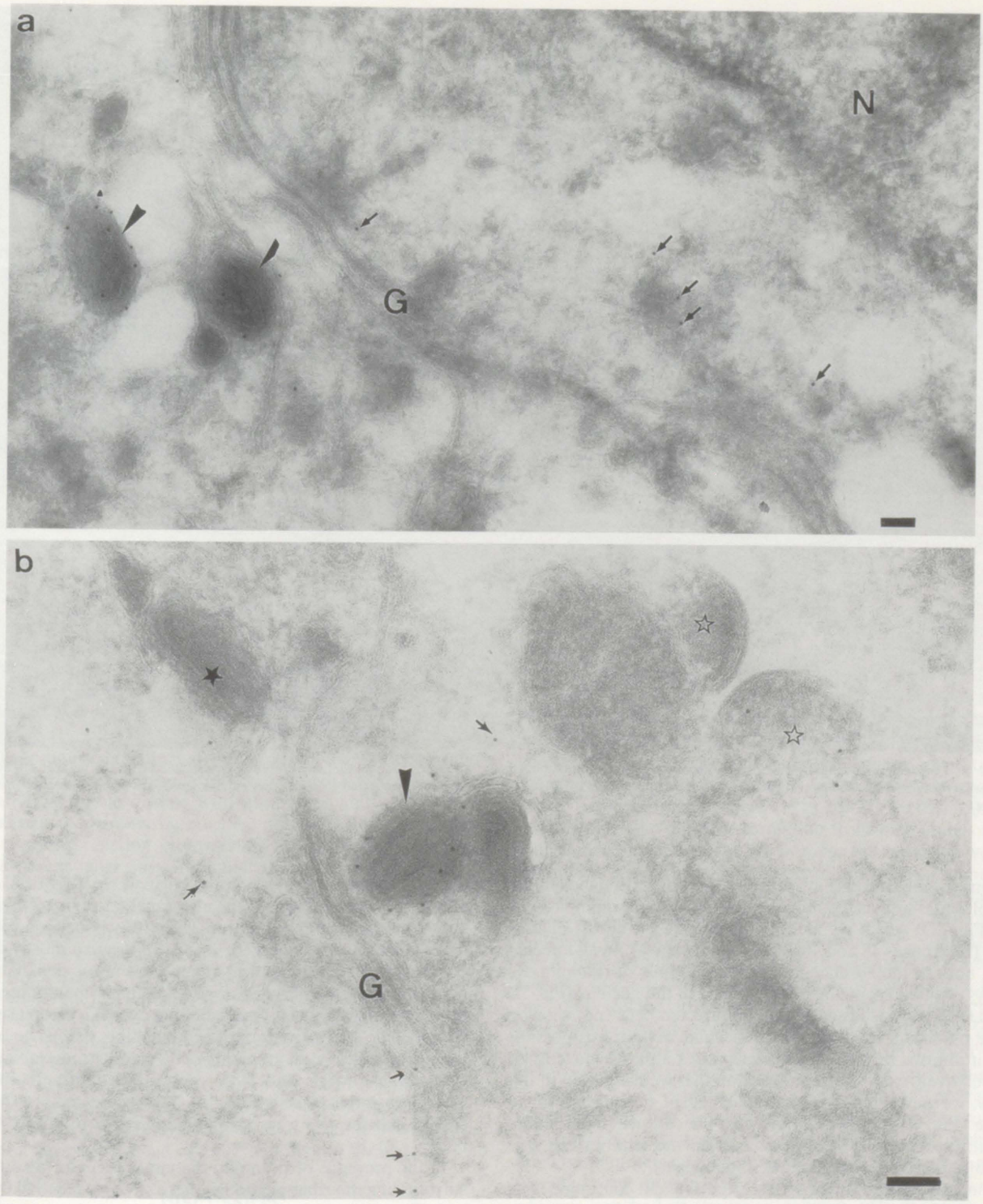


FIG. 3. Labelling for p32 in the perinuclear region of HeLa cells at 8 h postinfection. In addition to labelling, the IMV (arrowheads) gold particles are also associated with the peripheral elements of the Golgi complex (G, small arrows). Note that one of the IVs (open stars) and one IMV (filled star) are devoid of labelling. N, nucleus. Bars, 100 nm.

predominantly in the perinuclear region, as well as larger, discrete structures that were the most prominent labelled elements in these cells (Fig. 7B, asterisk in inset). These structures are most likely accumulated virions. In very flat cells, it is evident that they are made up of groups of particles (not shown). In such cells, it was also evident that these larger structures were not coincident with the viral factories, as defined by DNA staining (Fig. 7A and B; also insets). After even longer infection times, the diffuse cytoplasmic labelling as well as the number of labelled punctate structures increased (not

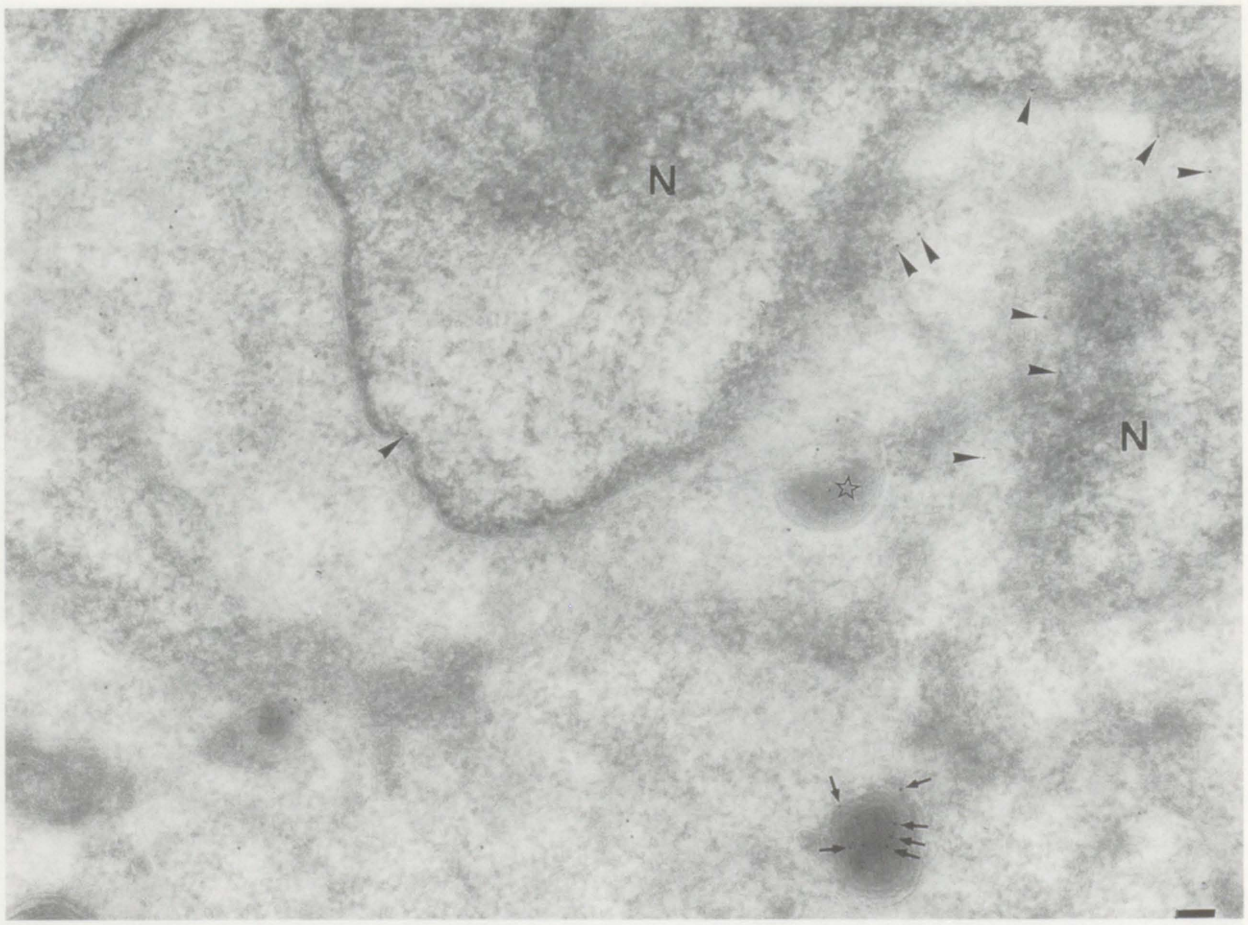


FIG. 4. Low-magnification image of HeLa cells at 8 h postinfection labelled for p32. Note the label that is preferentially associated with the nuclear envelope (N, nucleus [arrowheads]) as well as scattered in the cytoplasm. Both the IV (star) and a partially enwrapped IMV (arrows indicate gold) are labelled with anti-p32. Bar, 100 nm.

shown). In the presence of rifampin, anti-p14 also labelled the cytoplasm as well as the morphologically distinct rifampin bodies (Fig. 7D) which we identified with phase-contrast microscopy (references 45 and 46 and data not shown). In all infected cells, both in the absence and in the presence of rifampin, we always observed some labelling for p14 in the nucleus (Fig. 7B and D) which was absent from noninfected cells (not shown). Since p14 has a relatively low molecular weight, it is possible that it diffuses through the nuclear pores into the nucleus. At the relatively early times of infection that we have used in this study, we never observed any labelling of the plasma membrane (Fig. 6b and d). This was also the case when the immunofluorescence microscopy was carried out without cell permeabilization prior to labelling (not shown).

Immunoelectron microscopy experiments confirmed that the punctate labelling seen in control cells by immunofluorescence microscopy was due mainly to IMV particles (Fig. 8 and 9). Anti-p14 did not significantly label the IV (Fig. 8 and 9). However, an electron-dense intermediate form (45, 46) between the IV and the IMV form was strongly labelled predominantly on its outer membrane (Fig. 9). In general, the labelling of the IEV was variable. Figure 9e shows an example with significant labelling of the inner membranes. It seems likely that in the IEV the epitopes recognized by the antibodies are at least in part not accessible because of the binding of the additional membrane cisterna. We obtained similar results when we labelled cryosections of purified IMV or EEV particles. The purified IMVs were also labelled for p14 predominantly on their outer membrane with little associated with the inner membrane, whereas the intact EEVs were mostly devoid of labelling (data not shown). There was no obvious labelling of the plasma membrane or other cellular membranes, but there was often a low diffuse labelling over the cytoplasm (not shown). The overall pattern of p14 labelling, that is, no or very little labelling of viral crescents or IVs and strong labelling of intermediate forms and IMV, was fully confirmed with the SLO-permeabilized cells (Fig. 10). This argues against the possibility that the IVs were simply inaccessible to anti-p14 antibody.

In the presence of rifampin, the viral precursor membranes surrounding the rifampin bodies were strongly labelled by anti-p14 (Fig. 11b). Although there was always a low cytoplasmic labelling (Fig. 11b), the DNA crystalloids (D in Fig. 11c) were never labelled. When rifampin was washed out and the cells were chased in normal medium for 15 min, the viral crescents themselves were not labelled whereas the membranes connecting these viral crescents to the electron-dense rifampin bodies were positive for p14 (Fig. 11d). It remains to be established how p14 is excluded from the crescents during their formation. After longer chase times, the electron-dense intermediate form and the IMV were both strongly labelled by anti-p14 (data not shown).

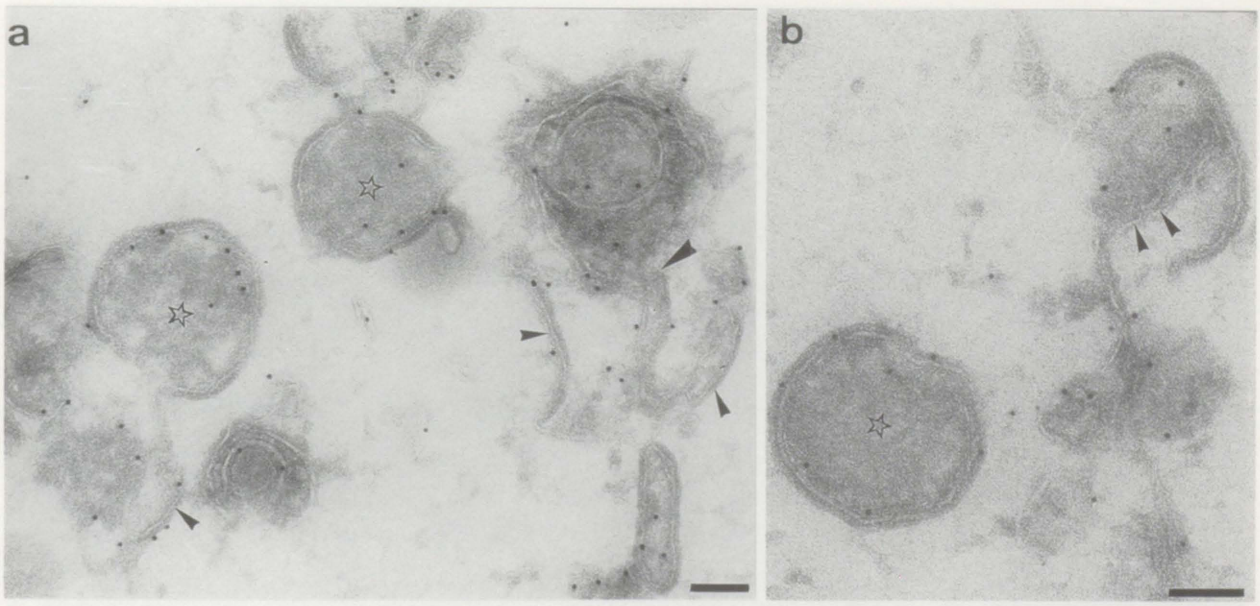


FIG. 5. Labelling of thawed cryosections of SLO-permeabilized HeLa cells at 8 h postinfection with p32. After the SLO permeabilization, the cytoplasm is extracted, and on the sections, there is a much higher degree of access for the anti-p32 antibody. Most of this label is membrane associated. The small arrowheads in panel a show labelling of viral crescent while the large arrowhead indicates a continuity between crescent membranes and an electron-dense membrane structure. Note the labelled membranes that appear to be partially enclosed by the developing crescent (arrowheads in panel b). Bars, 100 nm.

We also carried out double labelling with anti-p32 and anti-p14 and two sizes of gold (Fig. 12). This analysis confirmed the results from the single labelling, with p32 labelling all viral forms and strong labelling for p14 seen only in the intermediate stages. The IMVs were uniformly double labelled for both antigens.

Whole-mount labelling of purified virions. We confirmed that both p14 and p32 were exposed on the outside of the IMV by labelling whole virions with antibodies and gold before visualizing the virions by negative staining. Both antibodies gave a strong reaction in untreated virions (Table 1), and as expected, the label was essentially all abolished when the virions were treated with either trypsin (50 μg/ml, 37°C) or proteinase K (50 μg/ml, 4°C) (Table 1). When the virions were subjected to a variation of the treatment with NP-40 and reducing agent which has been widely used to separate envelope from cores (here, 1% NP-40 and 20 mM DTT [11, 21, 33, 43]), all the label for p14 and the bulk of label for p32 were removed relative to the untreated control. A surprising result came from pretreatment of the virus with 20 mM DTT alone before labelling. In the case of p32, this led to a loss of roughly half the label relative to the control. However, with p14 an almost fourfold increase was seen. A roughly twofold increase (≈80 gold particles per virion) was also seen when 1% mercaptoethanol was used instead of DTT (results not shown).

DISCUSSION

During the assembly of the first infectious form of vaccinia virus, at least four distinct morphological forms can be distinguished: the viral crescents, the IV, an electron-dense intermediate form, and the IMV itself (5, 13, 45). Our recent data indicate that the membranes of the crescents, the precursors of the IMV, originate from the intermediate compartment between the ER and the Golgi complex. This conclusion is based both on the existence of membrane continuities between the viral crescents and cellular membranes of the intermediate compartment and on the phospholipid composition of purified IMV particles (45). Vaccinia virus morphogenesis is clearly a complex, multistep process in which a large number of polypeptides must be assembled in a precise order to form a virus particle. The subviral localization of key structural proteins has, until now, relied mostly on the biochemical fractionation of purified IMV. Accordingly, the IMV proteins have been classified only as either detergent soluble, operationally defining the membrane proteins, or as detergent-insoluble, "core" proteins (e.g., see references 11, 21, 33, and 43).

To explain the crescent formation from membranes of the intermediate compartment, we propose the following working hypothesis: the formation of a specialized cisternal domain of the intermediate compartment is initiated by targeting vaccinia virus-encoded transmembrane proteins from the site of their synthesis, the rough ER, to the intermediate compartment where they are retained and therefore accumulate. We further envisage the crescent formation to be caused by an aggregation of these vaccinia virus membrane proteins, a process that is accompanied by an exclusion of cellular proteins. We further speculate that two kinds of protein-protein interaction would be involved in this process: first, lateral interactions within each membrane of a cisterna, and second, lumenal interactions which glue the two membranes together. All these processes are probably facilitated by vaccinia virus-encoded, peripheral membrane proteins. One obvious candidate for the latter is the vaccinia virus protein p65, the target of the drug rifampin, which is localized on the inner, concave, side of the crescents (46). The immunolocalization of the vaccinia virus proteins p32 and p14 in our present study should now be considered in the context of our assembly model.

p32, the product of the gene D8L, has all the hallmarks of a transmembrane protein, both from its predicted protein sequence and from its biochemical characterization (1a, 26, 32). On the basis of our immunogold labelling pattern for p32, we suggest that this protein is made in the rough ER membrane and subsequently transported to the intermediate compartment, where it is incorporated into the viral crescents. Bio-

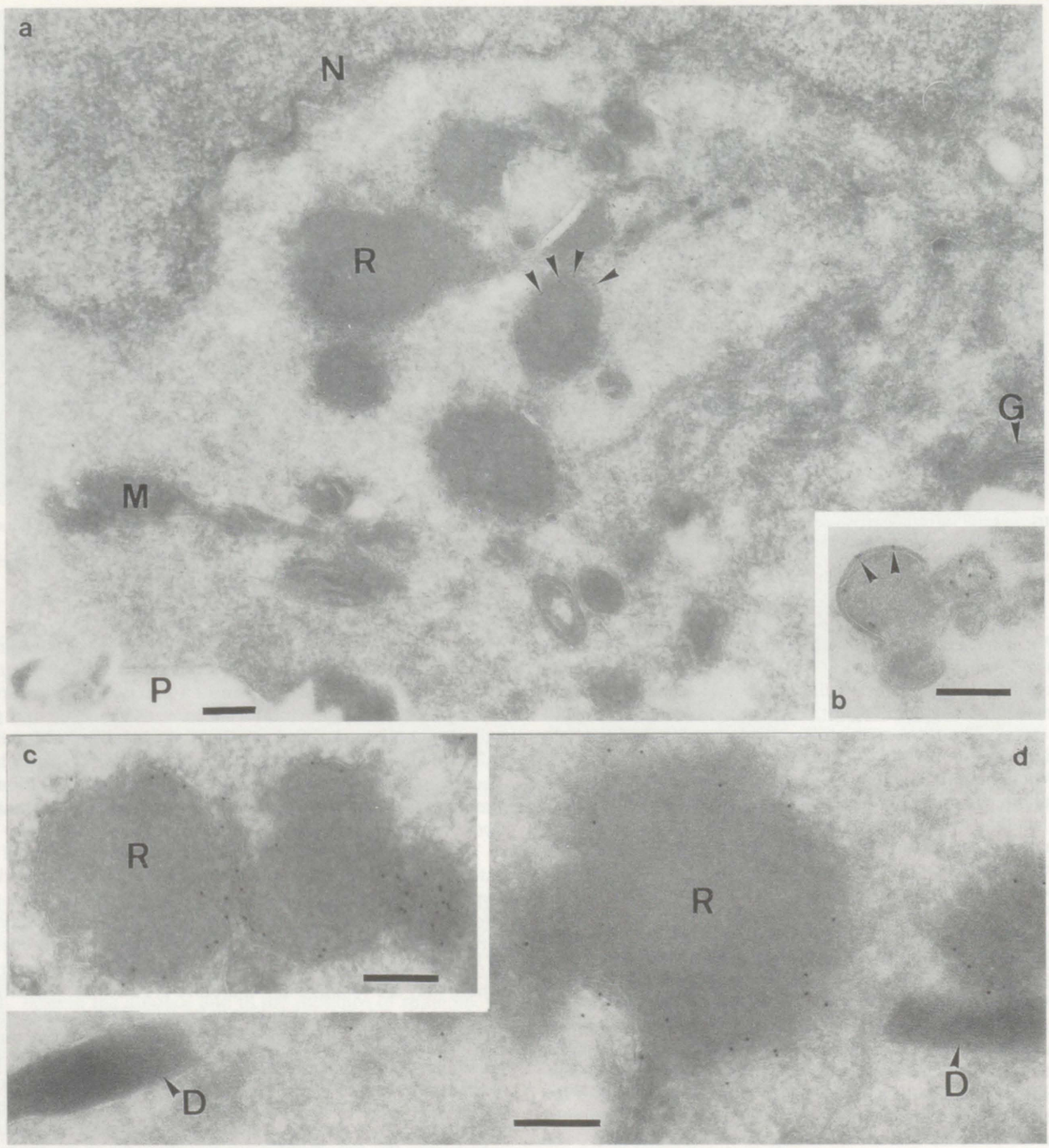


FIG. 6. Immunolocalization of p32 in cells infected in the presence of rifampin and after rifampin chase. Cryosections of HeLa cells infected with vaccinia virus (8 h) in the presence of rifampin (a, c, and d) and after chase of rifampin for 15 min (b) at 8 h postinfection were labelled with anti-p32 antibody. This antibody strongly labels the membranes (arrowheads) around the rifampin bodies (R in panels a, c, and d). Additionally, there is weak but significant labelling of cytoplasmic membranes but not the Golgi stacks (G in panel a), the plasma membrane (P in panel a), the mitochondria (M in panel a), or the DNA crystalloids (D in panel d). When rifampin is washed out, the viral crescents which assemble from the rifampin bodies are also labelled (arrowheads in panel b). N, nucleus. Bars, 200 nm.

chemical experiments are now in progress to try to confirm this working hypothesis. p32 was also localized in this study to the IV and the electron-dense intermediate form and, as expected, was found on the outer membrane of the IMV. The labelling of the IV was best demonstrated in cryosections of cells that had been permeabilized with SLO before fixation, a procedure which often improves access of antigens to their antibodies (25). When vaccinia virus assembly was blocked by rifampin, p32 accumulated on the viral precursor membranes associated with the rifampin bodies.

Collectively, these results agree with previous studies which have suggested that p32 is exposed on the outside of the IMV since a relatively large domain is removed by trypsin treatment of purified IMV (26, 32) and since some anti-p32 antibodies are neutralizing (2, 31a). Moreover, the p32 antibody labels intact IMV with immunogold followed by negative staining.

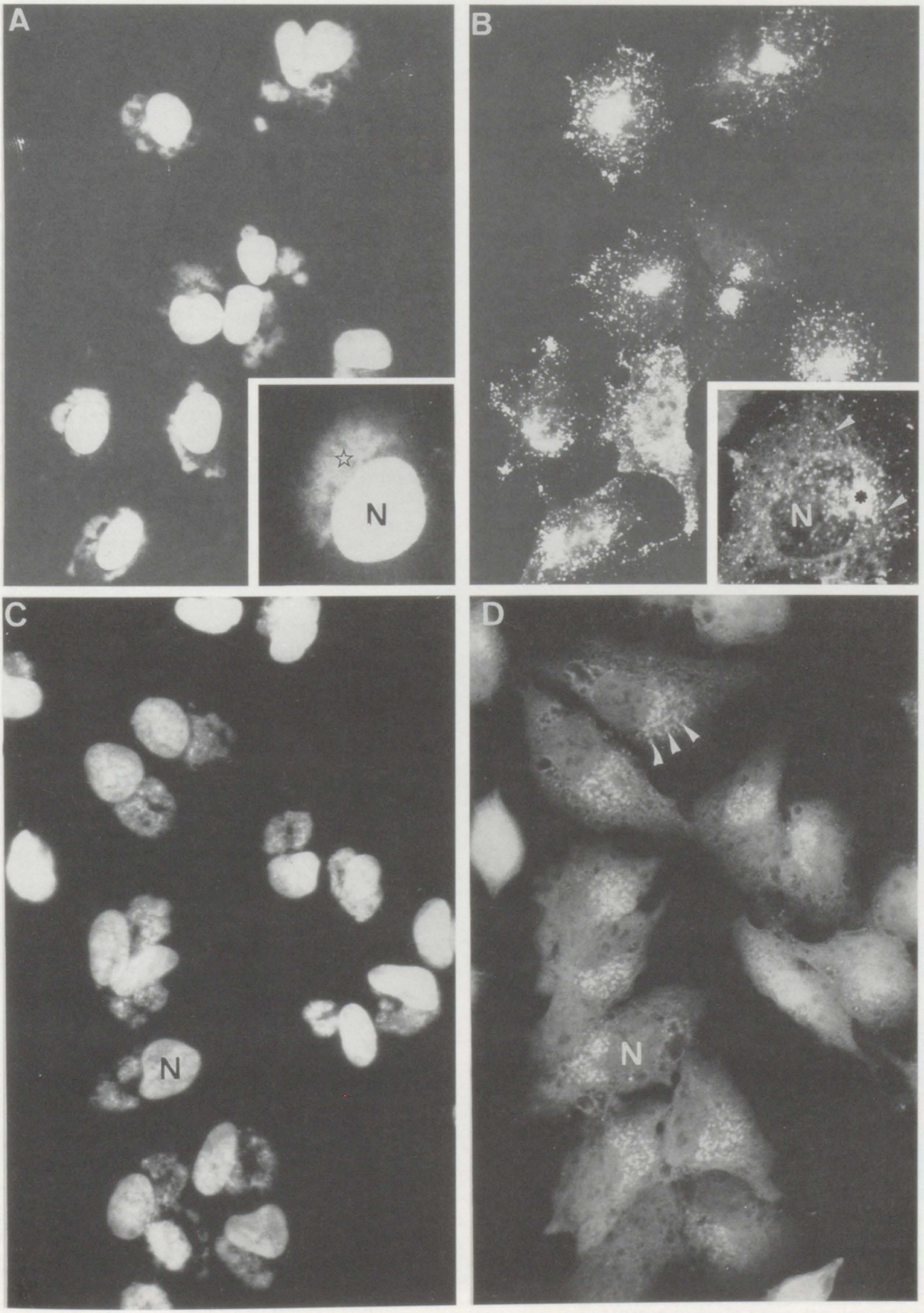

A
N
B
N
C
N
D
N

FIG. 7. Localization of p14 by immunofluorescence. Shown are vaccinia virus-infected HeLa cells 8 h postinfection in the absence (A and B) or presence (C and D) of rifampin. The cells were labelled with a fluorescent DNA dye (A and C) and with anti-p14 antibody followed by rhodamine-conjugated goat anti-rabbit antibody (B and D). In the absence of rifampin (B), anti-p14 gives a weak labelling of the cytoplasm and a strong labelling of punctate structures, probably individual virions, which accumulate in the perinuclear region (arrowheads) but which are also diffusely distributed throughout the cytoplasm, as is evident in the inset. The bulk of p14 labelling (asterisk in inset B) is clearly separated from the bulk of DNA (star in inset A). In the presence of rifampin (D), p14 accumulates on the rifampin bodies (arrowheads) easily identified in phase-contrast microscopy (not shown). The labelling of the cytoplasm in the presence of rifampin is stronger than in its absence (compare panel D with panel B). At these relatively early times of infection, there is no obvious labelling of the plasma membrane. N, nucleus.

and this label was essentially all lost when the virions were treated with proteases (Table 1). Additionally, it has been suggested that this protein functions as a ligand that facilitates the binding of IMV to the plasma membrane of susceptible cells (26, 27). In our EM sections, we also saw low but significant labelling for p32 on the inner membrane of the IMV, that is, the membrane that appears to be most closely associated with the DNA core (e.g., Fig. 2c and e). The significance of this observation awaits more detailed studies of the assembly process.

In contrast to p32, the amino acid sequence of p14 predicts a protein that lacks a putative signal sequence and a transmembrane domain. It contains only two very short, hydrophobic stretches: one of 5 amino acids at the amino terminus and one of 11 at the carboxy terminus (38). Our immunolocalization studies showed that, unlike p32, p14 was acquired at a distinct and later step of vaccinia virus assembly. Thus, while the early morphological forms of vaccinia virus were devoid of p14, there was strong labelling of the electron-dense intermediate form as well as the IMV. Importantly, and again in contrast to p32, most, if not all of the label for p14 was associated with the outer membranes of both the intermediate and the IMV forms. These observations are consistent with other data showing that p14 must be exposed on the outside of the IMV. Thus, some anti-p14 antibodies are neutralizing for IMV but not for EEV infection (6, 39). Further, this protein appears to be involved in the fusion of the IMV with the plasma membrane of the host cell (6, 16) and is essential for the intracellular wrapping of the IMV to form the IEV (41). That p14 is on the outside of IMV in significant amounts was also confirmed by labelling whole IMV with immunogold labelling followed by negative staining; almost all of this label is lost

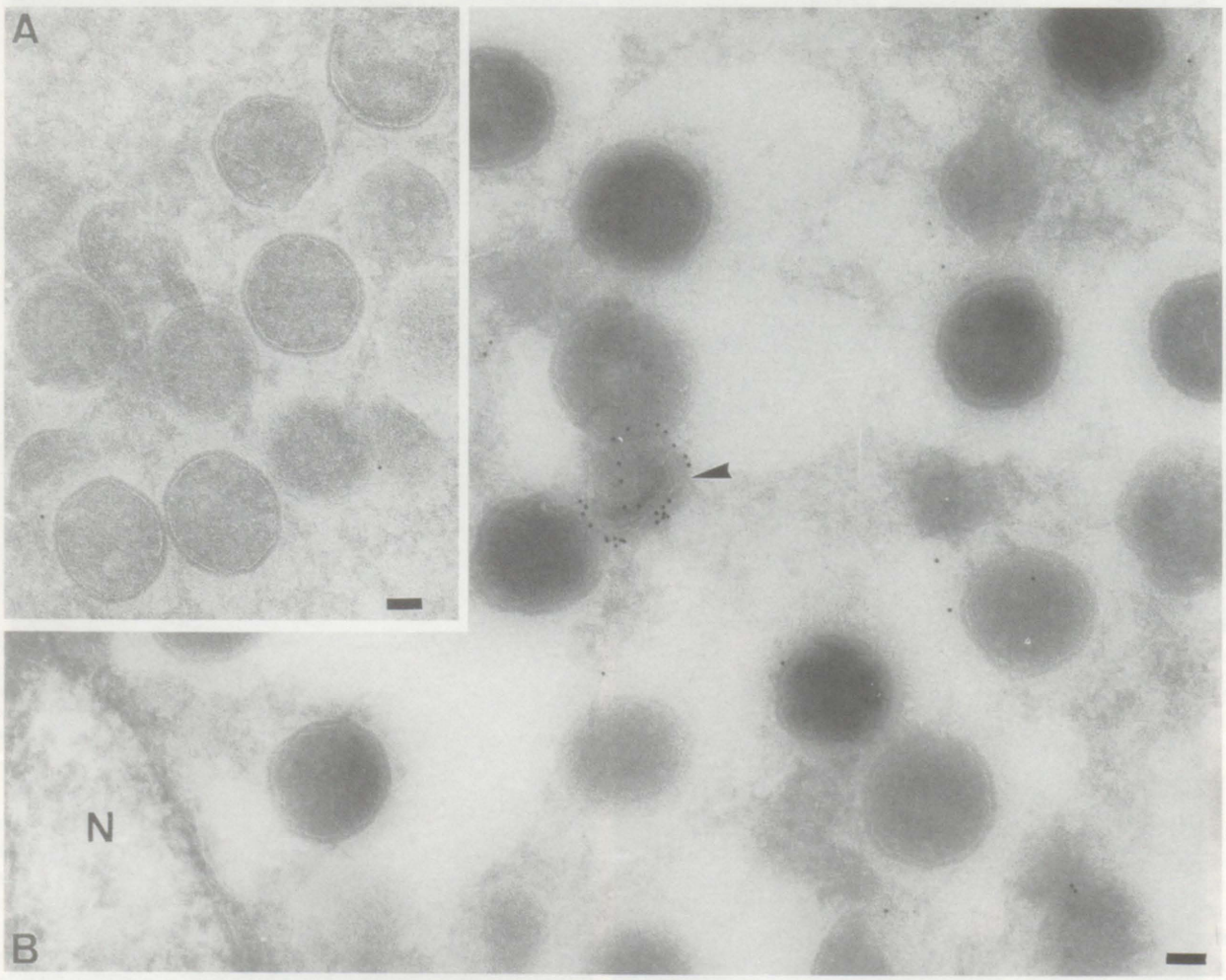


FIG. 8. EM immunolocalization of p14 in vaccinia virus-infected HeLa cells at 8 h postinfection. Most of the spherical IVs are either completely devoid of labelling or have a few single gold particles. In contrast, the IMV (arrowhead in panel B) is strongly labelled. N, nucleus. Bars, 100 nm.

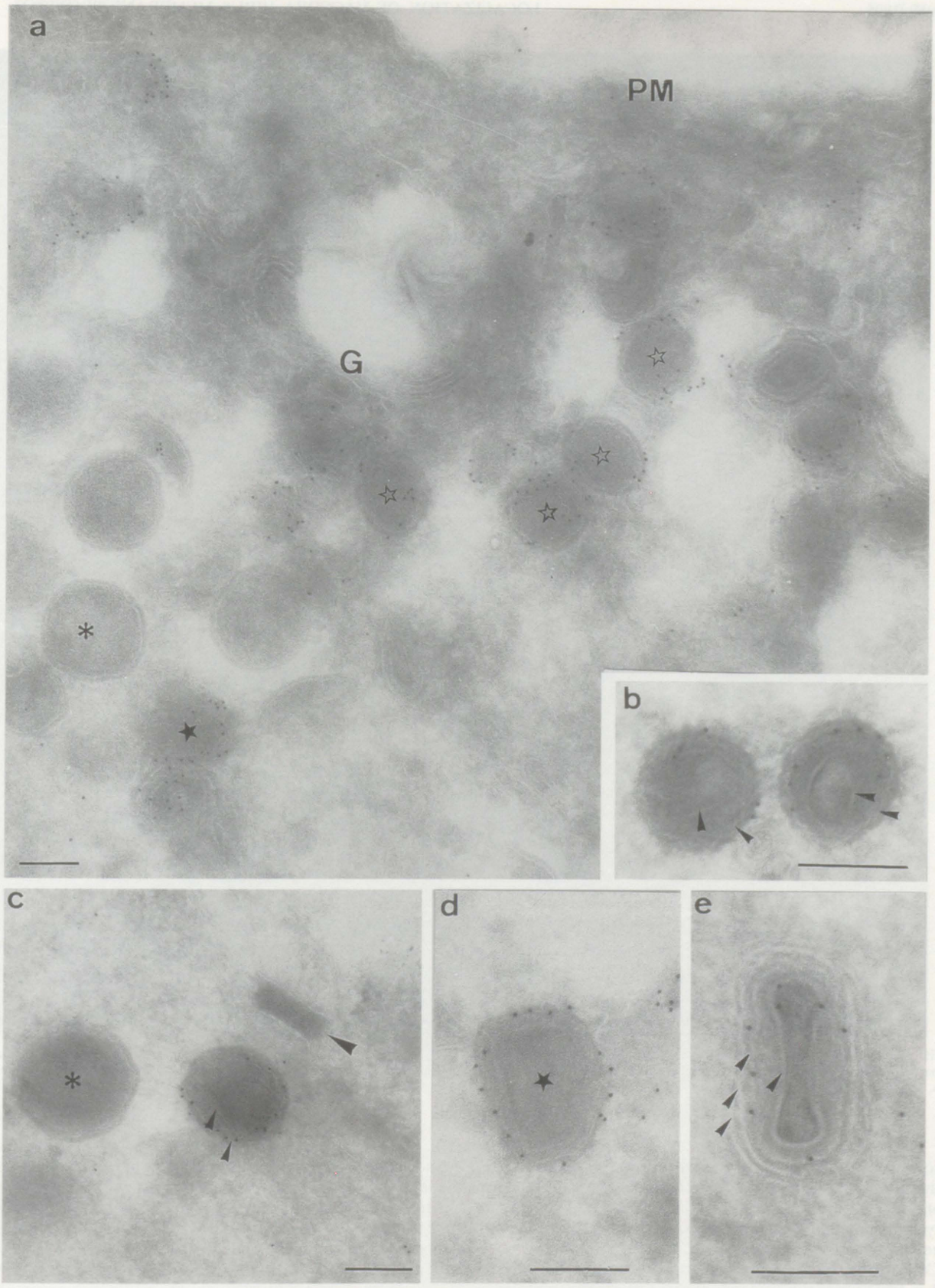


FIG. 9. EM immunolocalization of p14. Shown are cryosections of vaccinia virus-infected BHK cells at 10 h postinfection (a) and HeLa cells at 8 h postinfection (b to e). Anti-p14 does not label the immature virions (asterisks in panels a and c). The spherical intermediate form between the IV and the IMV, characterized by an outer membrane and a second, internal membrane around the core (arrowheads in panels b and c), is clearly labelled on its outer membrane. In some cases, a more electron-dense form of the IV (open stars in panel a) shows a strong labelling for p14. These forms presumably represent a stage just prior to the stages shown in panel a. The IMV (filled star in panels a and d) is strongly labelled on its outer membrane but not on its inner membrane. In panel e, an IEV particle is shown with its four distinct membranes (arrowheads); note that the labelling is restricted to the inner membranes. Large arrowhead in panel c, viral DNA. Bars, 200 nm.

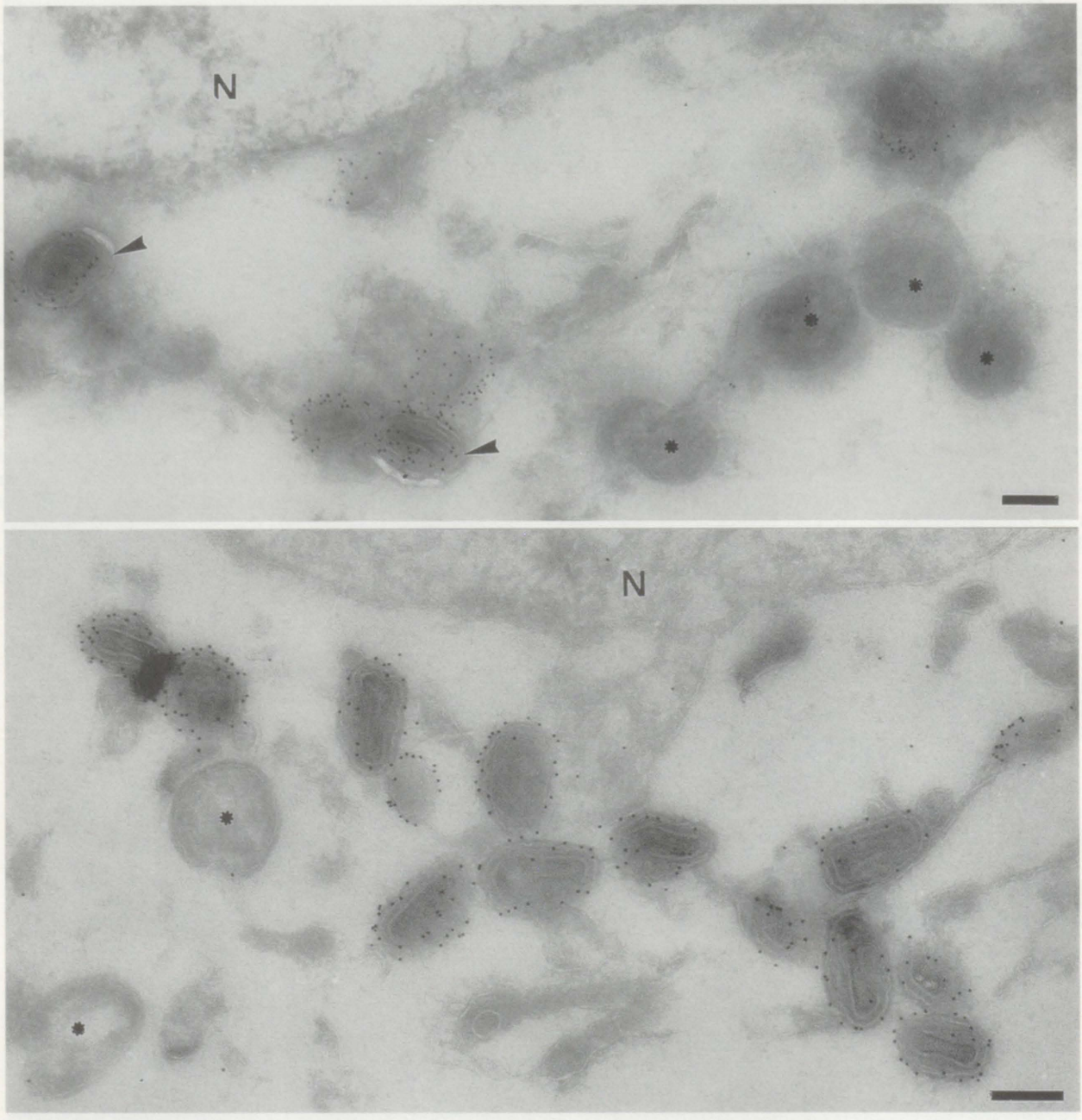


FIG. 10. Labelling of SLO-permeabilized, vaccinia virus-infected HeLa cells at 8 h postinfection with anti-p14 antibody. Even under this condition, the majority of IV particles (asterisks) have essentially no label while the IMV particles are strongly labelled on their periphery. The nuclear membrane (N, nucleus) is not labelled. Bars, 100 nm.

following treatment of the IMV with proteases (Table 1). Finally, upon treatment of [^{35}S]methionine-labelled IMV with proteinase K the band for p14 in sodium dodecyl sulfate-polyacrylamide gel electrophoresis is completely lost (unpublished data).

Collectively, the data are consistent with a model whereby p14 is synthesized on free cytoplasmic ribosomes and associates posttranslationally with the cytoplasmic domain of a membrane receptor. We propose that this putative membrane receptor becomes inserted into the early crescent but would only become active for binding p14 at the transition stage from the IV to the electron-dense intermediate form. The viral precursor membranes associated with the rifampin bodies were also labelled by anti-p14. Possibly, in the presence of rifampin, a significant amount of the putative p14 receptor in its active form might accumulate on the membranes of the rifampin bodies, but only the inactive form would be found on the crescents which form after washout of the drug. It remains to be determined whether or not the p14 which accumulates on these rifampin body membranes can be subsequently incorporated into IMV. One candidate for a p14 receptor is the 21-kDa protein, encoded by the gene A17L, which can be coprecipitated with antibodies directed to p14 (37). Since the amino acid sequence of A17L predicts two large internal hydrophobic

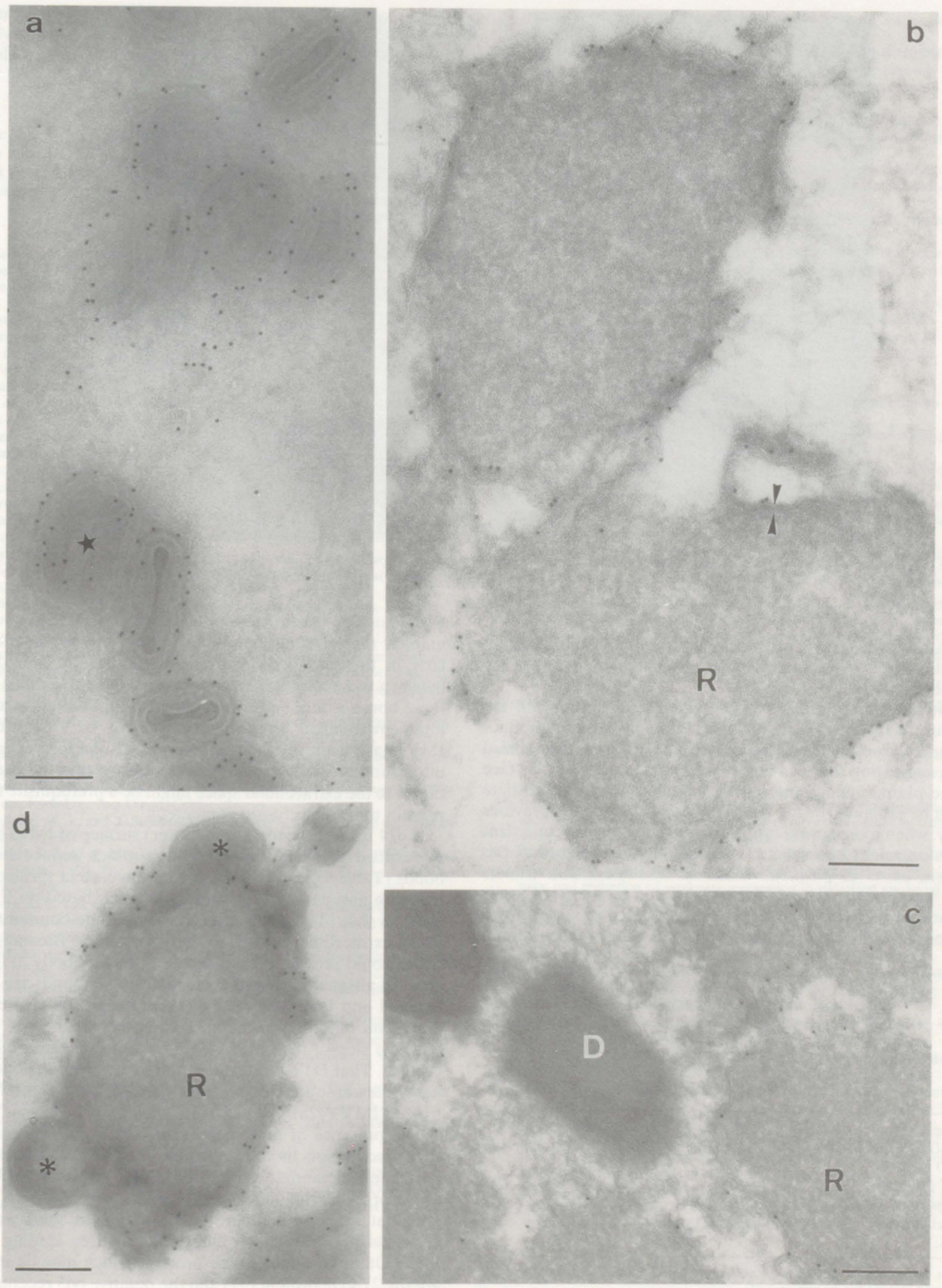


FIG. 11. Immunolocalization of p14 in the IMV and in cells infected in the presence of rifampin. Cryosections of vaccinia virus-infected HeLa cells at 15 h postinfection (a) and 8 h postinfection (b and c) and BHK cells (d) at 10 h postinfection were labelled with anti-p14 antibody. The cells in panels b and c were treated with rifampin, and those in panel d were treated with rifampin followed by a 15-min chase. Anti-p14 strongly labels the outer membrane of the IMV (a). In the presence of rifampin, p14 accumulates on the membranes (arrowheads in panel b) of the rifampin bodies (R) but is invariably absent from the viral crescents (asterisks in panel d) that are continuous with the membranes of the rifampin bodies. In panel c, the DNA-enriched crystalloid bodies (D) are not labelled for p14. Bars, 200 nm.

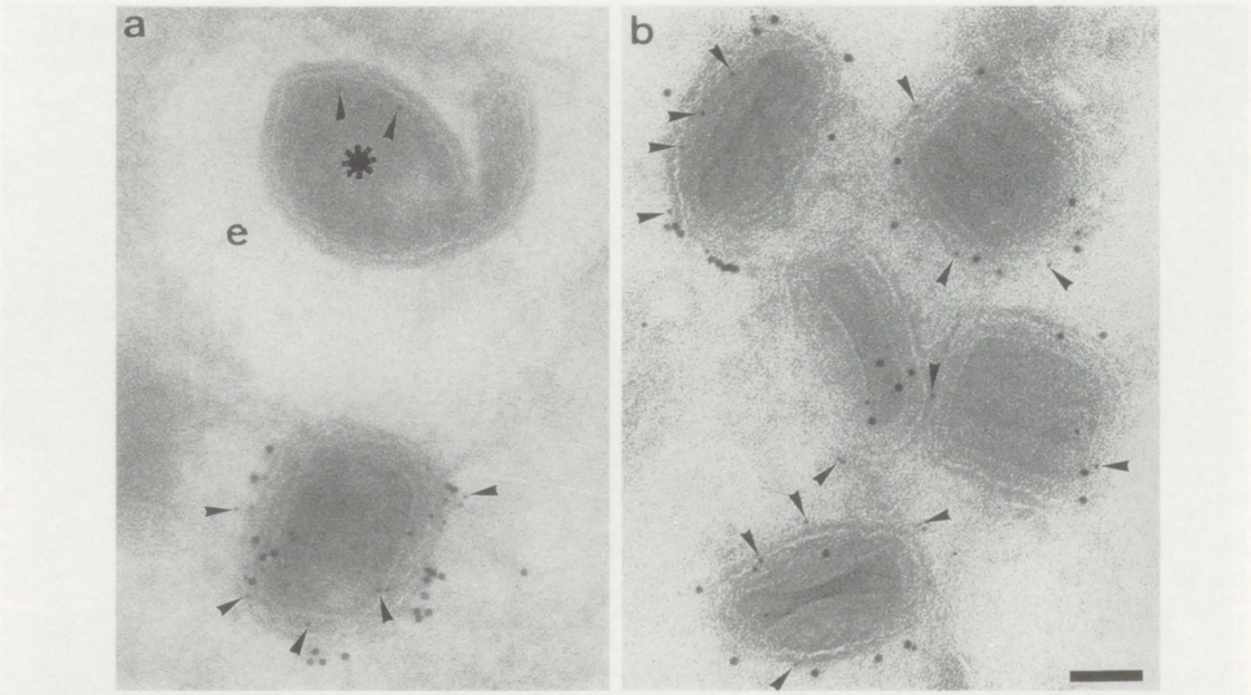


FIG. 12. Double labelling of HeLa cells at 8 h postinfection with anti-p32 (5-nm gold; arrowheads) and anti-p14 (10-nm gold). The IV (asterisk) has two gold particles for p32 but is not labelled for p14. On average, every IMV particle has at least some label for both antigens. Bar, 100 nm.

domains characteristic for membrane proteins, an interaction with this protein would provide a means to anchor p14 to the membrane (37).

Two previously published observations concerning p14 are difficult to reconcile with our data. First, earlier immunofluorescence experiments showed labelling of unpermeabilized cells, suggesting that p14 is localized on the extracellular face of the plasma membrane (40). This difference from our data might be explained by the later time points used in the previous study, when more severe cytopathic effects of the vaccinia virus infection might be expected. Second, it was shown that this protein exists in purified virions as disulfide-linked trimers (40). In our assembly model, p14 is located on the cytoplasmic surface of the IMV particles. Since the redox state of the cytoplasm is highly reducing (8, 14, 20, 22), we consider it unlikely that disulfide bonds, which can only form intracellularly in the oxidative environment of the ER, would form between p14 molecules on the intracellular IMV. Most likely, these bonds would be formed either in the oxidizing extracellular environment after the secretion of EEV or after the IMVs have been released by cell lysis. In the former case, an interesting possibility to consider would be that the oxidation of p14 in the extracellular space might be a prerequisite for this protein to become fusion competent.

TABLE 1. Labelling of intact, purified IMV

Treatment before labelling[a]	Gold particles/virion (mean ± SD)			
	p14		p32	
	No.[b]	%[c]	No.[d]	%[c]
Untreated	39.4 (4.8)	100	17.8 (4.2)	100
NP-40 (1%)–DTT (20 mM)	0.5 (0.6)	1.2	7.0 (2.1)	39.3
DTT (20 mM)	140 (12)	355.3	7.5 (6.5)	42.1
Trypsin (50 μg/ml)	0.9 (0.8)	2.3	3.1 (2.1)	17.4
Proteinase K (50 μg/ml, 4°C)	0.9 (0.9)	2.3	0.6 (0.8)	3.4

[a] In each case, the virions were adsorbed onto Formvar- and carbon-coated grids and treated for 30 min at 37°C.

[b] Labelled by a three-step protocol: the monoclonal anti-p14 (1) was labelled by rabbit anti-mouse antibody (3) followed by protein A-gold (10 nm).

[c] For the percentages, the values for untreated virus are normalized to 100%.

[d] Labelled by a two-step protocol: the rabbit anti-N terminus of p32 was visualized by protein A-gold (10 nm).

If p14 is on the cytoplasmic (outer) surface of IMV, how do we explain the fact that treatments which reduce disulfide bonds (Table 1) lead to a significant increase in surface labelling with anti-p14? The first explanation is based on the supposition that p14 has indeed formed disulfide-bonded trimers in the extracellular milieu, as discussed above. Breaking these bonds could provide greater access of the antibody to its antigen. An alternative possibility is that the S-S bonds are strictly lumenal and that DTT weakens the association between the outer and inner virion membranes such that the p14 on the opposite side of the outer membrane now becomes more accessible. That DTT loosens the contact between the outer and inner membrane is supported by cryo-EM images of DTT-treated IMV (42a).

The presence of neither p14 nor p32 is not obligatory for IMV production in cell culture (27, 32). Thus, besides the peripheral membrane protein p65 (48), no other viral membrane or membrane-associated proteins have yet been identified that are essential for the formation of the membrane crescents or for the morphogenetic changes leading to the IMV. Other transmembrane proteins which may be involved are the 21-kDa protein (37) and the putative p65 receptor (46). The complete sequencing of the vaccinia virus genome has predicted at least 30 further putative integral membrane proteins (15), which remain to be characterized. Our immediate goal is to determine which of these membrane proteins are

essential for the formation of the IV (IMV) and, more importantly, to elucidate how a macromolecular complex of the virus is able to assemble the crescents and the IV.

ACKNOWLEDGMENTS

We thank Kai Simons and Jacomine Krijnse Locker (EMBL) for many stimulating discussions during the course of this work. We also thank Rafael Blasco for critical evaluation of the manuscript. The manuscript was typed by Julia Pickles.

REFERENCES

1. **Cairns, H. J. F.** 1960. The initiation of vaccinia infection. Virology **11:**603.
1a. **Cudmore, S., and G. Griffiths.** Unpublished observations.
2. **Czerny, C. P., S. Johann, L. Hölzle, and H. Meyer.** 1994. Epitope detection in the intracellular naked orthopox viruses and identification of encoding genes. Virology **210:**764–767.
3. **Czerny, C. P., and H. Mahnel.** 1990. Structural and functional analysis of orthopoxvirus epitopes with neutralizing monoclonal antibodies. J. Gen. Virol. **71:**2341–2352.
4. **Dales, S.** 1963. The uptake and development of vaccinia virus in strain L cells followed with labelled viral deoxyribonucleic acid. J. Cell Biol. **18:** 51–72.
5. **Dales, S., and B. G. T. Pogo.** 1981. Biology of poxviruses. Virol. Monogr. **18.**
6. **Dallo, S., J. F. Rodriguez, and M. Esteban.** 1987. A 14K envelope protein of vaccinia virus with an important role in virus-host cell interactions is altered during virus persistence and determines the plaque size phenotype of the virus. Virology **159:**423–432.
7. **Doms, R. W., R. Blumenthal, and B. Moss.** 1990. Fusion of intracellular- and extracellular forms of vaccinia virus with the cell membrane. J. Virol. **64:** 4884–4892.
8. **Doms, R. W., R. A. Lamb, J. K. Rose, and A. Helenius.** 1993. Folding and assembly of viral membrane proteins. Virology **193:**545–562.
9. **Dubochet, J., M. Adrian, K. Richter, J. Garces, and R. Wittek.** 1994. Structure of intracellular mature vaccinia virus observed by cryoelectron microscopy. J. Virol. **68:**1935–1941.
10. **Earl, P. L., and B. Moss.** 1991. Expression of proteins in mammalian cells using vaccinia viral vectors, p. 16.19.1–16.19.10. *In* F. M. Ausubel et al. (ed.), Current protocols in molecular biology. Greene Publishing Associates and Wiley Interscience, New York.
11. **Easterbrook, K. B.** 1966. Controlled degradation of vaccinia virions *in vitro*: an electron microscopic study. J. Ultrastruct. Res. **14:**484–496.
12. **Essani, K., and S. Dales.** 1979. Biogenesis of vaccinia: evidence for more than 100 polypeptides in the virion. Virology **95:**385–394.
13. **Fenner, F., R. Wittek, and K. R. Dumbell.** 1989. The orthopoxviruses. Academic Press Inc., San Diego, Calif.
14. **Gething, M. J., and J. Sambrook.** 1992. Protein folding in the cell. Nature (London) **355:**33–45.
15. **Goebel, S. J., G. P. Johnson, M. E. Perkus, S. W. Davis, J. P. Winslow, and E. Paoletti.** 1990. The complete DNA sequence of vaccinia virus. Virology **179:**247–266.
16. **Gong, S., C. Lai, and M. Esteban.** 1990. Vaccinia virus induces cell fusion at acid pH and this activity is mediated by the N-terminus of the 14kDa virus envelope protein. Virology **178:**81–91.
17. **Griffiths, G.** 1993. Fine structure immunocytochemistry. Springer-Verlag, Heidelberg, Germany.
18. **Griffiths, G., and P. Rottier.** 1992. Cell biology of viruses that assemble along the biosynthetic pathway. Semin. Cell Biol. **3:**367–381.
19. **Grimley, P. M., E. N. Rosenblum, S. J. Mims, and B. Moss.** 1970. Interruption by rifampin of an early stage in vaccinia virus morphogenesis: accumulation of membranes which are precursors of virus envelopes. J. Virol. **6:**519–533.
20. **Helenius, A., T. Marquardt, and I. Braakman.** 1992. The endoplasmic reticulum as a protein-folding compartment. Trends Cell Biol. **2:**227–231.
21. **Holowczak, J. A., and W. K. Joklik.** 1967. Studies of the structural proteins of virions and cores. Virology **33:**717–725.
22. **Hwang, C., A. J. Sinskey, and H. F. Lodish.** 1992. Oxidized redos state of glutathione in the endoplasmic reticulum. Science **257:**1496–1992.
23. **Ichihashi, Y., M. Oie, and T. Tsuruhara.** 1984. Location of DNA-binding proteins and disulfide-linked proteins in vaccinia virus structural elements. J. Virol. **50:**929–938.
24. **Joklik, W. K., and Y. Becker.** 1964. The replication and coating of vaccinia DNA. J. Mol. Biol. **10:**452–474.
25. **Krijnse-Locker, J., M. Ericsson, P. J. M. Rottier, and G. Griffiths.** 1994. Characterization of the budding compartment of mouse hepatitis virus: evidence that transport from the RER to the Golgi complex requires only one vesicular transport step. J. Cell Biol. **124:**55–70.
26. **Lai, C., S. Gong, and M. Esteban.** 1991. The 32-kilodalton envelope protein of vaccinia virus synthesized in *Escherichia coli* binds with specificity to cell surfaces. J. Virol. **65:**499–504.
27. **Maa, J. S., J. F. Rodriguez, and M. Esteban.** 1990. Structural and functional characterization of a cell surface binding protein of vaccinia virus. J. Biol. Chem. **265:**1569–1577.
28. **Moss, B.** 1991. Vaccinia virus: a tool for research and vaccine development. Science **252:**1662–1667.
29. **Moss, B., and E. N. Rosenblum.** 1973. Protein cleavage and poxvirus morphogenesis: tryptic peptide analysis of core precursors accumulated by blocking assembly with rifampicin. J. Mol. Biol. **81:**267–269.
30. **Moss, B., E. N. Rosenblum, and E. Katz.** 1969. Rifampicin: a specific inhibitor of vaccinia virus assembly. Nature (London) **224:**1280–1284.
31. **Nagayama, A., B. G. T. Pogo, and S. Dales.** 1970. Biogenesis of vaccinia: separation of early stages from maturation by means of rifampicin. Virology **4:**1039–1051.
31a. **Niles, E. G.** Unpublished observations.
32. **Niles, E. G., and J. Seto.** 1988. Vaccinia virus gene D8 encodes a virion transmembrane protein. J. Virol. **62:**3772–3778.
33. **Oie, M., and Y. Ichihashi.** 1981. Characterization of vaccinia polypeptides. Virology **113:**263–276.
34. **Oie, M., and Y. Ichihashi.** 1987. Modification of vaccinia virus penetration proteins analyzed by monoclonal antibodies. Virology **157:**449–459.
35. **Paez, E., S. Dallo, and M. Esteban.** 1987. Virus attenuation and identification of structural proteins of vaccinia virus that are selectively modified during virus persistence. J. Virol. **61:**2642–2647.
36. **Payne, L. G., and K. Kristenson.** 1979. Mechanism of vaccinia virus release and its specific inhibition by N_1-isonicotinoyl-N_2-3-methyl-4-chlorobenzoylhydrazine. J. Virol. **32:**614–622.
37. **Rodriguez, D., J. R. Rodriguez, and M. Esteban.** 1993. The vaccinia virus 14-kilodalton fusion protein forms a stable complex with the processed protein encoded by the vaccinia virus A17L. J. Virol. **67:**3435–3440.
38. **Rodriguez, J. F., and M. Esteban.** 1987. Mapping and nucleotide sequence of the vaccinia gene that encodes a 14-kilodalton fusion protein. J. Virol. **61:**3550–3554.
39. **Rodriguez, J. F., R. Janeczko, and M. Esteban.** 1985. Isolation and characterization of neutralizing monoclonal antibodies to vaccinia virus. J. Virol. **56:**482–488.
40. **Rodriguez, J. F., E. Paez, and M. Esteban.** 1987. A 14,000-M_r envelope protein of vaccinia virus is involved in cell fusion and forms covalently linked trimers. J. Virol. **61:**393–404.
41. **Rodriguez, J. F., and G. F. Smith.** 1990. IPTG-dependent vaccinia virus: identification of a virus protein enabling virion envelopment by Golgi membrane and egress. Nucleic Acids Res. **18:**5347–5351.
42. **Rodriguez, J. R., D. Rodriguez, and M. Esteban.** 1992. Insertional inactivation of the vaccinia virus 32-kilodalton gene is associated with attenuation in mice and reduction of viral gene expression in polarized epithelial cells. J. Virol. **66:**183–189.
42a. **Roos, N., and G. Griffiths.** Unpublished data.
43. **Sarov, I., and W. K. Joklik.** 1972. Studies on the nature and location of the capsid polypeptides of vaccinia virions. Virology **50:**579–592.
44. **Schmelz, M., B. Sodeik, M. Ericsson, E. J. Wolffe, H. Shida, G. Hiller, and G. Griffiths.** 1994. Assembly of vaccinia virus: the second wrapping cisterna is derived from the trans Golgi network. J. Virol. **68:**130–147.
45. **Sodeik, B., R. W. Doms, M. Ericsson, G. Hiller, C. E. Machamer, W. van't Hof, G. van Meer, B. Moss, and G. Griffiths.** 1993. Assembly of vaccinia virus: role of the intermediate compartment between the endoplasmic reticulum and the Golgi stacks. J. Cell Biol. **121:**521–541.
46. **Sodeik, B., G. Griffiths, M. Ericsson, B. Moss, and R. W. Doms.** 1994. Assembly of vaccinia virus: effects of rifampin on the intracellular distribution of viral protein p65. J. Virol. **68:**1103–1114.
47. **Stern, W., and S. Dales.** 1976. Biogenesis of vaccinia: isolation and characterization of a surface component that elicits antibody suppressing infectivity and cell-cell fusion. Virology **75:**232–241.
48. **Zhang, Y., and B. Moss.** 1992. Immature viral envelope formation is interrupted at the same stage by lac operator-mediated repression of the vaccinia virus D13L gene as by the drug rifampicin. Virology **187:**643–653.

JOURNAL OF VIROLOGY, Nov. 1995, p. 7072–7086
0022-538X/95/$04.00+0
Copyright © 1995, American Society for Microbiology
Vol. 69, No. 11

Characterization of *ts*16, a Temperature-Sensitive Mutant of Vaccinia Virus

MARIA ERICSSON,[1] SALLY CUDMORE,[1] STEWART SHUMAN,[2] RICHARD C. CONDIT,[3] GARETH GRIFFITHS,[1]* AND JACOMINE KRIJNSE LOCKER[1]

Cell Biology Programme, European Molecular Biology Laboratory, 69012 Heidelberg, Germany[1]; Program in Molecular Biology, Sloan-Kettering Institute, New York, New York 10021[2]; and Department of Immunology and Medical Microbiology, University of Florida, Gainesville, Florida 32610-0266[3]

Received 15 May 1995/Accepted 8 August 1995

We have characterized a temperature-sensitive mutant of vaccinia virus, *ts*16, originally isolated by Condit et al. (Virology 128:429–443, 1983), at the permissive and nonpermissive temperatures. In a previous study by Kane and Shuman (J. Virol 67:2689–2698, 1993), the mutation of *ts*16 was mapped to the I7 gene, encoding a 47-kDa protein that shows partial homology to the type II topoisomerase of *Saccharomyces cerevisiae*. The present study extends previous electron microscopy analysis, showing that in BSC40 cells infected with *ts*16 at the restrictive temperature (40°C), the assembly was arrested at a stage between the spherical immature virus and the intracellular mature virus (IMV). In thawed cryosections, a number of the major proteins normally found in the IMV were subsequently localized to these mutant particles. By using sucrose density gradients, the *ts*16 particles were purified from cells infected at the permissive and nonpermissive temperatures. These were analyzed by immunogold labelling and negative-staining electron microscopy, and their protein composition was determined by sodium dodecyl sulfate-polyacrylamide gel electrophoresis. While the *ts*16 virus particles made at the permissive temperature appeared to have a protein pattern identical to that of wild-type IMV, in the mutant particles the three core proteins, p4a, p4b, and 28K, were not proteolytically processed. Consistent with previous data the sucrose-purified particles could be labelled with [^{3}H]thymidine. In addition, anti-DNA labelling on thawed cryosections suggested that most of the mutant particles had taken up DNA. On thawed cryosections of cells infected at the permissive temperature, antibodies to I7 labelled the virus factories, the immature viruses, and the IMVs, while under restrictive conditions these structures were labelled much less, if at all. Surprisingly, however, by Western blotting (immunoblotting) the I7 protein was present in similar amounts in the defective particles and in the IMVs isolated at the permissive temperature. Finally, our data suggest that at the nonpermissive temperature the assembly of *ts*16 is irreversibly arrested in a stage at which the DNA is in the process of entering but before the particle has completely sealed, as monitored by protease experiments.

Vaccinia virus (VV) morphogenesis has been extensively studied by electron microscopy (EM) and biochemistry (for reviews, see references 6, 11, 19, and 25). Viral DNA replication and assembly occur in the cytoplasms of infected cells, in discrete structures referred to as viral factories (2, 5, 20). The first characteristic viral structures to appear during assembly are crescent-shaped membranes (5, 7). We have recently shown that these crescents consist of two membranes that are continuous with the membrane of the intermediate compartment between the endoplasmic reticulum (ER) and the Golgi complex (43). The crescents mature into spherical immature virions (IVs), which are not sealed and which have not yet taken up the viral DNA. These IVs then undergo a complex series of maturational events, including uptake of the genome and proteolytical processing of viral core proteins (26, 40, 47, 49). The product of these events is the first infectious form of the virus, which we have proposed be called the intracellular mature virus (IMV) (43). In most cell types a variable fraction of the IMVs become further engulfed by a cisterna that originates from the trans-Golgi network, thereby forming the precursor of the second infectious form of the virus, the extracellular enveloped virus (14, 29, 39).

* Corresponding author. Mailing address: Cell Biology Programme, European Molecular Biology Laboratory, Postfach 10.2209, 69012 Heidelberg, Germany.

During the transition from the IV to the IMV, an intermediate structure can be seen by electron microscopy (13). This intermediate appears to be more condensed than the IV and can be characterized by the acquisition of p14, a peripheral membrane protein found also on the outside of the IMV (42). The transition from the IV to the IMV is further associated with a complex and poorly understood process by which the DNA enters the viral particle (5, 13, 24). Our understanding of the molecular mechanisms involved in the formation of the IMV lags significantly behind the descriptive morphological data. A serious obstacle in following the molecular events has been the difficulty in isolating intermediate stages. Whereas the IMV can be purified by using either sucrose or cesium chloride gradients (8), reports on the isolation of earlier stages of the assembly process have been sparse (36).

In the present study we have used a temperature-sensitive mutant of VV, *ts*16. This mutant VV was first described by Condit et al. (4) and was classified as having normal DNA and protein synthesis. More recently the mutation of *ts*16 has been mapped to a single amino acid substitution (Pro to Leu at position 344) in the product of the I7 gene (21). This gene encodes a 47-kDa late protein that has approximately 20% homology over a stretch of 200 amino acids to the *Saccharomyces cerevisiae* type II DNA topoisomerase. By EM it was shown that at the restrictive temperature of 40°C the assembly was arrested at a stage intermediate between the IV and the

IMV, a stage at which the DNA entry occurs. The mutant protein appeared to be made normally at 40°C, but it was not assessed whether it was present in the viral particles that accumulate at the nonpermissive temperature (21). In wild-type VV the I7 protein was associated with the viral core fraction, as analyzed biochemically (21). In this study we have further characterized the *ts*16 mutant using both morphological and biochemical approaches and have developed a procedure to purify the intermediate particle that was arrested at the nonpermissive temperature.

MATERIALS AND METHODS

Cells and viruses. BSC40 cells were grown in Dulbecco's modified Eagle's medium (DMEM) supplemented with 5% heat-inactivated fetal calf serum. HeLa cells were grown in Eagle's minimal essential medium supplemented with 10% heat-inactivated fetal calf serum and nonessential amino acids. The wild-type VV strain WR was propagated in HeLa cells grown at 37°C as previously described (9). VV *ts*16 was amplified in BSC40 cells at 31°C (permissive temperature).

Antibodies. The antibody recognizing p25 (L4R) was a kind gift from D. Hruby (48). The peptide antibody recognizing the COOH terminus of p4a (A10L) was a kind gift from R. Doms and was made by using the peptide MTDGDSVSFDDE. This peptide was coupled to keyhole limpet hemocyanin and used for three immunizations of rabbits, one primary immunization followed by two boosters at 4-week intervals. The anti-I7 antibody has been described earlier (21). The anti-DNA monoclonal antibody was purchased from Boehringer (Mannheim, Germany). The following antibodies were provided from the indicated sources: anti-p32 (D8L gene) antiserum (D8.1) from G. Niles (28), anti-p14 (A27L gene) monoclonal antibody (C3) from M. Esteban (32), anti-p4a/4a recognizing the precursor (p4a) and processed form of 4a (3160) (49), anti-p4b/4b and anti-p28/p25 (48) from D. Hruby, and the peptide antibody (B1) against the COOH terminus of p65 (D13L) from R. W. Doms (44).

EM. Confluent BSC40 cells were infected with VV *ts*16 virus in phosphate-buffered saline (PBS) (with Mg^{2+} and Ca^{2+}) at a multiplicity of infection of 10 at 31 and 40°C. After a 1-hour adsorption, the inoculum was aspirated, and the cells were washed once with PBS and then overlaid with DMEM which had been prewarmed to the appropriate temperature. At various times after infection, cells were processed for Epon embedding and postembedding immunolabelling as follows. For Epon embedding, cells were fixed on the dish for 60 min in 1% glutaraldehyde in 200 mM cacodylate buffer (pH 7.4), stained with a mixture of 2% OsO_4 and 1.5% KFe CN_6 for 1 h and with 1% magnesium uranyl acetate for 30 min, and then processed for conventional Epon embedding (12). For preparation of cryosections, infected cells were removed from the dish with proteinase K (25 μg/ml) on ice and then centrifuged at 800 × *g* for 3 min, and the pellet was fixed overnight with 8% paraformaldehyde in 250 mM HEPES (*N*-2-hydroxyethylpiperazine-*N*′-2-ethanesulfonic acid), pH 7.4. Prior to freezing in liquid nitrogen the cell pellets were infiltrated with 2.1 M sucrose in PBS for 15 min. Frozen samples were sectioned at −90°C, the sections were transferred to Formvar-coated copper grids, and immunolabelling was carried out as described elsewhere (12). The procedure for negative staining with ammonium molybdate-methylcellulose is also given in reference 12.

Visualization of isolated virus particles was performed by negative staining with 2% ammonium molybdate. To immunolabel the isolated virus particles, a drop of material was adsorbed to a copper grid for 5 min, and the grid was washed briefly in PBS and then incubated on a drop of antibody for 15 min. Following rinses on 4 drops of PBS for a total of 10 min the grid was incubated with protein A-gold for 15 min. A final 15-min wash on 4 drops of PBS was followed by a brief rinse in water before negative staining with ammonium molybdate for 1 min.

Proteinase K and DNase treatment of *ts*16-infected cells. BSC40 cells infected with *ts*16 for 24 h at 40°C were put on ice and rinsed twice in ice-cold streptolysin O (SLO) buffer (150 mM sucrose, 25 mM HEPES [pH 7.4], 115 mM potassium acetate, 2.5 mM $MgCl_2$). Cells were incubated with 2 U of SLO (Wellcome Diagnostics) per ml for 10 min on ice. To remove unbound SLO, the cells were washed in SLO buffer containing 1 mM freshly made dithiothreitol (DTT; Boehringer GmbH) and then permeabilized in this buffer by a 20-min incubation at 40°C. Cells were put on ice again, washed twice in SLO buffer, and overlaid with SLO buffer containing 1 mg of proteinase K per ml. For the treatment with DNase, the permeabilized cells were incubated for 30 min at 37°C in SLO buffer containing 500 U of DNase I (Sigma) per ml. In some experiments the permeabilized cells were incubated with distilled water for 10 min. The cells detached by themselves from the dish in the proteinase K solution or were scraped and transferred to an Eppendorf tube and incubated at 4°C on a rocking table. After 60 min cells were spun for 2 min at 2,000 × *g*, and the pellet was fixed with 1% glutaraldehyde in 200 mM HEPES (pH 7.4) for 30 min at room temperature. Cell pellets were processed for either Epon embedding or cryosectioning as described above.

Metabolic labelling. BSC40 cells in 35-mm-diameter dishes were infected as described above. After 1 h the cells were washed once in ice-cold PBS and then overlaid with prewarmed DMEM containing 30 μCi of [^{3}H]thymidine per dish. After 6 h of infection the cells were put on ice and the [^{3}H]thymidine-containing medium was removed. Then the cells were washed in ice-cold PBS and subsequently overlaid with prewarmed cysteine- and methionine-free DMEM containing 50 μCi of [^{35}S]Express (NEN, Dupont) per dish. After 22 h of infection, the ^{35}S label was removed and the cells were washed in ice-cold PBS and then further incubated in prewarmed normal DMEM for 2 h. Virus purification was carried out as described below.

To assay for posttranslational processing of viral proteins, 60-mm-diameter dishes of cells were infected with VV *ts*16 at 40°C and labelled from 5 to 8 h postinfection with 50 μCi of ^{35}S label per dish. Cells were washed three times in ice-cold PBS before incubation in normal DMEM at 31°C for different periods. When appropriate, rifampin was added during the 31°C incubation at a concentration of 100 μg/ml.

Isolation of VV *ts*16 viral particles and different treatments. After 24 h of infection, cells were scraped from the dish in the medium, centrifuged, resuspended in 10 mM Tris (pH 9.0), and then lysed by passage 15 times through a 27¾-gauge needle. After low-speed centrifugation (~800 × *g*) to remove the nuclei, the supernatant was layered onto a sucrose gradient.

Different conditions for sucrose gradient purification were tested. In preliminary experiments a 12-to-26% (wt/wt) sucrose gradient in 10 mM Tris (pH 9.0) was used. The sample was centrifuged at 4°C in an SW40 rotor for 30 min at 16,000 rpm (37). This procedure was later modified to a 12-to-40% (wt/wt) sucrose gradient centrifuged at 4°C for 30 min at 16,000 rpm or a 25-to-40% (wt/wt) sucrose gradient centrifuged for 20 min at 24,000 rpm. Fractions were collected from the top of the tube, and 100 μl from each fraction was counted in a Beckman liquid scintillation counter. For the immunoblotting, equal amounts of counts were run on 15% gels and transferred to nitrocellulose. The nitrocellulose was extensively blocked by using 5% milk powder in PBS–0.1% Tween 20 and incubated with the anti-I7 antibody at a 1:1,000 dilution followed by a goat anti-rabbit antibody coupled to horseradish peroxidase (Cappel, Durham, N.C.). Enhanced chemiluminescence (ECL; Amersham, Buchler GmbH, Braunschweig, Germany) was used to visualize the protein.

For the immunoprecipitation of the core proteins, 2% sodium dodecyl sulfate (SDS) (final concentration) was added to IMVs and mutant particles from the peak fractions, and the mixtures were incubated for 30 min at 37°C. The samples were centrifuged for 5 min at full speed in an Eppendorf centrifuge, the supernatant was diluted in 1 ml of detergent solution (23), 2 μl of anti-p4a/4a (3160), anti-p4b/4b (10098Q), or anti-p28/p25 was added, and the immunoprecipitation was performed as described previously (23).

For the proteinase K treatment of isolated virus particles, aliquots from the peak fractions of the gradients were incubated with equal volumes of a 200-μg/ml proteinase K solution in 10 mM Tris (pH 9) for 30 min on ice. To stop the reaction, 1 mM phenylmethylsulfonyl fluoride was added to the reaction mixture, and the sample was quick-frozen in liquid nitrogen. The sample was thawed rapidly, and Laemmli sample buffer was added prior to SDS-polyacrylamide gel electrophoresis (PAGE) analysis as described below.

To separate core from membrane fractions, wild-type and mutant particles were briefly sonicated and then incubated for 30 min at 37°C in 1% Nonidet P-40 (NP-40) and 20 mM (final concentration) freshly made DTT. The samples were layered on top of a 75-μl 36% sucrose cushion in an ultraclear centrifuge tube (Beckman) and centrifuged in a Beckman airfuge for 30 min at 26 lb/in^2. The supernatant, containing solubilized proteins, was concentrated by acetone precipitation at −20°C, and the pellet was directly resuspended in Laemmli sample buffer.

Gel electrophoresis and autoradiography. ^{35}S-labelled material from the peak fractions was diluted in Laemmli sample buffer containing 1% SDS and 0.5% β-mercaptoethanol and electrophoresed in an SDS–15% polyacrylamide gel. Gels were processed for fluorography, dried, and exposed to X-ray film at −80°C.

RESULTS

Morphology of VV *ts*16. Prior to the biochemical analysis, we characterized VV *ts*16 by conventional Epon embedding. Figure 1 illustrates representative sections of Epon-embedded BSC40 cells infected with VV *ts*16 for 24 h under permissive conditions (31°C) (Fig. 1a) and nonpermissive conditions (40°C) (Fig. 1b). At 31°C viral structures identical to those observed in cells infected with wild-type VV could be detected: these included crescent-shaped membranes surrounding discrete foci of viroplasm, spherical immature particles in close proximity to the viral factories, and brick-shaped mature virions more in the periphery of the cell (Fig. 1a).

In agreement with earlier data (21), no normal IMVs were apparent in cells infected at the nonpermissive temperature. Instead, spherical, often asymmetrical particles accumulated in the cytoplasm. A large number of these particles contained a

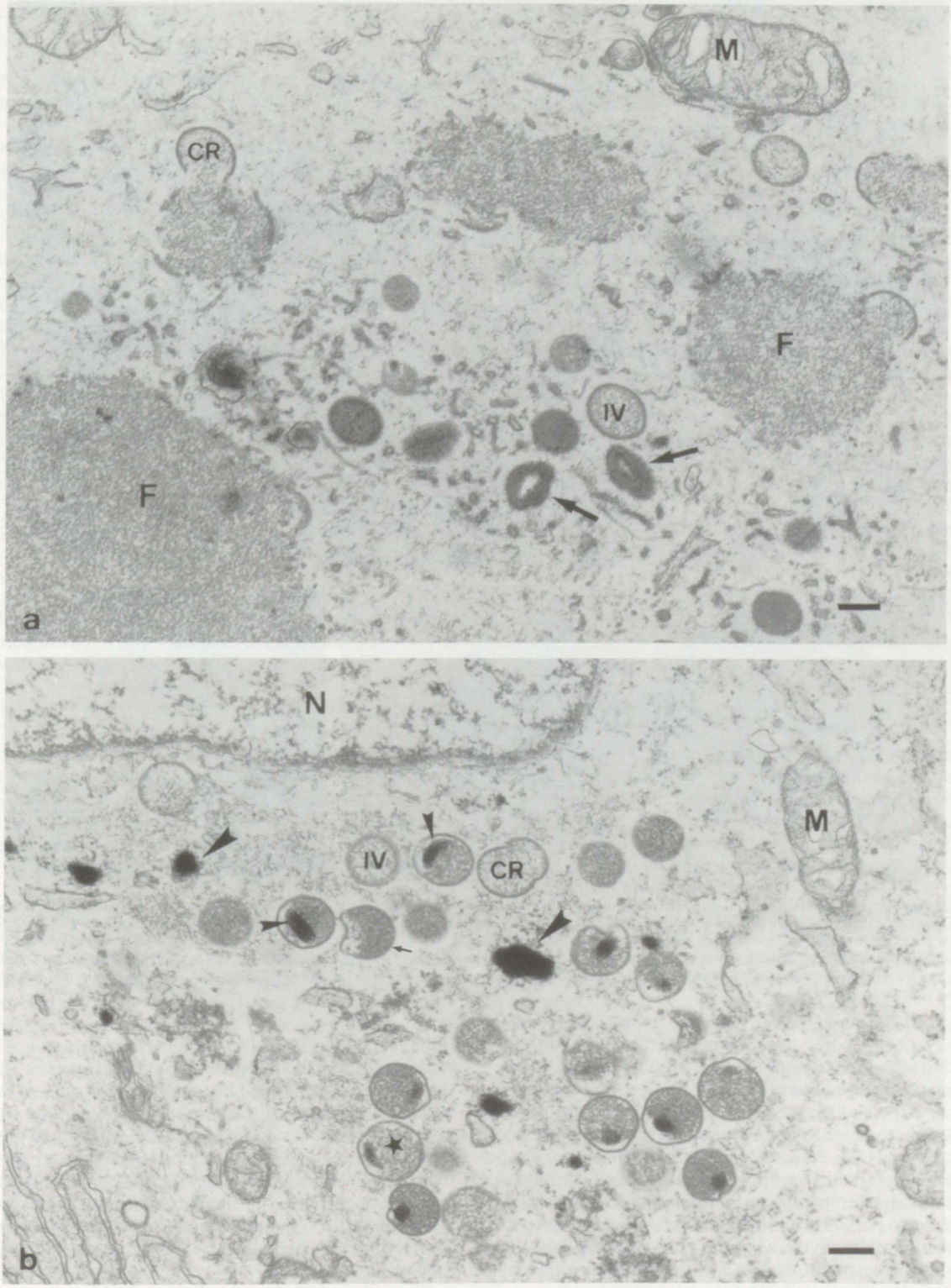


FIG. 1. Epon sections of BSC40 cells infected with *ts*16 for 24 h. (a) Cells infected at 31°C (permissive temperature) show VV at different stages of morphogenesis; the electron-dense viral factories (F) contain viral crescents (CR), spherical IV, and IMV (arrows). (b) Cells infected at 40°C (nonpermissive temperature) contain spherical particles, sometimes irregularly shaped (star), many of which contain a dense nucleoid (small arrowheads). These cells also contain viral crescents (CR), IVs, and DNA crystalloids (large arrowheads) but no IMVs. The small arrow denotes the irregular shape of some profiles of the IVs at the nonpermissive temperature. M, mitochondrion, N, nucleus. Bars, 200 nm.

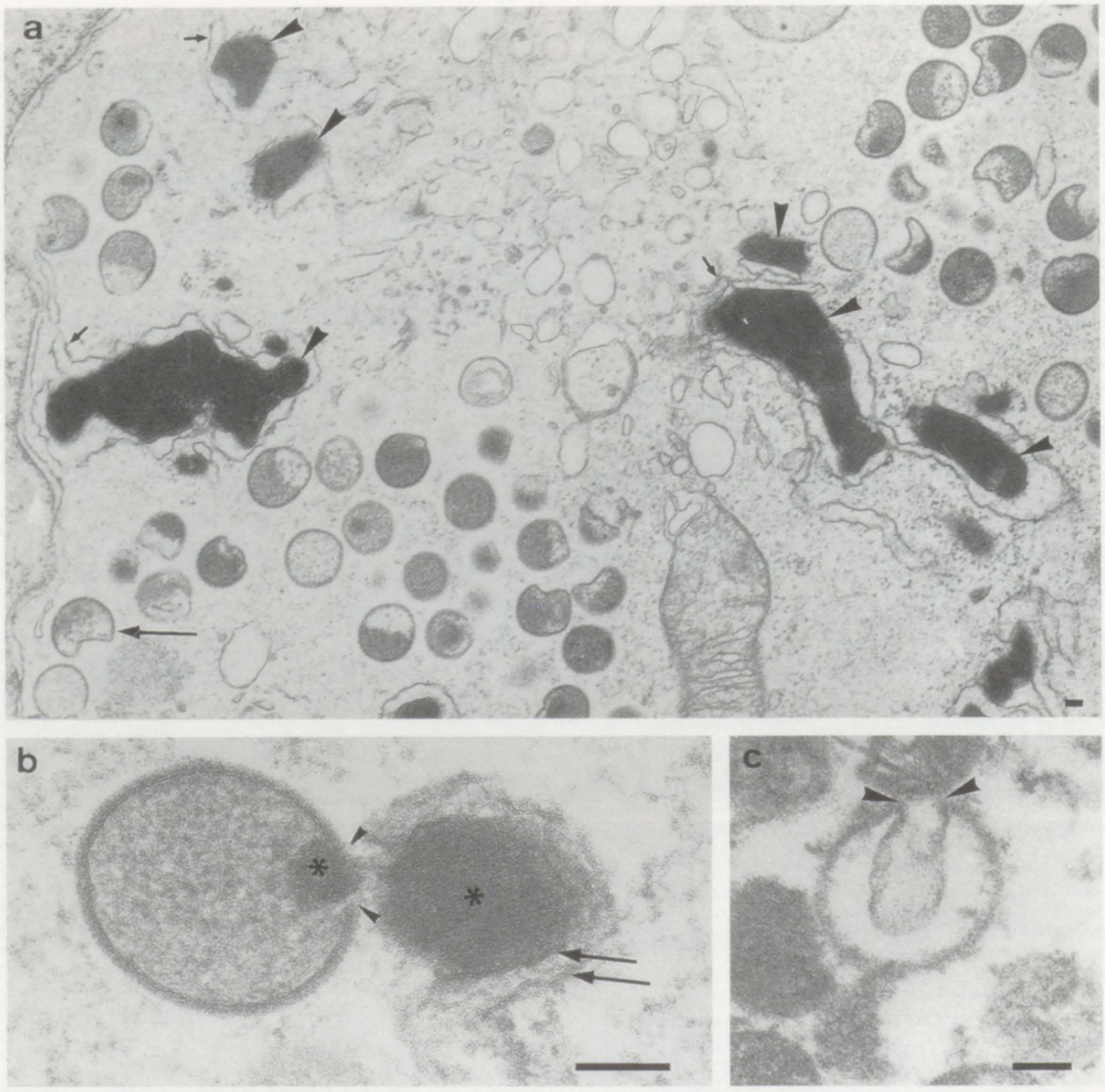


FIG. 2. (a) Epon section of a BSC40 cell infected with *ts*16 at the nonpermissive temperature for 24 h, showing the extensive accumulation of the viral DNA (arrowheads) that appears to be tightly associated with membranes of the ER (small arrows indicate ribosomes). (b) High-magnification view of the DNA (right-hand asterisk) from the same preparation, in which the parallel filaments are apparent. The two membranes that appear to enwrap the DNA are indicated by arrows. The large arrowheads and the left-hand asterisk show the site at which DNA appears to enter the IV. (c) Cryosection of a cell infected with *ts*16 for 24 h at the nonpermissive temperature and then permeabilized with SLO and incubated with DNase. The arrowheads show the points of invaginations of membrane(s) that would normally be filled with the viral DNA. Bars, 100 nm.

nucleoid and appeared to be denser than the spherical IV (Fig. 1b). At longer infection times (48 h) the particles became more irregular in shape and the envelope tended to collapse on one side of the sphere (Fig. 1b and 2a). Viral structures preceding the formation of the defective particles, such as crescent-shaped membranes and IVs, appeared to be mostly normal at the nonpermissive temperature. In Epon-embedded cells we could often see particles in which the viroplasm seemed to have condensed unevenly, leaving the particle partially empty (Fig. 1b). As discussed below, this was seldom seen with cryosections and may be an artifact of the plastic embedding.

In our extensive ultrastructural observations on VV assembly we have often noticed that the viral DNA associates closely with membranes (see also reference 13), and we suggest that this association may be important for DNA entry into the IV. In *ts*16-infected cells at the nonpermissive temperature this association of membranes with the DNA became much more evident, presumably because the entry process is arrested. At this temperature, large, filamentous aggregates of DNA accumulated, and most of them were associated with membranes after long infection times (Fig. 2a and b). In such preparations it became clear that these membranes represent the ER since they are clearly continuous with ribosome-associated membranes (rough ER). The significance of this membrane association of the DNA and its importance for the entry into the assembling VV particle must await more definitive experiments.

When the *ts*16-infected cells that had been arrested at the nonpermissive temperature were permeabilized with SLO and treated with DNase, the viral DNA was digested. In some of the defective particles the images we saw suggested that the sites previously filled with DNA were empty. For such particles we interpreted the images as suggesting that the DNA had pushed the membrane(s) into the particle, resulting in a dis-

tinct invagination (Fig. 2c; cf. Fig. 5e). The preservation of these preparations was, however, not good enough to enable us to conclude whether these invaginations possessed one or two membranes.

Figure 3 shows a panel of micrographs of the *ts*16 virus prepared under different conditions that have been selected to illuminate some features which we believe to be important for the normal assembly process and which are more easily visualized in the *ts*16 virus at the nonpermissive temperature. In Fig. 3a, which shows a cryosection of *ts*16 IVs visualized with ammonium molybdate, one IV (on the right) clearly has two membranes. These two membranes are normally so tightly juxtaposed that they appear as a single membrane (43). That they are indeed double membranes is demonstrated clearly in Fig. 3d, which shows an early step in the assembly of the IV, and more clearly in Fig. 3e, which shows an IV from a cell permeabilized with SLO and treated with proteinase K. In this image the IV shows two distinct bilayers. In a similar preparation (Fig. 3b) the structure of the DNA nucleoid is more evident following extraction of protein components. Finally, Fig. 3c shows a particle from a plastic-embedded section of a cell that was arrested for 6 h at 40°C and then switched to the permissive temperature. Although this particle is clearly abnormal it reveals structural features which are not obvious in normal IMVs; these include a peripheral cisterna, as well as the presence of at least one additional membrane bilayer around the core. The latter is electron transparent, suggesting that it does not enclose the DNA nucleoid or that the DNA was lost during specimen preparation.

Immunolocalization of viral proteins on thawed cryosections. We next analyzed VV *ts*16 infected cells using cryosections to immunolocalize the I7 protein as well as some of the major structural proteins of VV.

I7 protein. The thermosensitivity of VV *ts*16 has been mapped to the I7 gene, which encodes a 47-kDa polypeptide of yet-unknown function. The I7 protein is synthesized late in infection at both the permissive and nonpermissive temperatures, and it has been localized biochemically to the core of wild-type virions (21). In the latter study it was not determined whether the I7 protein is present in the particles that accumulate at the restrictive temperature. We therefore labelled cryosections of *ts*16-infected cells with an anti-I7 serum. In cells infected for 24 h at 31°C, viral factories were labelled, as well as the central part (viroplasm) of viral crescents and IV particles (Fig. 4a). Significant, but weaker, gold labelling was also seen on profiles of IMV particles that form at the permissive temperature (Fig. 4b). The labelling pattern resembled that found for core proteins in wild-type VV showing one or two gold particles over the central part of the IMV (41, 48). When infected cells were lysed with water for 5 min before fixation, there was a significant increase in the amount of label associated with the IV, presumably because of increased access of the antibody (Fig. 4d). Interestingly, at 40°C, labelling for I7 was present in the viral factories, but the viroplasms of the viral crescents, IVs, and the mutant particles seemed devoid of labelling (Fig. 4c). These results suggested that at the nonpermissive temperature VV *ts*16 fails to integrate the I7 protein into the particle (but see below). Experiments in which these cells at 40°C were lysed in water did not result in an increase in the labelling (not shown). In order to get a more objective impression, the gold labelling for I7 was quantitated. We compared the labelling in BSC40 cells infected at both temperatures with that in HeLa cells infected with the wild-type strain WR. As shown in Table 1, the IVs and crescents of *ts*16-infected cells had approximately six times more labelling for I7 at 31°C than at 40°C.

Collectively, these results show that the immunoreactivity for IVs in cells infected at the nonpermissive temperature is significantly lower than that seen with normal assembly intermediates.

Other viral proteins. We next undertook an extensive immunolocalization analysis to test for the presence in the mutant virus particles of proteins known to be in the IMV, using a spectrum of VV antibodies. For this we performed immunogold labelling on thawed cryosections using BSC40 cells infected with *ts*16 for 24 h at the permissive and nonpermissive temperatures.

The localization of the p14 and p32 proteins to wild-type VV has recently been described (42). The peripheral membrane protein p14 (gene A27L) is probably involved in the infection process (31–33) as well as in the wrapping of IMV by a Golgi-derived cisterna to produce the intracellular and extracellular enveloped viruses (34). We have shown by immunoelectron microscopy that in cells infected with wild-type VV, a monoclonal antibody against p14 labels the outer membrane of the IMV and an assembly intermediate between the IV and the IMV (see the introduction), whereas the IV particles are devoid of labelling (42). We rationalized this result by assuming that p14, which behaves as a peripheral membrane protein and lacks any hydrophobic stretch of amino acids long enough to span a membrane, is able to bind to a putative membrane receptor on the assembling particle only at a stage subsequent to the IV. As can be seen in Fig. 5a and b, after infection with *ts*16 at 31°C, the distribution of this antigen was comparable to that in wild-type VV, showing strong labelling of the IMVs but no labelling of IVs. In sections of cells infected with VV *ts*16 at 40°C, the mutant particles were strongly labelled for p14. The gold particles were often restricted to the irregular side of the sphere, which was irregular and flattened (Fig. 5c). In agreement with the labelling pattern seen at 31°C, the IVs and the crescents were not labelled (Fig. 5a and b).

The p32 protein (gene D8L) contains a single hydrophobic domain at its C terminus that could function as a membrane anchor (28). p32 binds to the plasma membrane of cells and is thought to have a function in virus entry (30). On cryosections of cells infected with wild-type VV, anti-p32 labelled the membranes of immature, intermediate, and IMV particles as well as additional membrane profiles in the cytoplasm (42). Essentially the same pattern was obtained when BSC40 cells were infected with *ts*16 both at the permissive (Fig. 5d) and at restrictive temperatures (Fig. 5e and f). Thus, the mutant particles appeared to contain a normal complement of p32 in their membranes.

The localization of the p65 protein (gene D13L), the target of rifampin (1, 45), during wild-type infection has also been previously examined by immunogold labelling (44). This protein is predominantly found on the inside of the forming crescents, suggesting that it might function as a part of a scaffold on the outside of the DNA-enclosing core. Although IVs and wild-type assembly intermediates are labelled strongly for p65, little labelling can be detected in mature virions; we presume that this is due to alteration or masking of the epitope. Sections of cells infected with VV *ts*16 at 31 and 40°C were labelled with a peptide antiserum (B1) raised against the COOH terminus of p65 (44). At 31°C, labelling was mainly observed on the inside of the inner membrane of viral crescents, IVs, and the intermediate form, but as with the wild-type virus, little label was detectable in the IMV (Fig. 6a). In cells infected at 40°C, crescents and IVs were labelled as expected; in addition, the most mature particles that assembled under this condition were strongly labelled, with most of the labelling being concentrated on the inner aspect of the viral membranes (Fig. 6b).

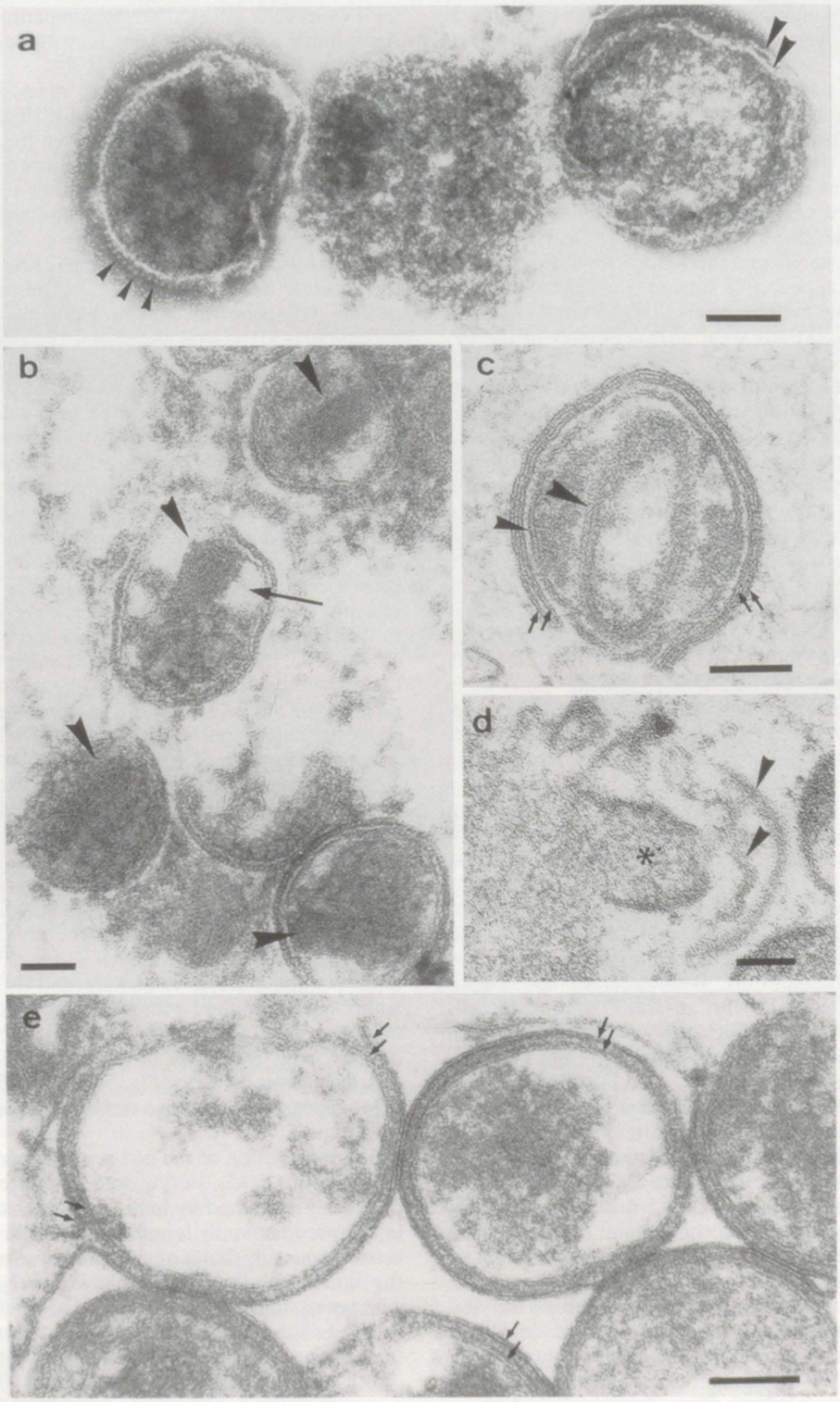


FIG. 3. Structural features of assembly intermediates in *ts*16-infected cells. (a) Thawed cryosection of a cell infected for 24 h at the nonpermissive temperature; the section was negatively stained with ammonium molybdate. The IV on the right has two membranes that are clearly separated from each other at one site (large arrowheads). In the particle on the left, the outer membrane is probably disrupted, revealing spike-like projections (small arrowheads). (b and e) IV particles from permeabilized BSC40 cells (24-h infection) that were treated with 1 mg of proteinase K per ml. (b) This treatment enhances the visibility of the viral DNA (arrowheads) by removing the bulk of the interior of the IV (arrow). (e) The two membranes of the IV (small arrows) are distinct. (c) Epon section showing a particle from a cell infected for 8 h at the nonpermissive temperature followed by a 1-h reversal to the permissive temperature. This particle, clearly abnormal, reveals a cisterna (arrows) on the periphery as well as one additional bilayer just beneath it (small arrowhead). A possible fourth bilayer indicated by the large arrowhead immediately surrounds the nucleoid, which in this case seems devoid of DNA. (d) Epon image from a cell infected for 24 h at the nonpermissive temperature to show the core (asterisk), possibly surrounded by a membrane, apparently in the process of being enclosed by a cisterna (arrowheads indicate the two membranes). Bars, 100 nm.

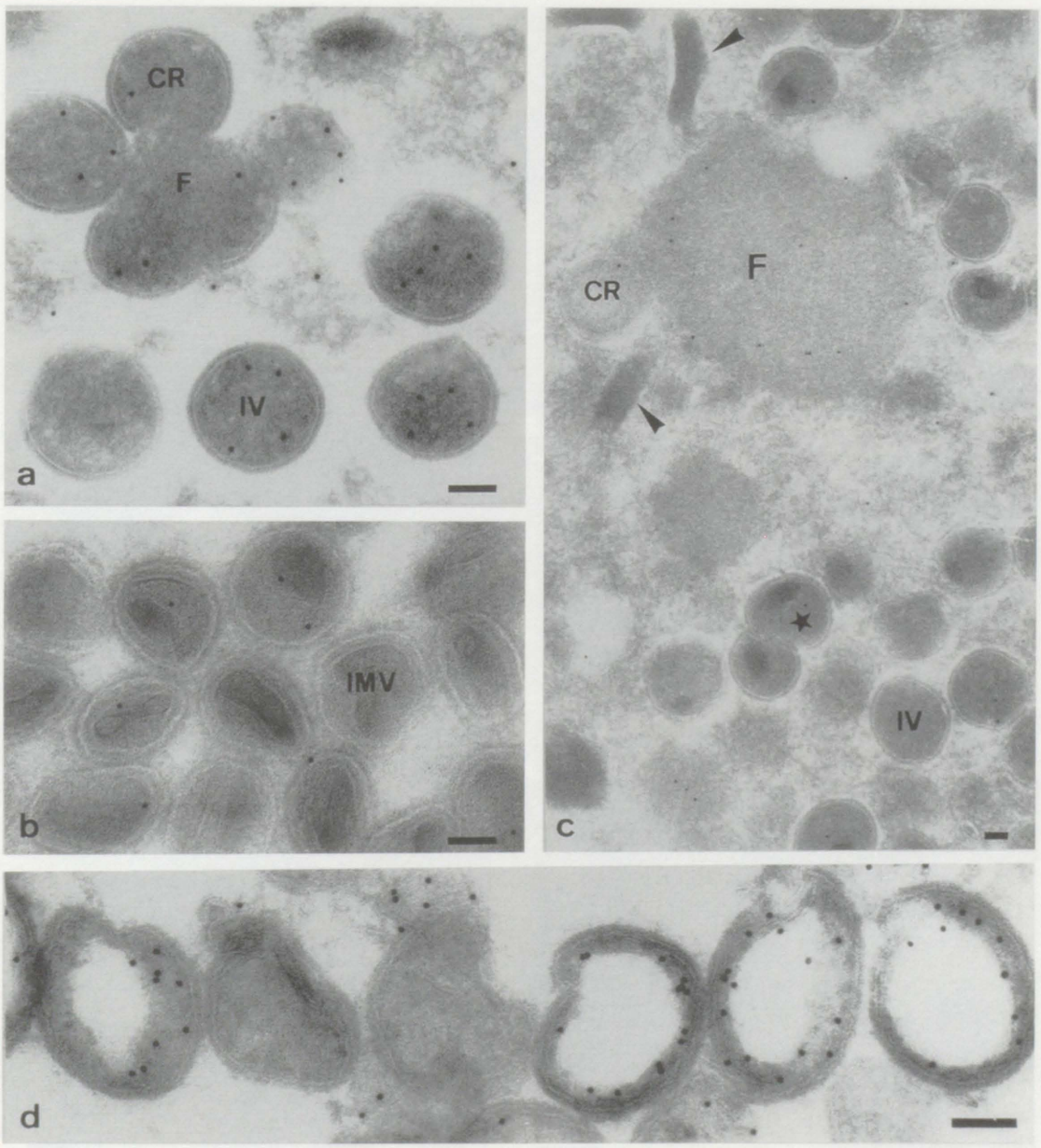


FIG. 4. Localization of the I7 protein. Cryosections of BSC40 cells infected for 24 h with *ts*16 at 31°C (a and b) and 40°C (c) and of HeLa cells infected with WR for 24 h at 37°C (d) were prepared. Sections were labelled with anti-I7 and then with 10-nm-diameter protein A-gold particles. At 31°C the anti-I7 serum significantly labels the viral crescents (CR) and IVs (a). The IMVs are labelled much less extensively: generally no more than one or two gold particles can be seen close to the core of the virion (b). At 40°C (c) the labelling is significantly weaker than at 31°C and predominantly localized to the viral factories (F). Viral crescents (CR), IVs, and the mutant virions (star) are almost totally devoid of labelling. Note the presence of small DNA crystalloids in close proximity to the viral factory (arrowheads). When HeLa cells infected with wild-type VV were incubated for 5 min in water before fixation followed by cryosectioning and immunolabelling, most of the IVs appeared empty but were labelled very strongly with the I7 antibody (d). Bars, 100 nm.

As described earlier for the IV of the wild-type virus, some gold particles were also seen on the outside of the viral particle: it should be noted that the size of the protein A-gold-antibody complex (~20 nm in length) is too large to enable us to be confident that this labelling indeed represents antigen on the particle surface. The fact that no labelling could be detected on the surface of isolated, negatively stained virions with this antibody (see below) argues against the presence of significant amounts of p65 on the outer surface.

The proteins 4a, 4b, and 25K (genes A10L, A3L, and L4R, respectively) are associated with the core of mature virions (35,

TABLE 1. Quantitation of VV I7 in BSC40 cells infected for 24 h with *ts*16 or WR

Virus strain	Infection temperature (°C)	Density of immunogold particles (mean ± SD)[a]	
		IV and CR	IM and IMV
*ts*16	40	0.39 ± 0.61	0.44 ± 0.62
*ts*16	31	2.39 ± 1.72	1.28 ± 1.07
WR	37	3.06 ± 2.26	1.44 ± 1.25

[a] Number of gold particles per square micrometer of micrograph. CR, crescent; IM, intermediate.

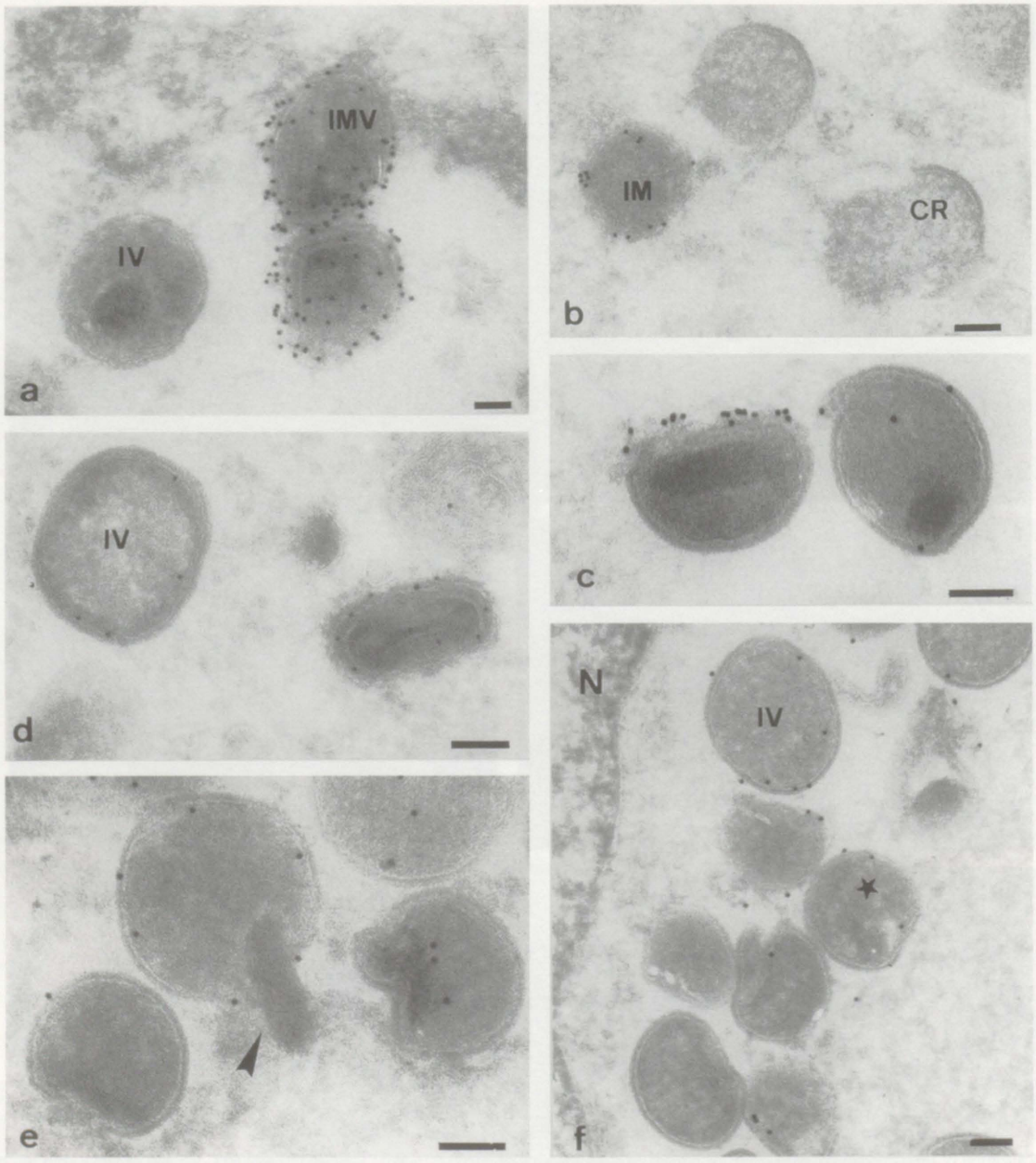


FIG. 5. Immunolocalization of p14 and p32 in cryosections of BSC40 cells infected with *ts*16 for 24 h at 31°C (a, b, and d) and 40°C (c, e, and f). The sections were labelled with either a monoclonal antibody specific for p14 (a to c) or a rabbit antiserum directed against p32 (d to f). At 31°C anti-p14 strongly labels the outer membrane of IMV (a) and the assembly intermediates (IM) (b). Viral crescents (CR) (b) and IVs (a) are not labelled. At 40°C anti-p14 labels the accumulated mutant virions strongly, often on the more irregular part of the outer membrane (c). Anti-p32 labels IMVs as well as IVs on the outer membrane at 31°C (d). At 40°C anti-p32 labels the membranes of the IVs and mutant virions (star) (f). Note the virion in panel e that is in the process of taking up the DNA (arrowhead). N, nucleus. Bars, 100 nm.

46, 50–52). Immunogold labelling with rabbit antisera against the three proteins gave very similar results and can be described collectively. Gold particles were evenly distributed in the viroplasm of the *ts*16 particles and in the viral factories under restrictive conditions, as was also seen in IVs during wild-type infections (Fig. 6c). Again, IMVs were labelled sparsely (results not shown). As for the p65 protein and the I7 protein, the failure to detect significant amounts of label for these proteins in the IMV core might be due to the fact that the antigens are not accessible in the densely packed IMV.

Labelling with anti-DNA antibodies confirmed that the dense nucleoids observed in the *ts*16 particles that accumulated at the restrictive temperature by using Epon embedding (Fig. 1) represented DNA (Fig. 6d). Labelling could also be detected on the larger crystalloids of DNA (data not shown) as well as on smaller structures of dense material in the cytoplasm, possibly representing smaller fragments of DNA ready to enter a viral particle (not shown). The fact that not all the DNA structures in profiles of the defective particles were labelled with anti-DNA (Fig. 6d) is probably due to their inaccessibility to antibody and to the fact that only the DNA appropriately exposed on the surface of the thawed cryosection will be labelled.

To summarize these results, most of the viral antigens ap-

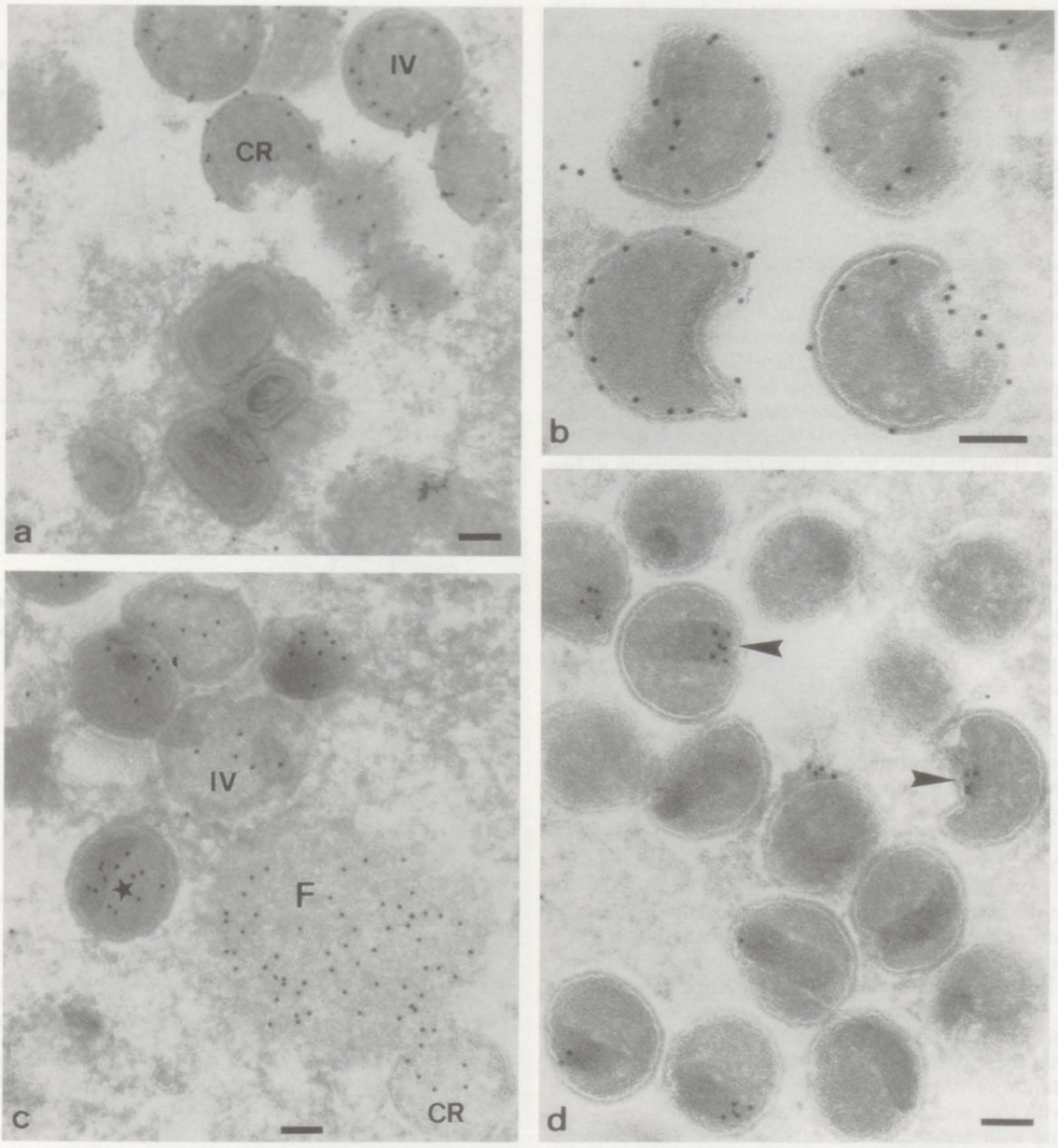


FIG. 6. Immunolocalization of p65, p4a/4a and the viral DNA in cryosections of BSC40 cells infected with *ts*16 at 24 h after infection. Sections of cells infected at 31°C (a) and 40°C (b) were labelled with antibodies against p65. At 31°C most but not all of the labelling is found on the inner side of the inner membranes of the IVs and the crescents (CR). IMVs are devoid of labelling. At 40°C the mutant virions are labelled similarly to the IVs, predominantly around the inner side of the inner membrane (b). (c) Immunolocalization of p4a/4a of cells infected at 40°C. Cryosections were labelled with an antibody recognizing both the precursor and the processed form of 4a. Anti-p4a/4a strongly labels the viral factories (F), the inside of the viral crescents, IVs, and the mutant virions (star). (d) Anti-DNA antibody labels the dense nucleoids (arrowheads) in the virions that accumulate at 40°C. In some virions the dense nucleoid that is clearly visible is not labelled, probably because of inaccessibility of the DNA to the antibody. Bars, 100 nm.

peared to localize to the mutant particle as expected for the assembly intermediate between the IV and the IMV, with two exceptions. The labelling for p14 was often polarized on one side of the particle, while no labelling for the I7 protein was evident in the defective particles.

Arrest of assembly of VV *ts*16 is not reversible. One important question was whether the spherical particles that accumulated at the nonpermissive temperature would form normal brick-shaped IMVs after being shifted to the permissive temperature. To investigate this, cells were infected at 40°C for 12 h and then shifted to 31°C and chased for up to 8 h in the presence of rifampin. Rifampin specifically inhibits VV assembly at a stage before formation of the crescents and is not known to have any effect on the maturation step leading from the IV to the IMV (13, 26, 27). Rifampin was added to block the putative formation of IMVs from remaining protein pools inside the cells. Despite a careful analysis of thin sections of such pulse-chased cells, no mature virions could be detected, suggesting that the *ts*16 particles which accumulated at 40°C do not mature into normal IMVs (Fig. 3c). In contrast, cells that were infected at the permissive temperature in the presence of rifampin formed normal amounts of IMV after washout of the drug (data not shown). Further evidence that the particles that accumulated at the nonpermissive temperature were irrevers-

ibly arrested came from the biochemical analysis of purified particles labelled under the pulse-chase conditions described above (see Fig. 9, lane C; see also below).

Isolation of *ts*16. In order to further characterize the spherical particles that accumulated at the restrictive temperature, we next attempted to purify them from infected cells. Initially we used a simplified version of the procedure described by Sarov and Joklik (36) to isolate intermediates of VV assembly. *ts*16-infected BSC40 cells were labelled with [^{3}H]thymidine and with ^{35}S, chased for 2 h in unlabelled medium, and homogenized. The homogenate was centrifuged gently to remove the nuclei, and the supernatant was layered onto a 12-to-26% (wt/wt) sucrose gradient and centrifuged for 30 min at 16,000 rpm in an SW40 rotor. Under these conditions one peak of radioactivity containing both [^{3}H]thymidine and ^{35}S label could be detected close to the bottom of the gradient, at both permissive and nonpermissive temperatures. Since our initial goal was to establish gradients that would separate the defective particle from the IMV, we modified the conditions in the following way. Cells were infected, labelled, and homogenized as described above. The supernatants were analyzed on either 12-to-40% (wt/wt) or 25-to-40% (wt/wt) sucrose gradients that were centrifuged for 30 min at 16,000 rpm or for 20 min at 24,000 rpm, respectively, in an SW40 rotor. Both sets of conditions gave similar results. Figure 7 shows the distribution of ^{3}H and ^{35}S labels over 12-to-40% gradients at 31 and 40°C. At both temperatures one peak, containing labelled DNA and protein, was detected at a position near the bottom of the gradient. Apparently, under the conditions used, we were unable to separate the IMV from the defective *ts*16 particles that accumulate at the nonpermissive temperature.

Characterization of the isolated particles. In order to analyze the particles found in the peak of ^{35}S and ^{3}H in the gradients in more detail we first performed a negative-staining EM analysis. As expected, brick-shaped particles, indistinguishable from isolated wild-type IMVs (Fig. 8c and e), were present in the peak obtained after infection at the permissive temperature. Consistent with the images obtained with Epon embedding and cryosections, at the nonpermissive temperature, the isolated particles had a spherical appearance with a diameter of about 270 nm. No brick-shaped virions could be seen in this fraction (Fig. 8a, b, d, and f). In some views it was evident that these particles were not complete spheres but had an indentation at one pole (Fig. 8b), in agreement with the analysis with thin sections (Fig. 2a and c).

Labelling with antibodies was carried out on these whole, isolated particles to examine which antigens were exposed on their surfaces. After labelling, the particles were negatively stained and examined by EM. The results of these experiments are illustrated in Fig. 8. The p14 antibody gave a very strong labelling on the mature IMV isolated from cells infected at the permissive temperature (Fig. 8c). At the nonpermissive temperature the isolated defective particles showed a variable labelling: some were labelled strongly, especially on one pole (Fig. 8d), while others seemed devoid of labelling (data not shown). This finding is consistent with the results from the immunolabelling on cryosections, where the labelling was mostly concentrated on one side of the particle.

Antibodies against the membrane protein p32 extensively labelled the outside of both mature virions and the defective particles (Fig. 8e and f). No significant labelling could be detected on the outer surfaces of these particles for I7, p65, or the core proteins 4a, 4b, and 25K (data not shown).

Protein composition of the isolated particles. *ts*16 has been classified as belonging to a group of mutants with wild-type protein and DNA synthesis (3). This finding was based on

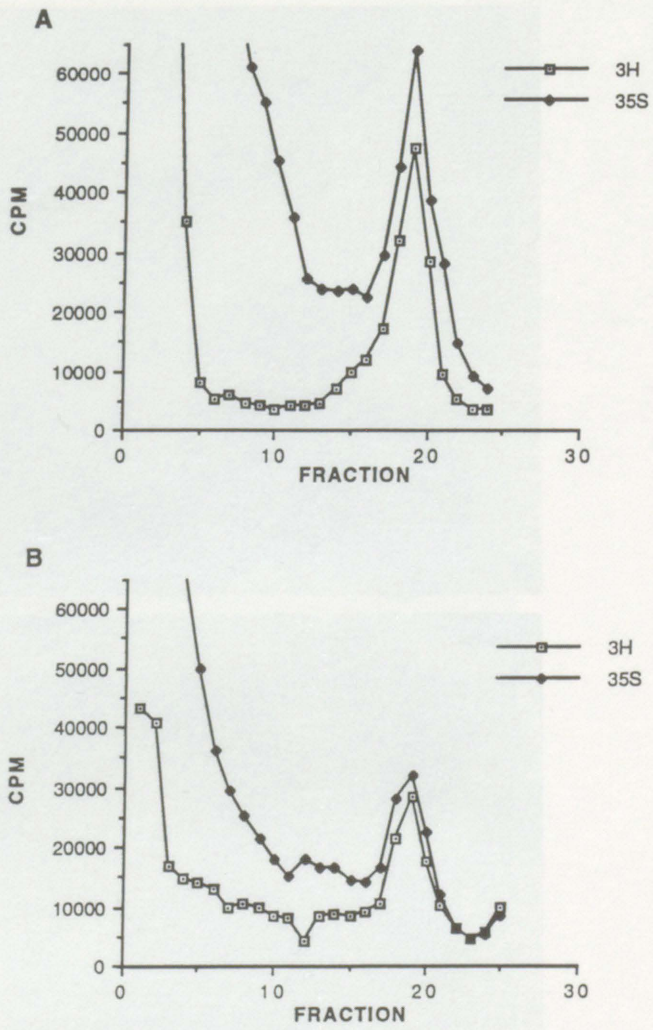


FIG. 7. Purification of VV *ts*16 on sucrose density gradients from BSC40 cells infected for 24 h under permissive (A) and nonpermissive (B) conditions. Infected cells kept at either temperature were labelled with [^{3}H]thymidine (3H) from 1 to 5 h postinfection and with ^{35}S label (35S) from 5 to 22 h postinfection. Postnuclear supernatants of infected cells were layered onto a continuous sucrose gradient and centrifuged for 30 min at 16,000 rpm in an SW40 rotor. Fractions were collected from top to bottom, and radioactivity was counted.

SDS-PAGE of pulse-labelled, infected cells grown at 40 and 31°C. We next analyzed by SDS-PAGE the protein composition of the defective particles, isolated as described above. The protein patterns of *ts*16 grown at 31 and 40°C were compared with that of purified IMV. As expected, the protein pattern of *ts*16 grown at 31°C was identical to that of purified IMV (not shown). The composition of the defective particles, however, appeared to be different. The most striking difference was that the core proteins p4a, p4b, and p25 were in the uncleaved precursor form and now appeared as bands of 95, 65, and 28 kDa, respectively (Fig. 9, lane B; Fig. 10). As shown by immunoprecipitation, at the permissive temperature the proteins migrated mainly as 62-, 60-, and 25-kDa bands, which correspond to the sizes of the proteolytically cleaved products (Fig. 10) (26, 47, 49). Also, the relative abundance of some of the proteins in the defective particles appeared to be different from the abundance in the virus from cells infected at 31°C and that in wild-type IMV. Another striking difference was that in the defective particles there was an abundant band migrating

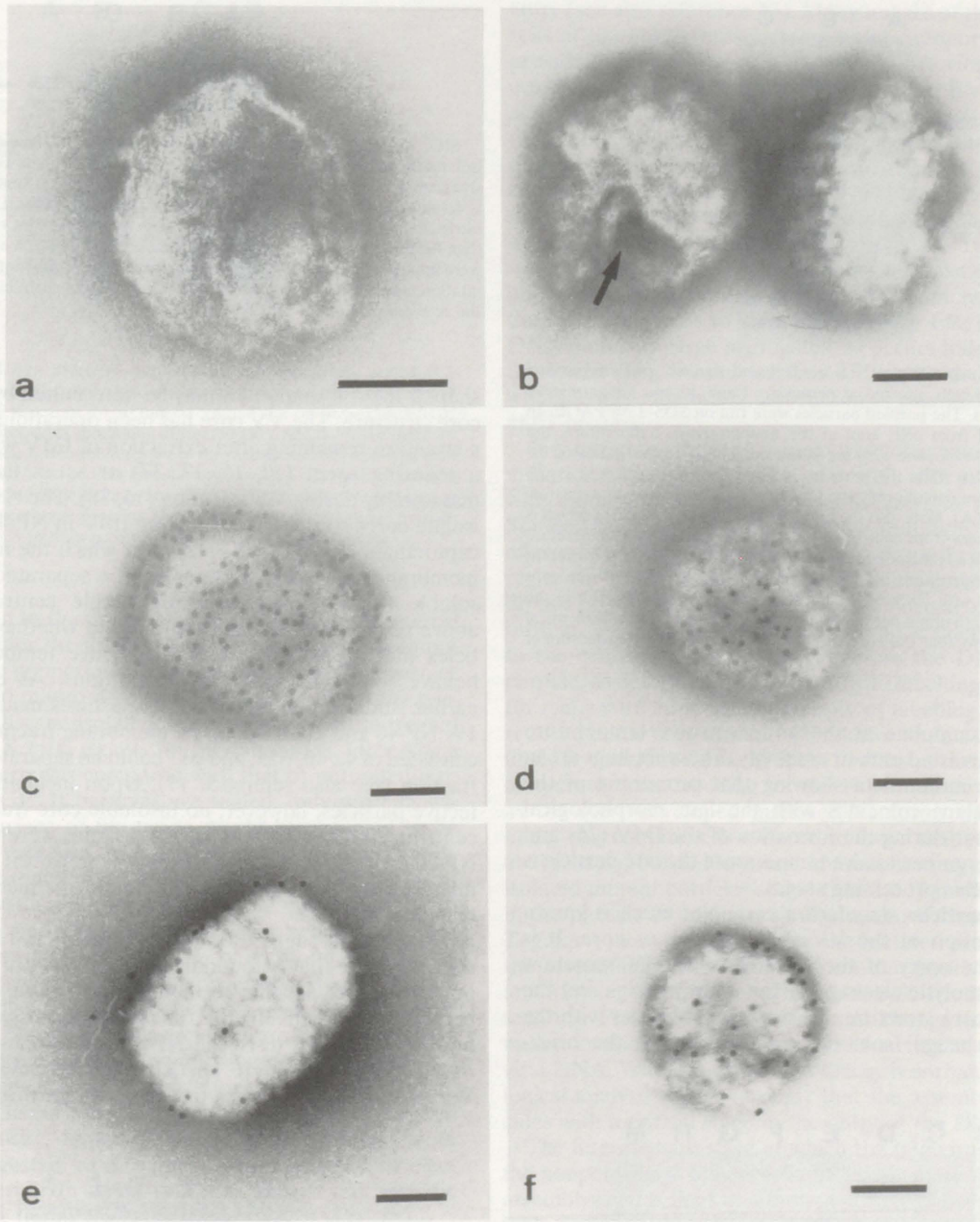


FIG. 8. Negative staining and immunogold labelling of sucrose-purified VV *ts*16 virions made at 31 and 40°C. Brick-shaped virions (c and e) were isolated from cells infected under permissive conditions, while spherical particles (a, b, d, and f) were obtained from cells infected under nonpermissive conditions. Some particles obtained from infected cells kept at 40°C are irregularly shaped and often have an indentation on one side (arrow in panel b). p14 (c and d) and p32 (e and f) are localized to the surface of the isolated particles in both IMV (c and e) and the mutant particle (d and f). Bars, 100 nm.

around 24 kDa while in the IMV a similar band seemed to run at about 20 kDa (Fig. 9, lanes B and C). The identity of this band was not further investigated.

To assess whether the I7 protein was present in the mutant particles, the labelled peak fractions of the gradients were run on SDS-PAGE and blotted onto nitrocellulose. Care was taken to load the same amount of radioactive counts of the particles isolated from cells infected at 31°C and those infected at 40°C. As a control, we also used labelled wild-type IMV, using five times more counts. To our surprise, and in obvious disagreement with the EM data, the I7 protein appeared to be present in roughly similar amounts in the mutant particles and in the viruses isolated from cells infected at the permissive temperature (Fig. 11). The I7 protein in the mutant particles, however, appeared to migrate slightly faster. The reason for this faster migration is at present not understood.

We further investigated whether the protein precursors that had accumulated during infection at 40°C would be processed following a temperature shift down to 31°C. BSC40 cells infected and labelled with ^{35}S for 24 h at 40°C were washed and then shifted to 31°C for various periods in the presence and absence of rifampin (see above). After the temperature shift, all three core proteins appeared to remain uncleaved (Fig. 9, lane C), in agreement with the EM data showing that the

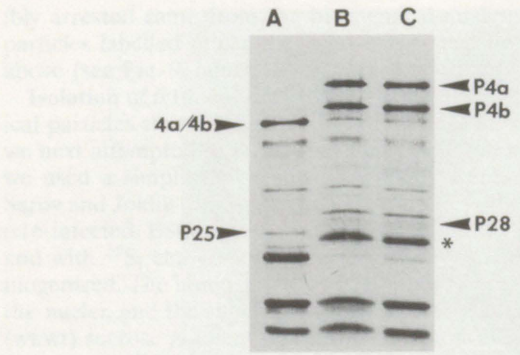


FIG. 9. Protein composition of ^{35}S-labelled and sucrose gradient-purified particles from BSC40 cells infected at permissive (lane A) and nonpermissive (lane B) temperatures. The purified particles were run on SDS–15% PAGE. In the particles isolated from cells kept at the nonpermissive temperature, the major core proteins (4a, 4b, and p25) are in their precursor forms (indicated for lane C by arrowheads), while the particles isolated from cells infected at the permissive temperature contain only the processed forms of these proteins (arrowheads beside lane A). Note also the band around 24 kDa (asterisk), which is present only in particles from cells infected at the nonpermissive temperature (lanes B and C), while a corresponding band running at about 20 kDa is present at the permissive temperature (lane A). Lane C, particles isolated from cells infected and labelled with ^{35}S at 40°C and then chased at 31°C for 6 h in the presence of 100 μg of rifampin per ml. The protein pattern in lane C is identical to that in B and shows that the core proteins have not been processed under these conditions.

particles that accumulate at the nonpermissive temperature are irreversibly arrested in their assembly. These findings are in agreement with earlier data showing that processing of the major core proteins coincides with the late morphological changes that occur during the formation of the IMV (26) and argue that at the nonpermissive temperature the *ts*16 particle is arrested before this processing stage.

The mutant particles may lack a core. Not much is known about the formation of the VV nucleocapsid, or core. It is assumed that the entry of the DNA into the IV somehow triggers the proteolytic cleavage of the core proteins and the formation of a core structure. This in turn coincides with the morphological change from the spherical IV to the brick-shaped IMV, a shape that may be determined by a underlying core structure. The VV core has been operationally defined as a structure remaining after extraction of IMV with NP-40 and a reducing agent (10, 16, 17, 37) or as an intermediate of disassembly during VV infection (15, 38). The classical assay to isolate cores consists of incubating IMV in NP-40 with β-mercaptoethanol or DTT at 37°C, after which the membrane and membrane-associated proteins can be separated from the insoluble (brick-shaped) core by simple centrifugation (see above references). We therefore asked whether the *ts*16 particles that accumulate at the restrictive temperature would behave similarly under these conditions. As expected from earlier studies upon incubation of particles made at 31°C with 1% NP-40 and 20 mM DTT, a membrane fraction that mainly consisted of 4a/4b, p25, and p11 could be separated from a core fraction (see also reference 17). Upon incubation of the defective particles, however, no insoluble core fraction could be centrifuged down. Instead all the proteins were now soluble in NP-40–DTT (Fig. 12). An exception, however, was a protein migrating as an 11-kDa species, some of which could be detected in the pellet.

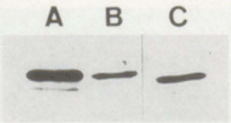


FIG. 11. The I7 protein is present in wild-type IMVs (lane A) and in particles isolated from VV *ts*16-infected cells at the permissive (lane B) and nonpermissive (lane C) temperatures. ^{35}S-labelled IMV and the peak fractions from virions isolated as described for Fig. 5a and b were run on SDS-PAGE and blotted onto nitrocellulose. About five times more counts were loaded for the wild-type IMV than for the others, while for the peak fractions from Fig. 5a and b equal counts were applied. The nitrocellulose was incubated with the I7 antibody at a 1:1,000 dilution, and the proteins were detected by enhanced chemiluminescence. Only the relevant part of the blot is shown.

These results suggest that the detergent- and DTT-insoluble core structure that is found in the IMV has not yet assembled in the *ts*16 particles that accumulate at the nonpermissive temperature. Alternatively, the *ts*16 particles possess a core that, however, does not resist the NP-40–DTT treatment.

The defective VV *ts*16 particles are not completely sealed. While the IMV is clearly a tightly sealed particle, the crescents

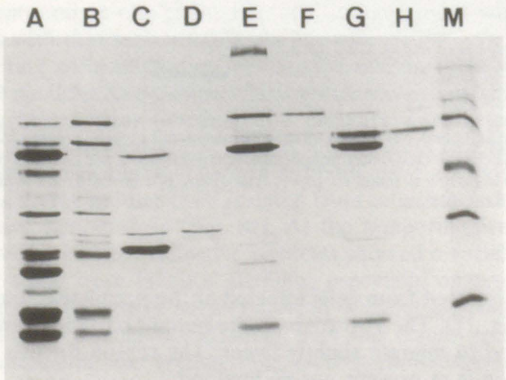


FIG. 10. Immunoprecipitation of p4a/4a, p4b/4b, and p28/p25 from IMVs and mutant particles. Lanes A and B, particles isolated from *ts*16-infected cells at 31 and 40°C, respectively. These particles were dissolved and immunoprecipitated with anti-p28/p25 (lanes C and D), with anti-p4a/4a (lanes E and F), and with anti-p4b/4b (lanes G and H) at 31°C (lanes C, E, and G) and 40°C (lanes D, F, and H). Lane M, ^{14}C marker. Although the antibodies immunoprecipitate bands of the expected size, they also appear to coimmunoprecipitate to variable extents the other core proteins. Note also that while at 40°C the three core proteins are quantitatively in their unprocessed precursor forms, at 31°C most but not all of these proteins are processed.

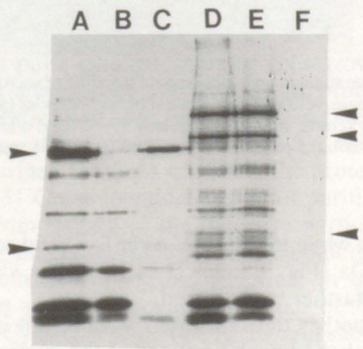


FIG. 12. *ts*16 defective particles lack an insoluble core fraction. ^{35}S-labelled and sucrose-purified mutant and wild-type particles were treated for 30 min at 37°C with 1% NP-40 and 20 mM DTT. The soluble and insoluble fractions were separated by centrifugation. Lanes A through C, particles isolated from cells kept at 31°C; lanes D through F, particles from 40°C infections. Lanes A and D, untreated particles; lanes B and E, detergent-soluble fractions; lanes C and F, insoluble fractions. Note that in the mutant particles only a faint band around 11 kDa can be detected in the insoluble fraction (lane F). The arrowheads point to the positions of the core proteins, p4a/4a, p4b/4b, and p28/p25 (top to bottom).

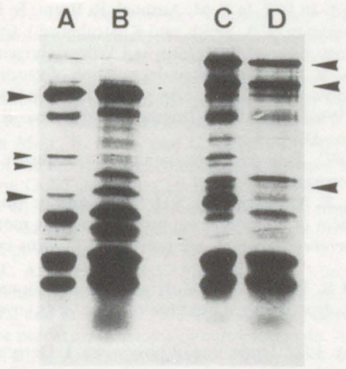


FIG. 13. Isolated *ts*16 defective particles are not completely sealed. ^{35}S-labelled and sucrose-purified wild-type and mutant particles were treated with 100 μg of proteinase K per ml for 30 min on ice and run on SDS–15% PAGE. Lanes A and C, control lanes containing untreated IMV and defective particles, respectively. Proteinase K treatment results in the digestion in the wild-type IMV of proteins running at 32 and 35 kDa (small arrowheads), while the core proteins are completely protected (lane B, large arrowheads). In the defective particles, in addition to the two membrane proteins, the core proteins 4a and 4b are partially digested, while the p25 protein is completely lost (lane D, arrowheads).

and IVs are open to the cytoplasm (43). It was thus of interest to find out whether the intermediate particles which accumulate in *ts*16 at the nonpermissive temperature were still open or whether they had matured beyond the stage at which the particles seal. For this the isolated mutant particles were treated with proteinase K (100 μg/ml) for 30 min on ice, after which the protein pattern was compared with that of untreated virions by SDS-PAGE. If particles are sealed, only proteins exposed on the surface of the virion would be expected to be accessible to the protease. As is evident in Fig. 13, virions made at the permissive temperature clearly lost proteins migrating at 35 and 32 kDa, while the core proteins were protected (18). In contrast, virions made at the nonpermissive temperature lost not only p35 and p32 but also the core proteins; p28 was completely lost, while p4a and p4b appeared partially digested. These results indicate that these particles were not completely sealed. That the particle is not as open as are the IVs was also suggested by a protease experiment using permeabilized cells (43). At the nonpermissive temperature, protease enters the permeabilized cells, as is evident by loss of the cytoplasmic and nucleoplasm density. However, the defective particles were only partially digested, as is evident by the presence of electron-dense material. In some of these images the periodic packed nature of the DNA is especially evident (Fig. 3b).

DISCUSSION

As a part of our effort in understanding how VV assembles we focused here on the characterization of *ts*16, a mutant virus that at the nonpermissive temperature is arrested at an interesting stage of its assembly. As shown by Kane and Shuman (21), and in more detail in this study, the block in assembly coincides with the complex morphological transition from the spherical IV, which does not contain DNA, to the brick-shaped IMV, in which the genome is fully enclosed in a sealed particle. In the normal assembly process this stage is relatively rare, which suggests that it is a relatively short-lived intermediate (13, 42).

Our extensive EM analysis of the assembly of wild-type VV has led us to believe that the viral DNA is packaged into a preformed nucleoid before it enters the viral particle and that these nucleoids may associate with cellular membranes prior to entry (see also reference 13). Many images of the *ts*16-infected cells at the nonpermissive temperature support this view and provided us with interesting images of the viral DNA and its possible entry process. From early on in our EM studies of VV assembly we had noticed that a small but consistent fraction of the viral DNA is present in roughly brick-shaped nucleoids that are tightly bound to cellular membranes. Some of these cisternae show above-background labelling for markers of the intermediate compartment (unpublished data) which we consider a specialized domain of the ER (22). The block in assembly of the mutant virus seemingly led to an exaggeration of one feature of the normal entry process, namely, the binding of the DNA nucleoids to membranes of the ER; in addition the DNA builds up large aggregates, as occurs following rifampin treatment (13). Further studies will be needed to determine whether this membrane association is essential for the DNA entry process.

It is intriguing that the protein which has undergone a point mutation in the *ts*16 virus is I7, a protein with partial homology with the type II topoisomerase of *S. cerevisiae* (21). Kane and Shuman logically suggested that the mutation in this protein affected the ability of the DNA to be properly packaged, leading to the block in assembly. Our data are consistent with, but do not prove, this hypothesis. During normal assembly the I7 protein, like all the core proteins we have examined, localizes to the central matrix of the IV before the DNA enters the particle, as determined by immunogold labelling. As is the case for many core antigens, the density of labelling is significantly reduced in the core of the IMV relative to that in the IV, most likely for steric reasons. In the *ts*16 virus at the nonpermissive temperature the labelling for the I7 protein of the IV, as well as the most developed intermediate forms that accumulate under this condition, is reduced to levels that are only slightly above background. However, immunoblotting analysis of the isolated mutant particles shows that the I7 protein is detected in the particle in amounts similar to those found in the IMV. Together, these data argue that the mutated protein can enter the assembling virion but in a form that poorly recognizes its antibody on the surface of formaldehyde-fixed, thawed cryosections. Presumably, the structural change induced by the mutation also impairs its proposed function in packaging the viral DNA. Whether or not this theory is correct, our morphological analysis argues strongly that the assembly block coincides with a critical stage in the entry of the DNA.

The intermediate stage at which the *ts*16 virus is blocked at the nonpermissive temperature is clearly more advanced in its assembly than is the IV, although at first glance both particles look similar. Thus, whereas random sections through the IVs invariably give rise to spherical profiles (although the particles are completely open and their contents completely digested with protease [43]), many profiles through the *ts*16 mutant particles are hemispherical at one pole only. In this study the three-dimensional appearance of these particles was best appreciated by the negative-staining EM approach, which showed that, when the orientation was favorable, these particles resembled a sphere with an indentation at one pole. From thin-section analysis it seems tempting to suggest that this indentation reflects the site at which the DNA enters the particle. Biochemically, as assayed by protease digestion of the isolated particles, the particles seemed partially open. In agreement with these data the EM analysis suggests that only a part of the electron-dense material around the DNA was sensitive to protease attack, unlike the IV, whose contents are essentially completely digested (see also reference 43).

While the *ts*16 particles are irreversibly arrested in their development, a number of proteins appear to be localized in a

manner indistinguishable from that in normal VV. Thus, besides the core proteins already mentioned earlier, p32, an outer membrane protein of IMV which is normally localized to the outer membrane of the crescents and IVs (42), shows the same uniform membrane localization in the *ts*16 particle at the nonpermissive temperature. Further, the p65 protein that genetic studies argue to be the target of rifampin localizes to the inner membrane of the spherical IV (44) as well as that of the defective *ts*16 particles. An interesting difference from the normal assembly process involved the peripheral membrane protein p14. This protein, which is an abundant component on the outer surface of the IMV, is not detected by immunogold labelling on the crescents or IV but is acquired in what appears to be a distinct step in the normal assembly process, the intermediate particle between the IV and the IMV (42). Such particles appear to be uniformly labelled with anti-p14 antibodies. Rodriguez et al. (31) have proposed that p14 binds to the integral membrane protein p21. The latter is therefore a candidate for being the receptor that might be activated for binding p14 only at the intermediate particle stage. The *ts*16 particle is clearly arrested at, or near, this intermediate stage since it is labelled strongly for p14 both on sections and on the outside of the isolated particles by negative staining. However, the distribution of label is abnormal in that p14 is clearly concentrated on some parts of the particle and depleted in others. We presume that this difference is somehow related to the defect in assembly, but further studies will be required to determine its significance. In contrast to labelling for p14, in preliminary studies antibodies to its putative receptor p21 label the membranes of the mutant particles in a uniform manner on sections (not shown).

The Condit collection of *ts* mutants of VV includes a number of examples in which a known protein is mutated and, as a result, a key step of assembly or disassembly of the virus is blocked. We believe that the combined morphological and biochemical analysis used here to characterize the *ts*16 mutant will continue to be a powerful approach to characterize other temperature-sensitive mutants with the expectation that these could open up key insights into the mechanisms of VV assembly and disassembly.

ACKNOWLEDGMENTS

We thank M. Esteban, E. Niles, D. Hruby, and R. Doms for antibodies.

J.K.L. was supported by a fellowship from the Human Frontier Science Program.

REFERENCES

1. **Baldick, C. J., and B. Moss.** 1987. Resistance of vaccinia virus to rifampicin conferred by a single nucleotide substitution near the predicted NH2 terminus of a gene encoding an Mr 62,000 polypeptide. Virology **156:**138–145.
2. **Cairns, H. J. F.** 1960. The initiation of vaccinia infection. Virology **11:**603–623.
3. **Condit, R. C., and A. Motyczka.** 1981. Isolation and preliminary characterization of temperature-sensitive mutants of vaccinia virus. Virology **113:**224–241.
4. **Condit, R. C., A. Motyczka, and G. Spizz.** 1983. Isolation, characterization, and physical mapping of temperature-sensitive mutants of vaccinia virus. Virology **128:**429–443.
5. **Dales, S.** 1963. The uptake and development of vaccinia virus in strain L cells followed with labelled viral deoxyribonucleic acid. J. Cell Biol. **18:**51–72.
6. **Dales, S., and B. G. T. Pogo.** 1981. Biology of poxviruses. Virology Monogr. **1981:**54–61.
7. **Dales, S., and L. Siminovitch.** 1961. The development of vaccinia virus in Earle's L strain cells as examined by electron microscopy. J. Biophys. Biochem. Cytol. **10:**475–503.
8. **Doms, R. W., R. Blumenthal, and B. Moss.** 1990. Fusion of intracellular and extracellular forms of vaccinia virus with the cell membrane. J. Virol. **64:** 4884–4892.
9. **Earl, P. L., and B. Moss.** 1991. Preparation of cell cultures and vaccinia virus stocks, p. 16.16.1–16.16.7. *In* F. M. Ausubel, R. Brent, R. E. Kingston, D. D. Moore, J. G. Seidman, J. A. Smith, and K. Struhl (ed.), Current protocols in molecular biology. Greene Publishing and Wiley Interscience, New York.
10. **Easterbrook, K. B.** 1966. Controlled degradation of vaccinia virions in vitro: an electron microscopic study. J. Ultrastruct. Res. **14:**484–496.
11. **Fenner, F., R. Wittek, and K. R. Dumbell.** 1989. The orthopoxviruses. Academic Press, San Diego, Calif.
12. **Griffiths, G.** 1993. Fine structure immunocytochemistry. Springer Verlag, Heidelberg, Germany.
13. **Grimley, P. M., E. N. Rosenblum, S. J. Mims, and B. Moss.** 1970. Interruption by rifampicin of an early stage in vaccinia virus morphogenesis: accumulation of membranes which are precursors of virus envelopes. J. Virol. **6:**519–533.
14. **Hiller, G., and K. Weber.** 1985. Golgi-derived membranes that contain an acylated viral polypeptide are used for vaccinia virus envelopment. J. Virol. **55:**651–659.
15. **Holowczak, J. A.** 1972. Uncoating of poxviruses. I. Detection and characterization of subviral particles in the uncoating process. Virology **50:**216–232.
16. **Holowczak, J. A., and W. K. Joklik.** 1967. Studies of the structural proteins of virions and cores. Virology **33:**717–725.
17. **Ichihashi, Y., M. Oie, and T. Tsuruhara.** 1984. Location of DNA-binding proteins and disulfide-linked proteins in vaccinia virus structural elements. J. Virol. **50:**929–938.
18. **Ichihashi, Y., T. Tsuruhara, and M. Oie.** 1983. The effect of proteolytic enzymes on the infectivity of vaccinia virus. Virology **122:**279–289.
19. **Joklik, W. K.** 1966. The poxviruses. Bacteriol. Rev. **30:**33–66.
20. **Joklik, W. K., and Y. Becker.** 1964. The replication and coating of vaccinia DNA. J. Mol. Biol. **10:**452–474.
21. **Kane, E. M., and S. Shuman.** 1993. Vaccinia virus morphogenesis is blocked by a temperature-sensitive mutation in the I7 gene that encodes a virion component. J. Virol. **67:**2689–2698.
22. **Krijnse Locker, J., M. Ericsson, P. Rottier, and G. Griffiths.** 1994. Characterization of the budding compartment of mouse hepatitis virus. J. Cell Biol. **124:**55–70.
23. **Krijnse Locker, J., J. K. Rose, M. C. Horzinek, and P. J. M. Rottier.** 1992. Membrane assembly of the triple-spanning coronavirus M protein. J. Biol. Chem. **267:**21911–21918.
24. **Morgan, C.** 1976. The insertion of DNA into vaccinia virus. Science **193:** 591–592.
25. **Moss, B.** 1990. Poxviridae and their replication, p. 2079–2103. *In* B. N. Fields, D. M. Knipe, R. M. Chanock, M. S. Hirsch, J. L. Melnick, T. P. Monath, and B. Roizman (ed.), Virology. Raven Press, New York.
26. **Moss, B., and E. N. Rosenblum.** 1973. Protein cleavage and poxvirus morphogenesis: tryptic peptide analysis of core precursors accumulated by blocking assembly with rifampicin. J. Mol. Biol. **81:**267–269.
27. **Moss, B., E. N. Rosenblum, E. Katz, and P. M. Grimley.** 1969. Rifampicin: a specific inhibitor of vaccinia virus assembly. Nature (London) **224:**1280–1284.
28. **Niles, E. G., and J. Seto.** 1988. Vaccinia virus gene D8 codes for a virion transmembrane protein. J. Virol. **62:**3772–3778.
29. **Payne, L. G.** 1978. Polypeptide composition of extracellular enveloped vaccinia virus. J. Virol. **27:**28–37.
30. **Rodriguez, D., J. R. Rodriguez, and M. Esteban.** 1992. Insertional inactivation of the vaccinia virus 32-kilodalton gene is associated with attenuation in mice and reduction of viral gene expression in polarized epithelial cells. J. Virol. **66:**183–189.
31. **Rodriguez, D., J.-R. Rodriguez, and M. Esteban.** 1993. The vaccinia virus 14-kilodalton fusion protein forms a stable complex with the processed protein encoded by the vaccinia virus A17L gene. J. Virol. **67:**3435–3440.
32. **Rodriguez, J. F., R. Janeczko, and M. Esteban.** 1985. Isolation and characterization of neutralizing monoclonal antibodies to vaccinia virus. J. Virol. **56:**482–488.
33. **Rodriguez, J. F., E. Paez, and M. Esteban.** 1987. A 14,000-M_r envelope protein of vaccinia virus is involved in cell fusion and forms covalently linked trimers. J. Virol. **61:**395–404.
34. **Rodriguez, J. F., and G. F. Smith.** 1990. IPTG-dependent vaccinia-virus: identification of a virus protein enabling virion envelopment by Golgi membranes and egress. Nucleic Acids Res. **18:**5347–5351.
35. **Rosel, J., and B. Moss.** 1985. Transcriptional and translational mapping and nucleotide sequence analysis of a vaccinia virus gene encoding the precursor of the major core polypeptide 4b. J. Virol. **56:**830–838.
36. **Sarov, I., and W. K. Joklik.** 1972. Isolation and characterization of intermediates in vaccinia virus morphogenesis. Virology **52:**223–233.
37. **Sarov, I., and W. K. Joklik.** 1972. Studies on the nature and location of the capsid polypeptides of vaccinia virions. Virology **50:**579–592.
38. **Sarov, I., and W. K. Joklik.** 1972. Characterization of intermediates in the uncoating of vaccinia virus DNA. Virology **50:**593–602.
39. **Schmelz, M., B. Sodeik, M. Ericsson, E. J. Wolffe, H. Shida, G. Hiller, and G. Griffiths.** 1994. Assembly of vaccinia virus: the second wrapping cisterna is derived from the trans Golgi network. J. Virol. **68:**130–147.
40. **Silver, M., and S. Dales.** 1982. Biogenesis of vaccinia: interrelationship between post-translational cleavage, virus assembly, and maturation. Virology **117:**341–356.

41. **Sodeik, B.** 1992. Das Assembly des Vaccinia Virus. Ph.D. thesis. European Molecular Biology Laboratory, Heidelberg, Germany.
42. **Sodeik, B., S. Cudmore, M. Ericsson, M. Esteban, E. G. Niles, and G. Griffiths.** 1995. Assembly of vaccinia virus: incorporation of p14 and p32 into the membrane of the intracellular mature virus. J. Virol. **69:**3560–3574.
43. **Sodeik, B., R. W. Doms, M. Ericsson, G. Hiller, C. E. Machamer, W. van't Hof, G. van Meer, B. Moss, and G. Griffiths.** 1993. Assembly of vaccinia virus: role of the intermediate compartment between the endoplasmic reticulum and the Golgi stacks. J. Cell Biol. **121:**521–541.
44. **Sodeik, B., G. Griffiths, M. Ericsson, B. Moss, and R. W. Doms.** 1994. Assembly of vaccinia virus: effects of rifampin on the intracellular distribution of viral protein p65. J. Virol. **68:**1103–1114.
45. **Tartaglia, J., A. Piccini, and E. Paoletti.** 1986. Vaccinia virus rifampicin-resistance locus specifies a late 63,000 Da gene product. Virology **150:**45–54.
46. **Van Meir, E., and R. Wittek.** 1988. Fine structure of the vaccinia virus gene encoding the precursor of the major core protein 4a. Arch. Virol. **102:**19–27.
47. **VanSlyke, J. K., C. A. Franke, and D. E. Hruby.** 1991. Proteolytic maturation of vaccinia virus core proteins: identification of a conserved motif at the N termini of the 4b and 25K virion proteins. J. Gen. Virol. **72:**411–416.
48. **VanSlyke, J. K., and D. E. Hruby.** 1994. Immunolocalization of vaccinia virus structural proteins during virion formation. Virology **198:**624–635.
49. **VanSlyke, J. K., S. S. Whitehead, E. M. Wilson, and D. E. Hruby.** 1991. The multistep proteolytic maturation pathway utilized by vaccinia virus P4a protein: a degenerate conserved cleavage motif within core proteins. Virology **183:**467–478.
50. **Weir, J. P., and B. Moss.** 1985. Use of a bacterial expression vector to identify the gene encoding a major core protein of vaccinia virus. J. Virol. **56:**534–540.
51. **Yang, W. P., and W. R. Bauer.** 1988. Purification and characterization of vaccinia virus structural protein VP8. Virology **167:**578–584.
52. **Yang, W. P., S. Y. Kao, and W. R. Bauer.** 1988. Biosynthesis and post-translational cleavage of vaccinia virus structural protein VP8. Virology **167:**585–590.

Appendix

A novel immunogold cryoelectron microscopic approach to investigate the structure of the intracellular and extracellular forms of Vaccinia virus

Norbert Roos[1, 4], Marek Cyrklaff[2], Sally Cudmore[1], Rafael Blasco[3], Jacomine Krijnse-Locker[1] and Gareth Griffiths[1]*

[1] Cell Biology Programme and [2] Biological Structures Programme, European Molecular Biology Laboratory, D-69012 Heidelberg, Germany.

[3] Centro de Investigacion en Sanidad Animal, INIA-MAPA, Valdeolmos, E-28130 Madrid, Spain

[4] Electron Microscopy Laboratory for Biology, University of Oslo, Blindern 0316 Oslo 3, Norway

* Corresponding author. Mailing address: Cell Biology Programme, European Molecular Biology Laboratory, Postfach 10.2209, D-69012 Heidelberg, Germany
Tel. +49 6221 387267, Fax +49 6221 387306

Key words: cryoelectron microscope, immunogold labelling, vaccinia virus
Running title: Structure of vaccinia virus

ABSTRACT

We introduce a novel approach for combining immunogold labelling with cryoelectron microscopy of thin vitrified specimens. The method takes advantage of the observation that particles in suspension are concentrated at the air-water interface and remain there during the subsequent immunogold labelling procedure. Subsequently, a thin aqueous film can be formed that is vitrified and observed by cryo EM.

In our view a key early step in the assembly of vaccinia virus, the formation of the spherical immature virus, involves the formation of a specialized cisternal domain of the intermediate compartment between the endoplasmic reticulum and the Golgi. Using this novel cryoelectron microscopy approach we show that in the intracellular mature virus (IMV) the core remains surrounded by a membrane cisterna that comes off the viral core upon treatment with dithiothreitol, exposing an antigen on the surface of the viral core. Complementary protease studies suggest that the IMV may be sealed not by membrane fusion but by a proteinaceous structure that interrupts the outer membrane. We also describe the structure and membrane topology of the second infectious form of vaccinia, the extracellular enveloped virus and confirm that this form possesses an extra membrane overlying the IMV.

INTRODUCTION

The classical view of the assembly of poxviruses such as vaccinia was that it involved a de novo synthesis of a single viral membrane in the cytoplasm (Dales and Mosbach, 1968). This assumes that the membrane arranges itself to build the first, morphologically distinct form of the assembling virus, the spherical immature virus (IV). The IV then encloses the viral DNA and develops further into the first infectious form, the brick-shaped, intracellular mature virus (IMV), previously referred to as the intracellular naked virus (reviewed by Dales and Pogo, 1981).

We have recently challenged this classical view and argued that both the IV and IMV possess two distinct, but tightly-apposed membranes, a consequence of their being derived from a specialized domain of the ER, the intermediate compartment (Sodeik et al., 1993; Krijnse-Locker et al., 1994). Although the presence of two tightly apposed membranes in the IV is difficult to show without using protease treatment, two distinct membrane profiles are visible in EM sections of the IMV using both thawed cryosections of fixed cells and epoxy resin sections (Dales and Pogo, 1981; Sodeik et al., 1993). This poses a dilemma (see below).

Whereas the IMV is not found in appreciable amounts in the extracellular medium of infected cells (except, presumably upon cell death), the extracellular enveloped virus (EEV) is actively released from the cell (Appleyard et al., 1971; Payne and Norrby, 1978; Payne 1978). In the process of EEV assembly, the IMV acquires two additional membranes derived from the trans Golgi network (TGN) cisternae forming an intracellular enveloped virus (IEV) that possesses four distinct membrane profiles in thin sections (Hiller and Weber, 1985; Schmelz et al., 1994). This second, cisternal envelopment of the IMV is critically dependent on at least two membrane or membrane-associated proteins; i.) a 14 kD protein on the surface of the IMV (Rodriguez and Esteban, 1987; Rodriguez and Smith, 1990; Sodeik et al., 1995) and, ii.) a 37 kD palmitylated protein in the cisterna derived from the TGN , which behaves as an integral membrane protein (Hiller and Weber, 1985; Schmutz et al., 1991, 1995) (Table 1). Two other integral membrane proteins of the wrapping cisterna, p21 and p42-50 are seemingly also essential for the formation of the four-membraned IEV (Duncan and Smith, 1992).

According to the available data, the IEV fuses with the plasma membrane, releasing the three-membraned EEV into the extracellular medium (Payne and Kristenson 1979; Hiller et al., 1981; Schmelz et al., 1994). The movement of the IEV through the cell in order to reach the plasma membrane is caused by the formation of filamentous actin tails behind the virus particles. These actin tails closely resemble the structures first described for Shigella bacteria (Clerc and Sansonetti, 1987). On reaching the plasma membrane, the virus particles project outward from the cell at the tip of virally-induced actin microvilli (Cudmore et al., 1995). Following exocytic

fusion the released EEV particles expose the lumenal domains of the EEV-specific spanning membrane glycoproteins. It is not yet clear whether any part of the 37 kD protein is also exposed on the EEV surface, but it is predicted (and recently shown; Schmutz et al., 1995) that the major part of this protein would be cytoplasmically disposed, both on the plasma membrane (after IEV fusion) and in the space between the EEV outer and inner membranes. Since both infectious forms of vaccinia, the IMV and the EEV (that has one additional membrane relative to the IMV) are both thought to enter the cell by fusing with the plasma membrane of the host cell (Doms et al., 1990), one has to assume that two different mechanisms of viral disassembly are employed. When the IMV infects cells it appears to release the viral core into the cytoplasm (Dales, 1963) where the early transcription machinery present in the viral core is activated. This event can be reconstituted in vitro (Kates and McAuslan, 1967). However, if the EEV fuses with the plasma membrane during infection it will seemingly put an intact IMV particle into the cytoplasm. The question therefore arises, how can an IMV particle previously assembled in the cytoplasm of an infected cell be disassembled in the cytoplasm of the cell it infects?

The novel technique developed during this study was to combine cryoelectron microscopy with a colloidal gold based immunolabelling procedure which was then used to investigate the structure of purified fractions of both the IMV and EEV. For the IMV a preliminary cryoelectron microscopic study has already been described (Dubochet et al., 1994). Two significant findings were reported in the latter publication; i.) the images of the IMV confirmed earlier data based on chemically-fixed material and showed two membrane-like domains that were separated by a layer of spike-like structures and, ii.) upon treatment of the IMV with NP40 and dithiothreitol (DTT), a treatment extensively used to prepare biochemical amounts of viral cores (Easterbrook, 1966; Holowczak and Joklik, 1967), the ensuing particles were covered by an array of spike-like projections morphologically similar to structures first described in conventional Epon sections in both the IV and IMV by Dales and Siminovitch (1961) and Dales (1963). Beneath this palisade of "spikes", an electron dense layer is seen.

Two different models can be envisaged to account for the observed features (Fig. 1). First, the two bilayers of the IMV seen in both conventional EPON sections and by cryo EM are the result of a separation of the two tightly apposed IV membranes (Fig. 2, model B). In this case the inner of these two membranes will constitute the core "membrane". Alternatively, the outer "membrane" of the IMV is , as in the IV, composed of two tightly apposed membranes (Fig. 2, model A). In that case the distinct core "membrane" must be additionally accounted for. One of our major goals at the outset of this study was to distinguish between these two models. Cryoelectron microscopy of thin films of vitrified suspensions is by far the most suitable method for observing delicate biological particles for high resolution electron microscopy (Dubochet et al., 1988). In most cases it helps to overcome the usual preparation artefacts due to

UNIVERSITY COLLEGE CORK Library

chemical fixation, staining and dehydration. In this method a drop of suspension is applied directly to a grid or a grid coated with a perforated carbon film. It was found recently that particles suspended in the solution tend to adsorb to, and concentrate at, the air-liquid interface in the holes of the grid (Johnson and Gregory, 1993). Most of the drop of suspension can be replaced by other buffers without loss of the particles adsorbed at the surface (Cyrklaff et al., 1994). These adsorption properties allow one to perform chemical treatments, staining and/or immunolabelling of the adsorbed particles under extremely mild conditions. Finally most of the drop is removed with a blotting paper and the residual thin layer containing the treated particles can be vitrified and observed in the cryoelectron microscope.

In the present study we have taken advantage of this observation in order to combine chemical treatment, uranyl acetate staining and immunogold labelling, employing a spectrum of antibodies, with cryoelectron microscopy using different forms of vaccinia virus. Using this approach we show that treatment of purified IMV with the reducing agent DTT disrupts the IMV in a reproducible fashion; it appears to loosen the interactions between the two outer membranes and thereby facilitates a peeling off of the cisterna. In this process a 39 kD core surface protein (Table 1) that is inaccessible to its antibody in intact IMV, becomes exposed. By use of structural disruption of the EEV, we could also confirm that this viral form contains one additional membrane (relative to the IMV) in which the spanning membrane protein, p42, (Table 1) is exposed on the outside. A second integral membrane protein, p37, (Table 1) is cytoplasmically buried in the space between the surface of the IMV and the EEV membrane. Collectively, our data suggest that, if the EEV fuses with a cell and releases an intact IMV into the cytoplasm, the presence of a reducing environment may be sufficient to induce an uncoating of the IMV into the transcription-competent core stage.

RESULTS

Our rationale in this study was to gain insights into the way vaccinia IMV and EEV are assembled. In order to achieve this we used a controlled process of disassembly of the viral particles and an electron microscopical preparation procedure in which the resulting viral structures are best preserved. Clearly, the best method which satisfied these requirements was the "fully-hydrated" method for cryoelectron microscopy (Dubochet et al., 1988). However, unlike most (periodic) viruses that have been studied by cryo EM (e.g. Stewart at al., 1991) both forms of vaccinia are relatively large. The roughly brick-shaped particles have approximate dimensions of 350 x 250 x 150 nm and are thus, perhaps, at the limit for this method. Since both infectious forms show at least two membrane profiles, it was clear that for interpreting the images the use of antibodies against proteins known to be localised to specific parts of the virus would be needed.

Whereas, for small viral particles, any bound IgG molecules, or even individual Fab fragments can be resolved without additional markers, for a large particle such as vaccinia an electron dense marker was essential. For this purpose, 5 and 10 nm gold particles conjugated to protein A were used for most experiments. We first visualized, either (unlabelled) intact IMV or viral cores (operationally defined), prepared using NP40 plus DTT, by cryo EM. Treatment of IMV particles with NP40 and a reducing agent such as DTT is a classical procedure for preparing vaccinia core particles (Joklik, 1964; Easterbrook, 1966) that are transcription-active in vitro (Kates and McAuslan, 1967). For both types of particles (IMV and cores) the images obtained (Fig. 1A, B and C) are similar to those observed by Dubochet at al. (1994) with the IMV displaying two electron dense layers that are presumably membranes. The space between these layers contains the ≈ 20 nm spike-like projections. When the cores were visualized, these spikes were visible as projections on their surface (Fig. 1B, C). In addition, we observed an additional set of spike-like protrusions of an average length of about 8 nm on the surface of the IMV (Fig. 5A). The molecular identity of these structures is unclear at present.

For immunogold labelling we first used two antibodies that recognise proteins on the surface of the IMV, namely the peripheral membrane protein p14 and the integral membrane protein p32 (Table 1). For labelling the surface of the viral core we used an antibody against p39 (Table 1) a protein first described by Rodriguez et al. (1987) and which we have characterized in more detail (Cudmore et al., manuscript in preparation). In the latter study labelling of viral particles followed by negative staining shows clearly that a-p39 does not label the intact IMV but strongly labels the surface of the (NP40 plus DTT-treated) viral cores. Antibodies against this protein also label the surface of the isolated natural cores that appear in the cytoplasm during the viral

infection process (Snijder et al. in preparation). These observations are confirmed in the present study (see below).

Treatment of IMV with DTT

The two membranes in the immature virus IV are so tightly apposed that they appear as a single membrane in most thin section images (see Sodeik et al., 1993; Dales and Pogo, 1981). However, in the IMV two distinct layers are evident in both thawed cryosections of aldehyde-fixed cells and by cryo EM of intact IMV virus. (Fig. 2A; Sodeik et al., 1993; Dubochet et al., 1994; see also Dales and Pogo, 1981). Prominent spike-like structures are especially visible in the space between these two layers in vitrified IMV preparations (Dubochet et al., 1994; Fig. 2B). The question therefore arises whether the two tightly apposed membranes seen in the IV separate in the IMV. In this case, the spike-like projections would be lumenal structures that perhaps cross-link the two membranes of the cisterna (Fig. 2, model B). Alternatively, the IMV has an outer layer that, as in the IV, is actually composed of two tightly-apposed membranes and it possesses an additional electron dense layer close to the viral DNA. If this is the case, the spikes must be cytoplasmically-disposed structures, that might cross-link the inner, cytoplasmic surface of the cisterna with the surface of the core outer layer (Fig. 2, model A).

To try to resolve this issue we looked for treatments that would disrupt the organization of the different layers, without destroying membrane structure. Inspired by the work of Easterbrook (1966) we found that the most striking effect was obtained using DTT, a treatment we expected to disrupt anz disulfide bonds in the virus. The same effects were also seen with 2-b-mercaptoethanol (results not shown). As shown in Fig. 3 incubation of IMV on the EM grid with 20 mM DTT for short periods (5-30 min) resulted in a statistically significant swelling of the IMV (untreated average (n=25): length 338 nm ± 13 nm (S.D.), width 267 nm ±18 nm (S.D.); treated average of the non-disrupted particles (n=25): length 356 nm ± 15 nm (S.D.), width 289 nm ± 15 nm (S.D.). Under this condition the IMV surface antigens p14 (not shown) and p32 (Fig. 4) remained fully exposed, with essentially no labelling seen with the antibodies against either p39, or with a control, irrelevant antibody. However, with increasing times of treatment a higher percentage of particles became disrupted and the particles labelled for p39 (see below). Representative images of this disruption process are shown in Fig. 3.

The disruption of the IMV with DTT was also visualized by a number of novel modifications of the bare-grid method. First, the virus could be chemically cross-linked using brief exposures (seconds to minutes) to low concentrations of aldehydes (not shown). This approach became more important for the studies with the EEV (see below). Second, the viruses, either with or without DTT treatment, could be exposed for a few seconds to low concentrations of uranyl acetate, which was subsequently replaced by pure water prior to freezing (positive staining; Fig.

3 F-I, Fig. 4). This treatment showed that whereas intact IMV were refractory to the stain, the stain clearly entered the particles that had been affected by DTT. Figure 3 shows different images of the DTT-induced disruption, a process which ultimately exposes the viral core, and thus may resemble the natural uncoating process that occurs during infection. In addition to the swelling with DTT we also noted a separation of the outer membrane(s). This separation process often appeared to be initiated at the corner of the particle (Fig. 3A, 3F). In Fig. 3G the two membrane profiles of the outer cisterna are evident (see also Fig. 3E), while Fig. 3F, 3G and 3I suggest that DTT induces a peeling off of this outer cisterna. In some cases this outer cisterna forms long, 20 nm diameter tubules resembling the so-called "surface tubular elements" first described by Stern and Dales (1976). In all cases where disruption occurred the surface of the core became exposed, as evident by the core spike elements (Fig. 3 panels A, C, D, E, F, H, I). Occasionally, the cores themselves also appear to become disrupted by DTT (Fig. 3I).

In order to examine this DTT-induced uncoating process in more detail we next analysed the pattern of labelling for the IMV surface antigens p14 and p32 and the core surface protein p39 (see Table 1) on such disrupted particles. A summary of the key findings is as follows: p39 was localized exclusively to the exposed core, identified by the presence of the 20 nm spike-like projections on their surface (Fig. 5, panels E-F). In contrast, antibodies against the surface membrane proteins p14 and p32 labelled only the outer membrane of the IMV (Fig. 5, panels A-D). Following disruption of the outer cisterna, the labelling for p14 and p32 was restricted to the membrane fragments that were attached to the cores devoid of labelling. The labelling density seen on such membrane fragments was similar to that seen on the surface of intact IMV.

In the next series of experiments we asked whether the approach introduced here for single immuno-labelling could also be applied for a double labelling procedure. For this the IMV was first labelled with antibodies against one of the surface membrane proteins p14 or p32 (Table 1) followed by protein A-gold. The IMV was then treated with DTT, briefly fixed (less than 1 min) with glutaraldehyde (Slot et al., 1991) and then labelled with an antibody against another vaccinia protein, or with control antibodies, followed by a different size protein A-gold complex. As shown in Fig. 4 this double labelling procedure facilitated a visualization of the disruption of the IMV by DTT. Whereas the outer membranes labelled for p14 and p32, the core, which became exposed following disruption, could be specifically labelled only with a-p39 (Fig. 4C). The findings that DTT treatment leads to the exposure of epitopes on a core surface protein argues strongly for model A rather than B in Fig 1.

Protease treatment of IMV

The above experiments with DTT suggested that the outer membrane of the IMV might not form a completely uniform cover around the IMV, that is, that the outer cisterna that enwraps the

viral core may not have fused with itself (Fig. 1, model Ai). We therefore asked whether this cisterna could be sealed by a proteinaceous structure such as a 'pore' or 'focal contact' (Fig. 1, model Aii or iii). If so, such a structure might be accessible to protease treatment. In extensive (unpublished) studies with proteases we had noticed that different IMV preparations behaved very irreproducibly towards proteases. In many experiments relatively high concentration of proteases digested IMV surface protein (such as p14) without affecting core proteins such as p4a or p39; in others, however , core proteins became digested within (2 hrs of treatment.

We therefore carried out a systematic study using two proteases, proteinase K (4°C) and trypsin (37°C) and assayed their effects both by biochemical analysis and by negative staining EM (Fig. 6). We emphasize that the goal of the latter approach in this study was simply to evaluate whether or not stain entered the particle, not to provide any structural details. Whereas the majority of intact IMV particles exclude stains such as uranyl acetate this stain can enter particles that have been disrupted, for example, with DTT, as mentioned.

IMV were treated with 100 or 200 (g/ml of either proteinase K at 4(C or trypsin at 37(C for either 1 or 2 hrs. In this experiment, treatment with 200 (g/ml proteinase K (4(C) for 2 hrs, a concentration which completely digested the surface protein p14 after 30 min, failed to significantly digest the core proteins (not shown). Similarly, by negative staining there was little difference in the staining appearance between untreated particles and those treated with 200 (g/ml proteinase K for 2 hrs (Table 2). In the case of trypsin at 37°C all treatments completely removed the surface protein p14 (Fig. 7). In contrast, at least 2 hrs was needed to show visible signs of degradation of the core proteins p39 and p4a. By 4 hrs these proteins were essentially completely digested (Fig. 7). These results were again complemented by the EM negative staining approach (Table 2). The images from this experiment also showed a significant fraction of particles that were obviously disrupted after 2 hrs although many apparently intact particles that either excluded or included stain were also seen (Fig 6). In some experiments 100-200 (g/ml proteinase K for 2 hrs at 4°C also led to an opening of the majority of the particles as seen by an immunoblotting analysis of p39 and p4a (not shown). Collectively, these data argued that whereas the IMV has an inherently high resistance to proteases, at a certain threshold of activity the particle opens. The simplest interpretation of these data is that the outer cisterna of the IMV is sealed by a proteinaceous structure although other interpretations cannot be ruled out. We stress that we have not yet seen any convincing evidence of any potential pore or other notable local structures on the IMV surface by cryo EM.

Extracellular Enveloped Virus (EEV)

The extracellular form of the IHD-J strain of vaccinia was purified from the medium of (the relatively high EEV yielding) rabbit RK13 cells and examined by cryo EM. In agreement with

the current ideas on this viral form, these particles appeared to have one additional membrane bilayer that was clearly resolved (Fig. 8A). However, in only few EEV particles did this membrane uniformly and tightly surround the particle and even in this case the interaction between the outer membrane and the underlying IMV was rather loose. In most cases the membrane appeared to have little contact with the IMV and was often disrupted (Figs. 8A; see also Payne and Kristenson, 1979). A brief fixation (seconds) of the EEV adsorbed to the grid with 0.5% glutaraldehyde increased the fraction of intact EEV particles considerably. When the outer membrane was completely removed the surface of some of the underlying IMVs was much rougher in texture (Fig. 8B) than the surface of purified IMV (Fig. 1A). This surface appearance of the IMV resembled the structures described earlier as surface tubular elements by Stern and Dales (1978). The significance of these structures remains to be established.

Because of this tendency for the EEV to disrupt we decided to investigate the topology of some key membrane proteins using the immunogold method in the absence of any treatment. In any one preparation one could clearly identify both intact and disrupted particles. In these experiments the structure of underlying IMV was rarely affected (except for the sometimes rougher surface texture, as mentioned).

Immunolabelling of EEV

For the EEV we selected two antibodies which pilot experiments revealed to be especially interesting. The first was p42 (Table 1) (Englestadt et al., 1992; Isaacs et al., 1992; Wolffe et al., 1993). This protein is enriched in TGN-derived membranes that wrap around the IMV to form the IEV, the precursor of the EEV (see Fig. 9). According to current ideas the IEV fuses with the plasma membrane, thereby releasing the EEV (Payne , 1980; Schmelz et al., 1994). As a result lumenal epitopes that are buried within the wrapping cisterna become exposed on the surface of the EEV (see Fig. 9).

The bulk of p42, like the haemagglutinin (Shida 1986; Schmelz et al., 1994) should be exposed on the outside of the EEV with the predicted small cytoplasmic domains of these proteins lying directly above the IMV. As expected from this model, a monoclonal antibody against p42 labelled the outside of the outer membrane of the EEV (Fig. 8D). In those cases where the membrane was disrupted, the newly exposed surface was clearly devoid of labelling (not shown). However, this newly exposed surface, as expected, labelled strongly for the IMV surface protein p14 (Fig. 8C). The second interesting protein we examined in the EEV was p37 (Table 1) (Payne, 1978; Hiller and Weber, 1985; Hirt et al., 1986) that is essential for IEV/EEV formation (Blasco and Moss, 1991). The available biochemical data argue that this protein, which has covalently bound palmitate, is an integral membrane protein, although it has not been established whether the protein is inserted into the rough ER or, as favoured by Hiller and Weber

(1985) based on immunofluorescence microscopy analysis, whether it somehow inserts directly into Golgi membranes by a post-translational mechanism.

Labelling of thawed cryo sections of vaccinia infected cells shows that Golgi/TGN as well as the wrapping membranes and the EEV are enriched for p37 (Schmelz et al., 1994). The data obtained using a combination of immunogold labelling for p37 followed by cryo EM argue that, in the EEV this protein is localized to the space between the outer membrane and the surface of the IMV. Thus, the a- p37 had no access to its antigen in intact EEV (in contrast to the a- p42) but following disruption/vesiculation and resealing of the outer membrane there was strong labelling of now exposed cytoplasmic side of the membrane (Fig. 8E). These data are summarized schematically in Fig. 9).

DISCUSSION

In the present paper we have studied the structure of vaccinia virus by cryo EM, and in particular taken advantage of a recent finding by Cyrklaff et al. (1994). This shows that particles floating at the water-air interphase on a holey EM grid will remain there for the time needed to replace all the solutions simply by gentle changes of the underlying solvent. Here, we adapted this technique for combining the advantages of immunogold labelling with the high resolution structural preservation that is routinely obtainable using cryo EM (Dubochet et al., 1988).

Using this novel approach we investigated both the structure and the topology of some key proteins in both the IMV and EEV forms of the poxvirus vaccinia, which probably represents the most complex form of all viruses. For the IMV our work extends the preliminary findings of Dubochet et al. (1994) who first described the appearance of the IMV by cryo EM. The images in the latter reference supported the notion that the IMV has two membrane-like 'layers'. Further, they confirmed earlier data from negative staining EM that there are prominent, spike-like projections visible in IMV in images of conventional thin sections, as well as in vitrified preparations, which appear to be on the surface of virus treated with NP40 plus DTT, the chemically prepared viral 'core'. The latter view is supported by our data in this study which also show a correlation between the presence of the spikes on the core surface, that is exposed by DTT treatment, with a strong surface labelling for p39. Both the presence of spikes as morphological entities, as well as labelling of their surface with α- p39 is also evident on the natural viral cores isolated during the infection process (Snijder et al. in preparation). The strong labelling for p39 on the surface of the NP40/DTT-prepared cores, on the core surface exposed after DTT alone, as well as on the 'natural' cores, argues that the same surface becomes exposed in all three conditions.

The model which emerges from the present study, in conjunction with our earlier data (Sodeik et al., 1993), is shown in Fig. 2A. This model argues that the tightly apposed cisterna which incompletely surrounds the spherical IV overlays the major spike-like projections that protrude from the surface of the viral core. This scheme is the simplest way to explain how DTT leads to the exposure of epitopes for p39, which is a cytosolic protein, on the surface of the core. We presume that DTT, a potent reducing agent, disrupts intra-lumenal disulfide bounds that stabilize the membrane-membrane interactions of the cisterna. According to current dogma, disulfide bonds can only form in the oxidising environment of the endoplasmic reticulum and not in the highly reducing environment of the cytosol (Hwang et al. 1992, Doms et al. 1993). The images of the DTT-induced disruption process lead us to suggest that the IMV outer cisterna does not fuse with itself but is rather interrupted in some way.

The notion that the outer cisterna of the IMV is not fused together (as in Fig 2Ai) was also supported by the experiments with proteases showing that, whereas the IMV particles resisted relatively high concentration of protease for relatively long periods, above a certain threshold of protease activity viral core proteins became almost completely accessible to digestion. We tentatively propose therefore that the IMV outer cisterna is 'glued' together by a (relatively protease-resistant) proteinaceous structure. Since we have failed to see convincing evidence of any 'pore' structure (Fig 2Aii) by cryo EM we speculate that the ends of the cisterna may be sealed by a protein 'plug' or 'focal contact' that tightly glues the end of the cisterna with the rest of the (same) cisterna (Fig 1Aiii).

The second important question raised by this study is the nature of the membrane-like electron-dense layer that is clearly seen beneath the spike layer of the cores, both in vitrified specimens (Dubochet et al., 1994; this study) and in thawed cryosections of IMV (Sodeik et al., 1993). We intend to address this question, is it a membrane, by analysing the biochemical composition of cores produced during the infection process. As shown in this study an obvious candidate protein that may at least compose part of the core surface spikes is p39.

The ability of reducing agents to simulate an uncoating process may be of physiological significance. The available data on the infection process for both IMV and EEV, while not definitive, have been interpreted as evidence for a fusion process in both cases (Granados 1973, Armstrong et al., 1973; Chang et al., 1978; Payne and Norrby, 1978; Doms et al., 1990). If the EEV fuses with the plasma membrane it would release an intact IMV into the cytoplasm. Our data now provide a plausible explanation for how such viruses could begin to disassemble as soon as they are exposed to the reducing environment of the cytosol. Such a view would also agree with the studies of Munyon et al (1967), who showed that, while intact IMV cannot undergo the remarkable in vitro transcription process that is observed with pure cores, treatment of IMV with either DTT or 2-b-ME (in the absence of detergents) also leads to significant increases in the measured in vitro transcription rates.

The novel cryo EM approach also provided interesting data with respect to the EEV. Whenever we have isolated this form and examined it by either negative staining or, following aldehyde fixation by cryo sectioning, we were always surprised at the extreme lability of these particles. Unexpectedly, this lability was also evident in the cryo EM images, even when the virions were taken from the extracellular medium without centrifugation and in the absence of chemical fixation. That aldehyde fixation facilitated the preservation of these particles suggests that at least a part of the disruption we observed occurs during the storage and/or labelling steps. Only a minority of the particles had a complete and intact outer membrane and, even in those cases, this membrane did not appear to interact tightly with the surface of the IMV. The presence of this

loose outer membrane on the physiologically most important infectious form of vaccinia (Payne, 1978) is surprising. In the simplest model one might argue that this outer membrane is simply a transient coat that is lost to expose the IMV prior to infection. However, such a phenomenon would be difficult to reconcile with experiments showing that antibodies against IMV block infection of the IMV but fail to prevent infectivity of EEV particles (Appleyard and Andrews, 1974; Payne, 1980).). This view is also inconsistent with the fact that purified EEV enter cells more rapidly than does the IMV (Payne and Norrby, 1978; Doms et al. 1990). Moreover, there are significant differences in the susceptibility of IMV and EEV to both temperature and metabolic inhibitors (Payne and Norrby, 1978).

A possible solution to the apparent paradox that the most infectious form of vaccinia is surprisingly labile, at least relative to the more robust IMV, comes from older (Stokes 1978, Hiller at al. 1979) and more recent (Cudmore et al., 1995) observations on the mechanism by which the EEV exits from infected cells. These data argue that the IEV, the intracellular precursor of the EEV, is propelled through the cell by an actin-based tail structure (Cudmore et al., 1995) similar to the structure first described for Shigella (Clerc and Sansonetti, 1987) and subsequently for Listeria (Tilney et al., 1989; Theriot, 1994; see Cossart 1995 for a review). The actin tail then somehow propels the IEV to the tip of a newly formed microvillus. One can speculate that the IEV subsequently fuses with the plasma membrane at the tip of the microvillus, releasing the EEV to the outside. Thin section EM images suggest that the EEV remains attached to the plasma membrane for extended periods since they are relatively easy to find in thin sections. The EEV can then fuse with and infect a neighbouring, uninfected cell. In this scenario an important extracellular role of the EEV would be as a transient and perhaps predominantly cell-associated form that facilitates rapid cell to cell transfer. In further agreement with this view is the recent identification of a distinct class of plasma membrane-attached EEV, the CEV (cell associated virus) form (Blasco and Moss 1992).

Our immunolabelling data on the EEV fit clearly into existing models. Thus, the EEV has one extra membrane relative to the IMV and that membrane is enriched in p42 (Englestadt and Smith, 1993; Schmelz et al., 1994), p21 (Duncan and Smith, 1992; Payne, 1992), the haemagglutinin (HA) (Shida, 1986) and a recently identified 43-50 kD membrane protein (Parkinson and Smith, 1994). All these proteins are predominantly exposed on the outer surface of the EEV and, for p42 we show this directly in this study. More significantly, we showed that p37 (Hiller et al. 1981; Hiller and Weber, 1985; Schmelz et al., 1994, Schmutz et al., 1991) is exposed to its antibody on the inner aspect of the outer membrane of the EEV only following disruption, in agreement with the recent biochemical data of Schmutz et al. (1995). This protein has been postulated to interact with a protein(s) on the surface of the IMV. The best candidate for the latter is, as previously proposed by Rodriguez and Smith (1990), p14, which here became

exposed to its antibody only following disruption of the outer membrane of the EEV, as expected if the outer membrane directly covers the surface of the IMV.

We believe that the novel approach of immunogold labelling, in combination with cryo EM of vitrified particles will be a useful approach for any particle in the range of 50 - 500 nm. Since the antibody-gold complex is relatively large (minimum size ≈ 20 nm) we emphasize that this is not a high resolution labelling technique per se. Available methods that could be applied to improve the spatial resolution of the immunolabelling would give only modest, but nevertheless important gains (Griffiths, 1993). However, by combining the immunolabelling with methods to disrupt or digest biological particles in a controlled fashion, we believe this approach can best be used for identifying layers or domains in other complex macromolecular structures such as nuclear pores, centrioles, kinetochores, or perhaps defined fragments of chromosomes, under conditions which avoid most of the artefacts associated with more conventional EM methods.

MATERIALS AND METHODS

Antibodies and protein A-gold: The following antibodies were used. Mouse monoclonal a-p14 (Dallo et al., 1987; Sodeik et al., 1995) provided by Dr. M. Esteban; rabbit α -p39 provided by Dr. M. Esteban; mouse monoclonal α -p42 (Schmelz et al., 1994) provided by Dr. G. Hiller and mouse monoclonal α -p37 (Schmelz et al., 1994); provided by Dr. G. Hiller). Protein A-gold was purchased from Dr. Jan Slot (University of Utrecht, Stichting MEMO, Utrecht, Netherlands).

Cells and viral strains: Preparation of IMV: Hela cells (ATCC CCL2) were grown in Eagle's minimal essential medium (MEM) supplemented with 10% fetal calf serum (heat-inactivated), non-essential amino acids, 2 mM glutamine, 100 U/ml penicillin and 100µg/ml streptomycin. The cells were grown as adherent cultures at 37°C in a 5% CO2 incubator for two days to 80% confluency. For the preparation of purified IMV we used both wild type WR virus and a WR deletion mutant (vRB12), lacking the EEV protein p37 (gene F13L; Blasco and Moss 1992) that fails to produce IEV and EEV. Since this deletion mutant does not readily spread from cell to cell, special care was taken to infect cells at relatively high multiplicity of infection (MOI). The use of this vRB12 mutant ensures that IMV preparations are devoid of EEV particles.

The routine procedure was to infect 4 flasks (175 ml) at a MOI of approximately 3 for 48 hrs, after which the IMV was released by freeze-thawing. This virus preparation was used to infect 6 plates (24 x 24 cm) of 70% confluent Hela cells. This generally led to complete cytopathic effects (CPE) at 48 hrs post-infection. The cells were harvested by scraping and centrifuged for 10' at 1500 rpm. The cells were broken with 12 strokes of a dounce homogenizer and the nuclei removed by centrifugation at 1000 g. The IMV was subsequently purified by pelleting at 24000 rpm through a 36% sucrose cushion (in 10 mM Tris pH 9.0), followed by sedimentation at 15000 rpm for 17 min in a 25-40% sucrose gradient using an SW27 rotor and the subsequent band finally concentrated by pelleting for 30' at 24000 rpm in a SW40 Beckman rotor. (Doms et al., 1990). Such IMV preparations usually contained from 1010-1011 particles/ml. All cell culture material was obtained from Gibco, GIBCO BRL (Gaithersburg, MD).

Preparation of EEV: Most of the virus present in the medium from infected cells 24 hrs post-infection is EEV (Payne and Kristenson, 1979). Since EEV is a very fragile form of vaccinia and has the tendency to loose its outer membrane when exposed to mechanical stress we tried to avoid any unnecessary manipulation. For many, but not all experiments, we took the EEV directly from the medium of IHD-J infected RK13 cells 48 hrs after infection without further purification (Payne 1979). In order to increase the number of viral particles, we reduced the

amount of medium to a minimum. Confluent monolayers in 25 cm2 flasks were infected with IHD-J and incubated in 2 ml of MEM containing 2.5% foetal calf serum. Sometimes the medium was clarified by low speed centrifugation and the amount of free virions in the medium estimated by negative staining.

Partial disruption of virus particles: For this, the particle suspension was applied to a perforated carbon grid, allowed to adsorb for 3-10 min depending on particle concentration. The grid was than washed briefly in 10 mM Tris pH 9.0 and incubated on 20 mM DTT in 10 mM Tris pH 9 at 370C or room temperature for 5-30 min in a humid chamber. The grids were subsequently rinsed with 10 mM Tris buffer (pH 9) and either frozen immediately or used for further labelling experiments as described below.

Protease digestion studies: Sucrose gradient purified IMV was mixed with an equal volume of 200 or 400 µg/ml trypsin, in 10 mM Tris, pH 9, containing 20 mM CaCl2. Alternatively 200 or 400 µg/ml protease K on ice was used. Final concentrations of proteases used were 100 or 200 µg/ml. Incubation at 37°C was continued for 30, 60, 120 or 240 min. Subsequently, digestion was blocked for 10 min on ice using 1 µl of aprotinin stock solution (4 mg/ml) and 1 µl of bovine trypsin inhibitor (20 mg/ml) (Sigma) in the case of trypsin or 2 mM PMSF (Sigma) for the protease K. The samples were snap frozen in liquid nitrogen and stored at -20°C before analysis using 15% SDS-Page. Samples were rapidly thawed by incubation at 95°C with Laemli sample buffer, the gels run and the proteins transferred to nitrocellulose and blotted for p39 p14 and 4a (a gift from Dr D Hruby - see vanSlyke et al., 1991), as described (Ericsson et al., 1995)

For negative staining aliquots of the virus plus protease were adsorbed to glow-discharged, carbon-coated grids, rinsed briefly with distilled water and negatively stained with 2% uranyl acetate.

Labelling of virus particles: Labelling experiments were performed as follows: after the 3-5 ml drop of particle suspension had been left for a given time on the grid (the side coated with the perforated carbon film), the grid was washed on 1 ml droplets of Hepes buffer (100 mM pH 7.4) four times for 2 sec and once for 2 min. The grid was subsequently placed on a small droplet (5-10 ml) of antibody solution for 15-30 min followed by a further washing step with buffer (4 x 2 sec and 1 x 2 min). The grid was then subjected to a protein A-gold solution for 15 min, washed (4 x 2 sec and then 2 x 2 min). In the case where antibodies which do not bind to protein A (i.e. mouse primary antibodies) were used, the grid was incubated on a secondary antibody solution, prior to another washing step before it was exposed to the protein A-gold solution. For double labelling we followed the general regime used for labelling of cryosections

with somewhat reduced incubation times. Blotting and vitrification took place as described below (Slot et al., 1991). In the few cases where we tested the use of fixatives the grids were either placed briefly (sec-min) on drops of formaldehyde solution (4% in HEPES 100 mM, pH 7.4) or glutaraldehyde solution (0.5% in HEPES 100 mM, pH 7.4).

Specimen preparation for cryoelectron microscopy: The thin film vitrification method is described in detail elsewhere (Dubochet et al., 1988; Roos & Morgan, 1990). A 3-5 ml droplet of suspension was put on a grid supporting a perforated carbon film with hole diameters between 2 and 5 mm. The drop was left on the grid for 1-3 min in the case of IMV and up to 10 min in the case of EEV. Blotting paper (Whatmann nr. 1) was then firmly applied to one side of the grid for about 1 sec. The plunger holding the grid was immediately released and, within about 0.1 sec, the grid was plunged into a liquid ethane slush cooled with liquid nitrogen, thus vitrifying the thin liquid film.

Cryo-electron microscopy: The vitrified samples were either stored in liquid nitrogen or observed immediately. Transfer and observations were made with a side entry, cryo-transfer holders (Gatan 626 (Gatan, Varrendale, Pa) and Oxford Instruments, CT-3500(Oxford Instruments, Oxford, UK) in a specially adapted cryo-electron microscope the Jeol-2000EX (JEOL, Tokyo, Japan, equipped with a Gatan TV camera, model 622-0600 with an image intensifier). The microscope has an efficient blade-type anti-contaminator. Observations were made under minimum irradiation conditions at magnifications ranging from X 3000 to 40000 and at 3.5-10.5 mm under focus. Micrographs were recorded on Kodak SO-163 electron microscopy film and developed in full strength D-19 developer for 12 min (speed: ca. 2.2 μm2/electron x OD unit). Magnification was calibrated with a cross-grating replica, with an estimated error of 2%.

ACKNOWLEDGEMENTS

We would like to thank the following for their generous gift of antibodies: Dr. M. Esteban for providing the α-p14 and α-p39, Dr. E. Niles for the α-p32, Dr. G. Hiller for the α -p42 and α -p37 and Dr. D. Hruby for the α-4a. We are also grateful to Dr. K. Simons for his critical comments on the manuscript.

TABLES

Table 1

Virus	Protein	Gene	Location
IMV	p14	A27L	outer surface of IMV cisterna
	p32	D8L	outer surface of IMV cisterna
	p39	A4L	surface of the core
EEV	p37	F13L	inner surface of the outer membrane of EEV
	p42	B5R	surface of the EEV

Table 2

Effect of proteases on IMV as seen by negative staining

	% of total*		
	INTACT	'OPEN'	DISRUPTED
Control	89	6	6
Proteinase K:			
100 μg - 1 hr	88	9	3
200 μg - 1 hr	85	10	5
100 μg - 2 hr	89	1	10
200 μg - 2 hr	83	2	15
Trypsin:			
100 μg - 1 hr	92	4	4
200 μg - 1 hr	75	6	19
100 μg - 2 hr	71	25	4
200 μg - 2 hr	8	27	65

* For each value a total of 200 particles were counted. Examples of intact particles as well as particles that appear intact but 'open' to stain are shown in Fig. 6A. Disrupted particles were defined as particles with gross morphological alterations (see Fig. 6B).

FIGURE LEGENDS

FIG. 1. Vitrified IMV particles: (A) untreated IMV particles, (B) and (C) isolated cores after NP-40 / DTT treatment. The large arrows show the outer membrane of the IMV, while the large arrowhead indicates the core outer layer. The small arrow points to the IMV surface spike projections, while the more prominent 20 nm spike on the surface of the core is indicated by small arrowheads. The asterisk depicts one of the very few partially disrupted IMVs found. We believe the extraneous material surrounding the cores in B and C represents remnants of the outer cisterna which are not extracted by the detergent.
(bar = 100 nm)

FIG. 2. Models of IMV formation and location of key proteins in relation to the enwrapping membranes of the intermediate compartment (IC) that we propose to be directly continuous with the rough endoplasmic reticulum (RER). The upper part of this model is based on our previous study (Sodeik et al., 1993); see Griffiths and Rottier, 1993 for review) and argues that the IV is a highly-apposed cisterna derived from the IC. In model A the key point is that the IV cisterna remains tightly apposed to and overlies the spikes which are on the surface of the core. A second set of (8 nm) surface spikes is evident on the surface of the IMV. In model B the spikes are shown as lumenal structures. In both models DTT is envisaged as having its effect by reducing intra-lumenal S-S bonds and thereby affecting intra-lumenal protein-protein interactions. In model A the composition of the core "membrane" is left open, while in B it represents the inner membrane of the IV-derived cisterna after a process of separation. The results in this study argue strongly against model B. Nevertheless, the precise structure of the outer surface remains to be solved. Based on both the structural data and the accessibility of core proteins to proteases, we suggest that the cisterna is not fused with itself (Ai) but may be glued together by a proteinaceous plug. The absence of any structural data for a 'pore' (Aii) makes us favour the view that the putative proteinaceous structure may be covered by an overlap in the cisterna (Aiii).

FIG. 3. Effect of 20 mM DTT at 370C for 10 min (panels (B), (C), (F) and (G)) or 30 min (panels (A), (D), (E), (H) and (I) on intact IMV. Panels (A)-(E) show unstained cryo EM preparations, while (F)-(I) are preparations stained for a few seconds with 0.3% uranyl acetate. The initial effects of DTT include swelling of the outer cisterna (B, D, G). Subsequently the particle appears to uncoat (A, C, D, E, F, H, I) exposing the major core spike (small arrowheads). In panels (G) and (E) the small arrows reveal the two membranes of the outer cisterna. In (F) the large arrowheads indicate the ends of the cisternae that appear to be peeling off the core surface. The tubule seen in (D) (arrow) is probably an artefact of the DTT induced

uncoating process that resembles the surface tubular elements seen in classical negative stain images.(bar = 100 nm)

FIG. 4 (A) and (B) show IMV particles treated with DTT (20 mM for 10 min) and labelled for p32. In (A) the particles are swollen while in (B) disruption is evident. The preparation in (B) and (C) is stained with 0.3% uranyl acetate. The arrowheads indicate the ends of the outer cisterna. (C) shows a double labelling experiment. The intact IMV was first labelled with p32 followed by 5 nm proteinA-gold. The particles were subsequently treated with 20 mM DTT for 10 min and labelled for p39 followed by 10 nm proteinA-gold. The image selected shows two intact particles (left) adjacent to a released core (asterisk). Whereas the intact IMV labels strongly for p32 the core labels strongly for p39.

FIG. 5. (A) shows undisrupted IMV particles labelled with α-p14. (B) (C) and (D) depict IMV particles exposed to DTT (20 mM for 30 min at 370C) prior to immuno-labelling with a-P14 while (E) and (F) show labelling for p39. These data show that α-p14 labels the outer membrane of IMV but not the exposed core, whereas a-p39 labels the core but not the outer membrane. (bar = 100 nm)

FIG. 6. Negative staining of vaccinia virus IMV. A shows a control virus preparation with two intact (I) particles that exclude stain and one open (O) but structurally intact particle that stain has entered. B is from a preparation treated in suspension with 200 μg/ml trypsin for 2 hrs showing one particle that we classify as normal and intact (I). The remainder either appear disrupted or include stain. The star indicates a side view of a particle into which stain has entered. Bars 100 nm.

FIG. 7. Protease treatment of purified IMV. The virus was treated for different times with two concentrations of trypsin at 370C. Immunoblots are shown for the core proteins, p39, 4a and the IMV surface protein, p14. While the outer surface protein p14 is completely digested at the earliest time points, p39 and 4a resist significant degradation until 2 hrs. After 4 hrs both proteins are essentially completely digested.

FIG. 8. Cryo EM of EEV. The EEV has one additional membrane relative to the IMV (Fig. 2A). The outer membrane (small arrowheads) is extremely fragile in isolated preparations.(A) untreated EEV; this preparation was taken directly from the extracellular medium of infected RK13 cells without centrifugation and vitrified. The asterisk depicts one of relatively few particles where the outer membrane remained intact. Very often they appear as shown in (B). In this example the outer membrane has been removed exposing the outer surface of the IMV. We have no explanation for the ruffled appearance of these particles which contrasts with the smooth

appearance of isolated IMVs (see Fig. 2A) but note the resemblance to the so-called surface tubular elements seen in classical negative stain preparations of IMV. In (C) the preparation was labelled with α-p14. Whereas this protein is not exposed in undisrupted particles, following disruption (in this case partial disruption) the epitopes for p14 are exposed and accessible for labelling. (D) shows particles that have been immuno-labelled with a-p42 showing the strong surface labelling on the outside of the EEV. (E) Whereas intact EEV does not label with a-p37, disrupted particles expose the cytoplasmic aspect of the outer membrane and become labelled. (bar = 100 nm)

FIG. 9. Model to show the membrane topology in the IEV and EEV. The IMV acquires two additional membranes from the TGN to form the IEV. The outer membranes of the IEV is lost upon fusion with the cell membrane and the EEV released into the extracellular medium. The bulk of p42 and HA are in the lumen of the IEV and become exposed on the surface of the EEV. In contrast p37 is cytoplasmically disposed and is not exposed on the surface of the EEV unless the particles are disrupted. p14, which covers the surface of the underlying IMV, may interact with p37 although, until now, no evidence for such an interaction has existed.

REFERENCES

Appleyard,G., Hapel,A.J. and Boulter,E.A. (1971) J. Gen. Virol., 13, 9-17.

Armstrong,J.A., Metz,D.H. and Young,M.R. (1973) J. Gen. Virol., 21, 533-537.

Blasco,R. and Moss,B. (1991) J. Virol., 65, 5910-5920.

Blasco,R. and Moss,B. (1992) J. Virol., 66, 4170-4179.

Chang,A. and Metz,D.H. (1976) J. Gen. Virol., 32, 275-282.

Clerc,P. and Sansonetti,P.J. (1987) Immun., 55, 2681-2688.

Cossart,P. (1995) Curr. Opin. Cell Biol., 7, 94-101.

Cudmore,S., Cossart,P., Griffiths,G. and Way,M. (1995) Nature...

Cyrklaff,M., Adrian,M. and Dubochet,J. (1990) J. Electron. Microsc. Tech., 16, 351-355.

Cyrklaff,M., Roos,N., Gross,H. and Dubochet,J. (1994) J. Microsc., 175, 135-142.

Dales,S. (1963) J. Cell Biol., 18, 51-72.

Dales,S. and Siminovitch,L. (1961) J. Biophys. Biochem. Cytol., 10, 475-503.

Dales,S. and Mosbach,E.H. (1968) Virology, 35, 564-583.

Dales,S. and Pogo,B.G.T. (1981) Virology monographs. Springer Verlag, Vienna.

Dallo,S., Rodriguez,J.F. and Esteban,M. (1987) Virology, 159, 423-432.

Doms,R.W., Blumenthal,R. and Moss,B. (1990) J. Virol., 64, 4884-4892.

Doms,R.W., Lamb,R.A., Rose,J.K. and Helenius,A. (1993) Virology, 193, 545-562.

Dubochet,J., Adrian,M., Chang,J.-J., Homo,J.-C., Lepault,J., McDowall,A.W. and Schultz,P. (1988) Q. Rev. Biophys., 21, 129-228.

Dubochet,J., Adrian,M., Richter,K., Garces,J. and Wittek,R. (1994) J. Virol., 68, 1935-1941.

Duncan,S.A. and Smith,G.L. (1992) J. Virol., 66, 1610-1621.

Easterbrook,K.B. (1966) J. Ultrastr. Res., 14,484-496.

Englestad,M. and Smith,G.L. (1993) Virology, 194, 627-637.

Englestad,M., Howard,S.T. and Smith,G.L. (1992) Virology, 188, 801-810.

Ericsson,M., Cudmore,S., Shuman,S., Condit,R.C., Griffiths,G. and Krijnse Locker,J. (1995) J. Virol., 69, 7072-7086

Granados,R.R. (1973) Virology, 52, 305-309.

Griffiths,G. and Rottier,P. (1992) Semin. Cell Biol., 3, 367-381.

Griffiths,G. (1993) Fine structure immunocytochemistry. Springer Verlag, Berlin, Heidelberg, New York.

Hiller,G., Weber,K., Schneider,L., Parajsz,C. and Jungwirth,C. (1979) Virology, 98, 142-153.

Hiller,G., Eibl,H. and Weber,K. (1981) J. Virol., 39, 903-913.

Hiller,G. and Weber,K. (1985) J. Virol., 55, 651-659.

Hirt,P. and Hiller,P. (1986) J. Virol., 58, 757-767.

Holowczak,J.A. and Joklik,W.K. (1967) Virology, 33, 717-725.

Hwang,C., Sinskey,A.J. and Lodish,H.F. (1992) Science, 257, 1496-1502.

Isaacs,S.N., Wolffe,E.J., Payne,L.G. and Moss,B. (1992) J. Virol., 66, 7217-7224.

Johnson,R.P.C. and Gregory,D.W. (1993) J. Microsc., 171(2), 125-136.

Joklik,W.K. (1964) J. Mol. Biol., 8, 262-276.

Kates,J.R. and McAuslan,B. (1967) Proc. Natl. Acad. Sci. USA, 57, 314-320.

Krijnse Locker,J., Ericsson,M., Rottier,P.J.M. and Griffiths,G. (1994) J. Cell Biol., 124, 55-70.

Munyon,W., Paoletti,E. and Grace,J.T. Jr. (1967) Proc. Natl. Acad. Sci., 58, 2280-2287.

Parkinson,J.E. and Smith,G.L. (1994) Virology, 204, 376-390.

Payne,L.G. (1978) J. Virol., 27, 28-37.

Payne,L.G. (1979) J. Virol., 31, 147-155.

Payne,L.G. (1980) J. Gen. Virol., 50, 89-100.

Payne,L.G. (1992) Virology, 187, 251-260.

Payne,L.G. and Norrby,E. (1978) J. Virol., 27, 19-27.

Payne,L.G. and Kristenson,K. (1979) J. Virol., 32, 614-622.

Payne,L.G. and Kristenson,K. (1990) Virus Res., 17, 15-30.

Rodriguez,J.F. and Esteban,M. (1987) J. Virol., 61, 3550-3554.

Rodriguez,J.F. and Smith,G.L. (1990) Nuc. Acid Res., 18, 5347-5351.

Rodriguez,J.F., Paez,E. and Esteban,M. (1987) J. Virol., 61, 395-404.

Rodriguez,J.F. and Smith,G.F. (1990) Nuc. Acid Res., 18, 5347-5351.

Roos,N. and Morgan,A.J. (1990) Cryopreservation of thin biological specimens for electron microscopy: Methods and applications. Oxford Science Publications.

Shida,H. (1986) Virology, 150, 451-462.

Schmelz,M., Sodeik,B., Ericsson,M., Wolffe,E.J., Shida,H., Hiller,G. and Griffiths,G. (1994) J. Virol., 68, 130-147.

Schmutz,C., Payne,G., Gubser,J. and Wittek,R. (1991) J. Virol., 65, 3435-3442.

Schmutz,C., Rindisbacher,L., Galmiche, M.C. and Wittek,R. (1995) Virology, 213, 19-27.

Slot,J.W., Geuze,H.J., Gigengack,S., Leinhard,G.E. and James,D.E. (1991) J. Cell Biol., 113, 123-135.

Sodeik,B., Doms,R.W., Ericsson,M., Hiller,G., Machamer,C.E., von't Hof,W., von Meer,G., Moss,B. and Griffiths,G. (1993) J. Cell Biol., 121, 521-541.

Sodeik,B., Griffiths,G., Ericsson,M., Moss,B. and Doms,R.W. (1994) J. Virol., 68, 1103-1114.

Sodeik,B., Cudmore,S., Ericsson,M., Esteban,M., Niles,E. and Griffiths,G. (1995) J. Virol., 69, 3560-3574.

Stern,W. and Dales,S. (1976) Virology, 75, 232-241.

Stewart,P.L., Burnett,R.M., Cyrklaff,M. and Fuller,S.D. (1991) Cell, 67, 145-154.

Stokes,G.V. (1976) J. Virol., 18, 636-643.

Theriot,J.A. (1994) Semin. Cell Biol., 5, 193-199.

Tilney,L.G., Connelly,P.S. and Portnoy,D.A. (1990) J. Cell Biol., 111, 2979-2988.

vanSlyke,J.K., Whitehead,S.S., Wilson,E.M. and Hruby,D.E. (1991) Virology, 183, 467-478.

Wolffe,E.J., Isaacs,S. N. and Moss,B. (1993) Virol., 67, 4732-4741.

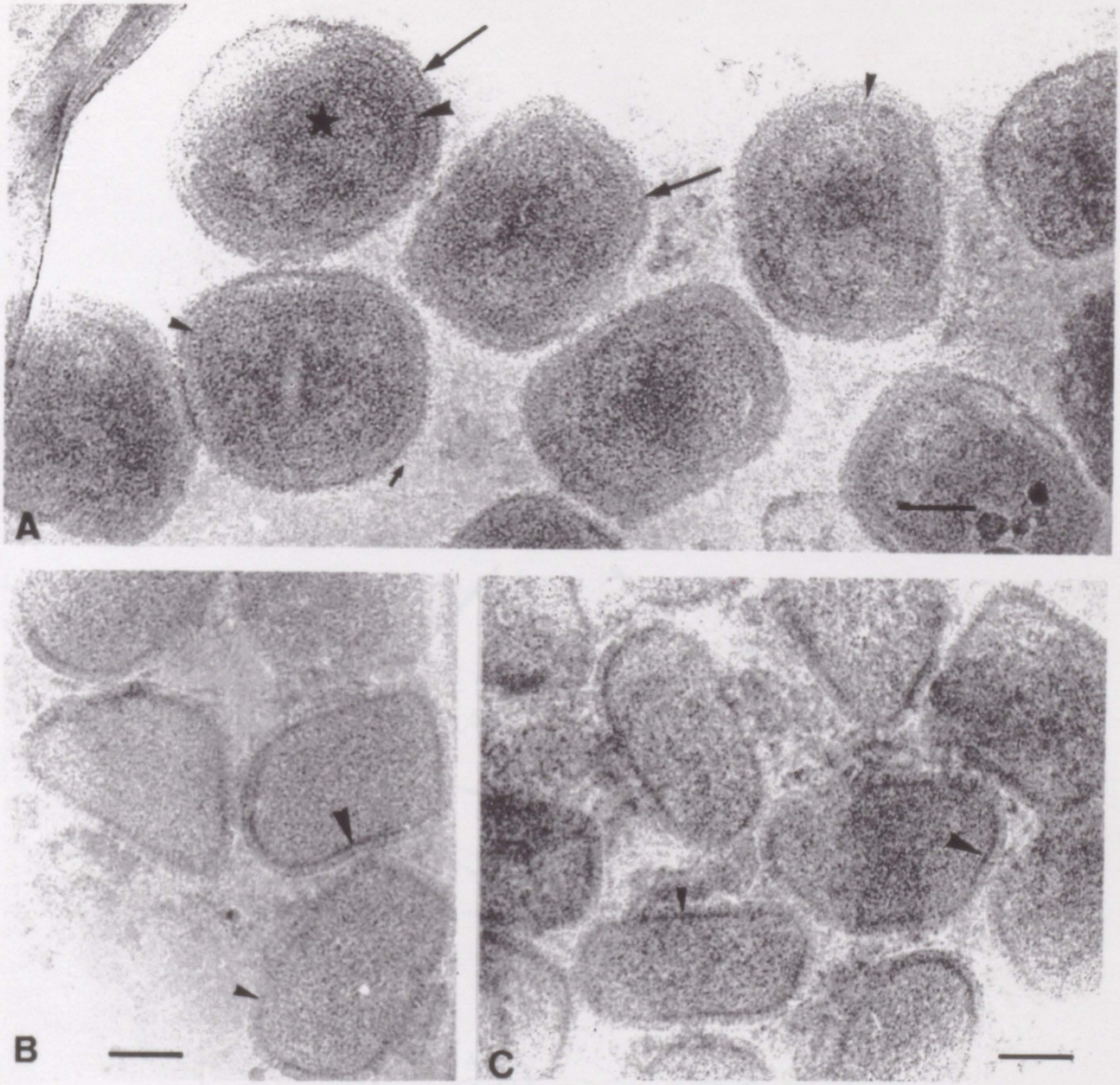
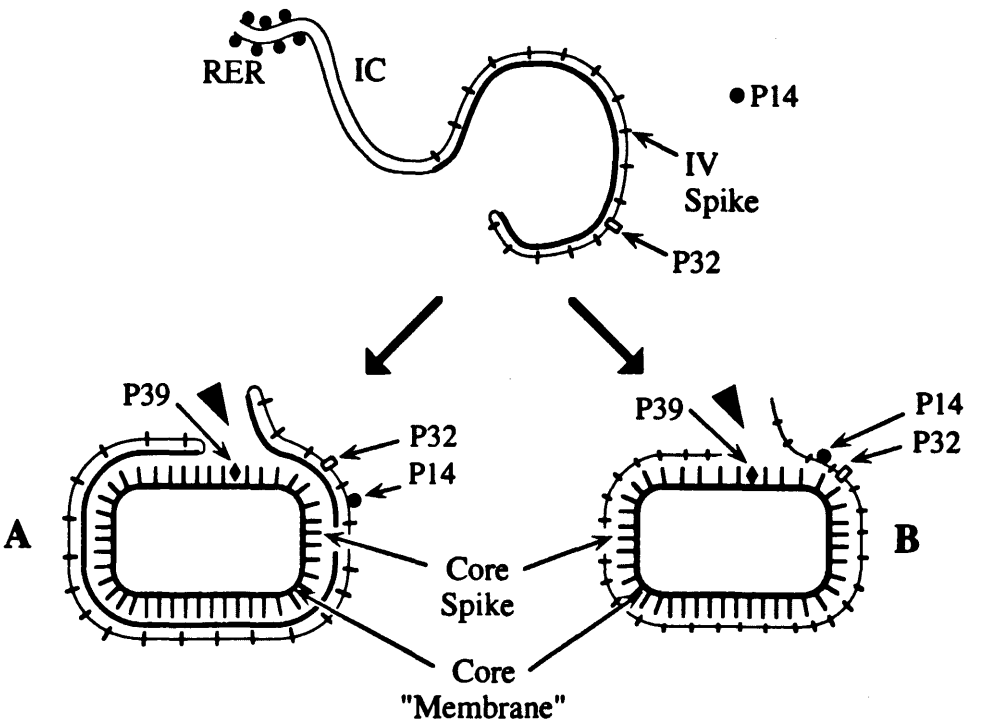


FIG. 1

A novel immunogold cryo EM method to investigate the structure of the IMV/EEV
Roos,N., Cyrklaff,M., Cudmore,S., Blasco,R., Krijnse-Locker,J., Griffiths,G.


RER
IC
P14
IV
Spike
P32
P39
P32
P14
A
Core
Spike
Core
"Membrane"
P39
P14
P32
B

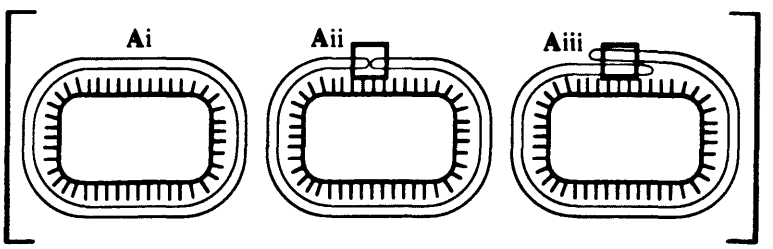
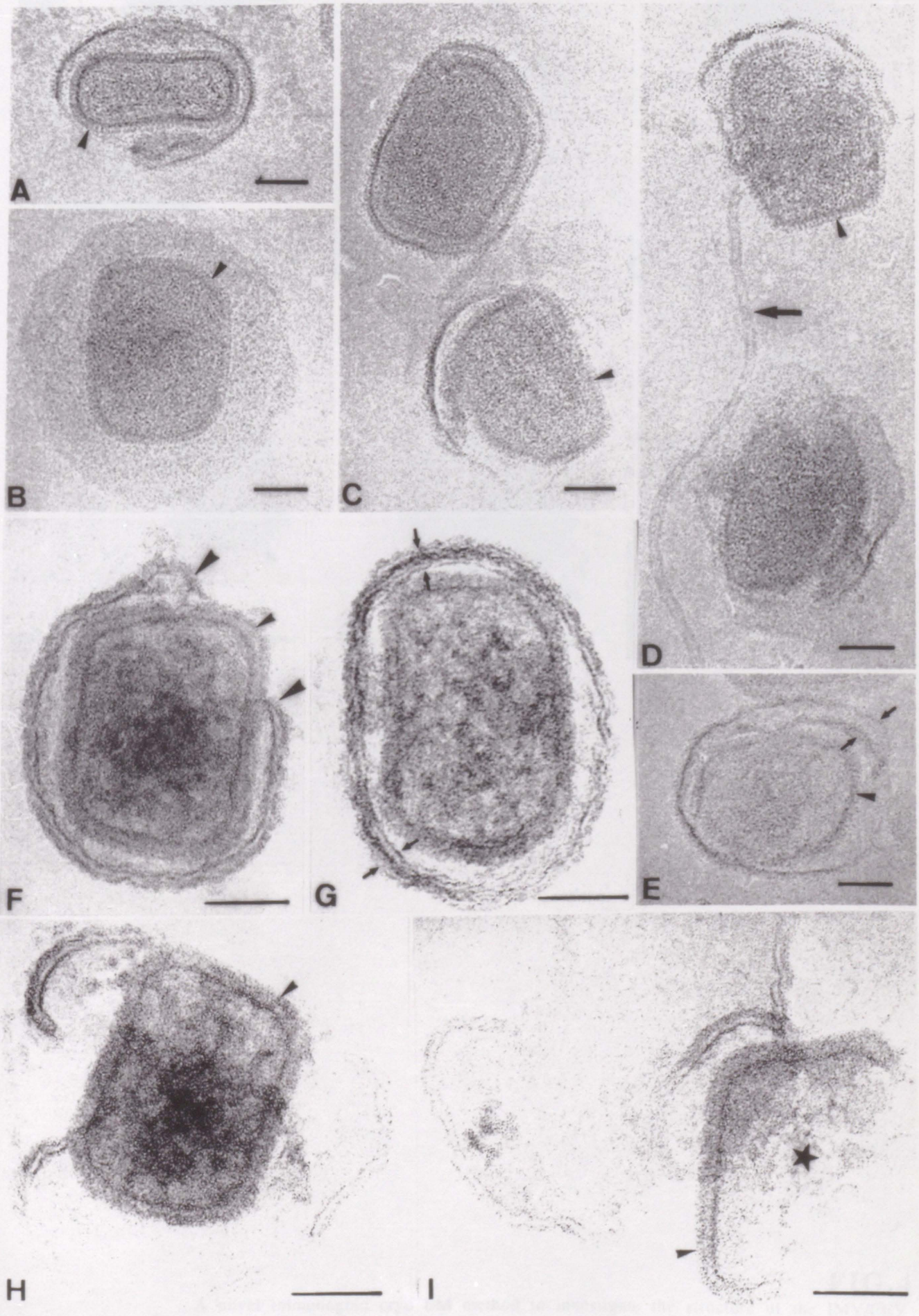

Ai
Aii
Aiii

FIG.3

A novel immunogold cryo EM method to investigate the structure of the IMV/EEV
Roos,N., Cyrklaff,M., Cudmore,S., Blasco,R., Krijnse-Locker,J., Griffiths,G.



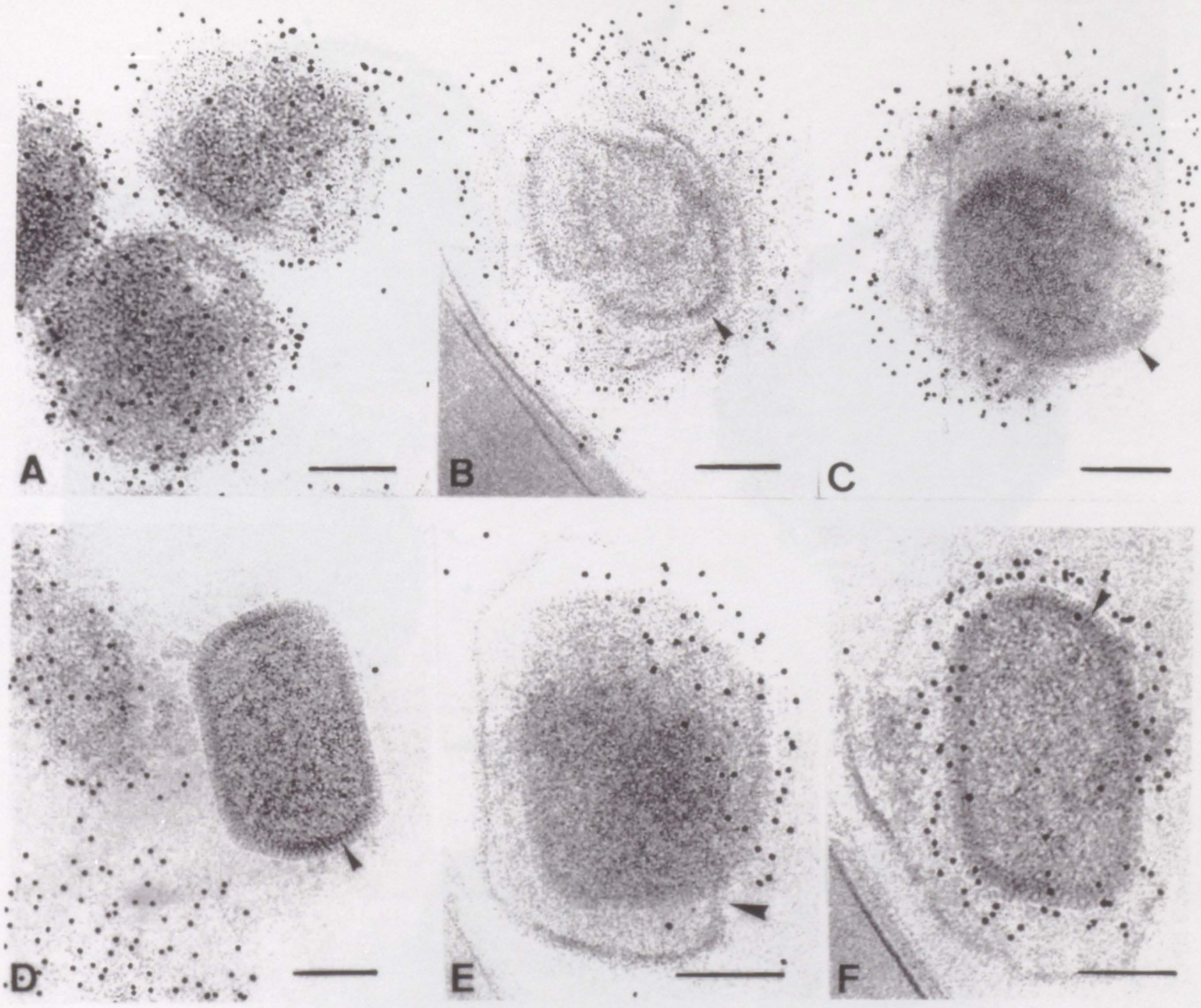


FIG.4

A novel immunogold cryo EM method to investigate the structure of the IMV/EEV
Roos,N., Cyrklaff,M., Cudmore,S., Blasco,R., Krijnse-Locker,J., Griffiths,G.

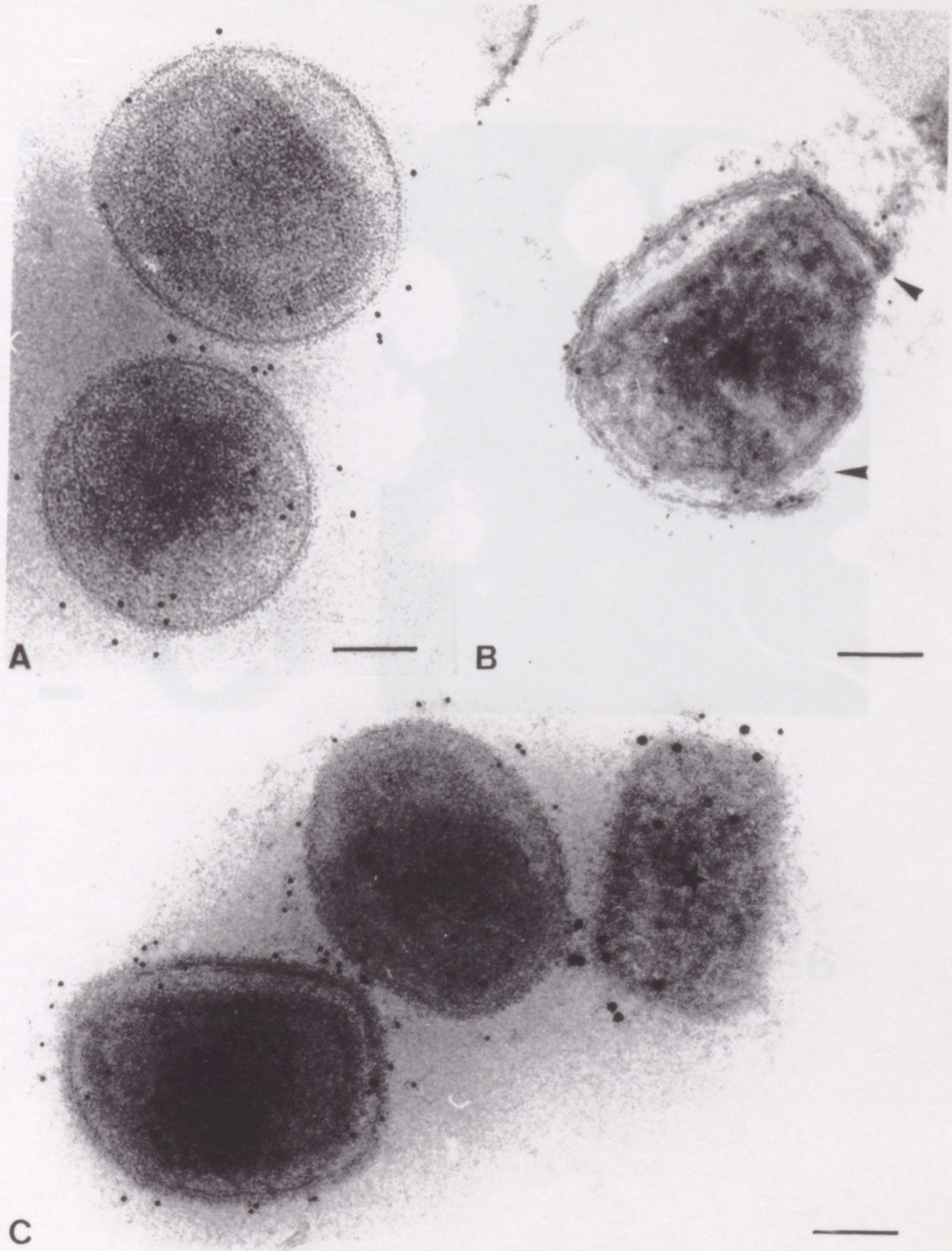
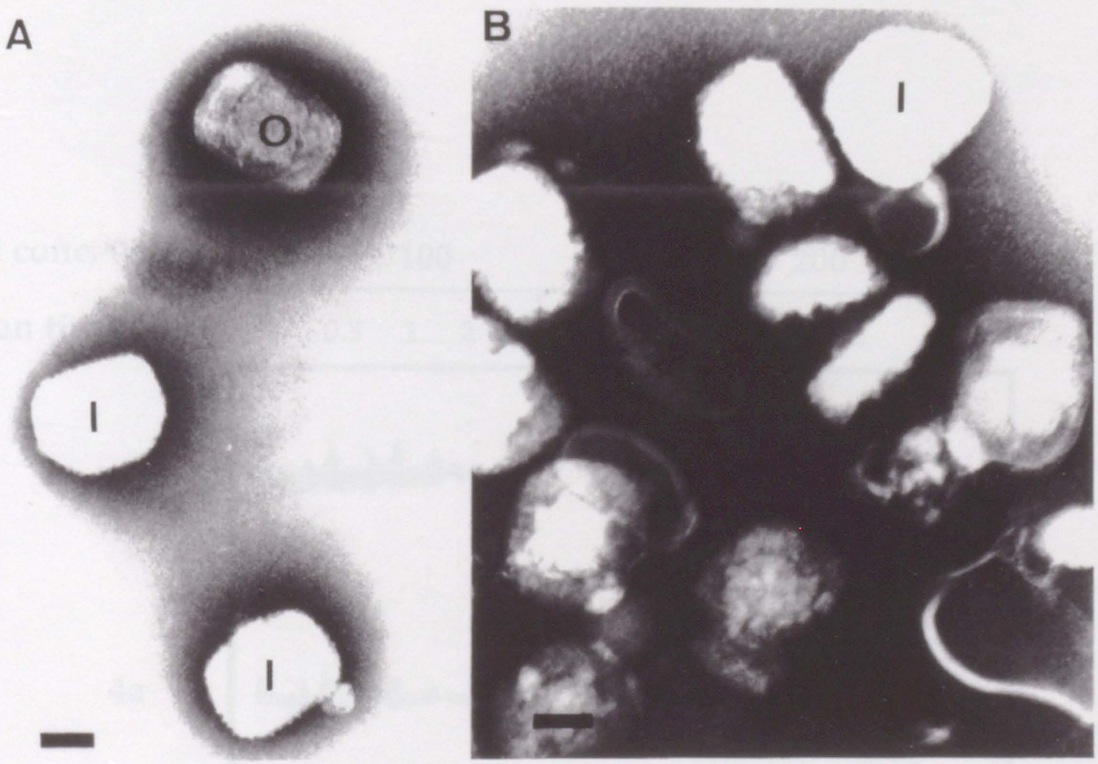
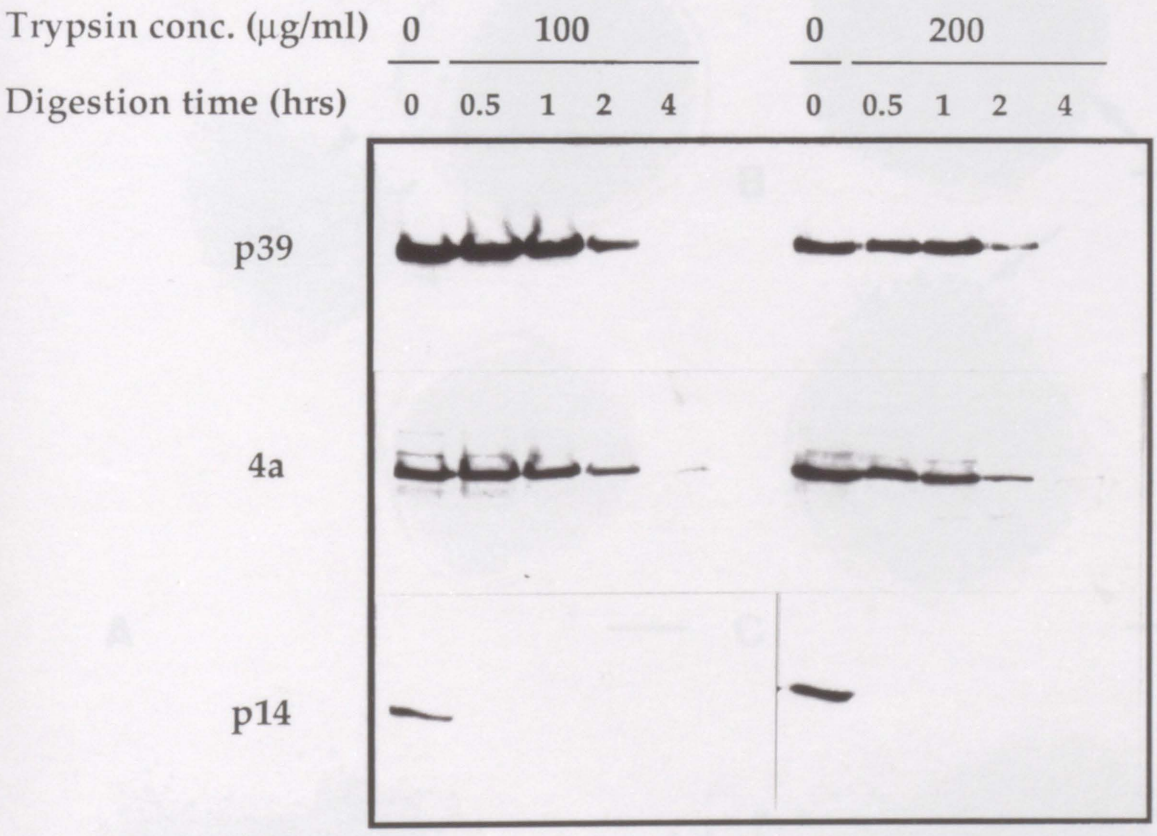


FIG.5

A novel immunogold cryo EM method to investigate the structure of the IMV/EEV
Roos,N., Cyrklaff,M., Cudmore,S., Blasco,R., Krijnse-Locker,J., Griffiths,G.



6


Trypsin conc. (μg/ml)
0
100
0
200
Digestion time (hrs)
0
0.5
1
2
4
0
0.5
1
2
4
p39
4a
p14

7

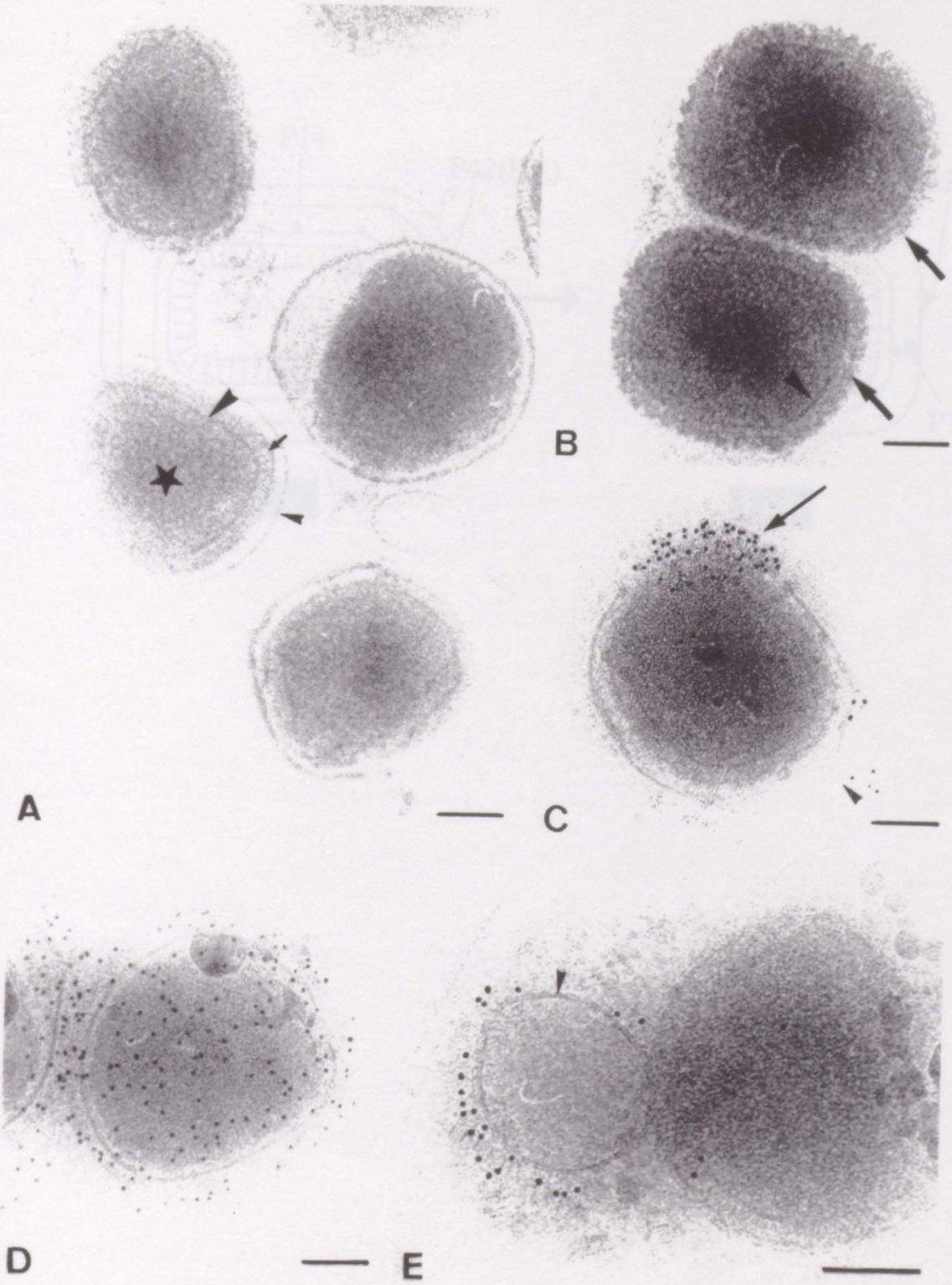


FIG 8

A novel immunogold cryo EM method to investigate the structure of the IMV/EEV
Roos,N., Cyrklaff,M., Cudmore,S., Blasco,R., Krijnse-Locker,J., Griffiths,G.

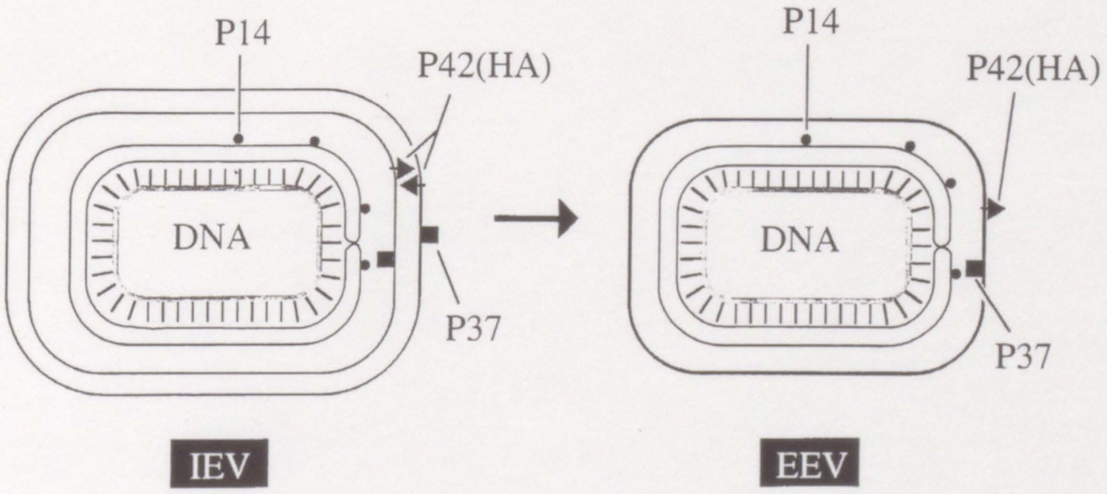


FIG 9

A novel immunogold cryo EM method to investigate the structure of the IMV/EEV
Roos,N., Cyrklaff,M., Cudmore,S., Blasco,R., Krijnse-Locker,J., Griffiths,G.